# Imperial College London

# Ephrin-B2 is a glioblastoma oncogene that drives perivascular invasion and proliferation

AUTHOR:

BENJAMIN KRUSCHE

SUPERVISOR:                                          IMPERIAL COLLEGE LONDON

DR. SIMONA PARRINELLO              MRC CLINICAL SCIENCES CENTRE

A thesis submitted to Imperial College London for the degree of Doctor of Philosophy

June 11, 2015

# Table of Contents

# Abstract

Glioblastoma multiforme (GBM) are the most aggressive and devastating tumours of the brain and are essentially incurable. They are defined by diffuse invasion of the surrounding brain parenchyma along preexisting structures like the vasculature. Glioma stem cells (GSC) are thought to be largely responsible for tumour recurrence following treatment due to their high resistance to therapy, their ability to recapitulate tumours from single cells and their marked invasive potential.

Here we show, that normal neural stem cell in the subventricular zone are compartmentalised by endothelial ephrinB2 and their proliferation limited through activation of p53 in an Eph signalling dependent manner. GSCs however evade both compartmentalisation and proliferation inhibition and are able to invade perivascularly. Intravital imaging, coupled with mechanistic studies *in vitro* revealed that upregulation of ephrinB2 in highly aggressive, mesenchymal GSCs enables escape from endothelial compartmentalisation through homotypic forward signalling.

Surprisingly we also find that that ephrinB2 reverse signalling promotes tumourigenesis by mediating anchorage-independent cytokinesis through activation of RhoA. In preclinical models using human GSCs we show, that inhibition of ephrinB2 by RNA silencing or with ephrinB2-blocking antibodies strongly suppresses tumourigenesis of established glioblastoma by inducing cell-cycle arrest and blocking GBM/vascular interactions. Thus, ephrinB2 is an oncogene and represents an attractive candidate for anti-GBM therapies aimed at eradicating the GSC compartment by targeting both glioma invasion and proliferation.

# Declaration of Originality

I hereby declare that this thesis and the work presented in it was composed by and originated entirely from me and has not been submitted in any form for another degree or diploma at any other institution. Any information derived from the published or unpublished work of others has been acknowledged in the text and references are listed in the bibliography.

# Copyright declaration

NAME:                                                      DATE: JUNE 11, 2015

# Acknowledgements

*"Research is what I'm doing when I don't know that I'm doing"*

--- Wernher von Braun

The past four years would not have been possible without the guidance and the help of a whole host of people, to whom I am very glad I met. First and foremost, I am heartily thankful to my supervisor Dr. Simona Parrinello, whose encouragement, supervision and expertise from the very first day shaped my development as a scientist. She demanded a high standard from all her students and I hope this work lives up to that. Thanks for kicking my butt whenever necessary to ensure that something actually worthwhile got accomplished. Cristina Ottone was the person I worked most closely with in the lab and I owe a great deal for her unselfish help and unfailing support (the images in this thesis would have looked a lot worse without her). You taught me a lot, but almost more importantly were always there when I needed a second opinion be it in science or in life. Thank you for that! My utmost gratitude also goes to Mel Clements. What you accomplish in the lab is a little terrifying, but inspiring at the same time and I still wouldn't be done stitching up my mice were it not for you! Thanks to Ari, Tim and Liz for brightening my lab life, drawing snails on everything, choosing just the right tunes for a boring day in tissue culture and being not just colleagues but friends! My next work place will be so much more boring just because you all won't be there. Thanks also to my sister Lena whom I could always rely on to be there for me be it for complaining about my research or going on a spontaneous skiing weekend. On a personal level, I'd like to thank my parents. Without your unflagging support, I never would have made it over here in the first place, much less finished. I owe you both so much more than I could ever repay.

# List of Abbreviations

| | |
|---|---|
| BBB | Blood brain barrier |
| bEND3 | Brain endothelialpolyoma middle T antigen transformed endothelial cells |
| bmvEC | Brain microvascular endothelial cells |
| BSA | Bovine serum albumin |
| BTSC | Brain tumour stem cell |
| BrDU | 5-Bromo-2-Deoxyuridine |
| CSC | Cancer stem cell |
| cDNA | Copy DNA |
| $CO_2$ | Carbondioxide |
| DMEM | Dulbecco's modified Eagle's medium |
| DMSO | Dimethyl sulfoxide |
| DNA | Deoxyribonucleic acid |
| DUSP | Dual specificity phosphatase |
| ECM | Extracellular matrix |
| et. al. | et alii (lat.: and others) |
| Eph | Erythropoietin-Producing hepatocellular protein |
| Ephrin | Eph family receptor interacting protein |
| EGF | Epidermal growth factor |

| | |
|---|---|
| FACS | Fluorescence activated cell sorting |
| FAK | Focal Adhesion Kinase |
| FGF | Fibroblast growth Factor |
| GAP | Guanosine triphosphatase (GTPase)-activating protein |
| GAPDH | Glyceraldehyde-3-phostphate dehydrogenease |
| GBM | Glioblastoma |
| GDP | Guanosine diphosphate |
| GEF | Guanine nucleotide exchange factor |
| GFAP | Glial fibrillary acidic protein |
| GFP | Green fluorescent protein |
| GPI | Glycolsylphosphatidylinositol |
| GSC | Glioblastoma stem cell |
| GTP | guanosine triphosphate |
| HRP | Horseradish peroxidase |
| Ig | Immunoglobulin |
| imNSC | Immortalised neural stem cell |
| KD | Knock-down |
| KO | Knock-out |
| MAPK | Mitogen-activated kinase pathway |
| mRNA | Messenger RNA |
| NSC | Neural stem cell |
| PCR | Polymerase chain reaction |
| PI3K | Phosphatidulinositol 3-kinase |
| PDZ | Post-synaptic density-95/Discs Large tumour supressor / Zonula Occludens-1 domain |
| Q-PCR | Quantitative PCR |

| | |
|---|---|
| Rb | Retinoblastoma |
| RMS | Rostral migratory stream |
| RNA | Ribonucleic acide |
| RT-PCR | Reverse transcriptase PCR |
| RTK | Receptor tyrosine kinase |
| rpm | revolutions per minute |
| SAM | Sterile alpha motif |
| SDS-PAGE | Sodium dodecylsulfate polyacrylamide gel electrophoresis |
| SGZ | Subgranular zone |
| SH2 | Src homology 2 |
| SH3 | Src Homology 3 |
| SILAC | Stable isotope labelling with amino acids in cell culture |
| siRNA | silencing RNA |
| shRNA | Short hairpin RNA |
| SVZ | Subventricular zone |
| TCGA | The cancer genome atlas |
| WHO | World health organisation |
| WT | Wild type |

# List of Figures

# List of Tables

# Chapter 1

# Introduction

Glioblastoma multiforme (GBM) is the most common and aggressive type of primary brain tumour and one the most lethal forms of human cancer. Despite highly aggressive treatment, recurrence is inevitable resulting in a median survival of less than 15 months. GBM are characterised by diffuse invasion of the healthy brain parenchyma along preexisting structures. Furthermore, GBM contain a population of stem-like cells which are highly infiltrative and intrinsically chemo- and radio-resistant.

In this thesis I used a glioma stem cell model derived from neural stem cells of the subventricular zone to investigate glioma invasion and proliferation. I will therefore introduce the subventricular zone, one of the two neurogenenic stem cell niche in the adult brain which has not only been implicated in gliomagenesis but also shares great structural and functional similarities with the microenvironment controlling glioma stem cell maintenance and invasion. Furthermore, I will introduce a class of proteins which are highly expressed in a variety of stem cell niches and are known for both their tumour suppressing and promoting potential in glioblastoma: Eph receptors and their ephrinB2 ligands.

# 1.1   The subventricular zone

For most of the 20th century it was considered a dogma that neurons in the brain were not added or replaced in adulthood.

However, it is now very well established, that the adult mammalian brain contains two neurogenic regions capable of continuously generating new neurons: The subventricular zone (SVZ) of the lateral ventricle and the subgranular zone (SGZ) of the dentate gyrus. Parenchymal cells in both of these regions create a supporting niche structure which controls self-renewal and differentiation of the stem cells.

The concept of a niche providing signals to stem cells was first developed in 1978 by Schofield: he proposed that stem cells reside in fixed anatomical compartments, niches, which are crucial for the maintenance of cells with stem cell properties (Schofield, 1978). Initially progress in identifying these proposed niches was mostly made in *Drosophila* and *C. elegans* due to the anatomical complexity of mammals but in recent years enhanced experimental techniques led to the identification of various stem cell niches in adult mammals (reviewed in Li and Xie, 2005).

The stem cell niche of the subventricular zone is one of the best-characterised mammalian stem cell niches (Allen, 1912; Lewis, 1968; Blakemore, 1969) and cell proliferation within the SVZ has been demonstrated in a large number of vertebrates including mice, rats,monkeys and humans (Kornack and Rakic, 2001; Sanai et al., 2004; Eriksson et al., 1998).

The SVZ is located throughout the lateral wall of the lateral ventricles and consists of three neurogenic stem and progenitor cell types: quiescent type B neural stem cells, transit amplifying type C cells and type A neuroblasts. Type B-cells are a group of GFAP expressing cells which are thought to be *bona fide* stem cells: Doetsch et.al. showed that they are label retaining slowly proliferating cells which are able to regenerate the pool of immature precursors and neuroblasts after depletion by antimitotic treatment *in vivo* . Furthermore only type-B

cells but not other cell types of the SVZ are able to form neurospheres *in vitro* and can be differentiated into neurons, astroglial cells and oligodendrocytes (Doetsch et al., 1999a). Type B-cells lie just under a single sheet of ependymal cells that line the ventricle and separate the cerebrospinal fluid from the brain parenchyma with occasional processes of the type B cells intercalating between the ependymal layer (Doetsch, 2003; Doetsch et al., 1999b) Type B-cells give rise to the rapidly proliferating intermediate precursor cells (C-cells). Type C cells in turn give rise to neuroblasts (A-cells). Type A neuroblasts then migrate in chains along the rostral migratory stream (RMS) to the olfactory bulb where they differentiate into various interneurons (De Marchis et al., 2007 ; **Figure I).** This chain migration has been observed in the brain of adult rodents (Lois and Alvarez-Buylla, 1994) and primates (Kornack and Rakic, 2001). It is still debated whether the RMS exists in a similar fashion in humans whose SVZ has a unique structure compared to other mammals (Sanai et al., 2004; Curtis et al., 2007). The SVZ however does not only supply neurons for the olfactory bulb but also constantly produces new oligodendrocytes and it has been shown that in response to brain injuries it it also capable of supplying new astrocytes to replace damaged cells (Levison and Goldman, 1993; Alvarez-Buylla et al., 2000; Benner et al., 2013).

Apart from neural stem cells and their progeny the SVZ is composed of supporting parenchymal cells, namely ependymal cells and a specialised vasculature. These supporting cell types , similar to cells in other stem cell niches in the body are required to provide the appropriate environment for the stem-like populations: firstly, signals produced by the niche have to be able to control stem cell self-renewal, maintenance and survival (Li and Xie, 2005). Secondly, the niche has to provide an architecture which promotes polarisation of stem cells and therefore asymmetric cell divisions (Yamashita et al., 2010) and lastly, stem cells have to be anchored within the niche through interactions with stromal cells and the extracellular matrix. This ensures that the stem cells are kept in close proximity to the signals emanating from the niche which regulate them ( Jones and Wagers, 2008 ; **Figure II).**
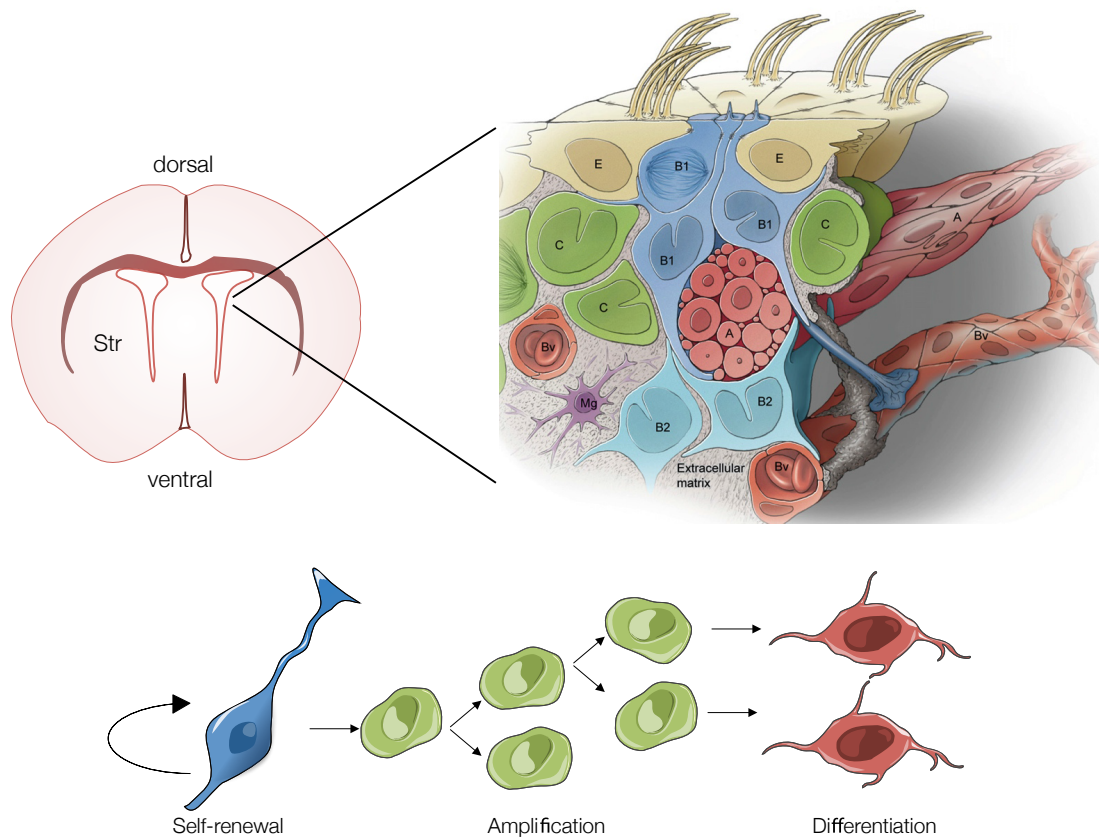
**Figure I:** **Schematics of the composition of the subventricular zone**. The SVZ is one of the two neurogenic stem cell niches in the adult brain (adapted from Ihrie and Alvarez-Buylla, 2011)

### 1.1.1    The vascular NSC niche

In recent years it has become more and more apparent that a specialised vasculature in the subventricular zone plays an important role in providing these crucial functions to ensure the right niche environment: an extensive network of blood vessels is present in the SVZ which is structurally different from non-neurogenic regions of the brain and also differs from the vasculature present in the subgranular zone (Tavazoie et al., 2008). Furthermore, both type-B NSCs and transit amplifying type-C cells are in close contact to the vasculature throughout their life cycle (Shen et al., 2008; Tavazoie et al., 2008). In fact, even migrating neuroblasts in the rostral migratory use blood vessels as a migratory scaffold and migrate parallel to vascular structures until they reach their final location in the olfactory bulb (Huntley et al.,
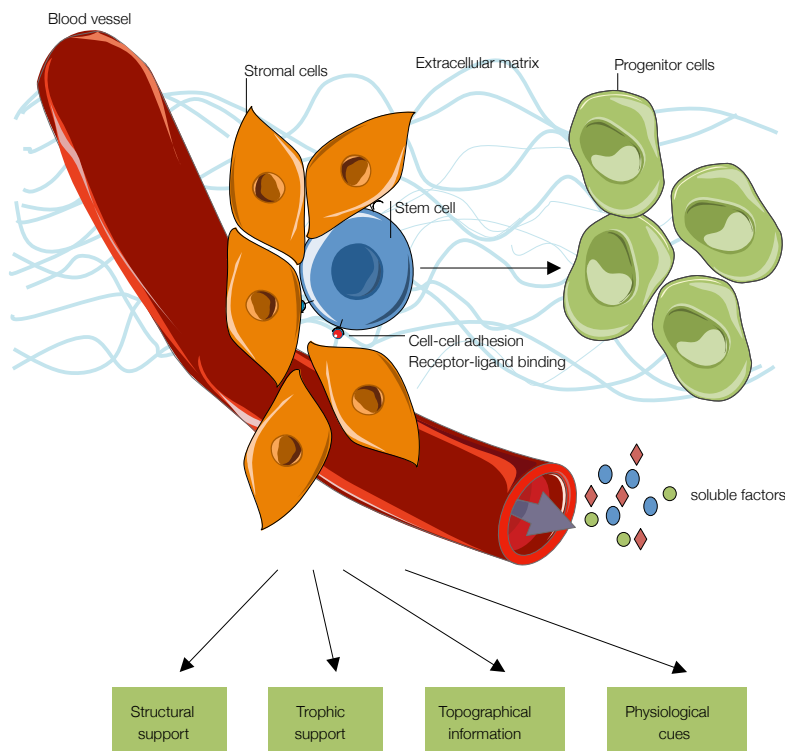
**Figure II:** **Summary of known key components of stem cell niches**. (adapted from Jones and Wagers, 2008)

2014; Nam et al., 2007). Blood vessels also support neurogenesis by secreting factors that further promote the differentiation of migrating neuroblasts into mature neurons (Goldman and Chen, 2011; Leventhal et al., 1999). Importantly, it is well established that quiescent type B stem cell form long cytoplasmic projections that make stable contacts with endothelial cells through specialised end feet poising them to receive spatial and regulatory cues from the vasculature (Tavazoie et al., 2008; Shen et al., 2008). Moreover, transplanted NSCs also actively home towards the vascular niche, attracted by endothelial secreted SDF1 (Kokovay et al., 2010). Endothelial cells secret a variety of soluble factors, that have been shown to promote self-renewal and control neurogenesis of adult NSCs: for example, PEDF released by endothelial cells promotes cell renewal *in vitro* and activates quiescent type-B cells *in vivo* (Ramírez-Castillejo et al., 2006). Similarly, Betacellulin and NT3 are released by the vasculature in the SVZ and regulate the self renewal and proliferation of NSCs (Delgado et al., 2014; Gómez-Gaviro et al., 2012). In addition, circulating blood can carry factors like hormones or cytokines that influence neurogenesis.

While many studies have found an important role for endothelial cells in neural stem cell activation, recent work from our group intriguingly also showed that the direct contact between quiescent type B stem cells and endothelial cells is critical for maintaining stem cell quiescence and identity. Mechanistically we showed that endothelial ephrinB2 and Jagged1 ligands suppress cell-cycle entry downstream of mitogens and induce the expression of stemness genes. *In vivo* ablation of either of these ligands leads to premature cell cycle entry of type B stem cells and a rapid depletion of the stem cell pool over time (Ottone et al., 2014). This data is particularly interesting as it shows how spatial information is integrated in stem cell niches to achieve the right balance of self-renewal and differentiation.

Together this data highlights the importance of endothelial cells as regulating components of a neuronal stem cell niche in the adult brain and raises important questions about what the role of this system is in the diseased state.

## 1.2 Glioblastoma

Most tumours in the brain originate from glial cells and are classified by their closest counterpart in normal tissue: astrocytomas, oligodendrogliomas and ependymomas (Ohgaki and Kleihues, 2005). Astrocytic gliomas are the most common and clinically relevant and were classified into a grade system by the WHO in the 1970s which has been updated in 2007 (Louis et al., 2007) based on their clinical and biological properties (Table I). WHO grade I only represents benign angiocentric gliomas in children and juveniles and is separate from grade II-IV which describe adult astrocytomas with progressing malignancy (Burger et al., 1985).

**Table I: Classification and grading of glioma subtypes according to the WHO**. (Louis et al., 2007)

| WHO-Grade | Tumour type | Histology |
|---|---|---|
| I | pilocytic astrocytoma | no pleomorphic cells and low proliferative potential |
| II | diffuse astrocytoma | usually nuclear atypia |
| III | anaplastic astrocytoma | usually nuclear atypia and mitotic activity |
| IV | Glioblastoma | nuclear atypia, mitosis, endothelial proliferation and/or necrosis |

Histological WHO-grade II tumours commonly have an isomorphous appearance whereas the anaplastic astrocytomas of WHO-grade III show an increase in cell density with frequent mitotic events. The decisive event for a tumour to be graded grade IV glioblastoma instead of grade III are areas of focal necrosis within the tumour and aberrant pathological neovascularisation (Burger et al., 1985).

Glioblastoma multiforme is the most aggressive and most common primary tumour of the

brain and despite extensive efforts in clinical and basic research, current therapeutic approaches are largely ineffective. GBMs almost invariably recur causing a median survival which for the last 20 years has remained steady at around 15 months. Several reasons underly the high recurrence rate and highly malignant nature of glioblastoma: GBM are highly invasive tumours and possess the marked ability to diffusely infiltrate the surrounding healthy areas of the brain which renders complete surgical resection near impossible (Smith and Jenkins, 2000; Pietsch and Wiestler, 1997; Cuddapah et al., 2014). Additionally, GBM are genetically highly heterogenous tumours in appearance and gene expression showing a wide variety of genetic abnormalities which causes highly variable response rates to standard chemotherapies (Mrugala, 2013). Treatment is further complicated by the presence of the Blood Brain Barrier, which although disturbed around the bulk of the tumour presents a significant barrier to efficient drug delivery to invading glioblastoma cells (Pitz et al., 2011; Agarwal et al., 2013). Lastly, glioblastoma contain a population of highly chemotherapy resistant cells stem-like cells which are able to reconstitute the tumour after treatment (Venere et al., 2011; Chen et al., 2012).

## 1.2.1 Cell of origin

It is still disputed from which cells in the healthy brain gliomas originate and whether the cell of origin is the same in all GBMs (Zong et al., 2012). This is partly due to the varied anatomical locations in which glioblastoma arise. There is supporting evidence, that gliomas originate in many cases from either of the normal stem cell niches in the brain (Alcantara Llaguno et al., 2009): gliomas commonly contain cells with varying grades of differentiation showing astrocytic, oligodendrocytic and even neuronal features. Strikingly however these different cell types carry common genetic alterations which hints at a clonal origin of these tumour cells. Moreover, the diverse lineages of the progeny of that clone suggest that the originally transformed cell must have had progenitor or stem like properties (Wang et al., 2009). Apart from these clinical observations there is experimental evidence showing that glioblastomas can arise from transformed neural progenitor cells. In independent studies

Holland et. al. (Holland et al., 2000) and Wang et. al. (Wang et al., 2009) showed that mutating different oncogenic pathways in neural progenitor cells of adult mice leads to the development of aggressive gliomas closely resembling their clinical counterpart.

However, other studies regard gliomagenesis as a multi-step process in which genetic alterations lead to progressive dedifferentiation and transformation of normal, differentiated cells. It has been shown for example, that loss of INK4A/Arf in combination with activation of oncogenic K-ras in mature astrocytes leads to the formation of tumour resembling glioblastoma (Uhrbom et al., 2002). Similar results have been reported for different combinations of oncogenes which also caused dedifferentiation of mature astrocytes and neurons and induced high grade glioma in mice (Friedmann-Morvinski et al., 2012; Bachoo et al., 2002; Radke et al., 2013).

## 1.2.2   Molecular pathology of glioblastoma multiforme

Despite their highly heterogeneous nature, extensive intratumoural variability (Inda et al., 2014) and ongoing debates about the cell of origin, great progress has been made in recent years in identifying key events during gliomagenesis (**Figure III**): the Cancer Genome Atlas (TCGA) has identified three main molecular pathways which are disrupted in the majority of all glioblastomas (TCGA, 2008):

1) the RTK/ras/PI3-K signalling axis,

2) the Retinoblastoma (Rb1) pathway and

3) the p53 tumour suppressor (TP53) pathway

Concurrently it has been shown, that inactivation of p53 combined with NF1 loss is sufficient to induce high malignant astrocytoma with full penetrance in mice (Zhu et al., 2005). Additionally, in a slightly different murine model Chow and colleagues discovered, that mutations in p53 and Rb pathways cooperate with loss of PTEN to induce highly aggressive astrocytoma (Chow et al., 2011). These studies highlight the important impact of these three pathways on

gliomagenesis and proof the validity of using key mutations as a model for glioblastoma.
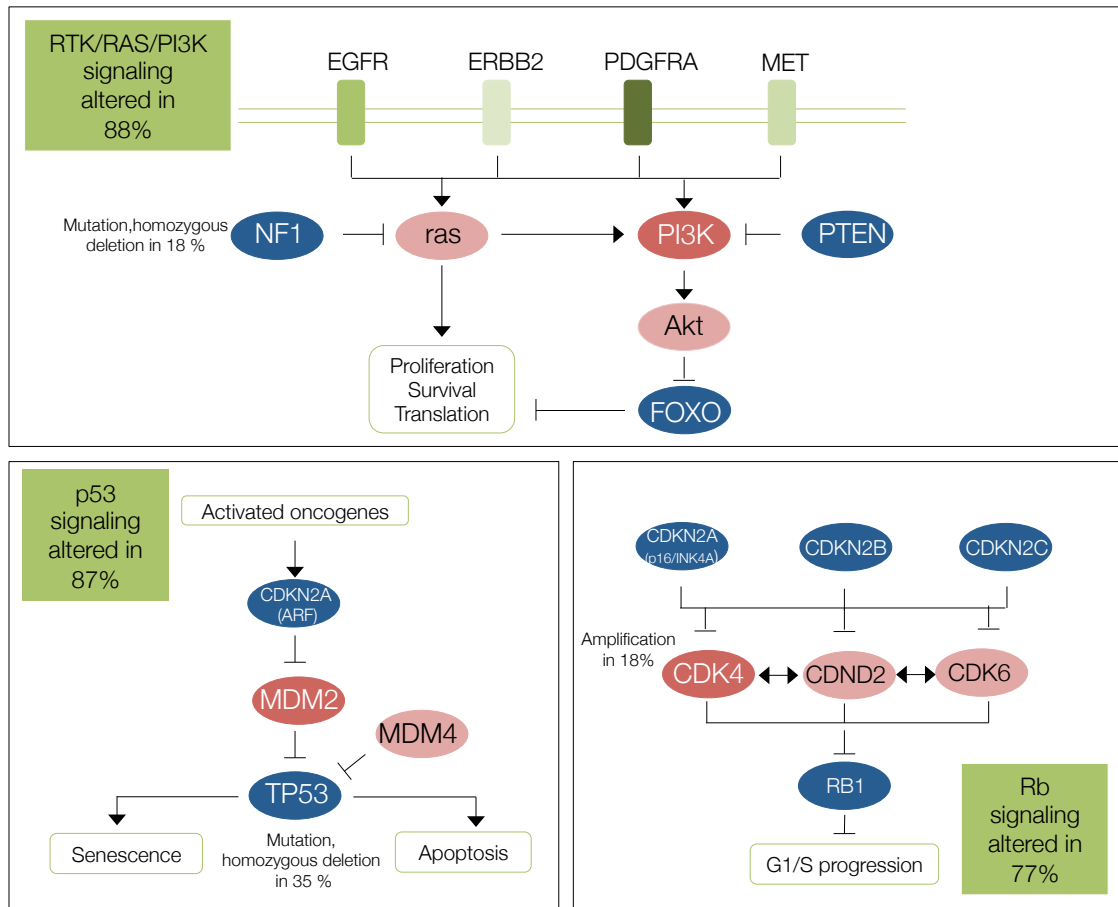


**Figure III: Frequent genetic alterations in glioblastoma**. (adapted from TCGA, 2008)

Expression profiling of a large number of glioblastoma patients made it possible to cluster glioblastomas into subgroups based on a combination of genes over- or under-expressed within each group. Four clinically relevant subgroups have been defined using the TCGA dataset: classical, proneural neural and mesenchymal glioblastoma(TCGA, 2008; Verhaak et al., 2010). Classical glioblastomas generally show gains on chromosome 7 accompanied by partial loss of chromosome 10 and focal losses on chromosome 9p21.3. These losses on chromosomal level lead to amplification of the *EGFR* gene with concomitant loss of the *PTEN* and *CDKN2A* tumour suppressors. In contrast to that virtually no abnormalities in *TP53*, *PDGFRA* or *IDH1* occur. Proneural glioblastomas have been defined as having either frequent overexpression or amplifications of *PDGFRA* or loss of *IDH1* function. A majority of all proneural glioblastomas also has mutations in the TP53 tumour suppressor pathway.

Interestingly *IDH1* mutations have also been associated with decreased mortality risk in patients (Dai et al., 2015). The neural subtype is not as well defined by gross genomic events but neural glioblastoma show high expression levels of neuronal markers such as *NEFL* or *GABRA1*.

The mesenchymal glioblastoma subtype is defined by deletions of a region on chromosome 17 containing the *NF1* tumour suppressor gene. Loss of this region is also frequently accompanied by loss of *TP53* and mutations of the Rb-signalling axis in this subtype (Verhaak et al., 2010). The high expression of mesenchymal and astrocytic markers in comparison to other tumour types is reminiscent of a epithelial-to-mesenchymal transition which has been linked to more dedifferentiated and aggressive tumours (Thiery, 2002). Some reports suggest that the mesenchymal glioblastoma subtype is also more aggressive due to the activation of gene programs promoting high rates of cell proliferation, angiogenesis and invasion (Bhat et al., 2011; Nakano, 2015). Interestingly, there is a clear shift specifically towards mesenchymal glioblastoma but not other subtypes in tumour progression and recurrence further strengthening the notion of mesenchymal glioblastoma as a more aggressive subtype (Phillips et al., 2006).

### 1.2.3   Cancer stem cells in glioblastoma

It is now well established that many tumours contain a small, relatively quiescent population of cells with stem cell properties called cancer stem cells (CSC). The CSC model describes tumours as a hierarchically organised tissue with the CSC population at the top. This population is able to generate the more differentiated bulk of the tumour which loses the capacity for self-renewal and tumourigenicity. (**Figure IV**).

CSCs were first identified in in acute myeloid leukemia (Bonnet and Dick, 1997) but similar results have since then been reported for prostate,liver,pancreas,breast and brain tumours (Collins et al., 2005; Li et al., 2007; Singh et al., 2003). Cancer stem cells bear remarkable sim-

Stochastic Model                    Cancer Stem Cell Model



Every cell within the tumour has the
potential to become tumourigenic

Only a subset of tumour cells,
known as cancer stem cells is tumourigenic
and these cells are defined by their capacity
for selfrenewal and differentiation plasticity
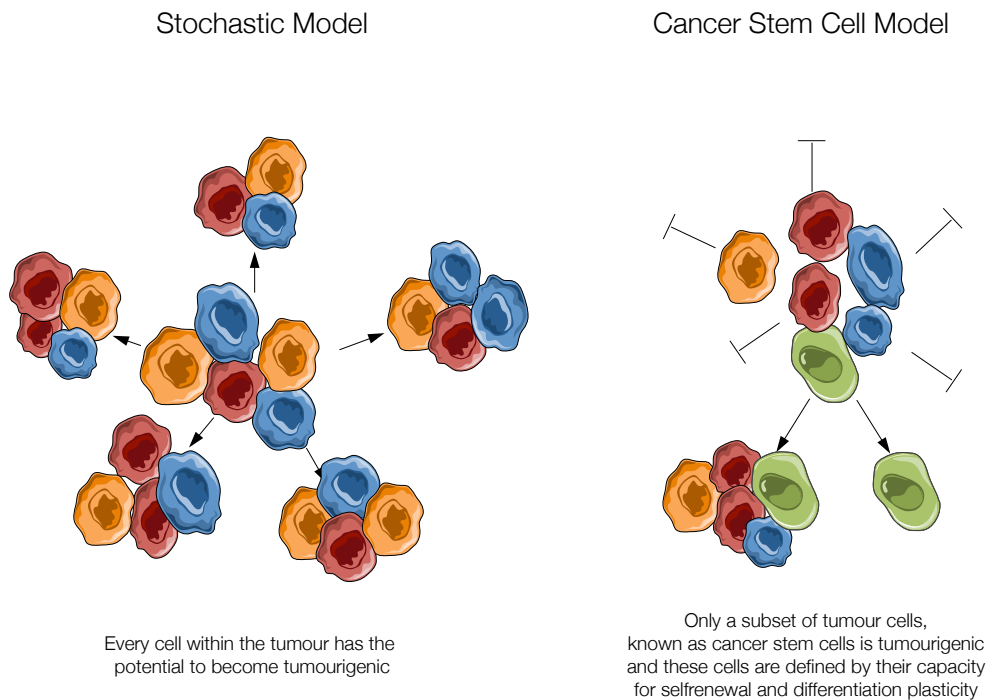
**Figure IV: Stochastic versus cancer stem cell models of tumourigenesis**.  According to the stochastic model, every cell has the potential to become tumourigenic. In contrast, the cancer stem cell model describes a hierarchical organisation of tumours where only a subset of tumour cells, called cancer stem cell, have the ability to self-renew and be tumourigenic. Green shading depicts cancer stem cells, other colours tumour bulk cells (adapted from Girouard and Murphy, 2011)

ilarities to normal stem cells in that they are able to self renew and differentiate into different cell types (Chen et al., 2012). In addition to that CSCs are highly resistant to chemotherapeutic treatment and it has been shown that a small number of CSCs is sufficient to reconstitute the tumour bulk. These characteristics make them highly likely to be the underlying cause of tumour recurrence (Todaro et al., 2007; Bao et al., 2006; Al-Hajj et al., 2003; Singh et al., 2004).

Evidence for a stem like population in glioblastomawas first presented by Steindler et. al. who showed that a subpopulation of cells isolated from human glioblastoma was capable of clonal expansion (Ignatova et al., 2002). This led to a number of similar reports by several groups which all showed that only a minority population of all cells isolated from glioblastoma have the ability to recapitulate the parent tumour (Singh et al., 2003; Yuan et al., 2004). Singh

et. al. identified and purified cells from primary human brain tumours which expressed the cell surface marker CD133 and possessed, in contrast to cells lacking this marker, a marked capacity for self-renewal and differentiation *in vitro* . Remarkably, injection of as few as 100 CD133 positive cells was sufficient to generate *de novo* tumours *in vivo* that were a phenocopy of the parental tumour whereas CD133 negative cells engrafted but did not cause tumour growth even if injected at much higher numbers (Singh et al., 2004). This study was seminal in that it showed for the first time, that brain tumours contain a transformed, undifferentiated cell population that was distinguishable from differentiated cells by the expression of a cell surface marker and was quickly followed by other reports proving that these stem-like cancer cells were indeed multipotent, that is, able to differentiate into different lineages in culture, and had the capability of long term clonal expansion and therefore possessed all characteristics of *bona fide* GSCs (Galli et al., 2004).

One of the hallmarks of glioblastoma is the inevitable recurrence of these tumours which is caused by a small population of chemotherapy resistant cells. In a seminal paper Chen and colleagues showed that this restricted population possesses all characteristics of GSCs and that these cells are largely irresponsive to temozolomide treatment due to their quiescent nature. Importantly, ablation of these Nestin positive GSCs significantly arrested tumour growth and development in mouse models (Chen et al., 2012). More recently, in a similar experiment it was shown, that loss of GSCs also leads to death, cell-cycle arrest and differentiation of the remaining tumour mass (Zhu et al., 2014). This highlights the crucial role of glioma stem cells in glioblastoma tumourigenicity.

### 1.2.4   GSC vascular niche

Glioblastoma are highly vascularised tumours characterised by extensive angiogenesis. The newly formed tumour-associated vessels display gross anatomical abnormalities are often tortuous, significantly larger than normal vessels and are highly permeable (Jain et al., 2007). A special relationship between glioblastomas and the vasculature was first described by Scherer in

the 1940s who observed tumour cells invading into the normal brain along preexisting blood vessels and found that glioblastoma cells regularly formed cuffs completely surrounding blood vessels (Scherer, 1940). It was presumed, that the main role of this extensive vascular network is to provide nutrients to support the aggressive tumour growth. Stem cells in various tissues inhabit protective niches and interestingly, neural stem cells lie in a vascular niche which regulates stem cell self-renewal through direct contact (Shen et al., 2004; Tavazoie et al., 2008; Ottone et al., 2014). Importantly, there is overwhelming evidence, that cancer stem cells in other solid tumours are highly dependent on similar vascular niches which regulate their stemness and proliferation (Cabarcas et al., 2011; Quail et al., 2012; Korkaya et al., 2011; Ye et al., 2014; Takakura, 2012).

Earlier experiments had shown, that CD133+ glioblastoma stem cells produce high levels of VEGF and actively promote tumour angiogenesis (Bao et al., 2006). This study showed, that GSCs actively shape their vascular microenvironment, suggesting that the vasculature might provide important survival and self-renewal cues for GSCs similar to normal stem cell niches in the brain. Interestingly, anti-VEGF treatment with bevacizumab, while not affecting the bulk of the tumour profoundly, seemed to selectively target GSCs resulting in a strong reduction in tumour growth (Leon et al., 1996; Vredenburgh et al., 2007). Proof that GSCs are indeed residing in a vascular niche was provided by elegant experiments of Calabrese and colleagues (Calabrese et al., 2007): they first showed using immunofluorescence and multiphoton microscopy that CD133+ Nestin+ GSCs were in close contact to the tumour vasculature in sections of human glioblastoma. When isolated, GSCs, but not other non-stem cells isolated from the tumour, migrated towards the vasculature and interacted intimately with endothelial cells *in vitro*. Crucially however co-implantation of brain tumour stem cells and endothelial cell into the brains of immunocompromised mice caused a strongly accelerated growth of these mixed populations compared to GSCs injected alone or combined with other cell types like astrocytes and fibroblasts. These experiments conclusively prove the important functional relationship between brain tumour stem cells and endothelial cells which mimics and exploits the signalling of the normal vascular stem cell niche (**Figure V**).
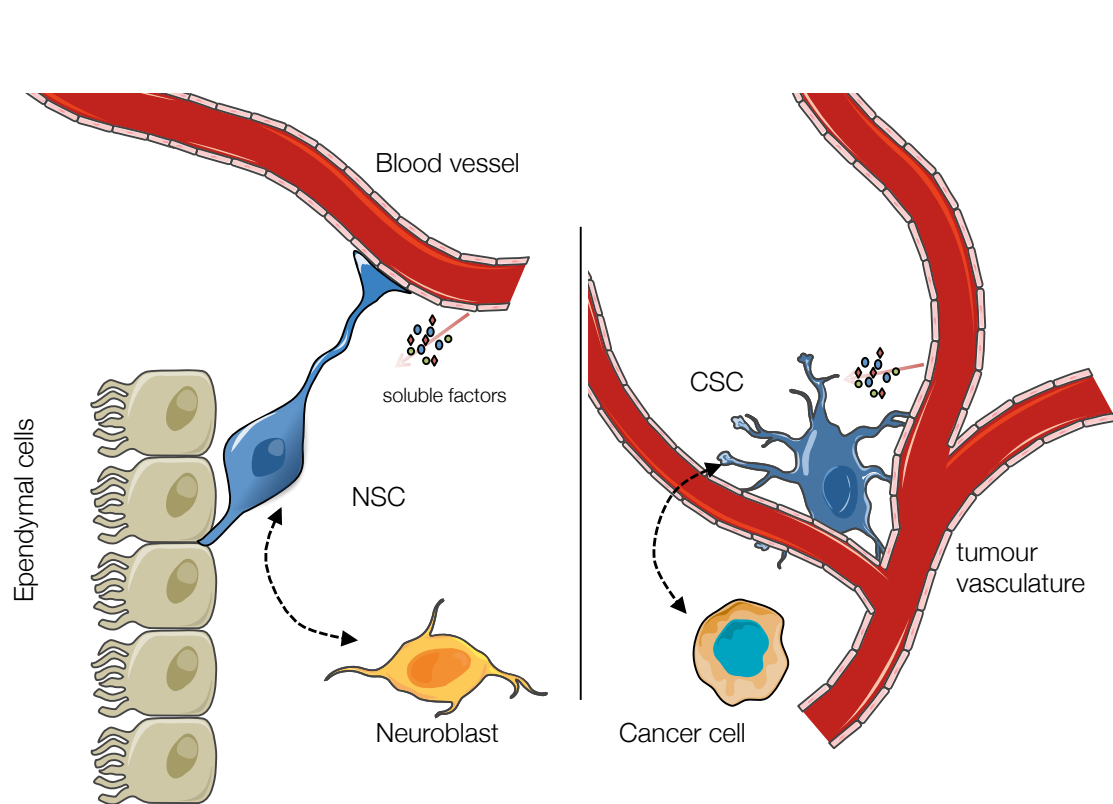
**Figure V:** **Stylised view of the normal and tumourigenic stem cell niche**. (adapted from Gilbertson and Rich, 2007)

Similar to the normal stem cell niche signalling between endothelial cells and CSCs through soluble factors has been shown to be important for tumour cell survival and proliferation (Galan-Moya et al., 2011). In the same vein, Charles et.al. provided evidence that soluble factors such as nitric oxide promote GSC maintenance through the activation of notch signalling (Charles et al., 2010). Intriguingly, GSCs are not only found in close proximity to vessels but actively intercalate their processes between endothelial cells to achieve direct contact (Farin et al., 2006). This close association bears a remarkable similarity to neural stem cells in the subventricular zone, where we have discovered a crucial role for direct cell contact between endothelial cells and NSCS to maintain the stem cell pool by supplying ephrin and Notch ligands (Ottone et al., 2014). Recently, it has been shown that endothelial cells in the glioblastoma vascular niche also express Notch ligands and through direct contact promote self-renewal and survival of GSCs (Zhu et al., 2011). Additionally, another study reported, that GSCs were located closely to SHH-positive endothelial cells in human tumour samples

and that activation of this pathway by endothelial cells *in vitro* and *in vivo* led to increased tumourigenicity and expression of stemness genes like Sox2 and CD133 (Yan et al., 2014). In addition to factors provided by endothelial cells themselves, the perivascular space seems to be enriched for extracellular matrix proteins, that are capable of promoting the survival and proliferation of GSCs. For example it has been shown, that Laminin $\alpha2$ is abundantly found in the perivascular region and possibly through activation of integrins regulates GSCs growth (Lathia et al., 2010, 2012).

Combined, these findings further highlight the similarities between normal and tumourigenic stem cell niches in the brain and provide strong evidence for the important role of endothelial derived signalling. It furthermore suggests that, paralleling our findings in the subventricular zone, ephrin dependent mechanisms could also play a vital role in regulating glioblastoma stem cell behaviour.

## 1.3  Glioblastoma invasion

Glioblastoma are practically incurable which is in no small part caused by diffuse invasion of single tumour cells into normal brain tissue. This makes complete surgical resection almost impossible and allows tumour cells to escape chemo- and radiation therapy (Cuddapah et al., 2014). Remarkably, glioblastoma rarely, if ever, metastasise outside of the brain and do not rely on intravascular or lymphatic spread unlike any other high-grade solid cancer (Beauchesne, 2011). This lack of extra cranial metastasisation might be caused by the inability of invading glioblastoma cells to penetrate the basement membrane and enter the blood stream, however it is also possible that extraneural tissues do not provide the right set of growth factors and attachment molecules necessary to provide glioma growth or patient survival is simply too short for extracranial metastases to be established (Bernstein and Woodard, 1995; Cuddapah et al., 2014; Lun et al., 2011). Instead glioma cells actively migrate through the extracellular space of the brain. Remarkably, this invasion almost invariably follows preexisting structures like white matter tracts and blood vessels resembling the migration pattern of brain cells during development (**Figure VI**).

This unique characteristic of glioblastoma was first observed by Scherer who described so called "secondary structures" which are formed by the interaction between glioblastoma cells and the neural microenvironment (Scherer, 1940). These early observations however were based on fixed slices of human tumour samples and did not allow for a dynamic analysis of these processes. One of the key questions left unanswered was, whether cells reach these secondary structures randomly, or whether an active homing response is involved. It was also impossible to assess whether these structures provide distinct advantages for the invasion of these cells or whether they simply proved to be the paths of least resistance.

These pathways through which glioma cells spread can roughly be divided into the perivascular space and the brain parenchyma. There are distinct differences between these two compartments which require a distinct ways of migration. The brain parenchyma contains the cell
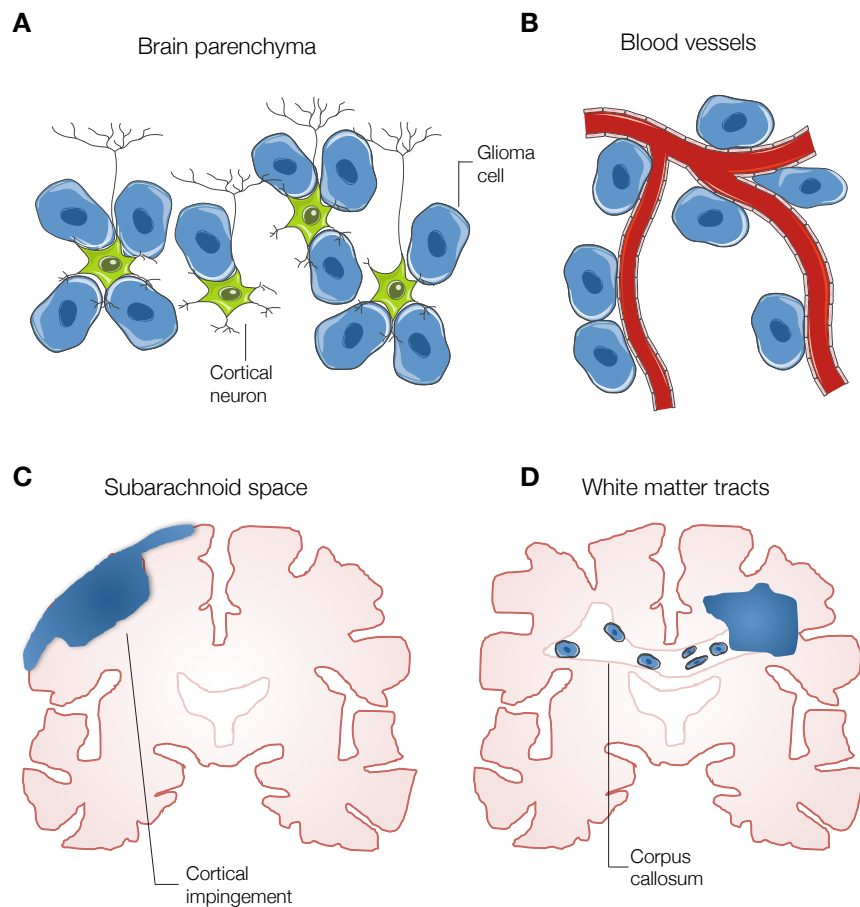
**Figure VI: Routes of glioblastoma invasion**. Glioblastoma cells invade along stereotypical routes termed "Scherer's structures": the brain parenchyma (A), pre-existing blood vessels (B), white matter tracts (either perifascicularly, intrafascicularly or interfibrillary) (C) and the subarachnoid space below the meningeal covering of the brain (D). (adapted from Cuddapah et al., 2014)

bodies and processes of neurons and glial cells and is therefore narrow, and offers a much greater physical resistance than the fluid-filled perivascular space which surrounds all blood vessels including arteries, arterioles and veins (Cuddapah et al., 2014).

### 1.3.1 Glioma cells utilise the vasculature as substrate for invasion

The predominant route of glioblastoma invasion follows the perivascular space surrounding blood vessels in the brain. Importantly, it has been shown, that the vast majority of human glioma cells in xenograft studies actively home towards vascular structures and migrate along

them, hinting at a distinct advantage for glioma cells to be in close proximity to the vasculature (Montana and Sontheimer, 2011; Farin et al., 2006). Interestingly, this attraction is maintained in slice culture experiments, where no blood circulates through the vessels. This strongly suggested that endothelial cells produce factors attracting glioma cells and therefore drive perivascular migration (Lugassy et al., 2002; von Bülow et al., 2001). Indeed, it was shown that endothelial-derived bradykin acts as a chemoattractant cue which directs invading glioma cells towards blood vessels (Montana and Sontheimer, 2011). In addition, the perivascular space is enriched in extracellular matrix proteins like fibronectin and vitronectin (Giese et al., 1994; Montana and Sontheimer, 2011) which can play a critical role in mediating glioblastoma cell invasion: cell migration is a highly coordinated biological process which requires a combination of many factors. To migrate a cell has to undergo vast changes in its cytoskeletal architecture to modify cell shape and stiffness enabling it to interact with the surrounding ECM: invading cells becomes polarised with the formation of a leading edge containing filopodia and lamellopodia. The extensions contain filamentous actin and signalling proteins which allow the cell to anchor to the ECM and pull the cell body forward through cytoskeletal contraction (Demuth and Berens, 2004). Although ECM molecules are required as fixed anchoring points they also present a physical obstacle to cell migration. This is why glioma cells frequently over express a number of secreted proteases like matrix metalloproteinases (MMPs) which can cleave the proteoglycans and other molecules making up the ECM and provide a space in which the cell can migrate (Mentlein et al., 2012).

*In vivo* 2-Photon microscopy revealed that the environment and the composition of the ECM surrounding blood vessels might indeed be advantageous for glioma invasion as perivascular invading glioma cells moved with higher velocity and more efficiently than cells which were not associated with the vasculature (Winkler et al., 2009).

Fascinatingly, glioma cells do no only migrate in close proximity to blood vessels but actively dislodge astrocytic endfeet and other structures to gain direct contact with endothelial cells strongly suggesting the involvement of cell-contact dependent mediators (Watkins et al.,

2014). Endothelial cells however do not only provide a favourable environment for cell invasion but seem to be involved in controlling the proliferation of glioma cells as well: Farin and colleagues reported that in an *ex vivo* slice culture assay, cell division of singly invading glioma cells occurred preferably at vascular branching points, with multiple glioma cells stopping and entering cell division repeatedly at the same branch points. These findings strongly suggest that further signalling molecules expressed on endothelial cells provide an environmental signal favourable for cell division and that these branching points could therefore act as a niche for secondary tumour formation (Farin et al., 2006).

## 1.3.2 Invading glioblastoma cells are likely GSCs

Invasion of any cancer cell type is a multifactorial process involving complex interactions of the invading cell with the ECM and adjacent cells. Interestingly, the morphology of migrating glioma cells closely resembles the morphology of migrating glial progenitor cells during development in that they have a predominantly unipolar morphology with one long leading process (Farin et al., 2006) and invasion of glioma cells also follows similar pathways neural progenitor cells migrate on during development (Suzuki and Goldman, 2003; Dirks, 2001). In the adult brain, normal neural stem cells remain highly motile however this motility is regulated in a very strict manner (Puche and Bovetti, 2011). These similarities suggest, that an invasive phenotype of glioblastoma cells stems from the loss of normal inhibitory controls rather than the acquisition of a *de novo* feature (Demuth and Berens, 2004; Dirks, 2001). Moreover, both normal neural progenitors and invading tumour cells are attracted by cues from the vasculature and actively home towards it (Kokovay et al., 2010; Montana and Sontheimer, 2011) suggesting a possible stem-like nature of invading glioma cells. Additional support for this theory is provided by the cancer stem cell hypothesis (see **Chapter 1.2.3**). By definition, cancer stem cells are a subpopulation of all tumour cells, which alone express the right gene set to enable reconstitution of the tumour following therapy and are also able to recapitulate the whole tumour if injected into a different host. Invasion and furthermore

metastasisation require a very similar set of characteristics as it involves formation of a secondary tumour at a distant site (Sampieri and Fodde, 2012). Indeed, a number of studies show, that GSCs derived from human glioblastomas or xenografts possess an elevated invasive potential, both *in vitro* and *in vivo* compared to non-stem cells from the same tumours (Inoue et al., 2010; Cheng et al., 2011). Remarkably, following chemotherapeutic treatment, glioblastoma in patients often display an increased invasive activity and an elevated metastatic potential (de Groot et al., 2010; Pacholska et al., 2012). This not only suggests, that chemotherapy resistant GSCs are driving invasion of glioblastoma but even hints at a potential negative control of glioma metastasisation by non-stem tumour cells.

Interestingly, it has been shown in a variety of solid tumours, that cancer stem cells are indeed responsible for metastasisation: Bae et al. show, that only a subpopulation of prostate tumour cells is able to invade the surrounding tissue and promote metastasisation. This subpopulation expresses the stem cell markers Sox2 and Oct3/4 and depletion of these markers markedly suppressed the invasion of prostate cancer stem cells (Bae et al., 2011). Similar results have been reported for breast cancer where only CD24 and CD29 positive stem cells were capable of metastatatic colonisation of the lung (Malanchi et al., 2012). Further weight to the idea that cancer stem cells are indeed identical to invasive cells in tumours is lend by the main principal of the cancer stem cell hypothesis: According to this hypothesis only CSCs possess the potential to self-renew and create a secondary tumour at a distant side in the body (Baccelli and Trumpp, 2012). This would suggest, that even if non-stem cells possessed the ability to invade healthy tissue, only stem cells were able to thrive, proliferate and cause the formation of a metastasis. First experimental evidence for this hypothesis was provided using a mouse model of spontaneous breast tumour which metastasises to the lung: Malanchi and colleagues showed in a series of elegant experiments, that only a small population of cancer stem cells were uniquely able to form a metastasis in different tissues by actively modulating the microenvironment to render it suitable for further tumour growth. Indeed, ablation of this subpopulation or of the proteins controlling this phenotype, led to a complete lack of metastasisation in this model (Malanchi et al., 2012).

Given the evidence in glioblastoma and other solid tumours it is therefore highly likely, that invasive glioblastoma cells and glioblastoma stem cells are indeed the same cells. It is paramount to gain a greater understanding of the mechanisms which enable perivascular invasion in tumourigenic stem cells and to assess the contribution of GSCs in greater detail. This could lead to more targeted therapies which could prevent metastasisation of glioblastoma more effectively and pave the way to prolonged patient survival.

# 1.4 Ephs and Ephrins

Eph receptor tyrosine kinases and their membrane-bound ephrin ligands are critical mediators of contact dependent cell-cell communication, which control a variety of biological processes in development, adult tissue homeostasis and repair and, when deregulated, can contribute to many diseases, including cancer (Pasquale, 2008). The original receptor was cloned in 1987 by Hirai et. al and named after the cell type it was first discovered in: erythropoietin-producing hepatocellular (Eph) receptor (Hirai et al., 1987). A series of related proteins was discovered in the following years (Henkemeyer et al., 1994; Lhoták et al., 1991) leading to the need for a unified nomenclature which was introduced in 1997 (Eph Nomenclature Committee, 1997).

There are two subclasses of Ephs and ephrins in mammals named A and B based on sequence homology and partially on binding preference. The mammalian A subclass consists of nine members, EphA1-A8 and A10 whereas the B subclass has five members, EphB1-B4 and B6. The ligands are divided into 5 A subclass members, ephrin A1-A5 and three B type ephrins, ephrin B1-3.

## 1.4.1 Molecular structure of Eph and ephrins

The Eph receptors of both subclasses share strong structural similarities: The ephrin binding domains are located at the most distal part of the extracellular region of the receptor, further separated from the membrane by a cysteine-rich linker and two fibronectine type III repeats (Noren and Pasquale, 2004). In the absence of ephrin binding the tyrosine kinase domain of the Eph receptor interacts with the juxtamembrane domain so that it remains in an inactive conformation (Wybenga-Groot et al., 2001). In addition to the kinase domain most Eph receptors possess a PDZ-binding motif at the intracellular carboxy terminus and a Sterile Alpha Motif (SAM) domain (Wybenga-Groot et al., 2001; Nowakowski et al., 2002). Both, the A and B subclass of ephrins share a common extracellular domain with a conserved re-
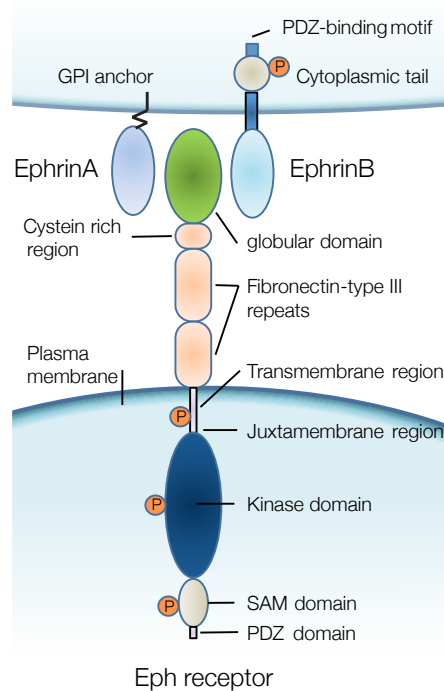
**Figure VII: Structure of Eph receptors and ephrin ligands**.   (adapted from Kullander and Klein, 2002)

ceptor binding domain and a spacer. They differ however in the way they are attached to the cell membrane (**Figure VII**): the A subclass is only attached to the cell membrane via a glycosylphosphatidylinositol (GPI) anchor whereas the B subclass of ephrins contains a transmembrane domain and a cytoplasmic tail with a PDZ-binding domain (Kullander and Klein, 2002). Within a subclass each Eph receptor can bind any ephrin. Generally speaking binding between the two subclasses does not occur with a few notable exceptions: EphA4 is able to bind both classes of ephrins (Kullander and Klein, 2002) and ephrinA5 was shown to bind and activate EphB2 (Himanen et al., 2004).

## 1.4.2   Eph/ephrin signalling

Both, Eph receptors and ephrin ligands are tethered to the cell membrane, so direct cell contact between neighbouring cells is needed for signal transduction. Upon binding of ephrin, ligands and receptors form clusters at the cell-cell interface. This multimerization is thought to cause autophosphorylation of Eph receptors on multiple cytoplasmic tyrosines which disrupts the inhibitor interaction between the kinase domain and the juxtamembrane domain allowing downstream signalling molecules containing SH2 motifs to bind and enhancing the kinase activity (Binns et al., 2000). A distinctive property of Eph-ephrin signalling is that upon binding to EphB receptors, the cytoplasmic tails of B-type ephrin also become phosphorylated on multiple tyrosine residues through the activity of associated SRC kinases (Palmer et al., 2002). The mechanism of signalling in A-type ephrins is less understood but possibly mediated through associated transmembrane proteins (Pasquale, 2008). Thus, Eph/ephrin signalling ultimately leads to cellular responses in both cell types: the conventional Eph receptor associated signalling is termed forward signalling whereas signalling in the ephrin expressing cell is dubbed reverse signalling (Klein, 2009). Interestingly both receptors and ligands are able to signal independently from each other by cross talking with other signalling pathways and modulating their function.

**Eph forward signalling**

Eph receptors remain in an autoinhibitory state unless bound to an ephrin ligand. Upon binding however, Eph receptor and ephrin ligands on adjacent cell surfaces are thought to cluster and form tetramers or higher order aggregates (Himanen et al., 2001). This clustering is believed to be crucial for the transactivation of eph receptors in cis through autophosphorylation of two juxtamembrane tyrosine residues (Kalo and Pasquale, 1999; Binns et al., 2000). Phosphorylation then causes the kinase domain to become converted to its active conformation which in turn causes phosphorylation of the tyrosine domains of adjacent Eph receptors and

other signalling molecules bound to the PDZ domain of Eph receptors (Kalo and Pasquale, 1999; Zisch et al., 2000; Kullander and Klein, 2002). Eph receptors are part of a complex network of regulatory pathways and Eph forward signalling is therefore known to act through a wide variety of mediators (Arvanitis and Davy, 2008). Many of the downstream effects of Eph forward signalling are regulated through small GTPases (Noren and Pasquale, 2004). Eph signalling has been shown to act through the Rho family of proteins (RhoA, Rac1 & CDC42) specifically by binding to Rho familyguanine nucleotide exchange factors (Rho-GEF). These Rho-GEFs trigger the exchange of GDP to GTP. This causes Rho-GTPases to switch from an inactive, GDP bound form, to an active, GTP bound, conformation. Rho proteins control a wide variety of effects through restructuring of the actin cytoskeleton. Both EphA and EphB differentially alter the activity of separate Rho-GTPases (Sahin et al., 2005). The Ras GTPase-activating protein, Ras-Gap acts in a similar way and binds to tyrosine residues on Eph receptors. This triggers the termination of downstream ras-Erk mitogen activated signalling (Holland et al., 1997). Eph receptors can, in addition to altering the activity of Rho & Ras GTPases also signal through integrin mediated pathways like FAK & Jnk which are involved in the adhesion of cells (Stein et al., 1998; Miao et al., 2000).

**Ephrin reverse signalling**

Similar to their Eph receptors, ephrins cluster upon binding, which triggers signal transduction in the ephrin expressing cell (Himanen et al., 2001). Ephrin-B ligands contain five highly conserved tyrosine residues which become phosphorylated upon binding to an Eph receptor (Brückner et al., 1997). In contrast to Eph receptors, ephrins do not possess an intrinsic kinase domain and they are thus dependent on other kinases to transduce signals. The most common signalling partner of ephrins are Src-family Kinases (SFK), which phosphorylate the tyrosine residues on ephrinB ligands (Palmer et al., 2002). This enables adapter proteins like Grb4 with an SH2 domain to bind to ephrinB ligands and potentially links them to a vast signalling network ranging from the modification of focal adhesion kinases (FAKs) to mito-

gen receptors like EGFR (Cowan and Henkemeyer, 2001). EphrinB's can also initiate reverse signalling through their PDZ domain. A number of PDZ binding proteins have been shown to interact with ephrins and have been implicated with regulating cell-cell contacts and the restructuring of the actin cytoskeleton (Palmer et al., 2002). Interestingly, there is increasing evidence that ephrin ligands are able to signal either independent of forward signalling or in addition to Eph binding through associated receptors which do not bind to the PDZ/SH2 domains (Daar, 2012). A number of studies suggests a competition based model for receptor independent ephrin signalling in which ephrins compete for binding sites in signalling complexes and therefore alter pathways, affecting, amongst others, cell-polarity and adhesion (Dravis and Henkemeyer, 2011; Lee et al., 2008).

## 1.5 Biological processes regulated by Eph/ephrin signalling

Consistent with the multitude of effectors, ephrin and Eph receptor activation has been linked to a great variety of biological functions (Kullander and Klein, 2002; Murai and Pasquale, 2003). This is further complicated by the fact that ephrin signals are regulated at several levels for example by integrating different degrees of activation of forward and reverse signals and also through heterooligomerization of A and B type receptors which depending on the respective ratios cause different outcomes (Janes et al., 2011). The best characterised function of ephrin signalling is to control cell positioning, adhesion and motility by modulating the actin cytoskeleton. For example, Eph receptors initiate repulsive responses that lead to the weakening of cell attachment to the extracellular matrix and retraction of cellular processes. This causes Eph receptor expressing cells to be repelled by their ephrin expressing counterparts (Murai and Pasquale, 2003).

This mechanism is not only important to establish tissue boundaries and ensure correct patterning during development but also to guide the migration of different cell types, for example during the migration of neural crest cells (Robinson et al., 1997) and in axon guidance (Marquardt et al., 2005). However, Eph/ephrins regulated a much wider variety of complex processes both during development and in the adult organism:

### 1.5.1 Eph/ephrin signalling in angiogenesis

The outgrowth of new sprouts from existing vessels or vascular remodelling of existing structures is called angiogenesis. Eph/ephrins have long been known to play a crucial role during vascular morphogenesis in the embryonic organisms. The principal proteins involved are ephrinB2 and EphB4 which are expressed in a reciprocal expression pattern in embryonic veins and determine the specification of vessels into arteries and veins (Wang et al., 1998; Brantley-Sieders and Chen, 2004). Interestingly however, the role of ephrinB2 and EphB4 is

not only limited to embryonic stages but the expression pattern persists in the adult organism and is required to ensure correct angiogenesis during cyclic vascular remodelling of the female reproductive tract and in wound repair. Importantly, it has been shown that many cancer cells actively exploit Eph/ephrins to induce tumour angiogenesis and facilitate endothelial cell migration and sprouting to ensure a constant supply of nutrients to the growing tumour mass (Pasquale, 2008; Brantley-Sieders and Chen, 2004).

## 1.5.2 Eph/ephrin signalling in the central nervous system

The role of Eph receptors and ephrin ligands in the developing nervous system has been extensively studied. Both ligands and receptors are highly expressed during development and it is well known, that they play a key role in the establishment of neuronal connections by guiding sprouting axons. It has been shown in numerous studies, that gradients of Eph receptors and ephrin ligands form boundaries which determine the direction of axonal growth (Pasquale, 2008; Poliakov et al., 2004; Luo and Flanagan, 2007). However, Eph/ephrins do not only control neural connectivity in the developing organism but it has been shown, that the Eph system is also involved in learning and memory formation by regulating the plasticity of neuronal connections. Treatment with various soluble Eph receptors or ligand affected the regulation of longterm potentiation and caused memory deficits, however the mechanisms underlying these effects remain unclear (Yamaguchi and Pasquale, 2004). More importantly however, Eph receptors and ephrin ligands play a crucial role in brain repair after injury. Several member of this family have been shown to be upregulated at sites of injury and developmental patterns of Eph/ephrin distribution are reactivated which may provide guidance cues to reestablish the appropriate connections. (Du et al., 2007). This highlights the sheer variety of physiological processes mediated by Eph/ephrin signalling in the normal and injured brain and their continued importance from development to the maintenance of an adult organism.

### 1.5.3 Eph/ephrin signalling in stem cell niches

While the short term effects of Eph-ephrin signalling have been relatively well studied long term effects of this signalling in the adult organism have just started emerging in recent years. Intriguingly Eph receptors and ephrin ligands are widely expressed in most stem cells throughout development and remain highly expressed even in adult stem cell niches. Studies have shown expression of a variety of Eph's and ephrins in adult stem or progenitor cells in the intestine, mammary glands, hair follicles, the epidermis and in both neurogenic stem cell niches in the brain (Batlle et al., 2002; Nikolova et al., 1998; Genander and Frisén, 2010). Both A and B type Eph's and ephrins are known to regulate proliferation of stem cells in hair follicle, epidermal and neural stem cells in the adult mouse however the exact mechanism is unclear (Genander et al., 2010; Conover et al., 2000). Our group has previously investigated the role of cell-cell contact dependent signalling in the vascular niche of the subventricular zone. Here we found that Eph-ephrin signalling between the stem cells and endothelial cells is required to maintain stem cell quiescence and identity. Depletion of EphrinB2 ligand from the vasculature caused a premature activation of the quiescent type B stem cells and a subsequent loss of this population over time. This highlights the importance of Eph-ephrin signalling not only in conveying short term positional cues but also in supporting long term homeostasis of stem cells (Ottone et al., 2014).

## 1.6 Eph/ephrin signalling in glioblastoma

A large body of evidence indicates that aberrant ephrin and/or Eph expression plays a key role in cancer development and progression but the mechanisms are still poorly defined (Wykosky and Debinski, 2008; Pasquale, 2010). Interestingly Eph signalling seems to play a dichotomous role in tumourigenesis in that it can either act as tumour suppressor or tumour promoters depending on tumour stage and signalling context. Eph receptors and ephrin ligands are frequently overexpressed in human gliomas and their expression often correlated with a higher proliferative and invasive potential.

### 1.6.1 EphA signalling in glioblastoma

EphA receptors and ephrinA ligands are frequently differentially expressed in GBM compared to healthy brain tissue. Interestingly, increasing evidence suggests a gradient of EphA/ephrinA expression with A-type receptors being highly expressed and poorly activated due to low ligand levels in more dedifferentiated, aggressive tumours cells, whereas elevated ephrinA expression can be found in more less invasive and proliferative tumours (Day et al., 2014). This model is supported by various studies demonstrating, that high expression of EphA2 and A3 receptors correlates with pathological grade, proliferation and worse prognosis for patient survival in GBM (Hatano et al., 2005; Wykosky and Debinski, 2008; Liu et al., 2007; Binda et al., 2012; Day et al., 2013). In contrast to that ephrinA1 ligand is lowly expressed in GBM and overexpression of ephrinA1 leads to reduced migration and proliferation of GBM cells (Liu et al., 2007). Similarly to that ephrinA5 expression is also low in GBM and it has been proposed that it acts as a negative regulator of EGFR by promoting degradation of the receptor and thus inhibiting proliferation (Li et al., 2009). Recent studies have shown a particularly important role for EphA2 and EphA3 in glioblastoma stem cells: both receptors were found to be most highly expressed on CD133 positive GSCs and actively maintain GSCs in a stem-like state by negatively regulating MAPK signalling (Day et al., 2013; Binda et al., 2012).

Several studies have also shown overexpression of other EphA receptors like EphA4, EphA5 and EphA7 in glioblastoma, however less is known about their functional significance (Fukai et al., 2008; Bruce et al., 1999; Wang et al., 2008).

## 1.6.2 EphB signalling in glioblastoma

The role of EphB/ephrinB signalling in glioblastoma is less well understood however it seems to become increasingly clear that they play a crucial role in promoting migration and invasion (Nakada et al., 2004, 2006, 2010). In strong contrast to the A type receptors and ligands both EphB and ephrinB proteins are overexpressed in glioblastoma and are frequently co-expressed in tumour cells. This suggests an important role for direct cell-cell interactions between individual glioblastoma cells which causes cell dispersion through repulsive Eph/ephrin signalling and therefore favours an invasive phenotype (**Figure VIII)**. This model would also explain high levels of EphB2 phosphorylation found in invading glioblastoma cells (Nakada et al., 2004, 2011). EphrinB2 and EphB4 are well known mediators of vascular sprouting and angiogenesis and it is not surprising that both have been found highly expressed in glioblastoma and linked to tumour angiogenesis (Day et al., 2014). The coexpression of EphB receptors and ephrinB ligands on endothelial cells and glioblastoma cells suggests a potential role for Eph/ephrin signalling at the glioblastoma cell- endothelial cell interface. The fact that glioblastoma cells invade along blood vessels and preferentially proliferate at vascular branching points highlights this interesting possibility (Farin et al., 2006).

Together these reports strongly suggest an important role for Eph/ephrin signalling in mediating GSC/vascular interactions which so far has only been addressed inadequately by previous research. An improved understanding of this interaction will pave the way for new, more effective GBM chemotherapies with the potential to block perivascular invasion, a main reason for tumour recurrence and aggressiveness.
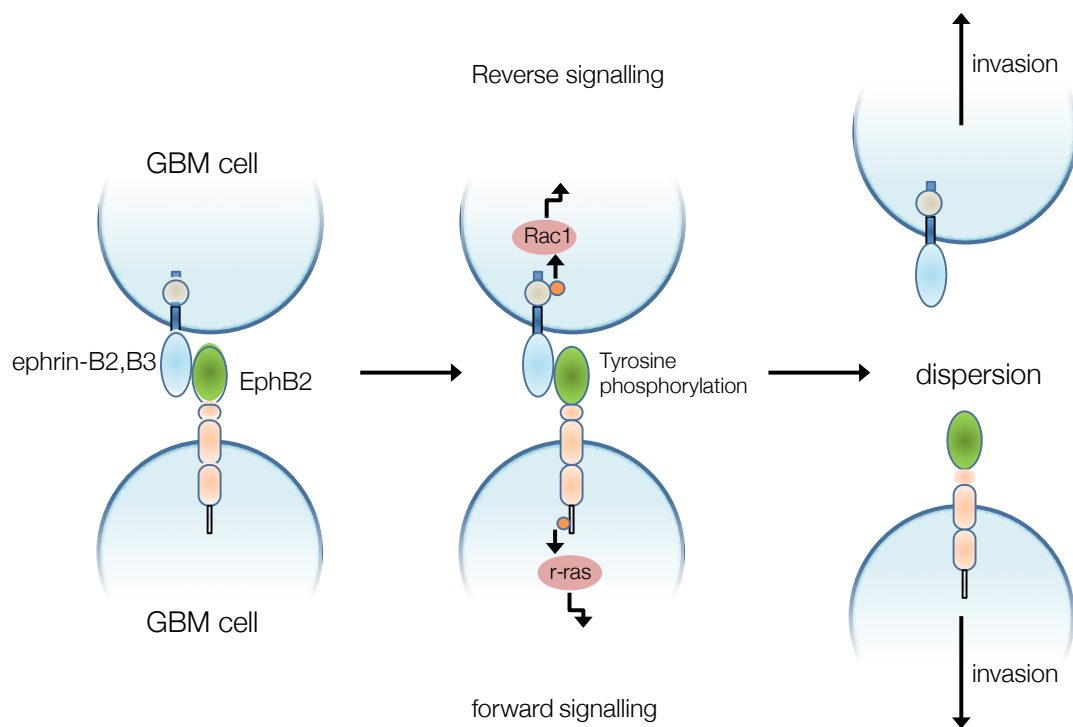
**Figure VIII: Putative model of EphB/ephrinB2 function in glioblastoma invasion.** Cell-cell contact causes activation of ligand and receptor and repulsive ephrin/eph signalling then leads to dispersion of the cells and favours an invasive phenotype (adapted from Nakada et al., 2011)

# Aims

We previously found that in the normal SVZ stem cell niche, physical contact with endothelial cells maintains type B cells as a population of quiescent undifferentiated stem cells. This response is triggered by ephrinB2 & Jagged1 ligand on the surface of endothelial cells. We showed that activation of Eph signalling specifically inhibits SVZ proliferation and profoundly affects stem cell morphology. The results therefore identify an important role for Eph signalling in regulating progenitor behaviour in the normal SVZ.

Elevated Eph and ephrin levels have also been observed in glioblastoma, the most common and aggressive tumour of the brain which is defined by diffuse invasion along preexisting structures, like the vasculature, and contains a population of glioblastoma stem cells, that reside in a vascular niche which bears remarkable similarities to the neural stem cell niche of the subventricular zone.

Consequently, the aim of this project is therefore to understand whether similar Eph/ephrin depending signalling mechanisms are important for the interaction of glioblastoma stem cells and the tumour vasculature.

This work will not only contribute to the understanding of glioblastoma invasion but also has significant potential to identify novel therapeutic targets for the treatment of these highly aggressive and deadly tumours.

# Chapter 2

# Experimental procedures

## 2.1 Antibodies

### 2.1.1 Primary Antibodies

**Table II:** Overview of primary antibodies used in this study

| Antigen | Host | Dilution WB | Dilution IF | Supplier |
|---|---|---|---|---|
| $\beta$-Tubulin | mouse | 1:5000 | - | Sigma |
| BrdU | mouse | - | 1:400 | Roche |
| Cd133 | mouse | - | 1:250 | Millipore |
| CD31 | rat | - | 1:400 | BD |
| cleaved caspase-3 | rabbit | - | 1:500 | Cell Signalling |
| Eph receptor B1+ B2 phospho Y 594 | rabbit | 1:1000 | 1:400 | Abcam |
| EphA4 | rabbit | 1:500 | - | Abcam |
| EphB2 | goat | 1:500 | - | Abcam |
| ephrinA5 | goat | 1:500 | - | R&D |
| ephrinB2 | rabbit | 1:250 | - | R&D |

**Table III Continued:** Overview of primary antibodies used in this study

| Antigen | Host | Dilution WB | Dilution IF | Supplier |
|---|---|---|---|---|
| Erk | rabbit | 1:15000 | - | Sigma |
| GAPDH | goat | 1:1000 | - | abcam |
| GFAP | goat | - | 1:1000 | Abcam |
| GFP | mouse | - | 1:400 | Millipore |
| N-Cadherin | mouse | - | 1:400 | BD Bioscience |
| Nestin | mouse | - | 1:400 | Millipore |
| Phalloidin-594 | - | - | 1:400 | Invitrogen |
| p-Erk | mouse | 1:10000 | - | Sigma |
| p-FAK | rabbit | 1:500 | - | Cell signalling |
| p-Src | rabbit | 1:1000 | - | Cell signalling |
| O4 | mouse IgM | - | 1:400 | R&D |
| Sox 2 | rabbit | - | 1:400 | Cell Signalling |
| SSEA1 | mouse | - | 1:400 | BD Pharmingen |
| Tuj1 | mouse | - | 1:500 | Covance |

## 2.1.2  Secondary Antibodies

**Table III:** Overview of secondary antibodies used in this study

| Antigen | Host | Conjugation | Dilution | Supplier |
|---|---|---|---|---|
| goat IgG | donkey | HRP | 1:5000 | R&D |
| mouse IgG | sheep | HRP | 1:5000 | R&D |
| rabbit IgG | donkey | HRP | 1:5000 | GE Healthcare |
| various IgG | donkey | Alexa Dyes | 1:400 | Invitrogen |
| mouse IgM | donkey | Alexa 555 | 1:400 | Invitrogen |

# 2.2  PCR-Primers

**Table IV:** Overview of mouse PCR Primers used in this study

| Name | | Sequence (5'->3') | Application | Source |
|---|---|---|---|---|
| Abl1 | fw | TGAGCAGAAAGATGCGCCTGAC | Q-PCR | Sigma |
| | rv | CGCTCATCTTCATTTAGGCTGCC | | |
| $\beta$-Catenin | fw | CTGCTCATCCCACTAATGTC | Q-PCR | Sigma |
| | rv | CTTTATTAACTACCACCTGGTCCT | | |
| Akt2 | fw | CCAACACCTTTGTCATACGCTGC | Q-PCR | Sigma |
| | rv | GCTTCAGACTGTTGGCGACCAT | | |
| BCL6 | fw | GACGTTGTCATCGTGGTGAG | Q-PCR | Sigma |
| | rv | GGTTGCATTTCAACTGGTCA | | |
| BLBP | fw | GGGTAAGACCCGAGTTCCTC | Q-PCR | Sigma |
| | rv | ATCACCACTTTGCCACCTTC | | |
| Bop1 | fw | TTACAGCCGCTTCATCCAGGAG | Q-PCR | Sigma |
| | rv | GGAAAGGCTGAAGGTCTCTTGG | | |

**Table IV Continued:** Overview of mouse PCR Primers used in this study

| Name | | Sequence (5'->3') | Application | Source |
|---|---|---|---|---|
| BTG2 | fw | GAGCGAGCAGAGACTCAAGGTT | Q-PCR | Sigma |
| | rv | CGATAGCCAGAACCTTTGGATGG | | |
| Casp1 | fw | GGCACATTTCCAGGACTGACTG | Q-PCR | Sigma |
| | rv | GCAAGACGTGTACGAGTGGTTG | | |
| Chi3l1 | fw | GCTTTGCCAACATCAGCAGCGA | Q-PCR | Sigma |
| | rv | AGGAGGGTCTTCAGGTTGGTGT | | |
| DLL3 | fw | CCAGCACTGGATGCCTTTTACC | Q-PCR | Sigma |
| | rv | ACCTCACATCGAAGCCCGTAGA | | |
| DNMT1 | fw | GGACAAGGAGAATGCCATGAAGC | Q-PCR | Sigma |
| | rv | TTACTCCGTCCAGTGCCACCAA | | |
| DUSP1 | fw | CAACCACAAGGCAGACATCAGC | Q-PCR | Sigma |
| | rv | GTAAGCAAGGCAGATGGTGGCT | | |
| DUSP2 | fw | AGATGGTGGAGATAAGTGCCTGG | Q-PCR | Sigma |
| | rv | AGATGGTGGCTGAGCGAGAGAT | | |
| DUSP3 | fw | GCCACAGATTTCATTGACCAGGC | Q-PCR | Sigma |
| | rv | CGTCCATCTTCTGCCGCATCAT | | |
| DUSP4 | fw | CTCCTGGTTCATGGAAGCCATC | Q-PCR | Sigma |
| | rv | GACGAACTCAAAAGCCTCCTCC | | |
| DUSP5 | fw | TCGCCTACAGACCAGCCTATGA | Q-PCR | Sigma |
| | rv | TGATGTGCAGGTTGGCGAGGAA | | |
| DUSP6 | fw | CTCGGATCACTGGAGCCAAAAC | Q-PCR | Sigma |
| | rv | TCTGCATGAGGTACGCCACTGT | | |
| DUSP7 | fw | GGTGGTGAGTTCACCTACAAGC | Q-PCR | Sigma |
| | rv | AGACACCACACTTCTTGGAGCG | | |

**Table IV Continued:** Overview of mouse PCR Primers used in this study

| Name | | Sequence (5'->3') | Application | Source |
|---|---|---|---|---|
| DUSP8 | fw | CTTATCCAGCCTGCTACACGGA | Q-PCR | Sigma |
| | rv | AGCTTGCTGAGCAGGATGGACA | | |
| DUSP9 | fw | GCCAAAGAAGAGTGGGATGCTG | Q-PCR | Sigma |
| | rv | GTTTCACACAGGTGAGGACACTC | | |
| DUSP10 | fw | CAGCCACTTCACATAGTCCTCG | Q-PCR | Sigma |
| | rv | GGGAGTTGTCACAGAGGTTTCC | | |
| DUSP16 | fw | ACTTCCTGCGAGTGCCTGTGAA | Q-PCR | Sigma |
| | rv | GTGGATAAGCACACAGCCATTGG | | |
| EfnA1 | fw | GCTGAAGGTGACTGTCAATGGC | Q-PCR | Sigma |
| | rv | CGGCACTGTAACCAATGCTGTG | | |
| EfnA2 | fw | GCTGACCGATACGCAGTCTACT | Q-PCR | Sigma |
| | rv | CAGGTAGTCGTTGATGCTCACC | | |
| EfnA3 | fw | CAAGTTCTCCGAGAAGTTCCAGC | Q-PCR | Sigma |
| | rv | CATCCTCAGACACTTCCAGTGC | | |
| EfnA5 | fw | TACGCCGTCTACTGGAACAGCA | Q-PCR | Sigma |
| | rv | GTCTTCTGGGACAGAGTCCTCA | | |
| EfnB1 | fw | GGCCAAGAACCTGGAGCCCG | Q-PCR | Sigma |
| | rv | GCACAGTGCTGCAAGCAGCC | | |
| EfnB2 | fw | GAGGGAGGGGTGTGCCAGACA | Q-PCR | Sigma |
| | rv | GACAGCGTGGTCGTGTGCTG | | |
| EfnB3 | fw | CAGGGGGTGTGCAAGTCGGG | Q-PCR | Sigma |
| | rv | CCTCACAACGCCGACCCTGG | | |
| Emx2 | fw | GCCTTTTGCAAAGGAGAGAA | Q-PCR | Sigma |
| | rv | GTGGGGTAAGGAAAGGAAG | | |

**Table IV Continued:** Overview of mouse PCR Primers used in this study

| Name | | Sequence (5'->3') | Application | Source |
|---|---|---|---|---|
| EphA1 | fw | CCCAAAACAGAGTGTCAGGACTG | Q-PCR | Sigma |
| | rv | CCTCGGTTCTTTCTTCACCAGC | | |
| EphA2 | fw | GGCTGTACTCAAGTTTACCACCG | Q-PCR | Sigma |
| | rv | CCGCTTTCAGTGTCTTGATGGC | | |
| EphA3 | fw | AGGAGAAGCGCCTTCACTTTGG | Q-PCR | Sigma |
| | rv | TTGGTGGCATCCAACTCCTTCG | | |
| EphA5 | fw | GGTACTGGAAGATGATCCTGAGG | Q-PCR | Sigma |
| | rv | CCAGACATCACTGGAAGAGGTG | | |
| EphA6 | fw | GGCATCTCAGAACAGCCTTGCT | Q-PCR | Sigma |
| | rv | TCGTGGAGGAATAGGTGAGCTG | | |
| EphA7 | fw | GATGTTGCCACACTTGAGGAAGC | Q-PCR | Sigma |
| | rv | ATGATGGTCCCTGCTACAGCCA | | |
| EphA8 | fw | TCAAACCAGGCACTCGCTACGT | Q-PCR | Sigma |
| | rv | CCGTGATGAGTGTCAGGCAGAT | | |
| EphA10 | fw | CTTGCTCTGCTTCTGGGACCTG | Q-PCR | Sigma |
| | rv | CGTGTTCATCCACGCCACTAATC | | |
| EphB1 | fw | GCAGCAGGAAACGAGCTTACAGCA | Q-PCR | Sigma |
| | rv | CCCATGATGCTCGCCTCGCTC | | |
| EphB2 | fw | GCCGTGGAAGAAACCCTGATGGAC | Q-PCR | Sigma |
| | rv | GCGGCGCCGGATGAATTTGG | | |
| EphB3 | fw | GGTCATCGCTCTTGTCTGC | Q-PCR | Sigma |
| | rv | TTCATCCCAGGAGCAATGT | | |
| EphB4 | fw | TGAATGGTGTGTGCTACCTTAGCC | Q-PCR | Sigma |
| | rv | CAGGAGAAAGAAACCCAATGC | | |

**Table IV Continued:** Overview of mouse PCR Primers used in this study

| Name | | Sequence (5'->3') | Application | Source |
|------|------|-------------------|-------------|--------|
| EphB6 | fw | CGAGAGGGCCAGTTCAGTAG | Q-PCR | Sigma |
| | rv | GCGAAGCAAGGAACTTGAAC | | |
| Erbb3 | fw | AGGCTCATTGCTTCTCCTGCCA | Q-PCR | Sigma |
| | rv | GAAAATGGGCGCATCGAGCACA | | |
| Fbxo3 | fw | GTGAGGAAGACCTGGATGCTGT | Q-PCR | Sigma |
| | rv | AGCGGTAGTGATTGGACAGTGC | | |
| FGFR3 | fw | ACAGGTGGTCATGGCAGAAGCT | Q-PCR | Sigma |
| | rv | CTCCATCTCAGATACCAGGTCC | | |
| Gabrb2 | fw | CTAAGGCGGTATCCACTGGATG | Q-PCR | Sigma |
| | rv | CTACGATGGAGAACTGAGGAAGC | | |
| GAPDH | fw | TGCACCACCAACTGCTTAG | Q-PCR | Sigma |
| | rv | GGATGCAGGGATGATGTTCA | | |
| MBP | fw | ATTCACCGAGGAGAGGCTGGAA | Q-PCR | Sigma |
| | rv | TGTGTGCTTGGAGTCTGTCACC | | |
| MEK1 | fw | AAGGTCTCCCACAAGCCATCTG | Q-PCR | Sigma |
| | rv | AGTTGCACTCGTGCAGTACCTG | | |
| NXK2-2 | fw | AGAGCCCTTTCTACGACAGCAG | Q-PCR | Sigma |
| | rv | GGATTTGGAGCTCGAGTCTTGG | | |
| Pax6 | fw | GCTTCATCCGAGTCTTCTCCGTTAG | Q-PCR | Sigma |
| | rv | CCATCTTTGCTTGGGAAATCCG | | |
| PDGFA | fw | CTGGCTCGAAGTCAGATCCACA | Q-PCR | Sigma |
| | rv | GACTTGTCTCCAAGGCATCCTC | | |
| RASA1 | fw | GCAAAACCCAGTATGGTCAGAGG | Q-PCR | Sigma |
| | rv | CCTGCTCAACTGGCAACGCATA | | |

**Table IV Continued:** Overview of mouse PCR Primers used in this study

| Name | | Sequence (5'->3') | Application | Source |
|---|---|---|---|---|
| SESN1 | fw | GCAGTTACAGGAATGCCGAGAG | Q-PCR | Sigma |
| | rv | CCTCAAAGTGCCGAGACACATC | | |
| Sncg | fw | CGTGGTACAAAGTGTCACCTCAG | Q-PCR | Sigma |
| | rv | GACCACGATGTTTTCAGCCTCC | | |
| Sox2 | fw | TCCAAAAACTAATCACAACAATCG | Q-PCR | Sigma |
| | rv | GAAGTGCAATTGGGATGAAAA | | |
| TLR2 | fw | ACAGCAAGGTCTTCCTGGTTCC | Q-PCR | Sigma |
| | rv | ACAGCAAGGTCTTCCTGGTTCC | | |
| TOP1 | fw | GAACAAGCAGCCTGAGGACGAT | Q-PCR | Sigma |
| | rv | CTGCTGTAGTGTGATGGAGGCA | | |
| TP53INP1 | fw | TCTCAGTGAGGCGAGTTGTGGA | Q-PCR | Sigma |
| | rv | ATCCACTGGGAAGGGCGAAAAC | | |
| TRADD | fw | GTTGGCTGACTGATGAAGAGCG | Q-PCR | Sigma |
| | rv | CACACGTCAGTTTGCAGAGCTC | | |
| RELB | fw | GTTCTTGGACCACTTCCTGCCT | Q-PCR | Sigma |
| | rv | TAGGCAAAGCCATCGTCCAGGA | | |

**Table V:** Overview PCR Primers for SP1 ChIP

| Name | | Sequence (5'->3') | Position on Promoter sequence | Source |
|---|---|---|---|---|
| SP1_1 | fw | CAGAGATAAAGGGCGCCTCC | 286-355 | Sigma |
| | rv | GGTTCCAGTGCTCTCCTGAC | | |
| SP1_2 | fw | TGTCCTGGAGCGCAGAGATA | 374-450 | Sigma |
| | rv | CAGTGCTCTCCTGACTGCTT | | |
| SP1_3 | fw | CAGGGTTGGTCGCCTCTTAG | 676-775 | Sigma |
| | rv | CCACGTCTCGCCCTATCCTA | | |
| SP1_4 | fw | TACTTGGCGGATCCCTCTGA | 840-958 | Sigma |
| | rv | CTAAGGCTCTCAGCCTCGTG | | |
| SP1_5 | fw | TACCAACGTCTGGGAGGACT | 1075-1159 | Sigma |
| | rv | CCGGGTCACACCTAACTTCC | | |
| SP1_6 | fw | CCCACTTTTGCCTCTCCGTA | 1273-1414 | Sigma |
| | rv | GGACTGTGCCTTCCACCTAC | | |

**Table VI:** Overview of human PCR Primers used in this study

| Name | | Sequence (5'->3') | Application | Source |
|---|---|---|---|---|
| GAPDH | fw | GTCTCCTCTGACTTCAACAGCG | Q-PCR | Sigma |
| | rv | ACCACCCTGTTGCTGTAGCCAA | | |
| EfnB1 | fw | CCTGGAGTTCAAGAAGCACCATG | Q-PCR | Sigma |
| | rv | TCAGGCGTCACAGCATTGGGAT | | |
| EfnB2 | fw | GCAAGTTCTGCTGGATCAACCAG | Q-PCR | Sigma |
| | rv | GCTGTTGCCGTCTGTGCTAGAA | | |
| EphB2 | fw | CGCCATCTATGTCTTCCAGGTG | Q-PCR | Sigma |
| | rv | GATGAGTGGCAACTTCTCCTGG | | |
| EphB3 | fw | AAGCAGCGACACGGCTCTGATT | Q-PCR | Sigma |
| | rv | GACACGTCGATCTCCTTGGCAA | | |

## 2.3    RNAi sequences

**Table VII:** Overview of siRNA sequences

| Gene | Name | Target sequence |
|------|------|-----------------|
| Dusp1 | Dusp1_4 | CTGTACTATCTTGTAAATAGA |
|       | Dusp1_5 | CCCGATGACATGCGCGTATGA |
|       | Dusp1_6 | ATCACGCTTCTCGGAAGGATA |
|       | Dusp1_7 | AAGCGCGGTGAAGCCAGATTA |
| Dusp2 | Dusp2_6 | TACAAGAGCATTCCAGTAGAA |
|       | Dusp2_7 | CAGCTTCATAGACTCGGTGAA |
|       | Dusp2_8 | CCCGAGGGTTCCGATCTATGA |
|       | Dusp2_9 | AACATTGAGGTTGTGTCAATA |
| Efnb2 | Efnb2_1 | CAGTATTATGCTTGAGTTATA |
|       | Efnb2_2 | AAAGTTTATATGGTTGATAAA |
|       | Efnb2_3 | CCCGGGTTAGACAATGATAAA |
|       | Efnb2_4 | TTGGCCAGTATGAATATTATA |

**Table VIII:** Overview of shRNA sequences

| Gene | Name | Target sequence |
|------|------|-----------------|
| Efnb2 | shEfnb2_1 | CCACAGATAGGAGACAAATTGCATATTAT |
|       | shEfnb2_2 | GTGTGCCAGACAAGAGCCATGAAGATCCT |
|       | shEfnb2_3 | GGTTGATAAAGACCAAGCAGACAGATGCA |
|       | shEfnb2_4 | GTTCTCAGACCTCCAGTGAGTACCTGACAA |

## 2.4 Media and solutions

### 2.4.1 Cell culture media

All media was purchased from Gibco (Life Technologies)

**Table IX:** Overview cell culture media recipes

| Name | Components |
| --- | --- |
| Dissection Media | HBSS |
| | 0.01 µg/ml FGF |
| | 0.02 µg/ml EGF |
| | 1 µg/ml Laminin |
| Trypsinisation solution | HBSS |
| | 0.5 % Trypsin |
| | 40 µg/ml DNAse |
| SVZ control media | DMEM-F12 |
| | 100 µg/ml Kanamycin |
| | 2 µg/ml Gentamycin |
| SVZ growth media | SVZ control media |
| | 1 % N2 (Invitrogen) |
| | 0.01 µg/ml FGF |
| | 0.02 µg/ml EGF |
| | 0.02 µg/ml BPE |

**Table IX Continued:** Overview cell culture media recipes

| Name | Components |
| --- | --- |
| Endothelial Media | DMEM |
| | 10% FCS |
| | 100 µg/ml Kanamycin |
| | 2 µg/ml Gentamycin |
| hGSC control Media | 500 ml DMEM-F12 |
| | 100 µg/ml Kanamycin |
| | 2 µg/ml Gentamycin |
| | 7.25 sterile glucose (Sigma, 2M) |
| | 5 ml of NEAA (PAA, 100x) |
| | 2.25 ml of HEPES (1M) |
| | 800 µl of BSA solution (75 mg/ml) |
| | 0.5 ml 2-mercaptoethanol (50mM, handle with care) |
| | 0.5 % N2 |
| | 1 % B27 |
| hGSC growth Media | hGSC control Media |
| | 0.01 µg/ml FGF |
| | 0.02 µg/ml EGF |
| | 1 µg/ml Laminin |

## 2.4.2 Western Blot solutions

**Table X:** Resolving Gel recipes

| Resolving Gel | 4% | 6% | 8% | 10% | 12% |
|---|---|---|---|---|---|
| 30% Acrylamide | 2ml | 3ml | 4ml | 5ml | 6ml |
| 4x Tris-HCl-SDS pH8.8 | 3.75ml | 3.75ml | 3.75m | 3.75ml | 3.75ml |
| APS | 100 µl | 100 µl | 100 µl | 100 µl | 100 µl |
| TEMED | 20 µl | 20 µl | 20 µl | 20 µl | 20 µl |
| $H_2O$ | 9.13 | 8.13 | 7.13 | 6.13 | 5.13 |
| **Total volume** | **15ml (vol for 2 1.5 mm gels)** | | | | |

**Table XI:** Stacking Gel recipes

| Stacking Gel | 4% | |
|---|---|---|
| 30% Acrylamide | 666 µl | 1.322ml |
| 4x Tris-HCl-SDS pH6.8 | 1.25ml | 2.5ml |
| APS | 50 µl | 100 µl |
| TEMED | 10µl | 15 µl |
| $H_2O$ | 3.024 ml | 6.088 ml |
| **Total volume** | **5 ml** | **10 ml** |

## 2.4.3 ChIP buffers

**Table XII:** Overview of buffers for ChIP

| Name | Components |
| --- | --- |
| Swelling buffer | 25 mM HEPES pH 7.9 |
| | 1.5 mM $MgCl_2$ |
| | 10 mM KCl |
| | 0.1% NP-40 |
| | complete mini protease inhibitor cocktail (Roche) |
| Sonication buffer | 25 mM HEPES pH 7.9 |
| | 140 mM NaCl |
| | 1mM EDTA |
| | 1 % Triton X-100 |
| | 0.1 % Na-deoxycholate |
| | 0.1 % SDS |
| Wash buffer A | 50 mM HEPES pH 7.9 |
| | 500 mM NaCl |
| | 1mM EDTA |
| | 1 % Triton X-100 |
| | 0.1 % Na-deoxycholate |
| | 0.1 % SDS |
| Wash buffer B | 20 mM Tris pH 8.0 |
| | 1mM EDTA |
| | 250mM LiCl |
| | 0.5 % NP-40 |
| | 0.5 % Na-deoxycholate |

**Table XII:** Overview of buffers for ChIP

| Name | Components |
| --- | --- |
| TE buffer | 10 mM Tris pH 8.0 |
| | 1 mM EDTA |
| Elution buffer | 50 mM Tris pH 7.5 |
| | 1 mM EDTA |

## 2.5 Cell culture techniques

### 2.5.1 Isolation and culture of neural progenitor cells

Primary neural progenitor cells from the murine subventricular zone were isolated from adult *Cdh5*(Pac)-CreERT2 or NF1$^{flox/flox}$ (Zhu et al., 2001) as previously described (Ottone et al., 2014). The mice were decapitated and skin and skull removed. The brain was then dissected from the brain stem and transferred into cold dissection media. The cerebellum and olfactory bulb were taken off and the remaining brain was cut into coronal sections of 200 μm thickness with a tissue chopper. The coronal sections were separated using micro forceps. The subventricular zone, lining the lateral ventricles, was micro-dissected and collected in a 1.5ml eppendorf tube containing dissection media. The explants were then incubated with trypsinisation solution for 5 minutes at 37 °C and pipetted up and down until no tissue pieces were visible. Trypsination was stopped by adding 5ml of endothelial media.Cells were then washed twice by centrifugation for 5 minutes at 1500 rpm and resuspension in prewarmed DMEM-F12 containing 3 % FCS and 0.02 μg/ml EGF. The isolated cells were plated on a poly-L-lysin coated 12 well cultured dish. After 48 hours the remaining other cell types were separated from the strongly adherent progenitor cells by rinsing the dish 10 times with PBS. Stem cells were then cultured in SVZ growth medium.

## 2.5.2 Culture of mammalian cells

All cell culture work was carried out in a class II microbiological safety cabinet (Nuaire) and cells were kept in dedicated cell culture incubators in maximum humidity and defined temperature and $CO_2$. Progenitor cells and the tumour progression series derived from them were cultured in SVZ growth medium at 37 °C in 5 % $CO_2$. Media was replaced every two days to ensure the freshness of all growth factors. The brain microvasculature endothelial cell line bEnd3 was cultured on tissue culture dishes in endothelial media at 37 °C in 5 % $CO_2$. Primary endothelial cells were obtained from Cell Biologics and cultured on cells coated with attachment factor in primary endothelial media. The retroviral packaging cell line, Phoenix and the lentiviral packaging cell line 293T were routinely cultured on tissue culture dishes in endothelial media. G7, G26, G144 and G166 were described previously (Pollard et al., 2009; Stricker et al., 2013). G7 was classified as proneural/classical, G26 carries NF1 deletions and p53 mutations, G144 and G166 are unclassified GSC cultures, with G144 displaying highly invasive behaviour upon intracranial transplantation and G166 forming more defined, less diffuse lesions. All human glioma stem cells were maintained in serum free HGSC growth media and cultured on laminin coated plates.

## 2.5.3 Viral infections

To enable the expression of specific gene constructs cells were infected using retro- or lentiviral vectors using Lipofectamine 2000 infection reagent (Invitrogen) according to the manufactures protocol. 293T cells were seeded at a density of $3*10^6$ cells on a 10 cm culture dish to achieve a density of 80 % on the following day. The day after 10 μg of plasmid containing the gene construct of choice was mixed with 7.5 μg of $\Delta 8.9$ gag/pol plasmid and 5 μg VSVG plasmid in 1.5 ml of Optimem media. 30 μL of Lipofectamine reagent was added to a separated tube containing 1.5 ml Optimem. Both tubes were incubated individually at room temperature for 5 minutes, mixed together and incubated for a further 20 minutes.

Endothelial media was removed from the 293T cells and the reagent mix added to the cells. 7 ml of Optimem containing 10 % FCS but no antibiotics was added and the cells cultured in a dedicated lentiviral cell culture incubator over night. The next morning the media was removed and replaced with 6 ml of endothelial media. Viral supernatant was collected the day after, filtered through a 0.2 μm mesh and 0.2 mg/ml Polybrene added. This supernatant was either snap-frozen on dry ice for later use or directly applied to the cells of choice. Cells were incubated for 3 hours with the viral supernatant for 2-3 consecutive days to achieve a maximum level of transduction efficiency.

### 2.5.4   Cell cycle analysis using propidium iodide and BrdU

To analyse the cell cycle profile a combination of propidium iodide to stain the DNA and BrdU, which is incorporated into DNA during cell division was used. This enabled us to clearly differentiate between the three main cell cycle phases: G1 (BrdU negative, DNA content: 1n), G2/M (BrdU negative, DNA content: 2n) and S-Phase (BrdU positive). For this end $1*10^6$ cells were treated with 10 μM BrdU for 60 minutes. The cells were then trypsinised, centrifuged for 5 min at 2000 rpm and 4 °C and fixed in 3 ml of 70 % EtOH over night at 4 °C. The alcohol was spun off and the cells washed twice with PBS at 2000 rpm for 5 minutes. To denature the DNA cells were resuspended in 2 M HCl and incubated for 30 minutes at room temperature with periodic vortexing. The acid was spun of and cells washed twice with PBS-T and then incubated in 100 μl of 1/50 diluted anti-BrdU antibody in PBS + 0.1 % BSA for 30 minutes at room temperature in the dark. Cells were washed twice with PBS-T and incubated with 100 μl of 1/50 diluted secondary antibody in PBS + 0.1 % BSA for 20 minutes at room temperature in the dark. Afterwards 1 ml of 1mg/ml RNase was added and the cells incubated for 30 minutes at room temperature in the dark vortexing every 10 minutes. Finally the cells were washed once, and resuspended in 750 μ L 10 μ g/ml propidium iodide. Cells were imaged on a FACS machine after 10 minutes of incubation.

## 2.5.5 Cell differentiation

To test the stem cell characteristics of our cells we subjected cells to two different differentiation protocols to induce differentiation into astrocytes/neuroblasts and oligodendrocytes respectively. Cells were seeded on PLL and laminin coated glass coverslips at a density of $6x10^4$ cells. For differentiation into astrocytic and neurogenic lineages cells were cultured in SVZ control media with 0.01 µg/ml FGF 1 % N2 (Invitrogen) and 2 % B27 for two days and then for another two days in SVZ control media only containing N2 & B27 as previously described (Ottone et al., 2014). To induce differentiation into oligodendrocytes we cultured cells in SVZ control media containing N2, B27 and 30 ng µl T3 for four days (Glaser et al., 2007). At the end of the differentiation protocol cells were fixed and stained for the relevant marker proteins.

## 2.5.6 Migration assays and quantification

For migration assays endothelial cells and imNSC/GSCs were plated at a density of $2x10^4$ cells into adjacent compartments of cell-culture silicon inserts (Ibidi) separated by a 500 µm gap. Alternatively one well of the insert was coated over night with 4 µg/ml of recombinant ephrinB2-Fc,ephrinA5-Fc,ephrinA1-Fc fusion proteins or Fc control (RD). For this the recombinant protein was mixed with fluorescently labelled anti-Fc antibody at a molar ratio of 1:2 in PBS, a volume of 75 µl of this solution pipetted into the compartments and incubated at 37 °C overnight. To remove the insert, the liquid in both compartments was removed and the insert slowly taken off with a pair of forceps by pulling carefully on the outer wall, as to not to destroy the cell monolayer. After removal of the insert, the cells were cultured in medium supplemented with 1 % Matrigel (Invitrogen) and live cell imaging was performed in a heated and $CO_2$ controlled chamber. Migration was quantified by tracing the boundary between GFP positive NSCs and non-stained bmvECs in ImageJ. To analyse the number of cell contacts individual frames from the videos of cells making initial contact with the ephrinB2-

Fc boundary were analysed by counting the total number of protrusions contacting other cells at this time. All counting was performed blind. Kymograph analysis was performed using an ImageJ macro. Quantification of the kymographs was performed by measuring pixel intensities 200 μm before and after the ephrinB2-Fc boundary at the last imaged time-point (60 h) to assess the proportion of cells that migrate over ephrin-B2 upon contact. The obtained values were expressed as relative cell densities by dividing the density of cells which migrated onto the layer ephrinB2 by the density of cells in the gap before encountering the ligand. To analyse scattering behaviour, cells were seeded sparsely at 10000 cells/12 well and their migration tracked for 20 h. Collisions between single cells were quantified over 200 min and a minimum of 50 cells were counted per condition per biological repeat. Only head on collisions between exactly two cells which did not encounter another cell for 120 minutes around the time point of collision were considered.

### 2.5.7 Soft agar Colony formation assay

*In vitro* colony formation assays are a quantitative way to measure the ability of cells to grow without anchorage signals. Anchorage independent growth is usually seen as a sign of transformation and correlates well with *in vivo* tumourigenicity. For this, a 1 % base agarose and a 0.7 % top agarose dilution were prepared by mixing appropriate amounts of sterile agarose with water and heating it in the microwave until dissolved. The base agar solution was mixed with warm growth media and 1.5ml added to each well of a 6 well plate. The base agar was left at room temperature to solidify for 5 minutes. The top agarose solution was left in a water bath to cool down to no more than 40 °C. In the meantime cells were trypsinised and counted. 5000 cells were plated in each 6 well. To plate 1.5 ml of cell-suspension was mixed with 1.5ml 0.7 % Agarose solution. 1.5 ml of this mixture was plated on a 6 well coated with base agar. 3 ml were prepared to perform the experiment in duplicates. The plates were then incubated at 37 °C in a humidified incubator for 10 days. The media was replaced every other day to ensure stable concentration of growth factors. After 10 days all colonies were

stained with 2 % crystal violet for 10-30 minutes. The stain was washed off with $H_2O$ until a sufficient difference in colour between colonies and the agar was observable. The colonies were then counted using a dissecting microscope.

## 2.5.8 Suspension culture and cell retrieval

To enable FACS analysis of cells grown in suspension they were seeded in growth medium containing 1.8 % Methylcellulose which forms a semisolid hydrogel as previously described (Cremona and Lloyd, 2009). To prepare the methylcellulose medium 9 g methylcellulose powder was autoclaved in a 500 ml Duran bottle. Under a laminar flow cabinet 500 ml of 37 °C warm DMEM-F12 was added bit by bit to the autoclaved methylcellulose, stirring all the time with a sterile pipette to disperse the clumps. The bottle was then mixed on a heated magnetic stirrer at 60 °C for 2 hours to ensure even dispersion of the powder into a cloudy solution. The semi-dissolved methylcellulose solution was cooled to 4 °C over night to dissolve completely. To seed the cells the required volume of methylcellulose medium was warmed to 37 °C, serum and factors were added to at the concentrations used in SVZ growth medium and $1*10^6$ cells seeded in 10 ml of medium in a 50 ml centrifuge tube. To ensure the cells were evenly mixed the tube was inverted 20 times and then cultured upright in a humidified incubator at 37 °C for no more than 72 h. To retrieve the cells the methylcellulose suspension was first diluted 1:2 with warm DMEM-F12, mixed thoroughly and then a further 30 ml of cold DMEM-F12 were added and the tubes places on ice. The tubes were centrifuged at 500 g for 10 minutes at 4 °C and the medium aspirated to the 5 ml mark as the residual methylcellulose and the cells did not form a compact pellet as this point. The cells were then resuspended in 10 ml ice-cold PBS and transferred to a clean 15 ml tube. The suspension was centrifuged again at 500 g for 5 minutes at 4 °C. After this the cell pellet could be used for the desired application.

For analysis of binucleated cells, all cells were incubated with EdU (Life Technologies) for 4 hours in suspension and placed on PLL-coated coverslips 15 minutes before fixation and

staining. As the metaphase in mammalian cells typically lasts less than an hour (Alberts et al., 2008) we are able to distinguish between cycling (EdU positive) and cytokinesis arrested (EdU negative) cells. Cells were stained using the Click-iT®Plus Assay Kits for Flow Cytometry (Life Technologies) following the manufacturers protocol.

## 2.6 Protein analysis

### 2.6.1 Immunoblotting

Harvested cell pellets were lysed in 55 μL RIPA buffer and incubated on ice for 15 minutes, vortexing every 5 minutes. The lysates were then centrifuged at 12000 g in a cooled table top centrifuge at 4 °C for 1 minute before transferring the cleared supernatant to a fresh 1.5 ml tube. The protein concentration was measured against a BSA standard using the Bio-Rad protein assay dye reagent. 6 x Laemmli sample buffer was then added and the samples boiled at 95 °C for 2 minutes to denature the protein completely. Samples were loaded onto polyacrylamide gels (see **Table X**), resolved by SDS gel electrophoresis (SDS-PAGE) and transferred to PVDF membranes (Millipore). The membranes were blocked for 1 hour at room temperature in 5 % milk powder or 3 % BSA in TBS-T. Blocked membranes were incubated with primary antibody in blocking solution over night at 4 °C, washed 3x in TBS-T, and incubated for 1 hour in HRP-conjugated secondary antibody diluted in blocking solution. After 2x washes in TBS-T the membranes were washed in TBS and chemiluminescence detected using ECL Luminata Crescendo reagent (Millipore).

### 2.6.2 Immunoprecipitation

Freshly harvested, unfrozen cell pellets were used for immunoprecipitations to help preserve protein complexes. The pellets were lysed in NP40 or RIPA lysis buffer containing phos-

phatase inhibitors and the protein concentration measured using the Bio-Rad protein assay dye reagent. 500 μg protein was used for each IP. The lysates were diluted to 500 μl total volume in lysis buffer and pre-cleared using protein A or protein G sepharasoe beads rotating for 1 hours at 4 °C before incubating with 10 μ g bead bound antibody for 1 hour at 4 °C. Beads with bound protein were then washed 3 times in ice cold PBS containing phosphatase inhibitors and the samples boiled for 2 minutes at 95 °C in Laemmli buffer. The samples were then analysed using immunoblotting.

## 2.7 Immunostainings

### 2.7.1 Immunofluorescence

For analysis of protein expression cells in intact cells, cells were fixed and stained with fluorescent antibodies. The day before staining cells were plated on 13 mm diameter poly-L-lysine and laminin coated glass coverslips in 4 well plates at a density of 80000 cells/well. The next day cells were fixed in 4 % paraformaldehyde for 15 minutes at room temperature, washed twice in PBS and permeabilised with 0.5 % Triton in PBS for 10 minutes. Cells were washed 3x in PBS again and blocked in 3 % BSA in PBS for 30 minutes at room temperature. Cells were then incubated with primary antibody at the appropriate dilution at 4 °C over night. The next day cells were washed 3x with PBS and incubated with the secondary antibodies of choice for 1 hours at room temperature in the dark. Cells were washed 3x in PBS, and incubated with DAPI to counterstain the nucleus for 15 minutes. Finally, cells were washed 3x in PBS and after one short wash in dH$_2$O cells were mounted with Prolong gold antifade.

## 2.7.2 Immunofluorescence with signal amplification

Some proteins and phosphoproteins had levels to low to be detected by standard immunofluorescence. For these proteins, signal amplification with the Tyramine Signal amplification kit (Molecular probes) was performed. Cells were seeded and fixed as standard but all washes were performed with TBSTi. After fixation for 15 minutes cells were permeabilised with TBSTi containing 1 % NP40. Cells were washed in PBS (no phosphatase inhibitors as these might interfere with the $H_2O_2$ reaction). Endogenous peroxidase activity was blocked with 0.1 % $H_2O_2$ in PBS for 20 minutes at room temperature.. Cells were again washed 2x with PBS and no inhibitors and blocked with 3 % BSA in TBSTi for 30 minutes at room temperature. Cells were then incubated with primary antibodies in 3 % BSA at 4 °C over night. The next day cells were washed with TBSTi 3x before incubation with tyramine reagent. The following solutions were prepared freshly for that:

1. Prepare the tyramide working solution with 0.015 % $H_2O_2$ :

   (a) Prepare buffer X = 0.5 μL of 30 % $H_2O_2$ in 100 μL of component E (amplification buffer)

   (b) Prepare working solution: 1 μL of buffer X into 100 μL of amplification buffer

2. Dilute component A in working solution at 1:100

The cells were then incubated in the diluted component A for 10 minutes at room temperature in the dark. Afterwards cells were washed with TBS containing 0.1 % Tween for 3 times. Finally nuclei were stained with DAPI in PBS for 15 minutes, cells were washed 3x with PBS and a final quick wash in $dH_2O$ and mounted with prolong gold antifade.

### 2.7.3 BrDU incorporation

To analyse the percentage of cycling cells, BrDU incorporation was used as a measure of cell proliferation. The day before staining cells were plated on 13 mm diameter poly-L-lysine and laminin coated glass coverslips in 4 well plates at a density of 80000 cells/well. BrDU was added to the cells for 3 hours at a concentration of 10 μM. The cells were then fixed in 4 % paraformaldehyde in PBS for 15 minutes at room temperature. Fixed cells were then stained using standard immunofluorescence protocols.

## 2.8 DNA/RNA analysis

### 2.8.1 Trizol extraction for RNA

We isolated RNA from mammalian cells using Trizol reagent. As Trizol is neurotoxic it is advisable to use a fume hood for the extraction. We typically used a confluent 6 well but the volumes can be adjusted accordingly to different plate sizes. We first aspirated the media from the plate and lysed the cells by adding 1 ml of TRI reagent to a 10 cm for 5 minutes. 200 μl of Chloroform was added to separate protein and nucleotides, the sample vortexed for 15 sec and incubated for 15 minutes at room temperature before centrifugation at 4 °C for 15 minutes at max 13000 g. The colourless top phase contains the DNA. Only 150 μl of this phase was transferred to a new tube to avoid contamination of the RNA. This RNA was then precipitated by adding 500 μl of isopropanol per 1 ml of TRI reagent, the sample vortexed for 10 seconds and incubated at room temperature for 10 min. Next, the RNA was pelleted by centrifugation at 13000 g for 8 minutes at 4 °C and the pellet washed with 1ml μl of 75 % EtOH per 1 ml of TRI-reagent. After a final centrifugation at 10500 RPM for 5 minutes at 4 °C the pellet was air dried for 5 minutes and finally dissolved in 10 μl RNase free water.

## 2.8.2 Trizol extraction of DNA

It is also possible to isolate DNA using trizol. For this the steps up until phase separation are identical to the isolation of RNA. After phase separation however, the upper clear phase was removed as completely as possible. Afterwards 300 μl of 100 % EtOH per 1 ml TRi reagent was added to the remaining organic and interphase and gently vortexed. The samples were then incubated at room temperature for 5 minutes and centrifuged at 12000 rpm for 5 minutes.

The protein containing supernatant was removed and the DNA pellet washed two times in 0.1 M soduum citrate solution. 1 ml Na citrate per 1 ml Trizol was used again. The samples were gently vortexed and incubated at room temperature for 40 minutes with periodic mixing. The DNA pellet was then washed in 1 ml of 75 % Ethanol per 1 ml Tri reagent and incubated for 15 minutes at room temperature. Finally the DNA was centrifuged again for 5 minutes at 12000 rpm and air dried before resuspension in 50 μl of sterile water.

## 2.8.3 Reverse transcription PCR

To obtain cDNA from isolated RNA, the sample has to be reverse transcribed. We used the iScript cDNA Synthesis Kit (BioRad) for this. The reaction was set up by adding

4 μl 5x cDNA synthesis kit buffer

1 μl iScript enzyme mixture

x μl Nuclease-free water

x μl 1 μg RNA sample

to a total volume of 20 μl in a 0.2 ml PCR tube.

This reaction mix was then run in a thermal cycle with the following parameters:

5 min at 25 °C

30 min at 42 °C

5 min at 85 °C

Hold at 4 °C

30 µl of RNase free water was added after the reaction to obtain a total volume of 50 µl.

### 2.8.4 Quantitative RT-PCR

To quantitatively analyse cDNA and DNA we performed Q-PCR analysis using the MESA Blue PCR Master mix (Eurogentec). The reaction was set up by adding

0.5 µl Stock primer (10 µM)

10 µl Mesa Blue 2x PCR Master mix

8.5 µl $H_2O$

1 µl cDNA

to a final volume of 20 µl. We analysed the obtained Cycle over treshold (Ct)-values by normalising against a housekeeping gene and comparing the diferences with an internal control ($\Delta\Delta C_t$-method).

### 2.8.5 Chromatin Immunoprecipitation

To investigate the interaction between transcription factors and specific DNA promoter sequences we performed Chromatin immunoprecipitations (ChIP) as previously described (Stock et al., 2007). $5x10^6$- $1x10^7$ adherently growing cells were treated with 1% formaldehyde at 37 °C for 10 minutes to crosslink protein complexes with the bound DNA sequence. The reaction was then stopped by the addition of glycine to a final concentration of 0.125 M. The cells were washed in three times ice-cold PBS before 1 ml swelling buffer was added to lyse

the cells (10 min, 4°C). The cells were then scraped from the tissue culture plates and the nuclei isolated by dounce homogenisation (50 strokes, "tight" pestle). After resuspension in sonication buffer (50 mM HEPES pH 7.9, 140 mM NaCl, 1mM EDTA, 1% Triton X-100, 0.1% Na-deoxycholate and 0.1% SDS) the nuclei were sonicated to produce DNA fragments with a length of less than <1.6 kb using a diagenode biorupter. The resulting material was centrifuged twice at 4 °C for 15 minutes at 14000 rpm. In the meantime, 50 µl of protein-G-sepharose beads (Amersham Biosciences) were incubated with 10 µg protein specific or IgG control antibodies for 1 hour at 4 °C to bind antibodies to the beads. To prevent unspecific binding the beads were then blocked for 1 h at 4 °C using 1mg/ml sonicated salmon sperm DNA and 1mg/ml BSA on a rotating wheel. The beads were then washed twice in sonication buffer prior to use. The chromatin was precleared at 4 °C for 2 hours with 100 µl protein-G beads per IP in the presence of 0.05 mg/ml BSA and protease inhibitor cocktail on a rotating wheel. 50 µl of the precleared chromatin were used as an input sample and the remainder (∼700 µg) used for the immunoprecipitation. For this 10 µg of antibody bound to beads was incubated with 700µg pre-cleared chromatin over night at 4 °C on a rotating wheel. The beads were then washed for 5 min at 4 °C with 1 ml of each of the following washing buffers: 1x with sonication buffer, 1x with wash buffer A, 1x with wash buffer B, 2x with TE Buffer. The beads were collected by spinning at 200 g for 5 minutes at 4 °C.

To elude the bound protein-DNA complexes 150 µl elution was added to the beads and incubated at 65 °C for 5 min. The mix was transferred to a rotating wheel for 15 min at room temperature and the supernatant collected by centrifugation (3 min, 200 g). To maximise the elution efficiency the beads were then re-eluted and both eluates pooled to obtain a final volume of 500 µl. 450 µl TE buffer was added to the input sample to have an equal volume in all samples. To reverse the aldehyde cross-linking of the immunoprecipitated chromatin and the input we then added NaCl and RNase to final concentrations of 160 mM and 20 µg/ml respectively. After an overnight incubation at 65 °C the EDTA concentration was increased to 5 mM and 200 µg/ml proteinase K (Roche) added. To fully digest all protein the samples were incubated at 45 °C for 2 h. finally, the DNA was purified by phenol-chloroform

extraction and ethanol precipitation.

The concentration of the immunoprecipitated DNA was measured using the Quant-IT Pico Green kit (Invitrogen). This kit is designed to reliably and sensitively detect very low concentration of double-stranded DNA. We used 200 µl working dilutions of PicoGreen reagent in a 96 well plate. The standard curve (1-100 ng/ml) was set up using the phage DNA supplied with the kit. 1-2 /micro l of sample or input DNA was used per well. Note, that the input DNA has to be diluted $\sim$ 50 fold in order to be in the linear range of the standard curve. The fluorescence of the samples were measured at 480 nm excitation and 520 nm emmision wavelengths according to the manufactures instruction. All samples and inputs were diluted to 0.2 ng/µl and 2 µl of each used in a 25 µl Q-PCR reaction. To obtain the final result we used the percent input method. With this method, Ct-values obtained form the immunoprecipitated DNA are divided by the Ct calues of the input control. For this the input control ( 1% of the starting chromatin) is adjusted to 100 % by subtracting 6.644 from the Ct value of the input sample. The final result is then obtained using the following formula: $100 * 2^{(Adjusted input - Ct(IP))}$.

## 2.9 *In vivo* protocols

All animal work was carried out in accordance with the regulations of the Home Office and the ARRIVE guidelines. Efnb2i$\Delta$EC mice and recombination protocols were described previously (Ottone et al., 2014; Wang et al., 2010). Briefly, to induce recombination of the $EfnB2^{flox/flox}$ gene cassette 3 week old mice were injected with 200 µl of a 20 mg/ml Tamoxifen solution diluted in 25 % EtOH and 75 % vegetable oil for 3 consecutive days. Tamoxifen-injected Efnb2$^{flox/flox}$ CreERT2 negative litter mates were used as controls. C57Bl6 and CD-1 nude mice for tumourigenicity analysis were obtained from Charles River.

## 2.9.1 Craniotomies

Cranial windows were surgically implanted into mice to enable intravital imaging of GFP-labelled tumour cells according to previously published methods (Holtmaat et al., 2009). 6-8 week old $Efnb2^{i\Delta EC}$ or $Efnb2^{flox/flox}$ mice were anaesthetised with an intraperitoneal injection of 0.08 mg/g ketamine and 0.008 mg/g xylazine. To limit an inflammation response 200 µL of 4mg/ml dexamethasone was administered intramuscular. Before cutting of the skin a subcutaneous injection of 1mg/kg bupivacaine was given as local anaesthetic. The mouse was placed on a heating blanket and the head stabilised in a stereotactic frame. To protect the eyes from dehydration lacri-lube was applied. The scalp was washed with povidone-iodine surgical scrub and a flap of skin roughly 1 cm² in size covering both hemispheres removed with a sharp pair of scissors. 1% Xylocaine was applied to the exposed periosteum and the exposed cheek muscles. After that the periosteum was removed by gently scraping the skull with a scalpel blade to facility the glue sticking to the skull. To enlarge the potential area of the cranial window the temporalis muscle was separated. A thin layer of cyanoacrylate (vetbond) was then applied to the nearly dry skin, the temporalis muscle and the wound margins to prevent the seepage of serosanguinous fluid, sparing the area where the cranial window is to be placed. This layer of cyanoacrylate provides a better base for the dental acrylic which can be applied in a thin layer afterwards again sparing the area of interest. Using a fine dental drill a circular groove with a diameter of 3 mm was drilled 2 mm from bregma, 3.5 mm lateral. Care should be taken no to apply excessive pressure, always to drill on a low setting and to apply saline buffer regularly to prevent heating which could bruise the underlying brain structures. After thinning out the groove until it becomes almost transparent the remaining island can be carefully removed using angle-tipped forceps. Under ideal circumstances no bleeding of the dura should be observed. $2x10^3$ tumour cells were injected using a micromanipulator and a microinjection dispenser (picospritzer) at roughly 300 µm depth in the cortex. To minimise reflux of the cell suspension the needle was left in the brain for 5 minutes after the injection. Afterwards the optical window was completed by covering the hole with a circular coverglass

of 6 mm diameter, #1 thickness. The exposed surface of the brain should be wet so that no air is trapped between coverslip and brain but the surrounding skull needs to be dry. The optical window was sealed to the skull with dental cement covering all the exposed skull, the wound margins and the cover glass edges. A clean titanium bar with screw holes was embedded into the dental cement over the intact hemisphere to stabilise the mouse during imaging sessions. The mouse was then monitored until it woke up and supplied with wet food and additional nesting material. 5-7 days were allowed between the surgery and the start of the imaging protocol.

### 2.9.2 Intravital 2-Photon imaging

A purpose built microscope equipped with a tunable Coherent Ti:Sapphire laser and PrarieView acquisition software was used for all *in vivo* imaging experiments. Mice were anaesthetized with isoflurane and secured to a fixed support under the microscope. The eyes were coated with Lacri-lube (Allergan) to prevent dehydration, an underlying heat pad used to maintain body temperature (37 °C). To prevent dehydration isotonic saline solution was administered (i.p.) during long imaging sessions. Depth of anaesthesia was closely monitored. To visualise blood vessels 50 µl of a 3000MW dextran-Texas Red conjugate was injected intravenously prior to imaging. A pulsed laser beam with a wavelength of 910 nm was used to ensure that both GFP-tumour cells and Texas Red showed sufficient signal intensity.Animals were imaged a maximum of four times daily with cells imaged every 20 min up to 1 hour per session. After image acquisition individual frames were aligned and the displacement of single cells measured using ImageJ software.

### 2.9.3 Orthotopic xenografts and *in vivo* imaging

$5x10^4$ luciferase expressing Cells were injected into 6-8 week old CD-1 nude or C57-Bl6 mice into the right putamen (1mm rostral to bregma, 2mm lateral and 2.5 mm depth) as previously

described (Ozawa James, 2010). Mice were anaesthetised with an intraperitoneal injection of 0.08 mg/g ketamine and 0.008 mg/g xylazine and placed on a heating blanket. Before cutting of the skin a subcutaneous injection of 1mg/kg bupivacaine was given as local anaesthetic. To protect the eyes from dehydration lacri-lube was applied. The scalp was washed with povidone-iodine surgical scrub and an incision of the skin roughly 1 cm² in length was made along the midline. A small hole was drilled into the skull using a 25G needle. Cells were loaded into the hamilton syringe just prior to injection and needle kept in place for a further 5 minutes to ensure minimal reflux of the material along the needle tract. The wound was closed using sutures and the mouse placed into a warmed chamber until it recovered fully. At least 5 days were allowed between the surgery and the start of the imaging protocol. Tumour formation, growth and volume were indirectly calculated by sequential images taken with an IVIS Spectrum in vivo imaging system (Perkin Elmers). Following D-luciferin administration (Intrace medical) by intraperitoneal injection at 120 mg/kg, mice were anaesthetised (3 % isoflurane) and imaged under continuous exposure to 2 % isoflurane. Luminescent measures were performed once a week starting 5 days after cell implantation until day 40. Bioluminescence was detected by the IVIS camera system, integrated, digitised, and displayed. Pseudocolour scale bars were consistent for all images of dorsal views in order to show relative changes at tumour site over time. Tumours were quantified by calculating total flux (photons/s/cm2) using Living Image software (Xenogen, Caliper Life Sciences). For treatment experiments, PBS or B11 administration was started once the tumours reached a minimum signal intensity of $1 \times 10^6$ photons/s/cm2. Mice were then randomised into two groups prior to intravenous injection of 5 doses of either anti ephrinB2-scFv B11 (total dose 20 mg/kg) or PBS control over a period of 9 days. Survival curves were estimated using the Kaplan-Meier method. Significance was calculated using the log-rank Mantel-Cox test.

# Chapter 3

# Generation of a tumour progression series

## 3.1    Introduction of oncogenes into neural progenitor cells to create a tumour progression series

Glioblastoma is the most aggressive primary brain tumour and a large number of studies suggests a role for Eph/ephrin signalling in glioblastoma progression and invasion (Nakada et al., 2006; Binda et al., 2012; Liu et al., 2007).  However, due to the heterogeneity of glioblastoma mutations on one side and the complexity of the Eph/ephrin signalling system no mechanistic insights have so far been gained and it is still not understood whether the role of eph receptors and ephrins is tumour promoting or suppressing (Pasquale, 2010).  To dissect the role of Eph/ephrin signalling in glioblastoma in a well defined system instead of using established glioblastoma cell lines, we generated a murine glioblastoma stem cell model.  Recent efforts have been made by the Cancer Genome Atlas (TCGA) Research Network to identify common mutations and subtypes of Glioblastoma on a genome wide level (TCGA, 2008).  Four subtypes, defined by specific genetic mutations were defined: The classical subtype is defined by *EGFR* amplifications, rarely seen in the other three subtypes.  Proneural glioblastoma mainly occurred in younger patients and showed alterations of *PDGFRA* and point muta-

tions in *IDH1*. The neural subtype showed a distinct expression of neuron markers such as *NEFL* or *GABRA1*. Mesenchymal glioblastoma have been suggested to be a more aggressive subtype and the other three subtypes show a clear trend towards mesenchymal classification after recurrence (Phillips et al., 2006). Mutations in p53, NF1 and Rb pathway are frequently observed in this subtype (Verhaak et al., 2010; Phillips et al., 2006). Interestingly, it has already been shown previously that mutations within the p53,NF1 and Rb axis are sufficient to generate fully transformed cells which are able to induce high grade astrocytoma in the adult mouse brain (Chow et al., 2011). To generate a model of mesenchymal glioblastoma stem cells we isolated primary neural progenitor cells from the subventricular zone of adult mice and introduced genetic changes in these three pathways. We used two complementary strategies targeting the same pathways using different vectors. This approach enables us to exclude any artefacts possibly introduced by the specific chosen oncogene and helps us to pinpoint phenotypic changes to the exact genotype.

| **SVZ**<br>pBabe+pLXSN | → | **imNSC1**<br>pBabe SV40 largeT | → | **GSC1**<br>pBabe-IT + pLXSN h-ras |
|---|---|---|---|---|
| **SVZ**<br>NF1$^{fl/fl}$ | → | **imNSC2**<br>shp53 + pCMV-Cdk4 Nf1$^{fl/fl}$ | → | **GSC2**<br>shp53 pCMV-Cdk4 NF1$^{-/-}$ |
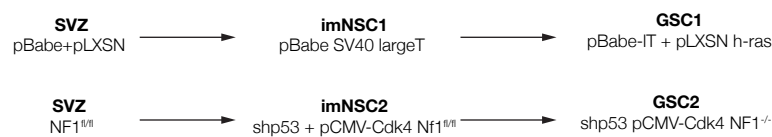
**Figure 1: Schematics of the tumour progression series**. Two independent tumour progression series were created using the pathways most commonly mutated in human glioblastoma

First we used a "classical" transformation regime introducing pBabe-SV40-largeT to immortalise adherently grown SVZ progenitor cells (imNSC1) and as a second step added pLSXN-hRas to fully transform these cells (GSC1). SV40 largeT antigene is known to inactivate both the p53 and Rb tumour suppressors (Ali and DeCaprio, 2001) whereas constitutively active Ras mimics the loss of NF1, a hallmark of mesenchymal glioblastoma. NF1 belongs to the family of ras-GAPs or guanosine triphosphatase (GTPase)-activating proteins. It catalyses the hydrolysis of GTP bound to hras to GDP, thereby converting hras from its active into the inactive form and therefore acting as a negative regulator of ras signalling (Cichowski and Jacks, 2001; Trovó-Marqui and Tajara, 2006). As this model is based solely on the exogenous expression of genes introduced with viral vectors it allowed us to rapidly test candidate

effectors by transforming NSCs isolated from mice carrying specific gene mutations, as previously reported in a similar model for postnatal astrocytes (Blouw et al., 2003). In the second approach we induced transformation by introducing defined genetic changes to rule out potential artefacts caused by overexpression of oncogenes. We isolated NSCs from NF1$^{flox/flox}$ mice and introduced a lentiviral construct carrying shRNA against p53 and afterwards infected the cells with pCMV-Cdk4. The Rb-Axis including *CDKN2A*, *CDK6* and *CDK4* is affected in the vast majority of all mesenchymal glioblastoma (Verhaak et al., 2010) and *Cdk4* amplifications have been found in 14 % of all tumours in the TCGA GBM cohort (TCGA, 2008). Both, the use of shp53 + Cdk4 and SV40-largeT oncogene which affects the same pathways are therefore highly clinically relevant. In a second step these cells were infected with either GFP-Adenovirus (imNSC2) or Cre-Adenovirus to induce recombination of the floxed alleles to create Nf1$^{-/-}$ cells (GSC2).

We immediately observed a distinct change in cells with impaired Nf1/ras signalling: Whereas imNSC1 and imNSC2 closely resembled cells infected with empty vector controls in that they grew in a well defined monolayer, GSC1/2 showed strong foci formation resembling a neurosphere like phenotype (**Figure 2a**).

Next we confirmed that the introduced oncogenes were indeed functional. To assess loss of p53 function we treated cells with Bleomycin, a radiomimetic that causes DNA double strand breaks and a subsequent p53-mediated cell cycle arrest (Nelson and Kastan, 1994). This treatment caused a complete cell cycle arrest of SVZ cells. In contrast to that, cells with impaired p53 function (imNSC1 & 2) showed no significant reduction in proliferation rate (**Figure 2b**).

To assess Rb function, cells were grown in growth factor depleted conditions which triggers an Rb-dependent cell-cycle arrest in normal cells. While control cells arrested to a large extend, imNSC1 and imNSC2 showed no significant decrease in proliferation rate (**Figure 2b**).

The MAPK/Erk cascade is a highly evolutionary conserved signal-transduction pathway that
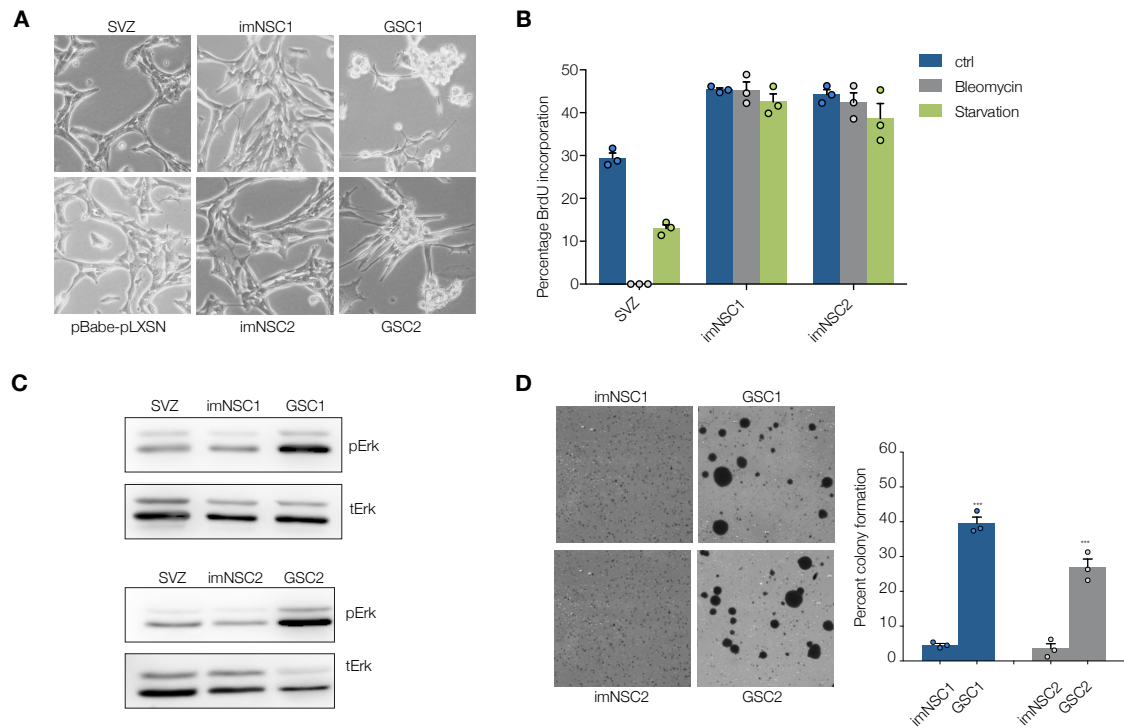
**Figure 2: Introduction of oncogenes to create a defined tumour progression series**. a) Phase contrast images showing the morphology of the generated cell lines b) Quantification of BrdU incorporation after treatment with 30 μM Bleomycin or factor depletion for 24 hours. c) Immunoblotting of cells grown in factor depleted conditions o/n. d) 5x10³ cells were seeded in soft agar and colony growth assessed via crystal violet staining after 10 days (left). Quantification of colony growth (right) error bars depict s.e.m. Students t-test.

controls the expression of important cell-cycle and differentiation specific proteins in response to stimulation by growth factors (mitogens) (Alberts et al., 2008). Overexpression of oncogenic ras or genetic deletion of the negative regulator NF1 causes increased phosphorylation of downstream targets like Erk in the absence of stimulating mitogens. Consistently we observed increased Erk phosphorylation in growth factor depleted ras infected or Nf1$^{-/-}$ cells(GSC1/2) but not in imNSC1/2 or control cells (**Figure 2c**).

One of the hallmarks of malignant cell transformation is the ability to grow anchorage independently in semi-solid medium, a property closely linked to *in vivo* tumourigenicity (Freedman, 1974). Therefore to test the malignancy of the generated cell lines we embedded 5x10³ cells in soft-agar and assessed their potential to form colonies. The majority of imNSC1 and imNSC2 cells remained as single cells and only less than 5 % generated small colonies as pre-

viously reported for normal stem cells (Gürsel et al., 2011). Whereas normal cells failed to proliferate significantly under these conditions, GSC1 and GSC2 cells embedded in soft-agar and cultured over 10 days formed large colonies indicating that GSC1/2 cells are indeed fully transformed cells (**Figure 2d**).

Thus we show that we have successfully generated cells, which express the desired constructs and are fully transformed *in vitro*.

## 3.2 Tumour model resembles mesenchymal Glioblastoma stem cells

To better characterise the resulting cells we used core genes defining the four Glioblastoma subtypes identified by TCGA (Verhaak et al., 2010) and checked their expression on mRNA level in GSC1 and GSC2 tumour cells. Consistent with the pathways we targeted to create our GSC model Q-PCR analysis indeed revealed revealed a higher relative expression of mesenchymal signature genes in comparison to genes associated with proneural, neural or classical subtypes in both cell types (**Figure 3a,b**).
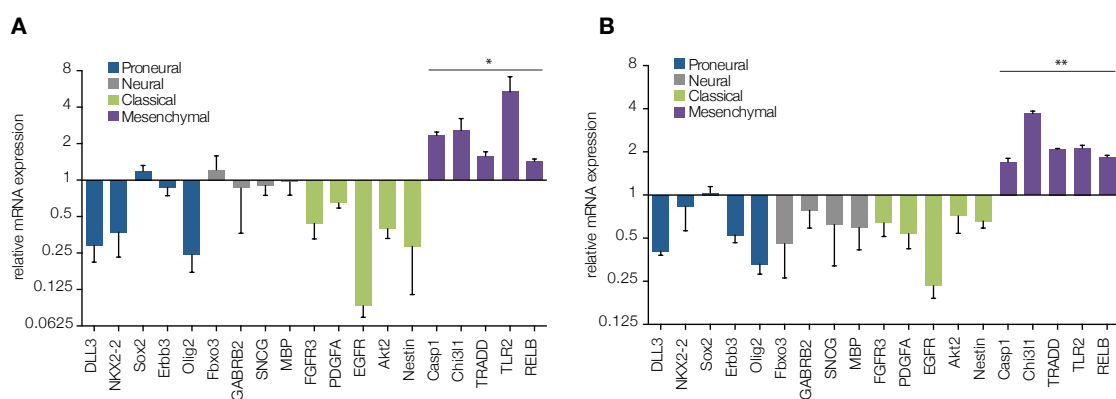


**Figure 3:** **GSC1/2 resemble mesenchymal glioblastoma cells**. a,b) RNA expression of specific marker genes associated with the GBM subtypes (classical=blue,proneural=grey,neural=red,mesenchymal=green) in GSC1 (a) and GSC2(b) respectively. Error bars denote s.e.m. Two-Way anova.

Glioblastoma in many cases originate from adult neural stem cells and throughout tumour

progression they retain a sizeable portion of cancer stem cells. Moreover, this relatively small population is highly invasive and thought responsible for tumour recurrence and chemotherapy resistance (Sadahiro et al., 2014; Oliver and Wechsler-Reya, 2004). Cancer stem cells are defined by their expression of stem-cell markers, their ability to grow clonally and their potential to differentiate into a variety of cell types. We first tested whether GSC1/2 cells retain their stem cell properties *in vitro* by testing for the expression of the known stem cell markers Sox2, CD133 and SSEA1. Both GSC1 and GSC2 homogenously express high levels of all these markers (**Figure 4a**). Next we seeded GSC1/2 at clonal dilution to assess their potential to form neurospheres (Ferrón et al., 2007) with high efficiency. Both cell lines readily divided at clonal dilution and formed neurospheres with 95 % efficiency (**Figure 4b**) which expressed high levels of Nestin (green). To confirm that GSC1/2 also remained tripotent stem cells we tested their ability to differentiate into neural and astrocytic lineages by either removal of growth factors or addition of 30 ng/ μL T3 to stimulate differentiation into oligodendrocytes (Glaser et al., 2007). After 4 days of treatment we were able to observe differentiation into astrocytes (GFAP+ Sox2-), Neuroblasts (Tuj1+) and Oligodendrocytes (O4+) **Figure 4c**. Quantification revealed that about 40 % of the cells differentiated into astrocytic lineages and 30% into a neural lineage **Figure 4c**.

All this *in vitro* data combined shows that the generated cells are *bona fide* mesenchymal glioblastoma stem cells.

## 3.3 GSC1/2 form mesenchymal glioblastoma *in vivo*

To assess their tumourigenic potential *in vivo* we first injected $5 \times 10^4$ GFP labelled GSC1/2 cells intracranially into the putamen, a structure in the dorsal striatum, of adult immuno-compromised CD1 nu/nu mice. This enabled us to test their ability to establish tumours in a neuroanatomical location relevant to human glioblastoma formation (Ozawa et al., 2002). Both cell types readily formed highly aggressive tumours with 100 % penetrance. The median
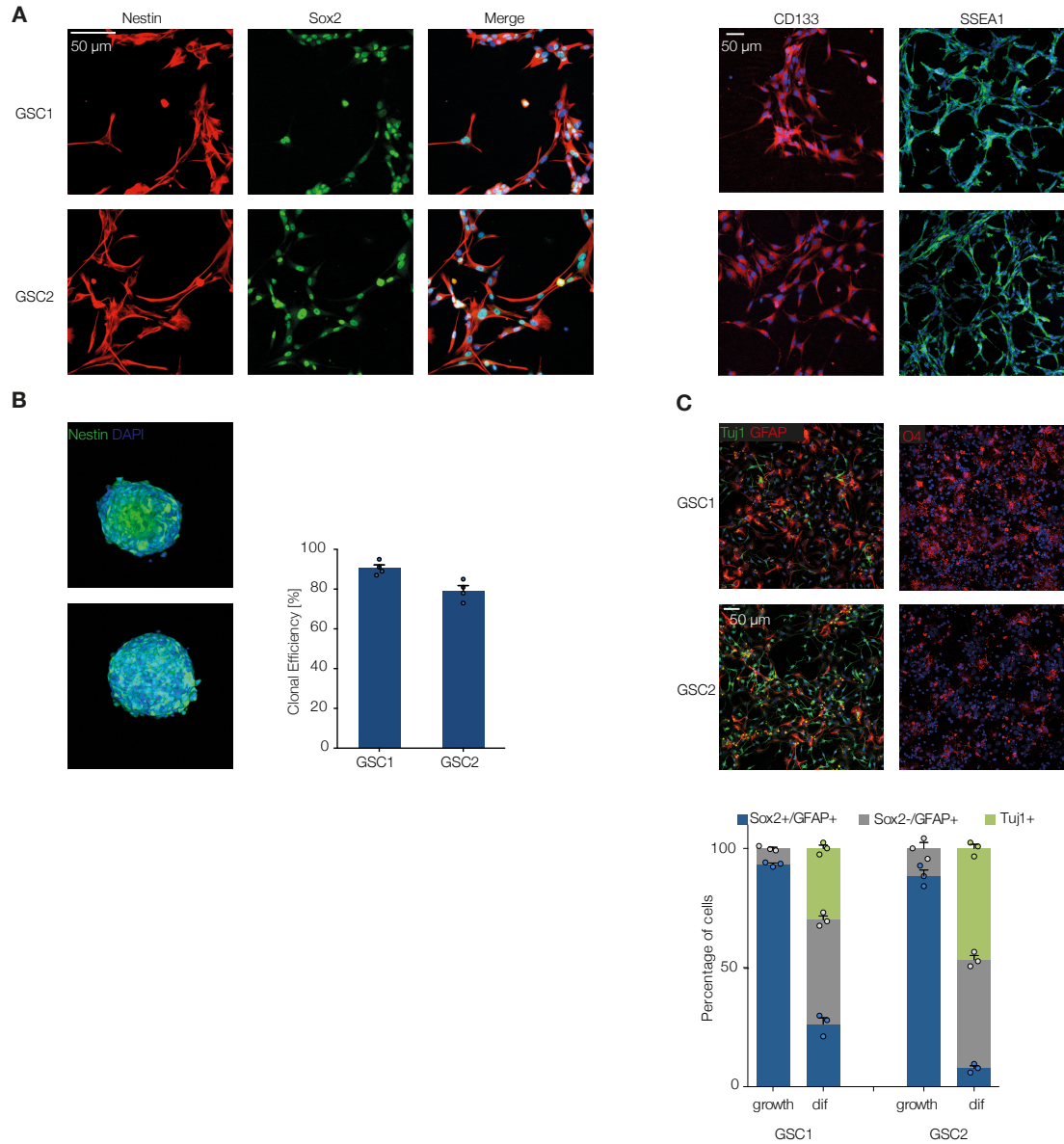
**Figure 4: GSC1/2 resemble mesenchymal glioblastoma stem cells.** a) Immunostainings of GSC1/2 for stem cell markers b) Representative immunofluorescence images of neurospheres formed after clonal dilution of cells stained with Nestin (green) and DAPI (blue). On the right, quantification of the efficiency of neurosphere formation. Error bars denote s.e.m. c) Immunofluorescence images of cells stained with Tuj1 (green) GFAP (red) or O4 (red) respectively after 4 days of differentiation (left). Quantification of the obtained cell types (right). Error bars denote s.e.m.

survival was 24 days for GSC1 and 38 days for GSC2 tumours respectively (**Table 2**).  One of the reasons for choosing a murine stem cell based system for our tumour model was the possibility to grow tumours in syngeneic immunocompetent mice. We therefore also injected GSC1 and GSC2 cells into fully immunocompetent C57/Bl6 mice.  Whereas GSC2 were not able to form tumours in this system GSC1 did so with a 56 % penetrance (5/9 animals) indicative of a more aggressive phenotype than GSC2.  We additionally injected GSC1 into the cortex of immunocompetent mice (see **Chapter 5**) and observed a penetrance of 75 % (9/12 animals) (**Table 1**).

**Table 1:** Penetrance of GSC1 injected into syngeneic mice

| Anatomical Location | Total tumours formed | Penetrance | Median survival |
|---|---|---|---|
| Striatum | 5/9 (1 censored) | 56 % | 73 days |
| Cortex | 9/12 (10 censored) | 75 % | 62 days |

censored mice died of other reasons than tumours

**Table 2:** Penetrance of GSC in nude mice

| Cell type | Total tumours formed | Penetrance | Median survival |
|---|---|---|---|
| imNSC1 | 0/5 | 0% | - |
| GSC1 | 5/5 (0 censored) | 100 % | 24 days |
| imNSC2 | 0/5 | 0% | - |
| GSC2 | 4/4 (1 censored) | 100 % | 38 days |

censored mice died of other reasons than tumours

A representative tumour formed by GSC1 in immunocompetent mice is shown in **Figure 5a**. We also processed these tumours for H&E staining (**Figure 5b**) The histopathology of the tumour resembled high grade astrocytoma given the degree of vascularisation (i), the high rate of proliferation (ii,iii) and the presence of focal necrosis (iv) (Louis et al., 2007).  Glial tumours are characterised by their expression of intermediate filament protein GFAP. We

therefore stained four GSC1 tumours formed in immunocompetent C57/Bl6 animals for GFAP (**Figure 5c**). We observed differing degrees of GFAP expression within the tumour indicating a degree of variability in the types of tumours formed after injection.

To better characterise the resulting tumours we also performed immunohistochemistry for CD133, Sox2 and Nestin. All tumours expressed high levels of all three stem cell markers both in the periphery and the in the centre of the tumour mass (**Figure 5d**).

The association of these cells with the vasculature was analysed by costaining for CD31, a vascular marker, and GFP. In all tested tumours we observed a strong association of tumour cells with the vasculature with tumour cells completely surrounding vessels in some instances (**Figure 5e i**). We also observed a smaller percentage of potentially invasive cells which were found removed from the main tumour mass and in direct contact with blood vessels (**Figure 5e ii**).

We wanted to ensure that the mesenchymal signature of these cells is retained *in vivo* and that the resulting tumours can indeed be classified as mesenchymal glioblastoma. We therefore isolated GSC1 tumours 30 days after injection and analysed the expression levels of key signature genes. GSC1 tumours show a significant enrichment for mesenchymal genes similar to the parental population. No significant association was found with signature genes of other GBM subtypes (**Figure 5f**).

We thus show that the generated GSC model indeed leads to the formation of highly aggressive mesenchymal glioblastoma with high penetrance.
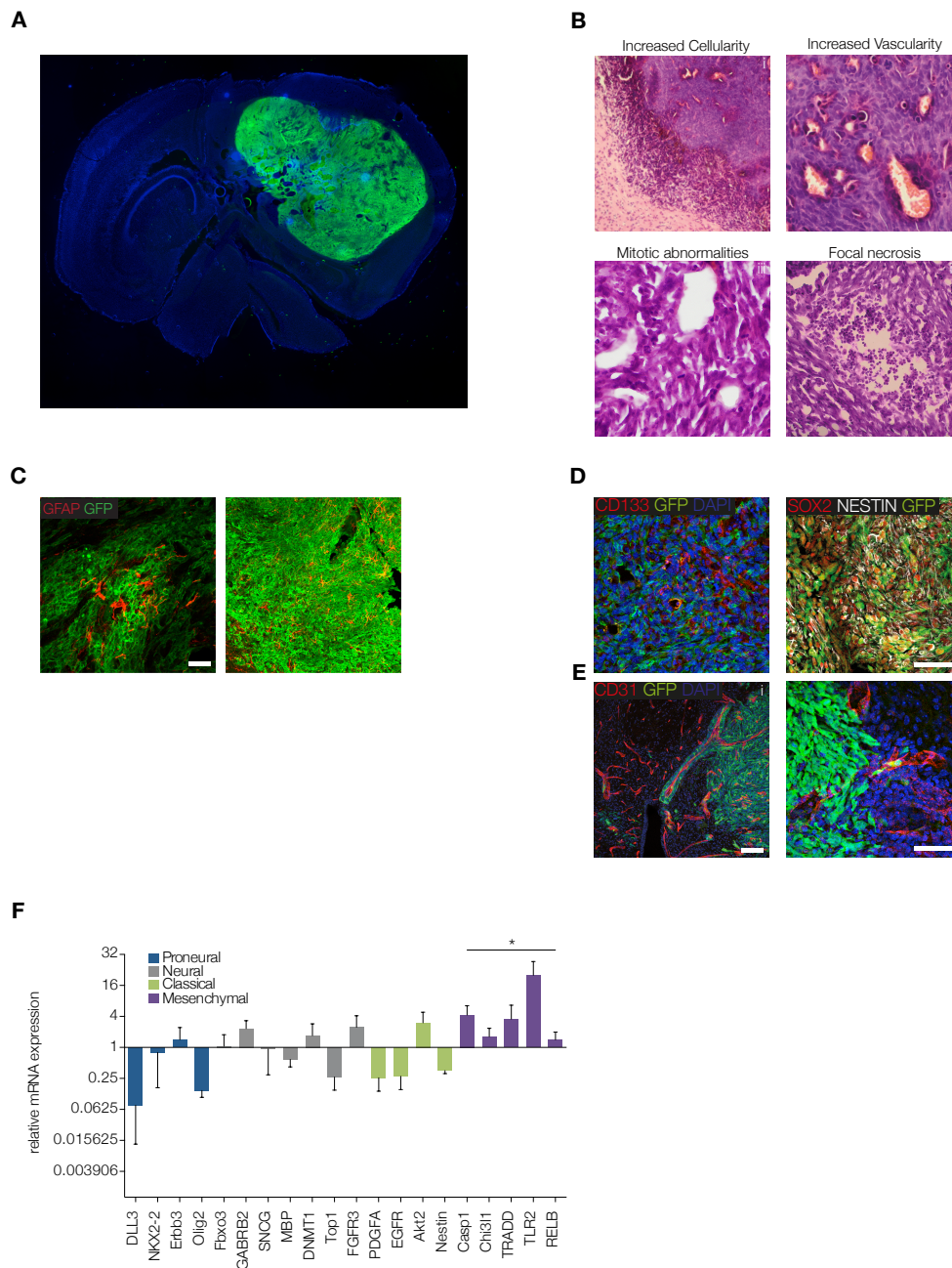
**Figure 5: GSC1 form highly aggressive astrocytoma in immunocompetent mice**. a) Representative immunofluorescence image of a coronal section of a C57-Bl6 mouse brain 60 days post intracranial injection of $5 \times 10^4$ GFP labelled GSC1 cells. b) H&E stains of the tumours showing all four hallmarks of high grade astrocytoma c) Immunohistochemistry of 2 different tumours stained with GFAP (red) and GFP(green). Scale bar = 50 μm d) Immunofluorescence pictures of representative tumours stained for stem cell markers CD133 (red),Sox2(red), Nestin(white) and GFP labelling the tumour cells (green). Scale bar = 50 μm e) Immunofluorescence pictures of tumours stained for endothelial marker CD31 (red) and GFP labeling the tumour cells (green). Scalebar = 50 μm f) quantitative RT-PCR analysis of three independent GSC1 tumours isolated from CD1-nude mice.

## 3.4 Conclusion

In this chapter we created a model system of mesenchymal glioblastoma by successively trans-forming adult neural stem cells isolated from the subventricular zone. The subventricular zone has long been implicated to play an important role in gliomagenesis (Recht et al., 2003; Oliver and Wechsler-Reya, 2004) and many studies in mouse models suggest a stem cell origin of glioblastoma (Chow et al., 2011; Wang et al., 2009; Abel et al., 2009). We chose to base our model on mesenchymal glioblastoma as it is generally characterised as the most aggressive and invasive human GBM subtype (Phillips et al., 2006). Additionally, recurrent glioblastoma, that had previous treatment show an enrichment for mesenchymal-associated genes under-pinning the importance of studying this subtype (Tso et al., 2006) . To model mesenchymal glioblastoma we introduced specific genetic changes most significantly associated with this subtype.

This approach has previously been used successfully to generate GBM of various subtypes from primary neural stem/progenitor cells (Bachoo et al., 2002; Ligon et al., 2007).A main advantage of using this approach over studying human cancer stem cells isolated from human patients is that it allows us to readily test candidate effectors by transforming neural stem cells from mice carrying specific mutations (Blouw et al., 2003). Importantly, these cells can then be tested *in vivo* in syngeneic, fully immune competent mice. Glioblastoma are immuno-genic tumours and it has become more and more apparent in recent years, that the effect of the immune system can't be neglected in murine tumour models (Ridley, 1977; Oh et al., 2014). The overexpression of oncogenes may cause artefacts, not typically observed in a nor-mal cellular context. Especially, high concentrations of constitutively active kinases like h-ras might cause the loss of substrate specificity (Hindley and Kolch, 2002). To exclude this pos-sibility we used two complementary strategies to generate a mesenchymal GBM model: First we utilised a "classical" transformation paradigm using SV40 largeT and h-ras oncogenes. We also used a more targeted approach by specifically silencing p53 and overexpressing Cdk4

in NSCs isolated from NF1$^{flox/flox}$ mice. In addition, we generated genetically matched non-transformed cells which enabled us to precisely study the phenotypical changes occurring during transformation and pinpoint them to exact genetic mutations. This is a unique advantage of creating a defined model system and not relying on GSCs isolated from human glioblastoma, which acquired a multitude of large-scale genomic aberrations during tumour progression. We next showed that all introduced oncogenes are functional and that the generated fully transformed cells indeed acquired a mesenchymal signature as predicted. GSC1 and GSC2 also both retain their stemness *in vitro* and are able to differentiate into neural and astrocytic lineages at similar efficiencies compared to established glioblastoma stem cell lines isolated from patients (Pollard et al., 2009).

Most importantly however we show that these cells formed highly aggressive tumours in neuroanatomical locations where GBM formation has been observed in humans: We injected cells into the putamen and the cortex (see **Chapter 5**) and obtained a penetrance of 56% and 75% respectively. In agreement with previous publications, the formed tumours associate strongly with the vasculature by coopting existing vessels and sometimes encapsulating them completely (Cuddapah et al., 2014; Farin et al., 2006). This tumours were classified by a trained pathologist as grade IV astrocytoma as H&E staining revealed increased cellularity, neovascularisation and focal necrosis. Furthermore, immunohistochemistry analysis showed expression of GFAP (Louis et al., 2007). GFAP expression was highly variable between different tumours which has however been previously observed in a similar model of GSCs generated from NSCs (Bachoo et al., 2002) and also in GSCs isolated from human glioblastoma patients (Pollard et al., 2009). In agreement with this and other publications we also observed a very high percentage of undifferentiated stem-like cells in tumours with fewer differentiated GFAP-positive cells (Chen et al., 2012). GSC2 did not form tumours in immunocompetent mice which could be caused by the fact that these cells were not isolated from inbred C57/Bl6 mice but a mixed background (Parrinello et al., 2008). Both tumours however formed highly aggressive astrocytoma in immunocompromised mice and retained their mesenchymal gene signature as confirmed by quantitative RT-PCR analysis.

Combined these results confirm that we successfully created two highly interchangeable model systems which resemble *bona fide* glioma stem cells and lead to the formation of tumours which effectively mimic important characteristics of human mesenchymal glioblastoma.

# Chapter 4

# Endothelial control of proliferation

## 4.1 Endothelial ephrinB2 enforces neural stem cell quiescence in a p53 dependent manner

We have previously shown that endothelial ephrinB2 suppresses cell-cycle entry of normal neural stem cells downstream of mitogens by mediating a G1-arrest (Ottone et al., 2014). We aimed to investigate how this arrest is affected by the introduction of oncogenes into normal neural stem cells. We therefore cultured normal stem cells (NSC), imNSC1 and GSC1 cells on either a confluent monolayer of brain endothelial cells (bEND) or 8 μg ephrinB2-Fc. Strikingly we found that the cell-cycle arrest in response to either co-culture with bEnd3 or ephrinB2-Fc was completely lost in both, imNSC1 and GSC1 (**Figure 6a**). We specifically introduced a vector expressing a dominant negative variant p53 into primary NSCS (p53) to see whether this phenotype was caused by lack of p53 function in largeT infected cells, or whether the inactivation of Rb was also needed. Intriguingly dominant negative p53 alone was sufficient to rescue the cell-cycle arrest in NSCs in response to Eph stimulation (**Figure 6a**).

In agreement with the loss of cell-cycle inhibition we also observed no decrease in cyclinD1
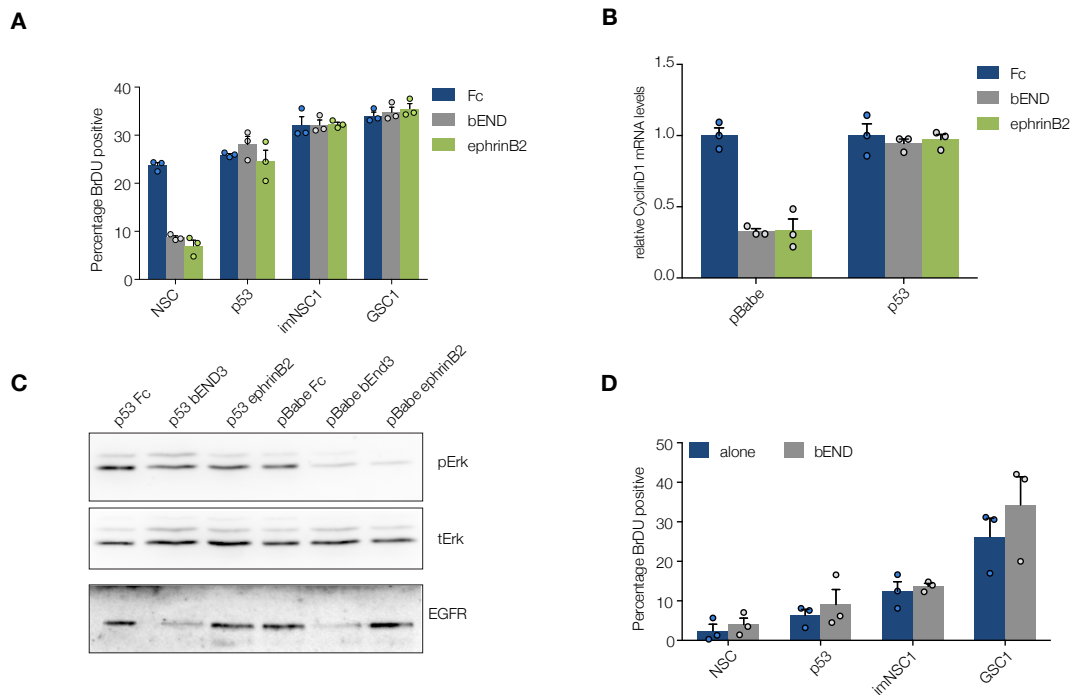
**Figure 6: p53 is sufficient to rescue ephrinB2 induced G1-S cell cycle arrest in NSC**. a) FACS analysis of BrDU incorporating cells cultured over night either on Fc-control (Fc), endothelial cells (bEND) or 8 µg/ml ephrinB2-Fc ligand (ephrinB2). Error bars depict s.e.m. b) quantitative RT-PCR analysis of cyclinD1 in cells cultured overnight either on Fc-control (Fc),endothelial cells (bEND) or 8 µg/ml ephrinB2-Fc ligand (ephrinB2).Error bars depict s.e.m. c) Western blot analysis of the depicted proteins of cells cultured overnight either on Fc-control (Fc), endothelial cells (bEND) or 8 µg/ml ephrinB2-Fc ligand (ephrinB2) d) FACS analysis of BrDU incorporating cells cultured for two days in factor depleted conditions either alone or on endothelial cells (bEND). Error bars depict s.e.m.

levels in co-cultures of p53 cells in contrast to NSCs which showed a strong reduction at mRNA level using quantitative RT-PCR (**Figure 6b**). We previously observed decreased pErk and EGFR levels in NSCs in response to overnight stimulation with endothelial cells. Interestingly while EGFR levels were still reduced in p53 cells to a similar extent as NSC controls no such reduction was observed in pErk levels. This suggests that pErk levels are not simply dampened by the absence of ras stimulation through EGFR receptor, but are regulated by an independent pathway (**Figure 6c**).

Given the differences observed in growth conditions we hypothesised that co-culture with endothelial cells might give an additional growth advantage to tumour cells compared to neural stem cells. We therefore cultured NSC, p53, imNSC1 and GSC1 cells on a monolayer

of endothelial cells for two days in the absence of mitogens (**Figure 6d**). However we did not observe a significant increase in the proliferation rate of any of the tested cell types.

Next we tried to identify the exact mechanism by which p53 mediates the Eph-dependent G1/S-arrest of neural progenitor cells. To consolidate the involvement of p53 in this system we initially checked the expression levels of p53 in NSC alone and compared it to those in co-culture. While we did not observe increased total p53 mRNA levels, we observed a strong increase in nuclear p53 in NSCs in co-culture with endothelial cells (**Figure 7a,b**). We then introduced Luciferase constructs containing either the p53 binding site or a mutated sequence which cannot be bound by p53 in NSCs and compared the p53 activity in cells cultured alone with cells cultured overnight on an endothelial cell monolayer or ephrinB2-Fc ligand. Bleomycin treatment served as positive control. Consistent with the previous findings, p53 activity was significantly increased in cells co-cultured with bEnd3 or treated with clustered EphrinB2 ligand (**Figure 7c**). Next, we checked the expression levels of a variety of known p53-downstream targets such as SESN1, BTG2 and p21. Interestingly while SESN1 and BTG2 mRNA levels were significantly increased we did not see an increase in p21 transcription levels (**Figure 7d**). As the dampening of pErk was lost in p53 negative cells, we reasoned that Erk dephosphorylation might be caused by transcriptional upregulation of a phosphatase through p53 activation. To test this hypothesis we cultured cells on endothelial cells in the presence of 5 nM calyculin A, a potent phosphatase inhibitor (**Figure 7e**). We observed a small increase of Erk phosphorylation in NSC co-culture treated with calyculin A compared to DMSO treated cells. A potential class of phosphatases involved in this are the dual specific phosphatases (DUSPs). DUSPs are Erk1/2 specific phosphatase and reports have identified several DUSPs as transcriptional targets of p53 (Huang and Tan, 2012). We therefore tested the expression levels of a panel of known DUSPs and observed a slight but significant upregulation of Dusp1, 2, 8 and 9 through contact with endothelial cells (**Figure 7f**). This hints to a possible role of this class of proteins in the dephosphorylation of Erk and the resultant cell cycle arrest in neural progenitor cells. Dusp1 and 2 are both known downstream transcriptional targets of p53 (Liu et al., 2008; Yin et al., 2003). We therefore tested several
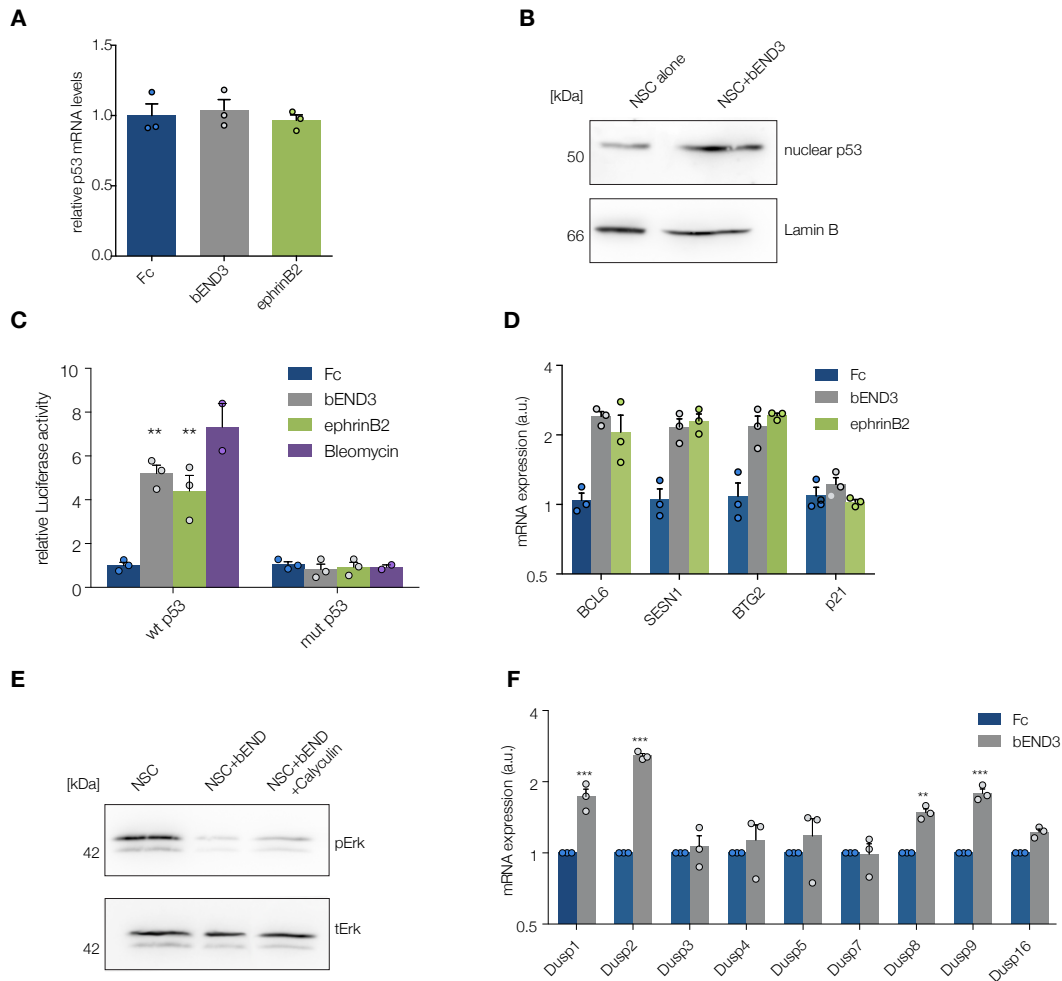
**Figure 7: Endothelial ephrinB2 activates p53 signalling in NSCs to mediate G1-1 arrest**. a) quantitative Q-PCR analysis of p53 mRNA levels in NSC cultured on Fc control (Fc), a monolayer of endothelial cells (bEND3) or coated ephrinB2 (ephrinB2) b) Western blot analysis of the nuclear fractions of cells cultured either alone or on top of a monolayer of endothelial cells (bEnd3) c) Relative Luciferase activity of cells transfected with Luciferase constructs containing either the wildtype p53 binding site (wt p53) or a mutated version sequence to which p53 does not bind to (mutant p53). Error bars depict s.e.m. One way anova with Tukey post hoc test d) quantitative RT-PCR analysis of NSCs cultured overnight on either Fc-control (fc), a monolayer of endothelial cells (bEND3) or clustered ephrinB2-Fc ligand (ephrinB2). Error bars depict s.e.m. e) Western blot analysis of NSCs cultured on a monolayer of endothelial cells and treated with either DMSO or 5nm calyculin A, a phosphatase inhibitor. f) quantitative RT-PCR analysis of the mRNA levels of different DUSPs in NSC after overnight culture on PLL (alone) or on a monolayer of endothelial cells (bEND3). error bars depict s.e.m.

siRNAs for their potential to knockdown Dusp1 & 2. siDusp1 6 and siDusp1 7 were able to cause a knockdown of Dusp1 of up to 80% without significantly affecting Dusp2 expression (**Figure 8a**). Dusp2 siRNAs were less efficient, however a pool of four siRNAs (siDusp 6-9) achieved a 75% knockdown on RNA level without affecting Dusp1, respectively (**Figure 8b**). We then tested whether knocking down Dusp1 or Dusp2 has an effect on pErk levels in cells co-cultured with endothelial cells over night (**Figure 8c**). We did not observe increased levels of phosphorylated Erk in either of the two knockdowns thus concluding that neither Dusp1 nor Dusp2 mediate Erk phosphorylation downstream of p53 in NSCs.
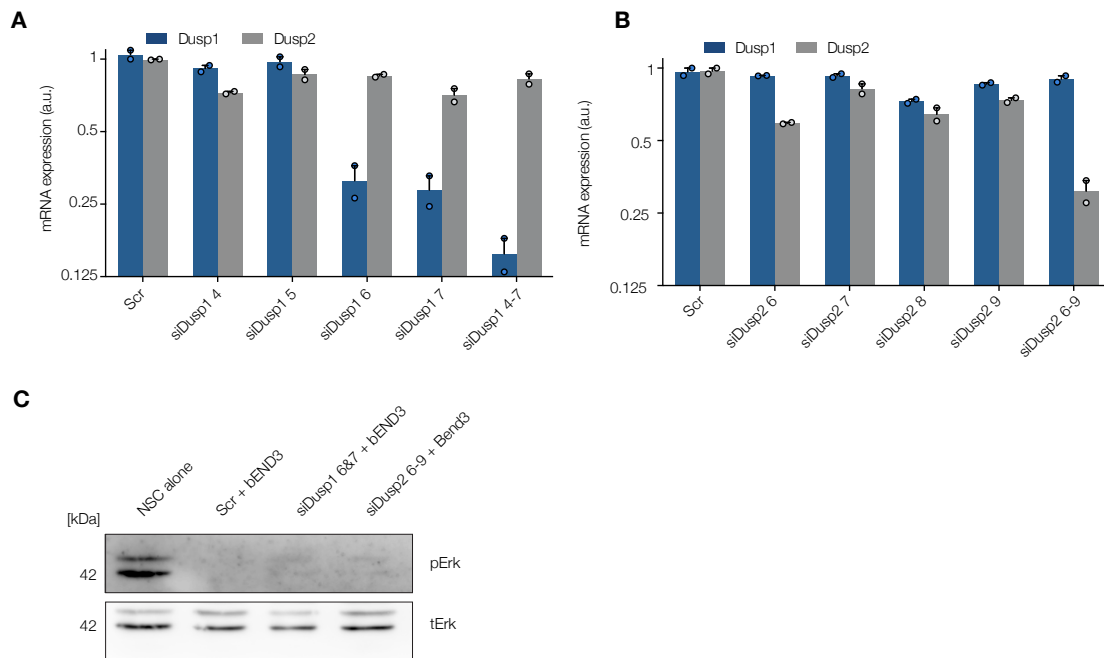


**Figure 8: Dusp 1 & 2 are not mediating pErk levels in NSCs.** a,b) quantitative RT-PCR analysis of a panel of siRNAs specific against Dusp1 (a) and Dusp2 (b) respectively. Error bars denote s.e.m. c) Western blot analysis of pErk levels in cells transfected with specific siRNAs against Dusp1 and 2 and then cultured over night on a monolayer of endothelilal cells (+bEND3).

Thus, we found a novel mechanism of cell-cycle regulation in neural stem cells which is mediated through Eph-forward signalling induced by ephrinB2 on endothelial cells. We obtained preliminary data suggesting that p53-dependent upregulation of a phosphatase might mediate this phenotype through Erk dephosphorylation and subsequent G1-arrest. However we did not identify a specific phosphatase responsible for this dephosphorylation and in the interest of time continued to pursue other, more promising projects.

## 4.2   Phosphoproteomics identifies potential links between Eph activation and p53 activity

We next tried to identify potential links between Eph activation and p53 relocalisation to the nucleus which in turn might lead to the upregulation of genes dampening Erk phosphorylation using more unbiased approaches. To this end we used a phosphoproteomics approach to gain an overview over all proteins which become tyrosine phosphorylated in response to activation of Eph-receptors which are phosphotyrosine kinases. Cells were labelled with heavy and light amino acids for SILAC analysis, then treated with either scraped endothelial cells or control medium for 10 minutes and an immunoprecipitation for tyrosine phosphorylated proteins performed before analysis of the obtained protein extracts using mass spectrometry. By physically scraping endothelial off the plate we avoid the use of enzymes like trypsin which can destroy the extracellular portions of membrane bound proteins like ephrinB2. The endothelial cells settle on top of the monolayer of NSCs during the 10 minute incubation but are easily removed by PBS washes as we have previously shown (Ottone et al., 2014). This protocol is sufficient to induce robust phosphorylation of Eph receptors as shown in **Figure 9a**. We first tested different lysis buffers for their potential to lyse cells effectively without destroying post-translational modifications. Lysis with NP40 buffer achieved the highest enrichment of tyrosine-phosphorylated proteins and was therefore chosen for further experiments (**Figure 9b**). We first tested the correlation of the two separate conditions by plotting the relative enrichment of each identified phosphorylated protein (**Figure 9c**).

Most proteins remained unchanged and align along the 90 % confidence band (dotted line). Additionally more proteins can be found which have higher phosphorylation levels after stimulation with endothelial cells. Thus, we were confident that the obtained data was not skewed by excessive experimental variability caused by technical errors during cell lysis and immunoprecipitation. Amongst the proteins with the highest fold change we found EphB2 (Ratio H/L 1.5262) suggesting, that we are indeed able to detect specific events following Eph phos-
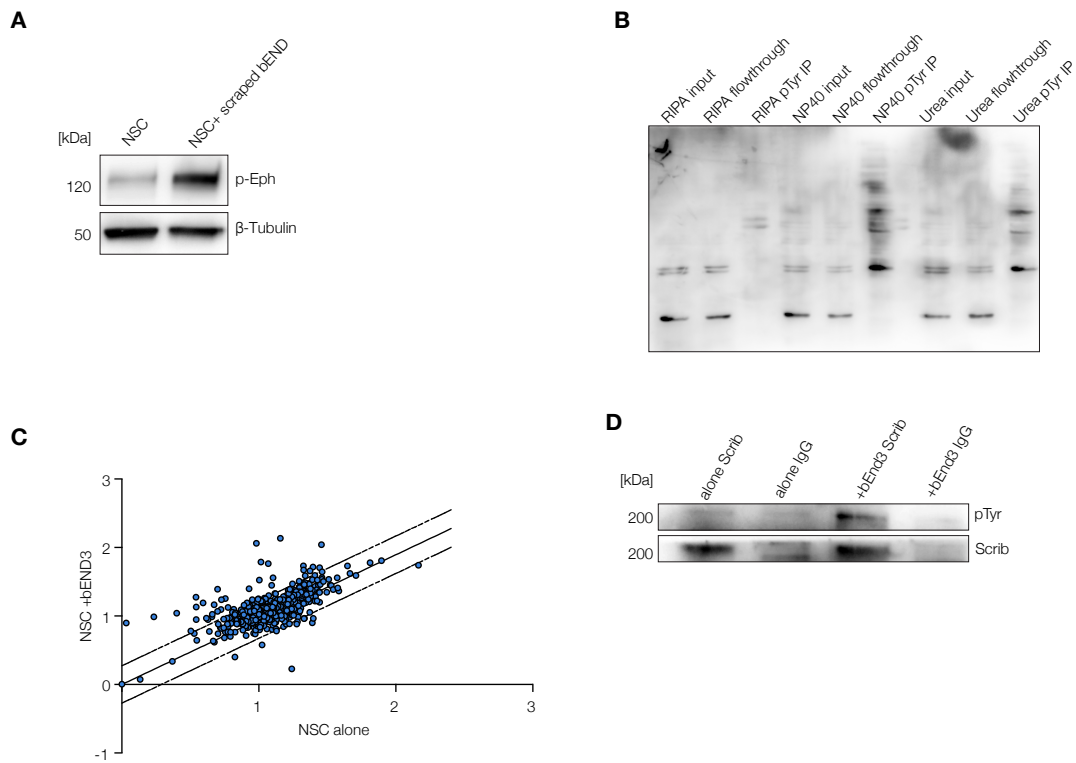
**Figure 9: pSILAC to identify phosphorylated proteins after stimulation with endothelial cells**. a) Western blot analysis showing the phosphorylation level of Eph-receptor after stimulation with scraped endothelial cells (bEND) for 10 minutes b) Western blot analysis of the levels of tyrosine-phoshorylated proteins (pTyr) pulled down using different lysis buffers. Input and flowthrough are shown as controls c) Correlation plot of pSILAC results of cells cultured alone and stimulated with endothelial cells. 90 % confidence interval is shown as dotted line d) Western blot analysis of specified proteins after immunoprecipitation with either IgG control (IgG) or Scribble specific antibodies (Scrib).

phorylation. The 10 highest ranking candidates are shown in **Table 3**

**Table 3:** Overview of top scoring proteins in pSILAC analysis

| Protein name | unique peptides identified | Ratio H/L |
|---|---|---|
| Protein Scribble homolog | 15 | 1.778 |
| Mitogen-activated protein kinase 6 | 7 | 1.7427 |
| Adenylate kinase isoenzyme 1 | 5 | 1.622 |
| Dehydrogenase/reductase SDR family member 1 | 25 | 1.5914 |
| Filamin-C | 48 | 1.5895 |
| Annexin A7 | 17 | 1.557 |
| Sorbin and SH3 domain-containing protein 2 | 10 | 1.536 |
| Ephrin type-B receptor 2 | 16 | 1.5262 |
| Phosphatidylinositol 3-kinase regulatory subunit alpha | 14 | 1.43443 |
| CD109 antigen | 24 | 1.4327 |

Protein Scribble homolog is commonly known as a mediator of cell polarity however it has been implicated to play a role in cell-cycle control and tumourigenicity in various systems (Humbert et al., 2003, 2008). Mammalian Scribble is a scaffolding protein which appears to be membrane bound and overlaps with cadherins localised at adherens junctions (Humbert et al., 2003). Interestingly, in *Drosophila*, loss of scribble leads to overproliferation and it has been shown to negatively regulate G1/S-Phase transition in epithelial cells (Dow et al., 2007; Nagasaka et al., 2006). We went on to confirm whether Protein Scribble homolog is indeed activated in our system by immunoprecipitation. After 10 minutes of stimulation with scraped endothelial cells we did indeed observe higher tyrosine phosphorylation levels of Scribble compared to mock treated controls (**Figure 9d**).

## 4.3 $\beta$-Catenin is not involved in mediating Eph signalling in NSC

Scribble as a scaffolding protein has a variety of binding partners which relay its signalling responses to the nucleus where transcription of target genes can be changed. Numerous studies have shown that Scribble is strongly linked with the Wnt signalling pathway, a crucial mediator of various cell functions including cell cycle progression (Davidson and Niehrs, 2010). The Wnt pathway critically relies on $\beta$-catenin which is a prominent binding partner of Scribble (Sun et al., 2009; Qin et al., 2005). $\beta$-catenin is a dual function protein, regulating cell-cell adhesion by binding to membrane associated proteins and also acting as a transcription factor in the nucleus (MacDonald et al., 2009). Interestingly, we previously observed a strong downregulation of EphB2 receptor in NSCs in response to co-culture on endothelial cells and $\beta$-Catenin has been shown to cause downregulation of EphB2 at the colorectal "adenoma-carcinoma" transition (Batlle et al., 2002). This made $\beta$-catenin a highly attractive candidate to mediate the effects downstream of Scribble phosphorylation. We therefore sought to understand whether activation of Scribble leads to relocalisation or a change in activation of $\beta$-catenin which could explain both, the downregulation of EphB2 in co-culture and be a possible pathway for the Eph-induced cell cycle arrest. Initially we performed cellular fractionation of NSC cultured alone or on a monolayer of endothelial cells. No change in the nuclear localisation of $\beta$-catenin or the total amount of protein was observed (**Figure 10a**). We then transfected NSC with TopFlash-vector, a plasmid containing a $\beta$-catenin responsive luciferase reporter construct. No significant change in $\beta$-catenin activity was observed in response to either overnight culture with endothelial cells or coated ephrinB2.

Thus $\beta$-catenin is not involved in mediating the G1 arrest induced by Eph/ephrin signalling in NSCs. pSILAC analysis proved to be a viable approach to find potential candidate proteins, though a more thorough analysis of more than one candidate protein and its downstream targets would be needed to identify the exact signalling pathway. However we conclude
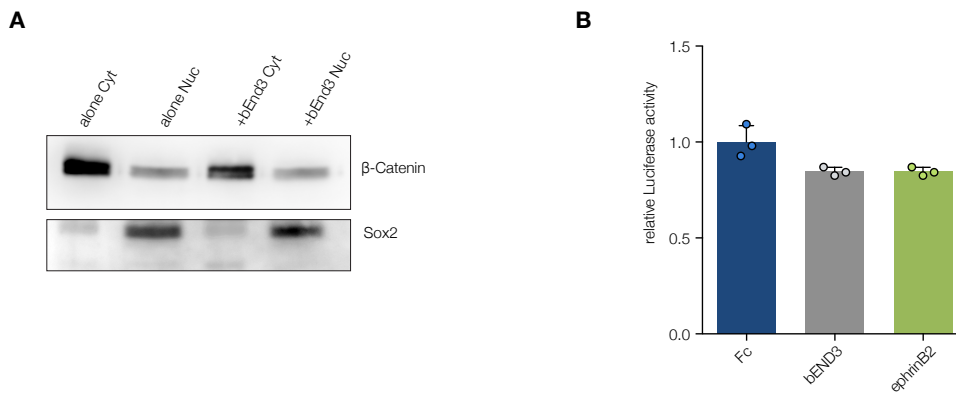
**Figure 10:** $\beta$-**catenin localisation and activity does not change in response to endothelial contact**. a) Western blot analysis of cellular fractions of NSC cultured either alone or on a monolayer of endothelial cells (bEND3) b) Relative Luciferase activity of cells transfected with Luciferase constructs containing $\beta$-catenin binding sites. Error bars depict s.e.m. One way anova with Tukey post hoc test

that ephrin-B2 ligands on the surface of endothelial cells inhibit progenitor cell proliferation through p53-signalling in a p21-independent manner. Instead, p53 activation downstream of Eph blocks proliferation via a decrease in MAPK signalling. Importantly, our results also show that loss of p53 function in transformed neural stem cells gives them a distinct proliferative advantage over normal NSCs in the context of a stem cell niche which strictly governs the proliferation rate of cells within it.

## 4.4 Conclusion

We have previously shown that direct contact with ephrinB2 on endothelial cells maintains stem cells of the subventricular zone in a quiescent stem-cell state by causing a G1/S arrest while at the same time profoundly affecting cell morphology (Ottone et al., 2014). Here we show that Eph-receptors on NSCs act as early tumour suppressors that limit proliferation through p53 induction in a p21-independent manner. TP53 is classically known as a DNA-Damage response gene that can arrest the cell to allow repair or initiate apoptosis if the damage is too extensive. In recent years, however, a crucial role for p53 in stem cell biology is emerging: p53 is constitutively expressed in a variety of adult stem cell niches (Bonizzi et al., 2012; Solozobova and Blattner, 2011). In neural stem cells of the SVZ specifically, p53 was shown to regulate self-renewal and differentiation and it has been shown that p53 knockout leads to increased proliferation of neural precursors (Armesilla-Diaz et al., 2009; Gil-Perotin et al., 2006). Our results are in agreement with a previously published report by Theus et.al. describing the regulation of p53 by EphB3 forward signalling in the SVZ during homeostasis and following traumatic brain injury (Theus et al., 2010). Our data however for the first time identifies endothelial cells and more specifically ephrinB2 as critical mediator of this phenotype. We next sought to understand the precise signalling pathway linking Eph activation to p53 regulation using both classical hypothesis driven approaches and unbiased proteome-wide screening techniques. Given their important role as major mediators of critical signalling pathways we first explored the possibility of DUSPs regulating the Erk 1/2 dephosphorylation downstream of p53 as we observed an increase in pErk levels in cells treated with a phosphatase inhibitor. We found a significant upregulation of a number of DUSPs, siRNA knockdown however did not alter the response downstream of endothelial contact. This could be due to the relatively low efficiency of the knockdown but more importantly, it has been shown on several occasions that knockdown of one member of the DUSP family can be compensated by other DUSPs (Huang and Tan, 2012). It would nevertheless be interesting to continue studying the potential involvement of phosphatases in this system, per-

haps looking at a broader panel using available microarrays. We then performed an unbiased analysis of the phosphorylation events immediately downstream of Eph activation following endothelial contact using mass-spectrometry. We identified Scribble as potential downstream effector of Eph which showed higher levels of tyrosine phosphorylation following stimulation with endothelial cells. Scribble, together with discs large (Dlg) and Lethal giant larvae (Lgl) is part of a group of highly evolutionary conserved proteins that link the seemingly unrelated functions of cell polarity and cell proliferation in epithelial cells (Humbert et al., 2003). Mammalian Scribble is an important regulator of cell polarity and has been implicated to act as a tumour suppressor by negatively regulating cell-cycle progression from G1 to S phase in epithelial cells (Nagasaka et al., 2006). Scribble acts as a scaffolding protein for regulators of canonical Wnt signalling like $\beta$-catenin to relay signalling from the membrane to the nucleus. $\beta$-catenin was a highly promising candidate to be a downstream effector of the p53 dependent cell-cycle arrest for several reasons: $\beta$-Catenin transcription is known to be controlled by p53 activation (Sadot et al., 2001) and is has been shown in multiple instances to regulate MAPK/Erk signalling (Jeon et al., 2007) and control the expression of cyclinD1 (Tetsu and McCormick, 1999). Interestingly, $\beta$-catenin activity has also been shown to cause downregulation of EphB2 (Batlle et al., 2002). We previously observed a strong downregulation of Ephb2 on NSCs in co-culture with endothelial cells, suggesting that $\beta$-catenin might indeed be involved in our system. However, no change in $\beta$-catenin activity or localisation was observed in co-culture with endothelial cells or on ephrinB2-ligand. A previous report using a similar model for SGZ neurogenesis identified $\beta$-catenin activity increased in a ephrinB2 dependent manner in the context of increased neurogenesis (Ashton et al., 2012). It is interesting to note that stimulation with ephrinB2 causes opposing responses with an increase in newborn neurons in the SGZ and a strong suppression of cell-cycle entry in the SVZ (Ottone et al., 2014). Our results therefore further highlight the differences between two superficially similar neurogenic niches in the adult brain. Our data might also further explain why loss of p53 signalling is such an important event in early gliomagenesis which occurs in nearly 90% of all glioblastoma (TCGA, 2008). In our system it enables mutated stem cells, the

likely cell of origin for a large percentage of glioblastoma , to escape the tight control of their microenvironment and proliferate unhindered. At the moment it is still not entirely known how Eph activation on the cell surface leads to p53 activation, Erk1/2 dephosphorylation and a cell-cycle arrest in G1-phase. It would therefore be of great interest to study and understand this pathway better, as the high frequency of p53-alterations in glioblastoma make any downstream effectors a very attractive target for potential new therapeutic approaches.

# Chapter 5

# Endothelial control of migration

## 5.1 Eph/Ephrin signalling compartmentalises normal neural progenitor cells but not GSCs

Glioblastoma are characterised by their diffuse invasion of healthy brain tissue along pre-existing structures (Scherer, 1940). A major route of invasion is perivascular migration along blood vessels (Farin et al., 2006). To assess the interaction of GSCs with syngeneic brain vasculature we injected GFP-labelled GSC1 and imNSC1 at a depth of 200-300 μm into the cortex of 6 week old mice under a chronic cranial window. Using 2-Photon microscopy we imaged these cells 7 days after injection *in vivo* in real time. (**Figure 11a**) GSC1 cells were able to migrate along the vasculature in single cells, and were frequently observed detaching from the main tumour mass and invading the surrounding healthy tissue. This migratory behaviour is very similar to previous observations on perivascular invasion by other groups (Farin et al., 2006). However, strikingly, imNSC1 were unable to migrate perivascular and remained in stationary groups (**Figure 11b**). This difference was not caused by the inability of imNSC1 to survive *in vivo* as at this early time point general cell morphology and occasional movement of cells within the bulk of the injected cells was very comparable to GSC1 cells.

93

This suggests that the vasculature compartmentalises normal neural progenitor cells *in vivo* .
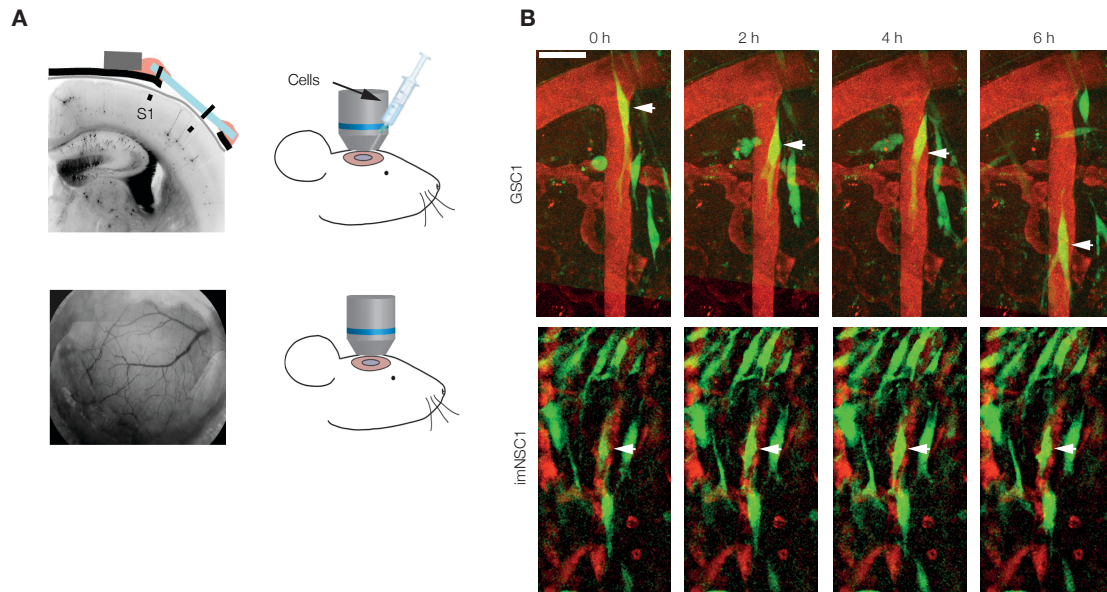


**Figure 11: The vasculature compartmentalises normal neural progenitors cells in vivo**.      a) Schematic of the craniotomy procedure b) Intravital 2-Photon stills of GFP-labelled imNSC1 and GSC1 cells injected into the cortex of syngeneic mice and imaged 7 days post injection over 6 hours through an intracranial window at a depth of 200 μm

It has previously been shown that infiltrating GBM cells primarily contact endothelial cells during perivascular invasion.  Indeed, studies suggests an active displacement of other cell types, like astrocytes, which would hinder the direct contact between endothelial cells and migrating glioblastoma cells (Cuddapah et al., 2014) Therefore, to dissect the mechanism of vascular compartmentalisation in more detail we developed an *in vitro* migration assay which mimics the response of infiltrating cells to the initial contact with endothelial cells. We used cell culture silicone inserts which divide the cell-culture dish into two compartments separated by a 500 μm gap. In each compartment different cell-populations can be seeded. After removal of the insert, the cells migrate towards each other allowing to study their behaviour upon contact. We seeded primary endothelial cells and normal SVZ progenitors in opposite compartments and performed time-lapse microscopy. Remarkably this assay closely recapitulated the results we observed *in vivo* . imNSC1 were strongly repelled when they came in contact with endothelial cells, this resulted in the two cell types remaining completely separated and forming a sharp boundary (**Figure 12a**) . This behaviour was significantly impaired

in GSC1 which started to migrate over and into the endothelial monolayer and failed to separate completely resulting in a significantly longer, less straight boundary. We repeated these measurements using imNSC2 and GSC2 to exclude the possibility that the observed phenotype is caused by artefacts induced by the overexpression of oncogenes. We observed very similar results using this complementary approach (**Figure 12b**). To quantify the differences in repulsion we measured the length of the boundary between endothelial and stem cells after 60 hours of migration. In agreement with our qualitative observation, a significantly longer boundary was measured in GSC1 and GSC2 cells compared to the respective immortalised controls (**Figure 12c**).

In a previous study we identified ephrinB2 as the ligand which is responsible for mediating the direct contact between endothelial cells and normal stem cells in the subventricular zone. We hypothesised that the same ligand might also be responsible for the compartmentalisation effect in this system as we previously observed a profound morphological change when neural stem cells were plated on a monolayer of endothelial cells. We therefore tested the role of ephrinB2 in our migration assay by using recombinant ephrinB2-Fc clustered with anti-Fc antibody substituting endothelial cells in our migration assay witha coating of recombinant ephrinB2-Fc. We first performed serial dilutions of the clustered antibodyFc complex to be able to determine the minimum concentration at which we observe phenotypical changes in the migration of imNSC1. To our great surprise we observed a strong repulsion of imNSC1 induced by ephrinB2 using this approach (**Figure 12d**). We decided to use 4 µg/ml recombinant clustered ephrinB2-Fc, as this concentration was sufficient to induce a strong migratory arrest in neural stem cells without cells escaping the compartmentalisation as seen with 3 and 2 µg. We then tested whether this effect was indeed specific for ephrinB2 by coating 4 µg Fc antibody control or ephrinA5-Fc and ephrinA1-Fc (ligands, which are also expressed on endothelial cells) clustered the same way as ephrinB2-Fc. No changes in the migration of imNSC1 were observed thus we conclude that ephrinB2 specifically compartmentalises imNSC1 (**Figure 12e**). Using this same coating approach we then tested the response of GSC1 to ephrinB2 and found that, strikingly, these cells were completely insensi-
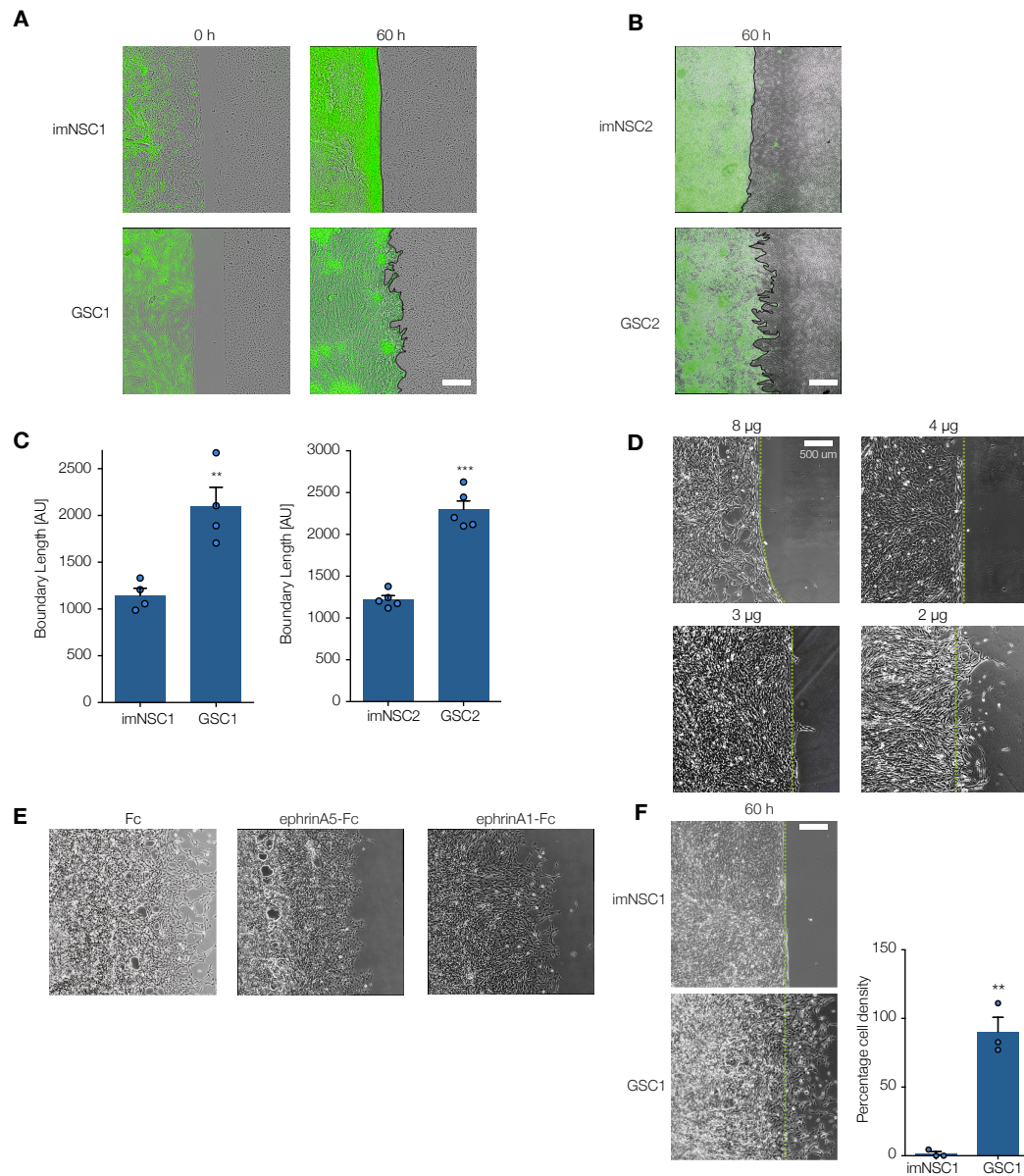
**Figure 12:** **Endothelial EphrinB2 regulates migration of normal progenitors cells but not transformed cells**. a) Representative images of imNSC1/GSC1 (green) migrating towards primary endothelial cells (unstained).b) Representative images of imNSC2/GSC2 (green) migrating towards primary endothelial cells (unstained). c) Quantification of the boundary length after 60 h. Error bars denote s.e.m. d) Representative phase contrast images of imNSC1 migrating towards different concentrations of coated ephrinB2-Fc. e) Representative images of imNSC1 migration towards Fc-antibody control (Fc) and ephrinA5/ephrinA1-Fc ligands respectively. f) Representative phase contrast images of imNSC1 and GSC1 migration towards an ephrinB2-Fc coat (left) .Quantification of the ratio of cell densities 200 μm before and after the boundary. (right)

tive to the repulsive cues of ephrinB2. Instead, they readily migrated over the coated protein layer and were not compartmentalised (**Figure 12f**). We again repeated these experiments using imNSC2 and GSC2 obtaining identical results. To quantify this behaviour we calculated the ratio of cell densities 200 μm before and after the coated ephrinB2-Fc layer. This quantification was a robust measurement showing that there is virtually no degree of compartmentalisation in GSC1 cells, as the cell densities on both sides of the ephrinB2-Fc layer were nearly identical (ratio near 100 percent). In stark contrast, the ratio dropped to almost zero in imNSC1 cells which were completely repelled (**Figure 12f**). We next wanted to test whether ephrinB2 is not only sufficient, but necessary, to induce compartmentalisation of imNSCs. For this we knocked down *Efnb2* in endothelial cells using siRNA (**Figure 13a**). Intriguingly, the knockdown severely disrupted their ability to compartmentalise imNSC1. This resulted in a significantly longer boundary (**Figure 13a**).

Having observed this novel compartmentalisation mechanism *in vitro* we wanted to assess whether ephrinB2 on endothelial cells also controls migration of imNSCs *in vivo* . For this we used mice bearing a $EfnB2^{flox/flox}$ allele combined with an inducible CreERT2-cassette under control of the endothelial cell specific VE-Cadherin promoter. This enabled us to specifically remove ephrinB2 from the vasculature by inducing recombination using tamoxifen injections. Two weeks after recombination we injected GFP labelled imNSC1 under a cranial window in these mice and monitored the migratory behaviour of GFP positive cells using 2-photon microscopy. Remarkably, genetic deletion of *Efnb2* on the vasculature enabled robust perivascular migration of single imNSC1 cells *in vivo* (**Figure 13b**). We quantified the total distance cells migrated perivascularly. This confirmed that imNSC1 in knockout mice indeed migrated significant distances along blood vessels albeit to a slightly lesser extent than GSCs in wild type mice (**Figure 13c**).

We therefore conclusively show that endothelial ephrinB2 compartmentalises normal neural progenitor cells and that ephrinB2 is both necessary and sufficient for this compartmentalisation response *in vitro* and *in vivo* .
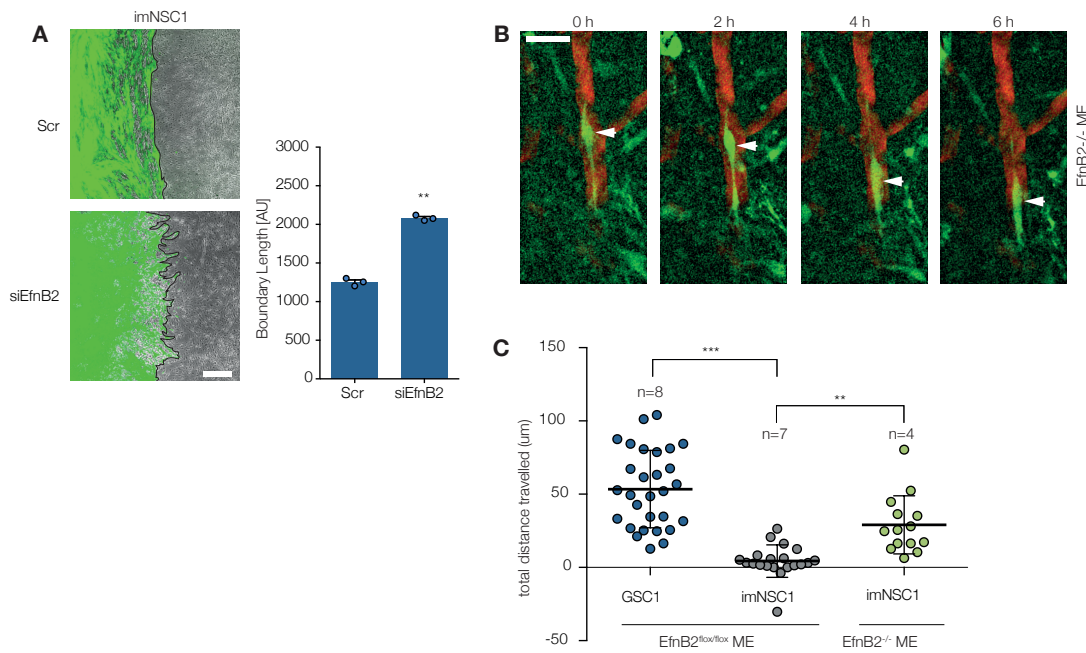
**Figure 13:** **Endothelial specific knockdown of ephrinB2 enables perivascular invasion of normal neural progenitors**.  a) Representative images of imNSC1 and GSC1 migrating towards coated ephrinB2-Fc ligand (left).  Quantification of the respective cell densities before/after the boundary (right).  b) Intravital 2-Photon stills of GFP-labelled imNSC1 cells injected into the cortex of endothelial specific EfnB2 knockout mice (EfnB2-/- ME) and imaged 7 days post injection over 6 hours through an intracranial window at a depth of 200 μm.  c) Quantification of the total distance travelled by perivascular migrating cells in wildtype (EfnB2 flox/flox ME) and endothelial specific EfnB2 knockout mice (EfnB2-/- ME)

# 5.2    Upregulation of ephrinB2 drives perivascular invasion of GSCs

Intriguingly, both our *in vitro* migration assay and the *in vivo* 2-photon microscopy showed that cells with impaired Ras signalling (GSC1,GSC2) became insensitive to compartmentalisation by endothelial ephrinB2. We reasoned, that changes in Eph/ephrin levels on GSCs might underly this change in behaviour, as a similar behavioural change has previously been reported in prostate cancer (Astin et al., 2010). We therefore analysed the expression levels of all Eph receptors and ephrin ligands using quantitative RT-PCR. We included control vector infected cells in our analysis to rule out changes induced by abnormal p53 and Rb signalling in imNSC12 which are unrelated to perivascular invasion. This analysis revealed that p53 and

Rb inactivation did not change the composition of Eph receptors and ephrin ligands substantially. Aberrant ras signalling did, however, cause strong downregulation of *Ephb2* receptor and a parallel upregulation of *Efnb2* ligand. The changes in EphA and ephrinA composition were more subtle, however an upregulation of *Efna5* and downregulation of *Epha4* could be detected at RNA level in GSC1 (**Figure 14a**). Overexpression of constitutively active kinase like h-ras might cause loss of their substrate specificity (Hindley and Kolch, 2002). This, in turn, could alter the expression of genes which are not functionally related in a physiological context but mere artefacts of the exogenous expression of high levels of an oncogene. To exclude this possibility we performed the same analysis on imNSC2 and GSC2 cells and obtained very similar results (**Figure 14b**), again seeing a upregulation of *Efnb2* and *Efna5* ligands, a significant downregulation of *Ephb2* receptor but no changes in *Epha4* levels.

We performed immunoblotting analysis to see whether the changes at RNA level are mirrored at protein level. This revealed that only EphB2 and ephrinB2 changed significantly whereas ephrinA5 and EphA4 protein levels remained unchanged in GSC1 (**Figure 14c**). We therefore concentrated on EphB2 and ephrinB2 as candidates which might be responsible for the loss of compartmentalisation in GSCs.

We first tested whether the downregulation of EphB2 was responsible for cells to become insensitive to compartmentalising stimuli by ephrinB2. For this we overexpressed EphB2 in GSC1 and monitored the migration of these cells towards a coated layer of ephrinB2-Fc using live-cell imaging. To quantify the expected shifts in phenotype we transformed the obtained live cell images into two dimensional space-time plots called kymographs. This produces a representation of a spatial position over time, with time being represented on one axis and the spatial axis set parallel to the direction of migration. The velocity of the forward edge of the migrating cells is therefore represented as the angle in relation to the horizontal. In cells exhibiting a compartmentalisation response a sharp change in the angle of progression ending in a line parallel to the time axis is observed, representing an un-shifting boundary over time. Cells which are insensitive to ephrinB2 continue to migrate at similar velocities upon
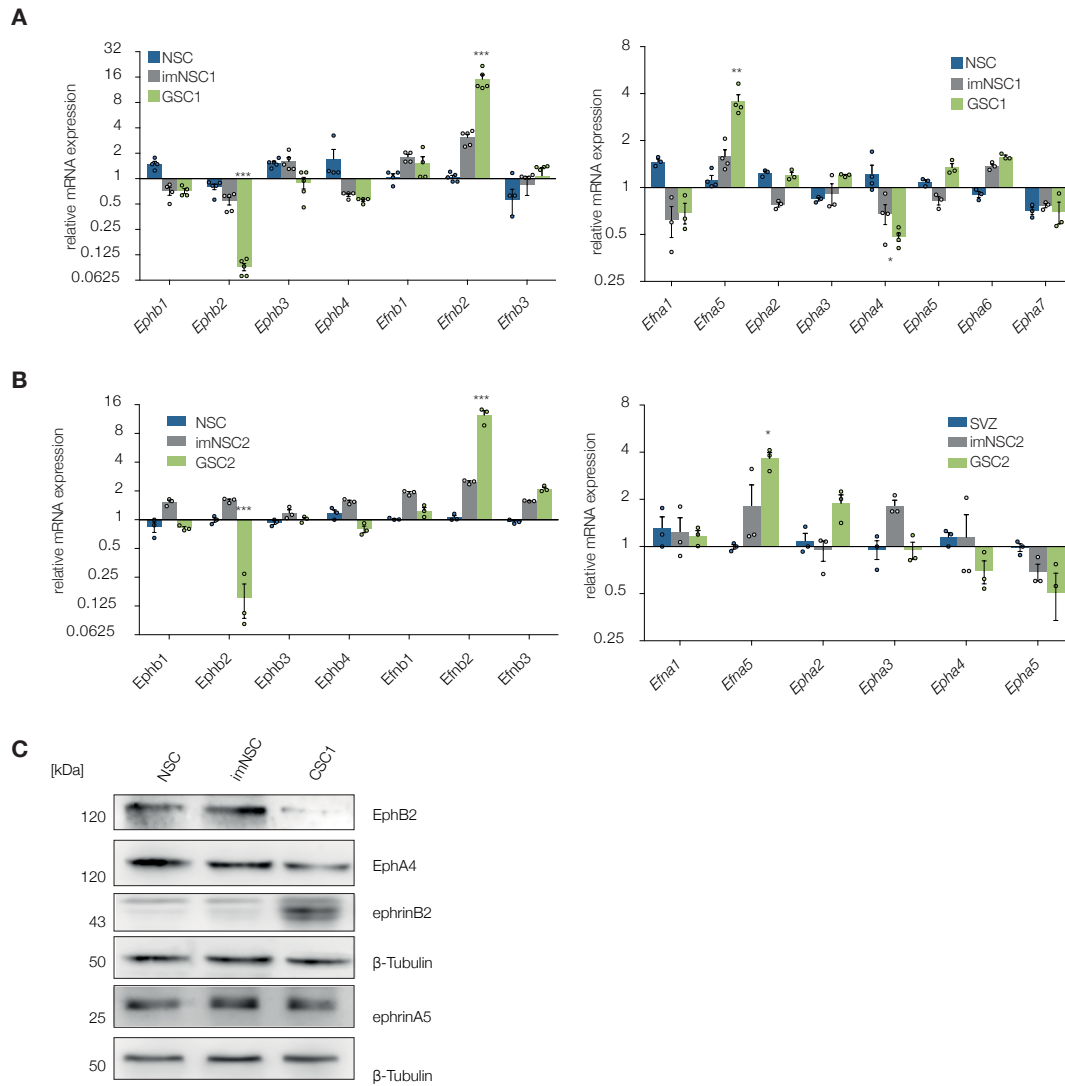
**Figure 14: Eph and ephrin levels change in a ras/Erk dependent manner in GSCs.** a,b) quantitative RT-PCR analysis of eph/ephrin levels in normal neural stem cells (NSC), imNSC1/2 and GSC1/2. error bars denote s.e.m. one way anova. c) Immunoblotting analysis of selected Eph receptors and ephrin ligands.

encountering the boundary and the angular change is therefore less pronounced or absent (**Figure 15a**). From these kymograph images we could then obtain the cell densities at any given point in time by plotting a brightness profile of a single line (i.e. single time point). This proved to be a very robust measurement of the degree of compartmentalisation as the ratio of cell densities 200 μm before/after the ephrinB2-Fc was close to 1 in GSC1 and 0 in imNSC1 respectively, giving us a broad range to quantify intermediate phenotypes (**Figure 15b**).

Surprisingly, overexpression of EphB2 in GSC1 did not change the migratory behaviour and the cells were still able to migrate over an ephrinB2 boundary (**Figure 15c**).

As EphB2 overexpression in GSC1 and genetic deletion of *Efnb2* in imNSC1 had no effect on the migration of these cells we next tested the role of ephrinB2. Remarkably, overexpression of ephrinB2 in imNSC1 was sufficient to overcome the compartmentalisation of imNSC1, and led to a migration pattern very similar to fully transformed GSC1 cells (**Figure 15c**). Conversely, genetic deletion of *Efnb2* in GSC1 completely restored boundary formation and the migratory behaviour of these cells was indistinguishable from imNSC1 control cells (**Figure 15c**).

We then tested whether ephrinB2 levels are also causative for the phenotypical changes observed in boundary formation with endothelial cells. Indeed, overexpressing ephrinB2 in imNSC1 was again sufficient to strongly interrupt boundary formation with bMVECs resulting in a much longer boundary than control cells. Mirroring this result, genetic deletion of *Efnb2* rescued the compartmentalisation phenotype in GSC1 cells and resulted in a straighter and better defined boundary when interacting with endothelial cells (**Figure 15d**).

As a next step we injected imNSC1 overexpressing full length ephrinB2 (imNSC1-EfnB2) and ephrinB2 knockout GSC1 (GSC1-*Efnb2*$^{-/-}$ ) intracranially into syngeneic mice and monitored their perivascular migration behaviour using 2-Photon microscopy. Strikingly we could observe the exact same behaviour as in our *in vitro* assay: ephrinB2 overexpression is sufficient to induce robust migration of otherwise stationary imNSC1 and genetic knock-
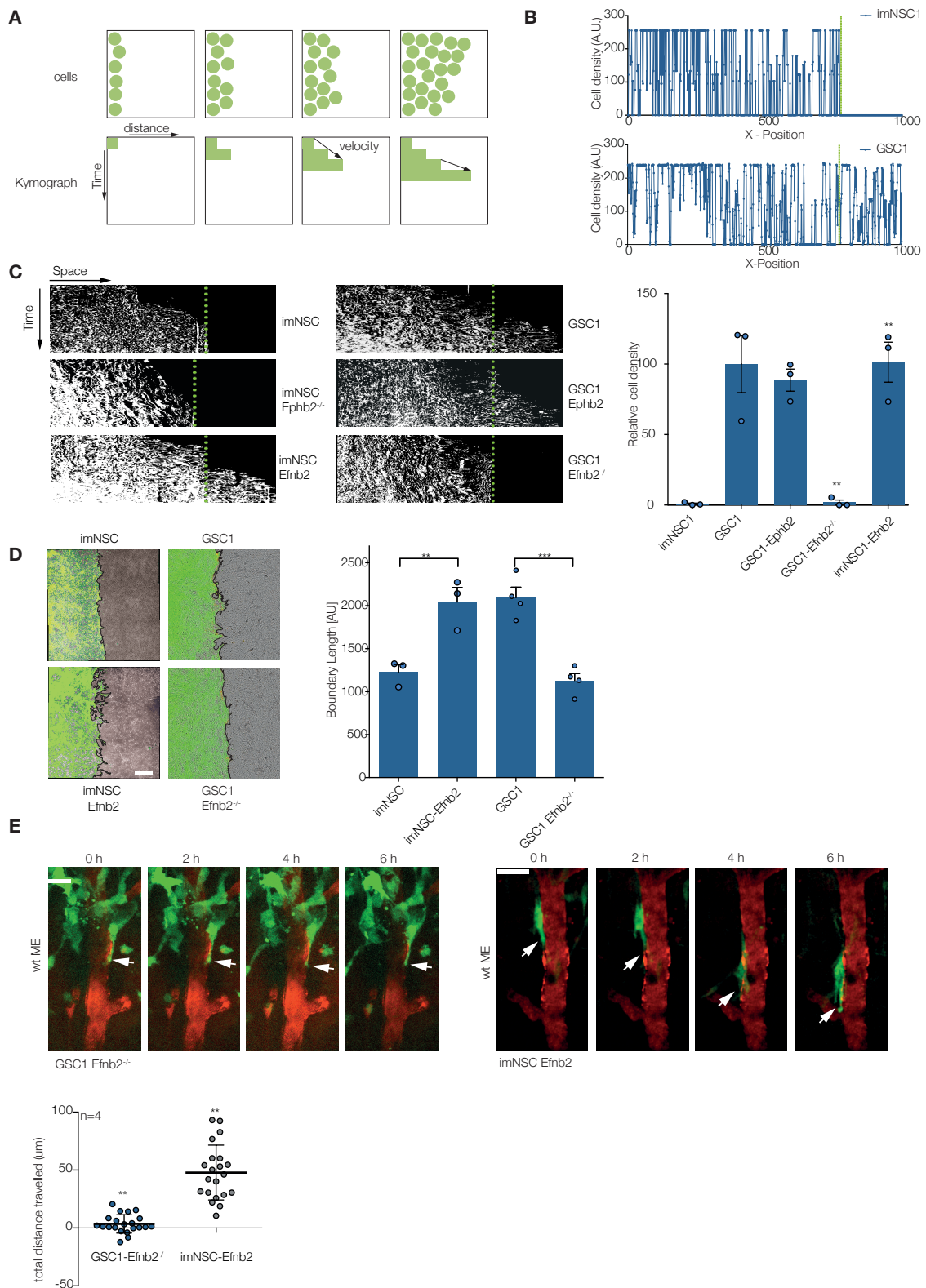
**Figure 15: EphrinB2 is necessary and sufficient to enable perivascular invasion.** a) Schematics detailing the transformation of a time lapse video into a two dimensional space-time plot called kymograph. b) Cell density plots of imNSC1 and GSC1 obtained from kymographs. c) Kymographs from time-lapse experiments of the indicated cell types migrating against coated ephrinB2-Fc over 60 h. Quantification of the kymographs is shown on the right. Error bars denote s.e.m. one way anova with tukey post hoc test. d) Representative images of imNSC1/GSC1 (green) migrating towards primary endothelial cells (unstained) (left). Quantification of the boundary length after 60 h. Error bars denote s.e.m. (right) e) Intravital 2-Photon stills of GFP-labelled imNSC1 and GSC1 cells injected into the cortex of syngeneic mice (top). Quantification of the total distance migrated. one way anova with tukey post hoc test (bottom).

out of ephrinB2 on GSC1 rescues compartmentalisation and renders these cells incapable of invading along vascular structures (**Figure 15e**).

Our observations show conclusively that escape from endothelial compartmentalisation *in vivo* is mediated by overexpression of full length ephrinB2 in GSCs.

## 5.3 EphrinB2 upregulation is dependent on Mek/Erk signalling and SP1 transcription factor

We wanted to further our understanding of the relationship between aberrant ras signalling and ephrinB2 overexpression in GSC1/2. We therefore tested a number of inhibitors targeting downstream effectors of ras: UO126 to inhibit MEK, Ly294002 to inhibit PI3K and JnkiII to inhibit Jnk-signalling. Whereas inhibition of PI3K and Jnk did not have an effect on ephrinB2 expression, UO126 significantly decreased ephrinB2 expression both on protein and RNA level (**Figure 16a,b**). UO126 did not alter the mRNA expression levels of any other ephrin ligand or Eph receptor and treatment with UO126 only marginally affected *Efnb2* expression levels in imNSC1 (data not shown). Again we repeated this experiment in our second model, GSC2, and obtained very similar results (**Figure 16b**).

In addition, we performed an unbiased *in silico* analysis of the murine *EfnB2* promoter to identify binding sites for transcription factors which become activated by MAPK signalling. We used the TRANSFAC database to score the potential binding sites (Heinemeyer et al., 1998). Amongst the highest scoring hits using this algorithm was SP1 with predicted binding sites over the full length of the *Efnb2* promoter (**Figure 16c**). SP1 is a known activating transcription factor which has been described extensively to act downstream of MAPK signalling (Tan and Khachigian, 2009). We therefore hypothesised that SP1 might mediate the upregulation of ephrinB2 through increased binding to the ephrinB2 promoter. To test this hypothesis we performed chromatin immunoprecipitation (ChIP) with a SP1 specific anti-
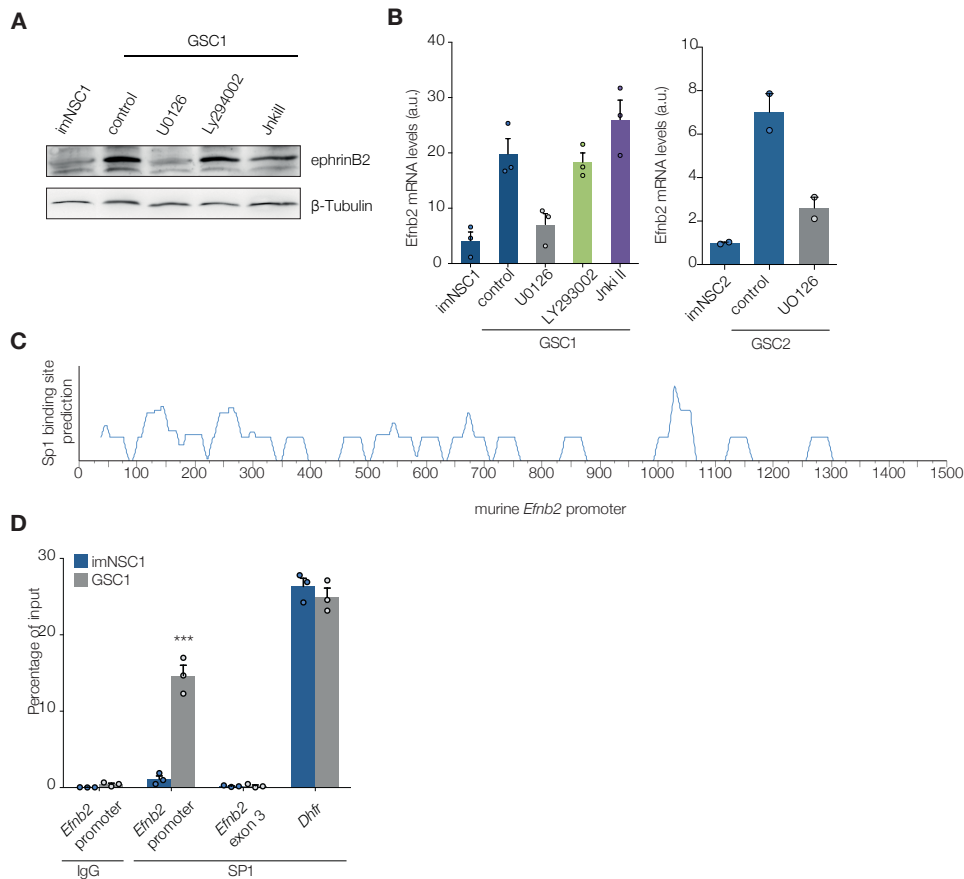
**Figure 16: Mek/Erk and SP1 control upregulation of ephrinB2**. a) Western Blot analysis of ephrinB2 levels in response to different inhibitors after overnight stimulation. b) Quantitative RT-PCR analysis of *Efnb2* levels in response to different inhibitors after overnight stimulation in GSC1 (left) and GSC2 (right) c) Predicted Sp1 binding sites shown as an overlay on the murine *Efnb2* promoter sequence d) Quantitative RT-PCR analysis of ChIP pulldowns using either control antibody (IgG) or an antibody specific for the SP1 transcription factor (SP1). Error bars denote s.e.m. one way anova with tukey post hoc test.

body and amplified the bound DNA using primers targeting the murine *EfnB2* promoter. A strong increase in SP1 binding throughout the whole length of the EfnB2 promoter was observed in GSC1 cells compared to imNSC1 cells. This increased binding was specific for the promoter region as no difference was observed using primers targeting exon 3, and similar levels of binding were observed for the promoter of the ubiquitously expressed DHFR gene (**Figure 16d**).

Thus we conclude that ephrinB2 expression in GSCs is dependent on aberrant ras/NF1 signalling which activates the MAPK signalling cascade. This in turn causes recruitment of SP1 to the *Efnb2* promoter and results in upregulation of ephrinB2 in tumourigenic cells.

## 5.4 Elevated ephrinB2 levels in GSCs cause hyperactivation of EphB signalling and insensitivity to migratory cues mediated by the vasculature

One of the key questions of the loss of compartmentalisation in GSCs was the exact mechanism that causes them to become insensitive to endothelial ephrinB2 and enables transformed cells to invade perivascularly. To gain insights into the potential mechanisms underlying this change in behaviour we analysed cells coming into contact with the ephrinB2-coating in greater detail. Interestingly we found that irrespective of the fact that all GSC cells eventually migrate into the ephrin-B2 coated well, a small percentage of cells was repelled on first contact with the recombinant ligand (**Figure 17a**).

A closer look at cells reaching the ephrinB2-Fc layer revealed an intriguing cell-contact dependent behaviour of tumour cells which migrate over the boundary: Whereas single cells, and cells in small groups, are invariably repelled independent of cell type, migration in larger groups of cells causes a switch in behaviour in tumour cells which renders them insensitive to the ephrinB2 ligand and enables migration into the coated well. In stark contrast,
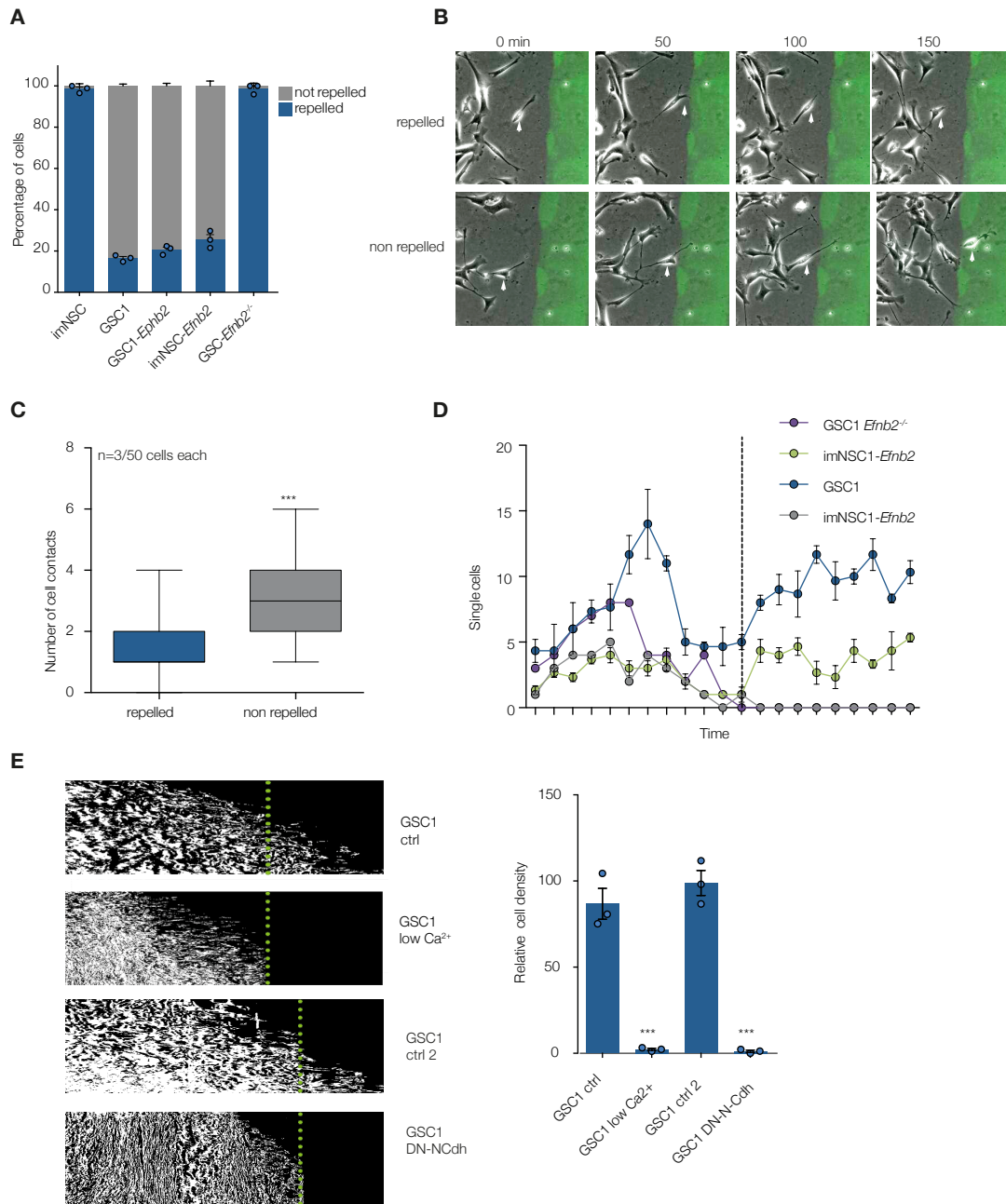
**Figure 17: The response to compartmentalisation signals by ephrinB2 is lost in a homotypic contact dependent manner**. a) Quantification of the initial response upon contact with ephrinB2. Error bars denote s.e.m. b) Stills of time lapse movies of cells contacting ephrinB2 boundary. c) Quantification of the number of contacts cells had in relation to their response shown in b. Error bars denote St.D., students t-test d) Quantification of the number of single cells at a given time point. n=3, error bars denote s.e.m. e) Kymographs of cells cultured in Calcium depleted media ($Ca^{2+}$) or transfected with dominant negative N-Cadherin (DN-NCdh) (left), Quantification of the kymographs is shown on the right. Error bars denote s.e.m. Student's T-test.

imNSC1s failed to overcome compartmentalisation independent of the number of cell contacts (**Figure 17a,b**). We therefore specifically quantified the number of cell-cell contacts of cells at the time of first contact with the ephrinB2 layer and found a strong correlation between the number of contacts and the outcome of the interaction between cells and ephrinB2 ligand: Cells which were repelled had an average of 1.57 cell contacts at the time of repulsion whereas non repelled cells contacted 3.32 adjacent cells on average when migrating over the ephrinB2 boundary (**Figure 17c**). To confirm this we quantified the number of cells which migrated as single cells and tracked the changes in each cell population over time. In all cell types a significant decrease of singly migrating cells was observed at the ephrin-B2 boundary (**Figure 17d**). This shows again, that all cells migrating alone or in small groups are repelled, which causes cells to "pile up" at the edge of the coated well. GSC1 and imNSC-*Efnb2* however, overcome this compartmentalisation through homotypic cell contacts which pushes adjacent cells over the boundary. As soon as cells are in full contact with the ephrinB2-Fc ligand, no bias towards a more grouped migration was observed and the percentage of single cells returned to normal levels.

To test the hypothesis that homotypic cell interactions are indeed responsible for the loss of compartmentalisation we cultured GSC1 cells in $Ca^{2+}$ depleted conditions and in a second experiment infected them with dominant negative N-Cadherin, the primary mediator of cell-cell adhesions in these cells. Both methods fully restored boundary formation whereas the respective control treatment did not affect the migration (**Figure 17e**). Thus we concluded that homotypic cell-cell interactions between GSCs cause a change in behaviour dependent on ephrinB2 overexpression resulting in insensitivity to compartmentalising signals mediated by endothelial ephrinB2.

As Eph/ephrin signalling is bidirectional, two possibilities arose: Increased ephrinB2 levels cause increased forward signalling and Eph phosphorylation through homotypic cell interactions resulting in a desensitisation to extrinsic ephrinB2, or higher levels of ephrinB2 cause increased reverse signalling through ephrinB2 itself altering the cell behaviour. To answer this

question we generated imNSC1 cells overexpressing a truncated version of ephrinB2 lacking the intracellular domain (imNSC-$\Delta$ C*EfnB2*). As the specific vector used did not contain any selection markers we used two complementary strategies to obtain a pure population expressing the truncated ephrinB2 construct: In the first approach we seeded imNSC1 infected with $\Delta$C *EfnB2* in clonal dilution and checked the clones for the presence of *EfnB2* cDNA (**Figure 18a**). The positive clones were then pooled and used for experiments. In the second approach we infected imNSC2 cells with the same vector, after infection stained these cells with an antibody detecting the extracellular portion of ephrinB2 and FACS sorted cells with high ephrinB2 expression levels. The sorted population was again checked for ephrinB2 expression using FACS staining and then used for experiments (**Figure 18b**). Both strategies yielded populations with a high level of $\Delta$C*Efnb2* overexpression as confirmed by Western blotting and FACS analysis (**Figure 18b,c**) Interestingly, overexpression of this truncated construct was sufficient for cells to escape compartmentalisation by ephrinB2 (**Figure 18d**) suggesting that Eph forward signalling is responsible for this phenotype. To confirm this we performed immunoblotting analysis to detect phosphorylated (i.e. activated) Eph receptors in these cultures. If ephrinB2 expression indeed activates Eph forward signalling higher phosphorylation levels are expected in these cultures. Indeed, while imNSCs only showed low basal levels of Eph activation (p-Eph), GSC1 and imNSC1-*Efnb2* displayed constitutively high p-Eph levels. We cultured these cell in $Ca^{2+}$ depleted conditions to assess whether this phosphorylation was dependent on cell-cell contacts, or whether ephrinB2 expression causes phosphorylation of Eph receptors on the same cell. Culture in low $Ca^{2+}$ reduced the levels of Eph phosphorylation in GSC1 and imNSC1-*Efnb2* to the basal levels of imNSC1 cells.

We aimed to understand how these higher basal levels affect the response of GSC1 cells to stimulation through extrinsic ephrinB2 expressed on endothelial cells. Interestingly, the high basal levels of Eph phosphorylation in GSC1 cells seemed to be saturating, as neither co-culture with endothelial cells nor with ephrinB2-ligand could stimulate a further increase Eph signalling in GSC1. This desensitisation was entirely dependent on the presence of ephrinB2 on GSCs as genetic deletion of *EfnB2* in GSC1 reduced basal levels to normal and fully
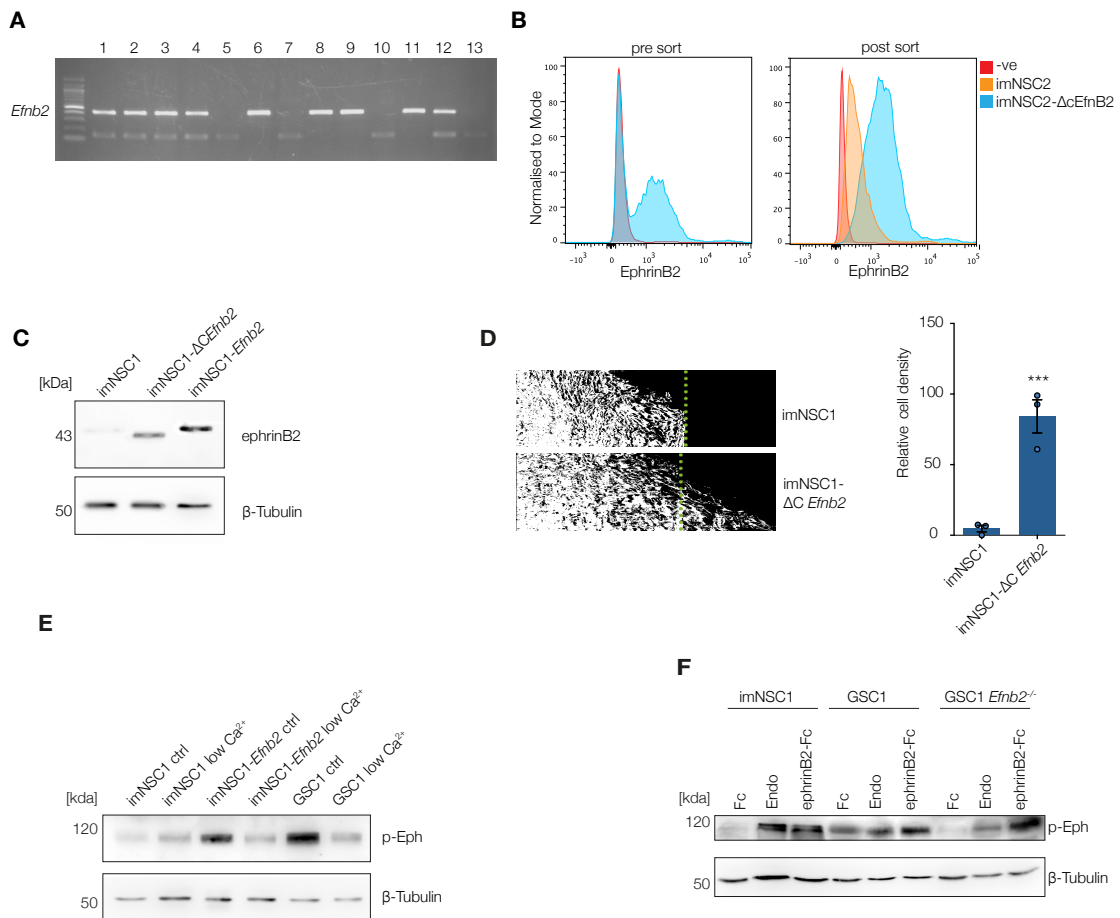
**Figure 18: EphrinB2 upregulation in GSCs desensitizes them to vascular repulsion by saturating Eph forward signalling**. a) Exemplary agarose gel of different clonally expanded imNSC1 cultures infected with Δ C*EfnB2*-vector. b) FACS profiles of cells stained with either secondary antibody control (-ve) or with an ephrinB2 specific antibody. imNSC2-Δ C*EfnB2* are shown before sorting (pre sort, left) and after FACS sorting (post sort, right) c)Western analysis of imNSC1 overexpressing either truncated ephrinB2 (Δ C*EfnB2*) or full-length protein (*Efnb2*) d) Kymographs showing the response of imNSC and imNSC overexpressing intracellular deleted ephrinB2( ΔC *Efnb2* (left). The quantification of the Kymographs is shown on the right. Error bars denote s.e.m. Students T-test. e) Representative western blot of the levels of phosphorylated Eph (p-Eph) of cells cultured in normal growth medium (ctrl) or calcium depleted medium (low $Ca^{2+}$) f) western blot analysis denoting cells cultured on Fc-control antibody (Fc), a mononlayer of endothelial cells (Endo) or 4 µg coated ephrinB2-Fc ligand (ephrinB2-Fc).

restored Eph stimulation by endothelial cells or ephrinB2-ligand **Figure 18f**).

Ephs are well known mediators of cell migration and are known to mediate repulsion between adjacent cells (Pasquale, 2008). To observe potential changes in the repulsive behaviour in our system we sparsely seeded imNSCs and GSCs and monitored their migration behaviour using live cell imaging. We observed a greater scattering of GSCs compared to imNSCs indicating either faster migration or increased homotypic repulsion (**Figure 19a**). To determine the cause we closely monitored head-on cell collisions between two cells and recorded their velocity 100 minutes before and 100 minutes after collision. Intriguingly, while their is no significant difference in the speed of migration before collision between imNSCs and GSCs, GSCs migrate significantly faster immediately after a collision and only return to their normal velocity about 150 minutes afterwards. In stark contrast, imNSCs continue to migrate at similar velocities before or after collision, even though these cells are still repelled upon collision. This is apparent as a change in their angular movement, resulting in a directed migration away from the point of collision.

To test whether this behaviour is indeed dependent on ephrinB2 overexpression we quantified the relative velocities of imNSC-*Efnb2* and GSC-*Efnb2*$^{-/-}$ before and after homotypic cell collisions. Again we observed that ephrinB2 is necessary and sufficient to induce the increased repulsion between cells as imNSC-*Efnb2* showed higher velocities after collisions whereas GSC-*Efnb2*$^{-/-}$ showed no such increase, and post-collisions velocities were similar to imNSCs (**Figure 19b**). As a second measurement we also recorded the time cell-protrusions from adjacent cells remained in contact after initial contact. A significant decrease in the contact time was observed in GSC1 cells compared to imNSC1: Whereas imNSC1 retained contacting protrusions for an average of 105 minutes GSC1 protrusions of contacting cells collapsed after only 41 minutes averagely. This, we interpreted as further proof of increased homotypic repulsion in GSCs (**Figure 19c**). Again, we wanted to assess wether this behaviour is purely dependent on the presence of ephrinB2. For this we also quantified the time imNSC-*Efnb2* and GSC-*Efnb2*$^{-/-}$ remain in contact after homotypic collisions. Indeed, whereas
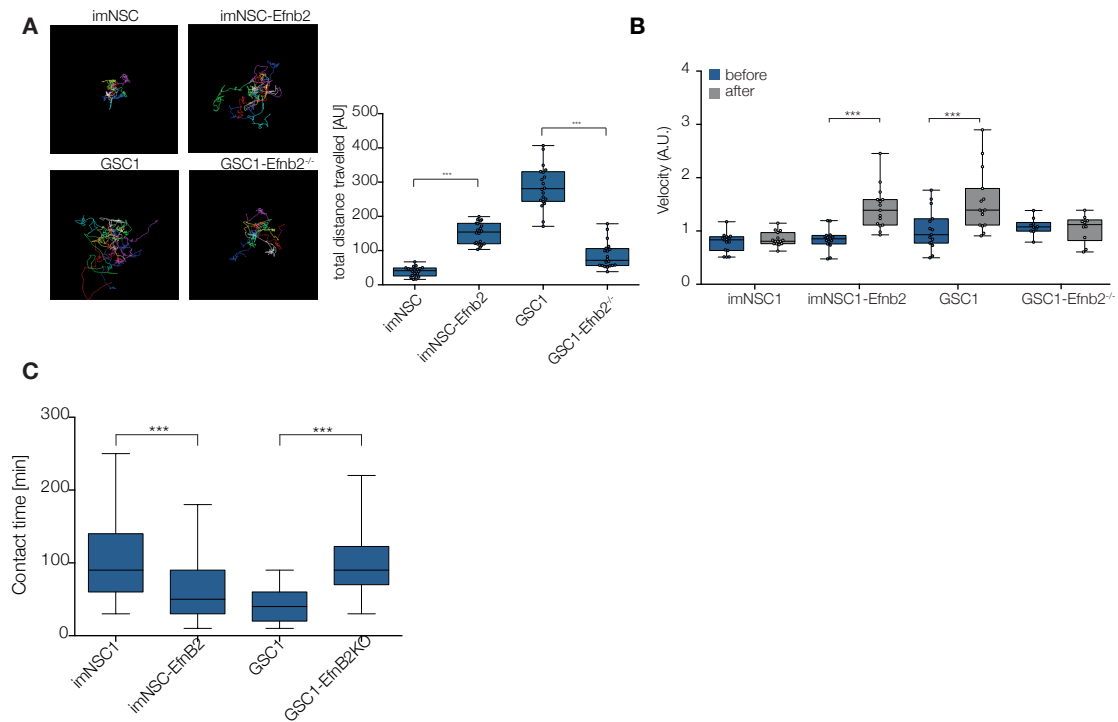
**Figure 19: Increased Eph forward signaling leads to increased repulsion and cell scattering**. a) Quantification of the velocities of indicated cells 100 minutes before (blue) and after (grey) head-on homotypic collisions in sparse culture. Error bars denote St.D., One-way anova with bonferonni post-hoc test. b) Quantification of the time contacting projections of adjacent cells remained stable. Error bars denote St.D. One way anova with tukey post-hoc test. c) Representation of the migration of tracked cells over 20 hours transformed into a common coordinate system (left). Quantification of the total migrated distance (right). Error bar denotes St.D., One way anova.

imNSC-*Efnb2* showed decreased contact times of only about 57 minutes, genetic deletion of *EfnB2* restored prolonged homotypic cell contacts and the average time GSC-*Efnb2$^{-/-}$* retained contacting protrusions was increased to 105 minutes, almost identical to the behaviour imNSC1 showed. (**Figure 19c**).

From this we conclude that increased ephrinB2 levels in GSCs lead to saturated levels of Eph phosphorylation rendering them insensitive to additional stimuli by endothelial cells. This process is accompanied by an increased repulsion between GSCs, resulting in greater scattering.

## 5.5 Conclusion

One hallmark of glioblastoma is their ability to extensively invade along preexisting structures, predominantly the vasculature in a process called perivascular invasion. Perivascular invasion is not only one of the most important mechanisms of glioma invasions but also critical during early primary glioma growth (Baker et al., 2014). In this chapter we identified ephrinB2 as a critical mediator of glioma perivascular migration. High levels of ephrinB2 signalling have previously been linked to an invasive phenotype (Nakada et al., 2010). However, while this emphasises the importance of ephrinB2 in GBM pathogenesis it remained unclear which exact mechanisms enable perivascular invasion in the context of the complex microenvironment of the brain. Intriguingly we found that while non-transformed cells readily associate with the abluminal side of the blood vessels, they are unable to migrate along the vascular space. This causes a compartmentalisation of immortalised neural progenitor cells which is consistent with previous observations that show that normal SVZ precursors actively home to the vasculature but remain stationary after initial contact is made (Shen et al., 2008; Nie et al., 2010). Mechanistically we found that ephrinB2 ligands on vascular endothelial cells mediate this compartmentalisation, which restricts the migration of SVZ progenitors by activation of Eph forward signalling. It is tempting to speculate that this compartmentalisation is also important for maintaining the proper niche structure in physiological stem cell niches like the subventricular zone, where ephrin ligands and receptors are known to be expressed on contacting endothelial cells and type B progenitor cells respectively (Ottone et al., 2014), and ablation of Eph receptors leads to abnormal polarisation and cell positioning (Chumley et al., 2007; Laussu et al., 2014).

A very similar role for Eph forward signalling has been reported in a variety of stem cell niches (Genander and Frisén, 2010; Genander, 2012) and interestingly it has been shown that this same signalling pathway also aids in constraining the migration of premalignant cells in a variety of tissues: in agreement with our study, activation of Eph signalling through ephrinB2

ligands in the surrounding normal tissue inhibits expansion and invasion of incipient lesions in colorectal cancer (Cortina et al., 2007). A similar mechanism has also been observed during prostate cancer development in that ephrin ligands on stromal cells repel normal and non-metastatic cells (Astin et al., 2010). Our findings therefore further strengthen the notion that during early tumourigenesis ephrins expressed in the normal tissue mediate tumour suppressive effects. We also identified the vasculature as a critical mediator of these effects. Given the ubiquitous expression of ephrins on endothelial cells it is tempting to propose a more general tumour suppressive mechanism of the vasculature which acts by limiting the expansion of incipient lesions via ephrinB2 signalling.

In striking contrast to the compartmentalisation observed in non malignant cells, transformation overrides vascular compartmentalisation and enables perivascular invasion of glioma cells. This has previously been observed by others but so far studies were limited to the observation of a phenotype without being able to explain the underlying mechanism (Farin et al., 2006; Winkler et al., 2009). It is important to note that invading glioblastoma cells almost invariably have direct contact with endothelial cells and not other cell types lining the vasculature, therefore validating our *in vitro* model (Watkins et al., 2014). We conclude that the ability of GSC to escape endothelial compartmentalisation depends on constitutive Eph forward signalling elicited by elevated ephrinB2 through homotypic cell-cell interactions within the tumour cell population. This in turn desensitises the receptor to further activation, thereby overriding the repulsion exerted by endothelial ephrinB2 and enabling unimpeded perivascular migration. This reliance on homotypic cell interactions is in agreement with other studies showing that phosphorylation of the EphB2 receptor promotes migration and invasion in glioblastoma(Nakada et al., 2004). Furthermore, the increase in ephrinB2 expression leads to increased homotypic repulsion between GSCs. This causes greater scattering of GSCs, i.e. "pushes" single cells out of a compact tumour mass leading to increased dissemination of single cells, promoting diffuse infiltration of surrounding healthy tissue as observed previously (Winkler et al., 2009).

EphrinB2 overexpression causes increased invasion along the vasculature by desensitising the cells to repulsion by extrinsic ephrinB2 expressed on endothelial cells and secondly enhances the general motility of GSCs by increasing homotypic repulsion. This ``hijacking'' of the signalling pathway through which the vasculature normally compartmentalises healthy tissues differs significantly from previous reports. It has been mentioned in studies investigating colorectal and prostate cancer invasion (Astin et al., 2010; Cortina et al., 2007) that tumour spread mainly depends on the downregulation of Eph receptors in a cell autonomous manner, whereas in our GBM model GSCs augment their tumourigenic potential in a non-cell-autonomous fashion through constitutive activation of Eph forward signalling. This suggests substantially different mechanisms to evade ephrin repulsion and subsequent compartmentalisation escape depending on the cancer type.

Thus we have, so far, shown that endothelial ephrinB2 is a critical tumour suppressor in early stages of tumour development by compartmentalising normal neural stem cells and limiting their proliferative potential. In later tumour stages, however, ephrinB2 upregulation on the tumour cells themselves overrides this compartmentalisation leading to extensive perivascular invasion.

# Chapter 6

# Cell autonomous Ephrin signalling

## 6.1  EphrinB2 is a glioblastoma oncogene

Given the important role of ephrinB2 in perivascular invasion we asked whether its expression might also have an effect on tumourigenicity. To this end we aimed to study the kinetics of tumour progression non-invasively using whole-body bioluminescence imaging of Luciferase tagged tumour cells. We first performed a pilot experiment by injecting $1 \times 10^5$ GSC1 intracranially in C57Bl6 mice to determine the right dose and length of incubation time following intraperetoneal injection of D-Luciferin substrate. We tested doses ranging from 1 to 6 mg D-Luciferin on the same set of three animals and measured the emitted photons over a period of 30 minutes in one minute intervals. Doses below 2 mg showed a significantly weaker signal over time, however the strength of the signal did not increase linearly at high doses (**Figure 20a**): whereas almost no difference could be observed between 6 and 2 mg of D-Luciferin a strong reduction in the maximal signal intensity from $2.2 \times 10^7$ to $1.5 \times 10^7$ photons/s/cm² was observed using 1 mg of D-Luciferin. The amount of photons emitted increased steadily over time in all tested concentrations and reached a plateau at about 10 minutes after injection. The signal intensity then remained relatively stable for 10-15 min-

utes independent of the injected amount before it began to decrease again. This is a typical pattern observed with luciferin based imaging methods (Kemper et al., 2006). From this set of experiments we decided to choose a dose of 2.4 mg of D-Luciferin and image 10 minutes after injection of the substrate. We additionally tested whether imaging the fluorescent GFP signal instead of measuring the luminescence was sufficient to image the tumours with high confidence as this would have significantly reduced the time each animal had to be kept under anaesthesia. We were able to detect signals in all mice using fluorescent imaging however as the signal to noise ratio was about 4-fold less using Epi-Fluorescence than with Luminescence and a strong unspecific signal was detected around the ears and snout, we decided to continue using Luciferase based imaging (**Figure 20b**).
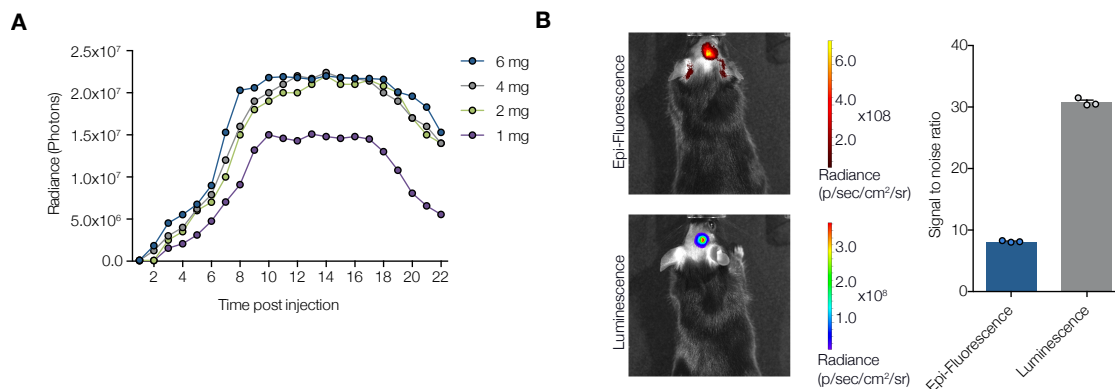


**Figure 20: Optimisation of IVIS imaging for monitoring of tumour growth**. a) Time course of bioluminescence intensities following injection of different amounts of D-Luciferin substrate b) Representative images showing the same tumour imaged using GFP-Fluorescence (top left) or bioluminescence following injection of 2.4 mg D-Luciferin (bottom left). Quantification of the signal-to-noise ratio in the obtained images (right). Error bars depict S.D.

To then study the effect of ephrinB2 on tumour growth we injected $5 \times 10^4$ luciferase tagged imNSC1, imNSC1-EfnB2, GSC1 and GSC1-EfnB2$^{-/-}$ into the putamen of Cd1-nude mice and non-invasively monitored their growth over time by measuring the increase of the Luciferin signal. We chose to use immunocompromised mice as injection of GSC1 into immunocompetent mice only generated tumours with a penetrance of 56 % in our tumourigenicity studies (see **Chapter 3**). The incomplete penetrance precludes rigorous assessment of the tumourigenic potential of lines derived from GSC1 cells in a syngeneic environment. Surprisingly, quantitative imaging revealed a complete dependence of tumour formation on

the presence of ephrinB2: while imNSC1 control cells did not form tumours, overexpression of ephrinB2 was sufficient to enable survival and proliferation of these cells *in vivo* as indicated by an increase of emitted photons over time (**Figure 21a**). Mirroring this, GSC1 cells readily proliferated *in vivo* whereas their ephrinB2 knockout counterpart GSC1-*Efnb2*$^{-/-}$ showed no increase in the Luciferin signal and initially an almost complete regression of the observable cell mass (**Figure 21a**).

This data was supported by the Kaplan-Meier survival analysis we performed (**Figure 21b**): mice injected with GSC1 tumours died within a median time of 24.7 days whereas all imNSC1 animals survived tumour-free beyond 150 days. Surprisingly, imNSC1-*Efnb2* tumours resulted in a similar median survival as GSC1 (28 days) . In stark contrast, GSC1 *Efnb2*$^{-/-}$ developed lesions with much slower kinetics in 7 out of 9 mice (median survival: 62 days) while the remaining two mice remained tumour free beyond 150 days. This suggests that ephrinB2 is a *bona fide* oncogene which can substitute for oncogenic Ras in mesenchymal glioblastoma.

To dissect the mechanisms involved in transformation by ephrinB2 we performed *in vitro* soft-agar assays. Growth in semi solid soft-agar mimics the loss of anchorage and niche specific signals *in vivo* and is thought to be a valid *in vitro* measure for *in vivo* tumourigenicity of cells (Freedman, 1974). Consistent with the *in vivo* findings we found a strong correlation between ephrinB2 levels and anchorage independent growth: the majority of imNSC1 and GSC1 *Efnb2*$^{-/-}$ cells remained as single cells and less than 5% of the cells generated small colonies (**Figure 22a**). Instead GSC1 and imNSC1-*Efnb2* cells formed large colonies at high efficiencies with very similar kinetics. This indicates that ephrinB2 drives anchorage independent proliferation *in vitro* and tumourigenicity *in vivo* and is sufficient to transform immortalised NSCs.

The previously observed effects of ephrinB2 on perivascular migration were mediated by Eph-forward signalling. We therefore tested, whether forward signalling is also important in mediating anchorage independent proliferation or whether ephrinB2-reverse signalling drives pro-
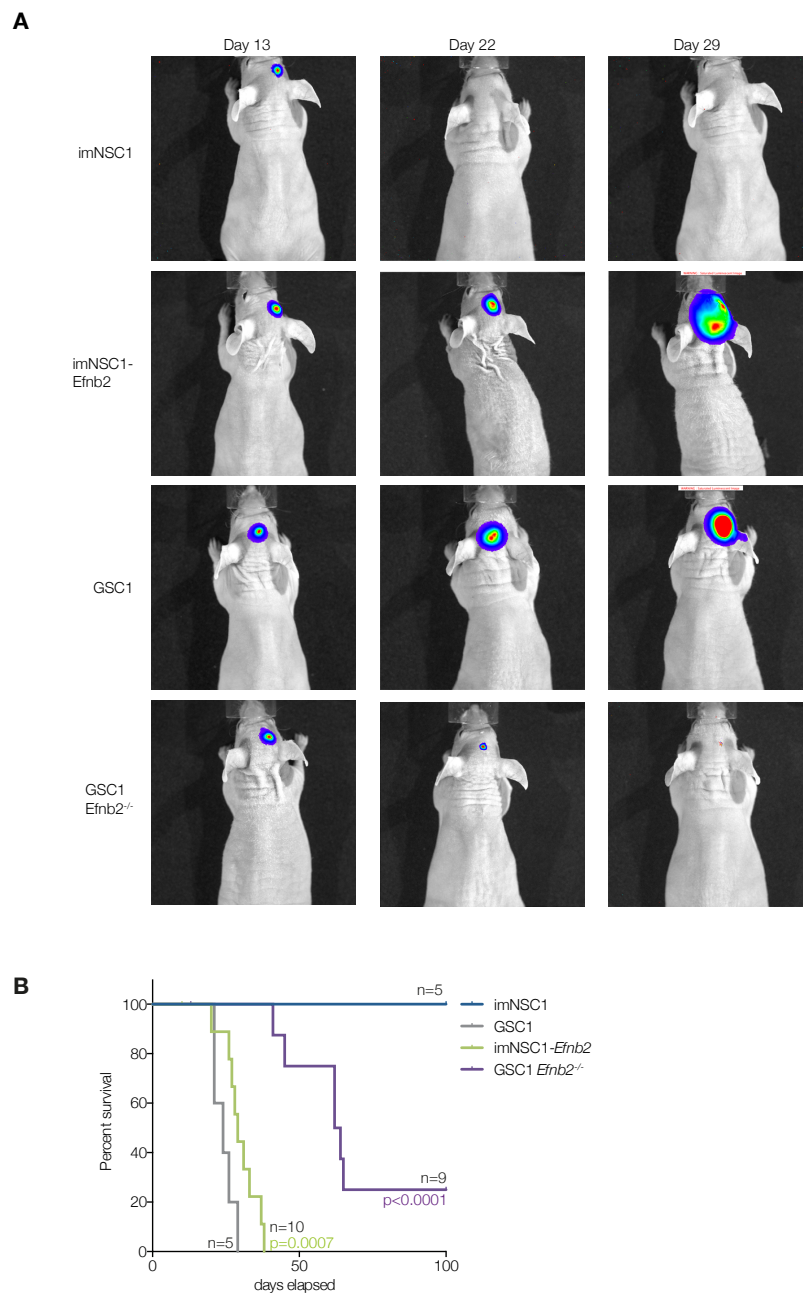
**Figure 21: EphrinB2 is an oncogene in glioblastoma.** a) Representative Bioluminescence images of CD1-nude mice at different time points during tumour progression after injection of imNSC1, imNSC1-*Efnb2*, GSC1 and GSC1 *Efnb2*$^{-/-}$ . b) Kaplan-Meier survival plots of the mice depicted in A. Significance is given relative to imNSC1 for imNSC1-*Efnb2* and relative to GSC1 for GSC1-*Efnb2*$^{-/-}$ .

liferation in the absence of anchorage signals. Intriguingly, and in contrast to the migration phenotype, proliferation in suspension depended entirely on reverse signalling as overexpression of an intracellular deleted variant did not enable imNSC1 cells to form colonies in soft agar (**Figure 22a**).

To rule out the possibility that the transforming ability of ephrinB2 is a peculiar feature of the largeT-ras model, we repeated this experiment with imNSC2, imNSC2-*Efnb2* and imNSC2-ΔC*Efnb2*. As the GSC2 progression series was not based on neural stem cells bearing an *Efnb2* floxed allele we relied on siRNA to achieve a knockdown of ephrinB2 instead. We used either control (Scr) or three different *Efnb2* specific siRNAs and observed a knockdown of over 90 % at protein level in GSC2 using siRNA 1 (**Figure 22d**). We then repeated the soft agar assay with the GSC2 progression series and obtained highly similar results confirming the generality of these findings (**Figure 22b,c**): all cells with functioning ephrinB2 reserve signalling (imNSC2-*Efnb2* , GSC2-scr) formed large colonies, whereas imNSC2, imNSC2-ΔC*Efnb2* and GSC2 si*Efnb2* were not able to proliferate in suspension.

This conclusively shows, that ephrinB2 reverse signalling controls anchorage independent proliferation, however it is not clear whether this effect is dependent on intercellular contacts or whether it occurs cell autonomously. To answer this question we transfected imNSC1-*Efnb2* with adenoviral particles expressing either GFP (ctrl) or a dominant negative variant of N-Cadherin (DN-NCdh). We have previously shown, that N-Cadherin is the dominant Cadherin expressed on these cells and that overexpression of this construct is sufficient to inhibit cell-contact dependent signalling (see **Chapter 5**). Transfection with this construct did not alter the ability of imNSC1-*Efnb2* to form colonies in soft-agar showing that ephrinB2 mediates proliferation in the absence of anchorage signals in a cell autonomous way.
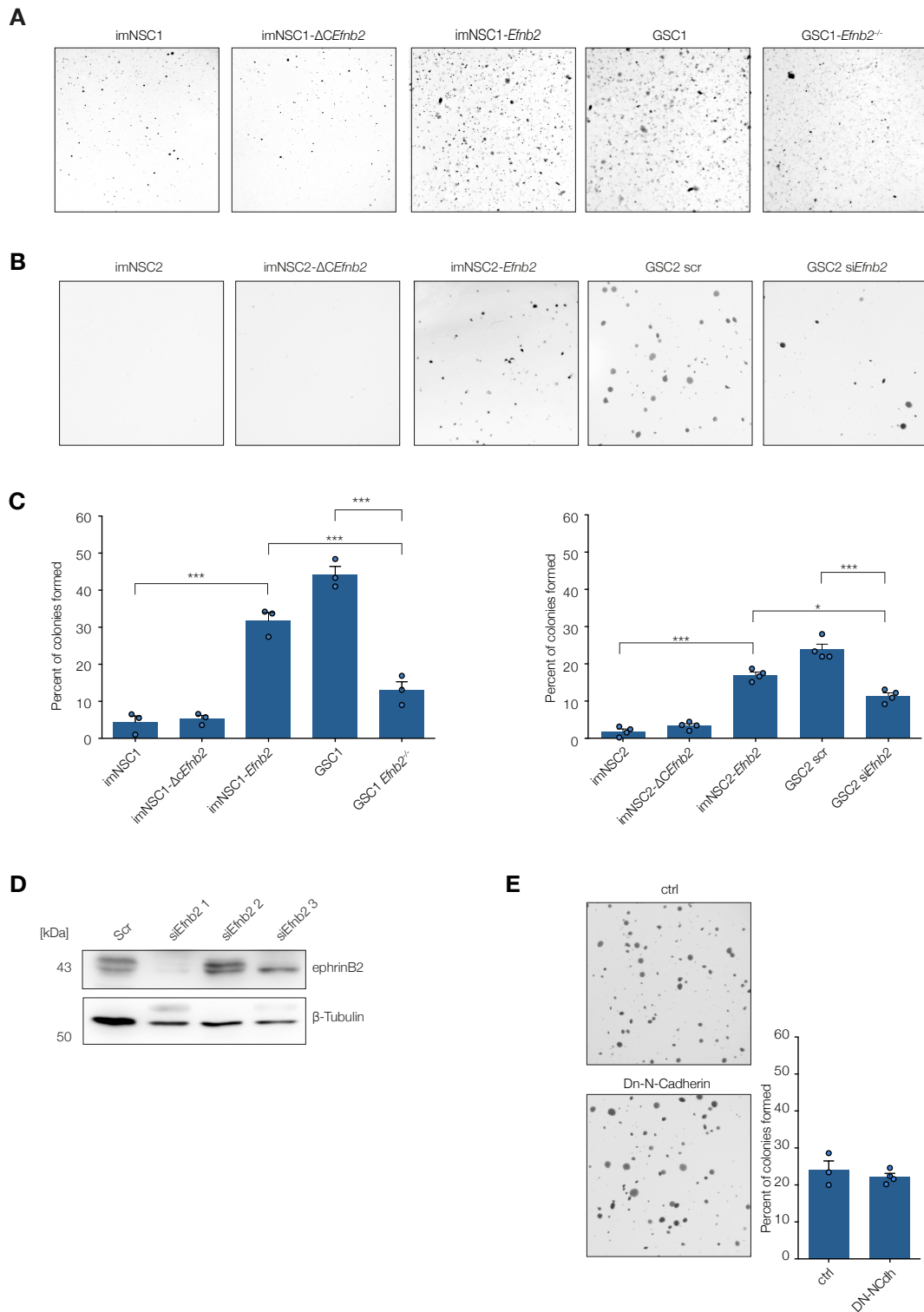
**Figure 22: EphrinB2 reverse signalling drives anchorage independent proliferation.**   a,b) Representative micrographs of GSC1 (a) and GSC2 (b) cells of indicated genotype grown in soft agar for 10d. c) Quantification of number of colonies formed in soft agar in all cultures, expressed as percentage over total number of seeded cells. n= 3, error bars depict s.e.m.  One way ANOVA with Tukey correction. d) Western analysis of ephrinB2 knockdown in GSC2 using either control (scr) or three different *Efnb2* specific siRNAs (si*Efnb2*1,2,3). e) Quantification of number of colonies formed in soft agar of imNSC1-*Efnb2* cells transfected with either GFP (ctrl) or dominant negative N-Cadherin (DN-NCdh) adenoviral particles

## 6.2 EphrinB2 enables progression through the G2/M checkpoint in suspension

We next asked how ephrinB2 expression might override the checkpoints that arrest cells in absence of normal anchorage signals. We therefore examined how culture in suspension affects the cell cycle progression of immortalised and transformed cells. To be able to retrieve single cells after suspension culture we used a modified version of the soft agar assay by replacing the agar with methylcellulose. Methylcellulose forms a semi solid medium in higher concentrations but returns to a liquid state upon dilution (Cremona and Lloyd, 2009). This approach enabled us to retrieve the cells by centrifugation and process them for immunostaining.

We seeded imNSC1, imNSC1-*Efnb2* , GSC1 and GSC *Efnb2*$^{-/-}$ in either adherent conditions or in methylcellulose culture for 72 hours, retrieved the cells by diluting the methylcellulose fivefold and analysed their cell cycle profile by FACS following propidium iodide (PI) staining. As expected, all cells in attachment proliferated efficiently, with cells expressing oncogenic ras showing a higher proportion of dividing cells in S-Phase (**Figure 23a,b**). In stark contrast, their behaviour in suspension was very distinct: while GSC1 in suspension were able to proliferate with similar kinetics as in attachment, imNSC1 did not: A strong increase of cells with 2n DNA content was observed with the PI profile also showing a smaller percentage of cells in S-Phase (**Figure 23a,b**). This difference in cell-cycle profiles was not due to an increased level of apoptosis in imNSC1 as both cell types showed similar numbers of caspase3+ cells in suspended cultures (**Figure 23c**). This data suggests that while imNSC1 are able to progress relatively normally through G1 and S-Phase in suspension (as predicted for they are lacking functional p53 and Rb signalling) , their progression through G2/M phase is blocked by an anchorage dependent checkpoint which is impaired in cells overexpressing oncogenic Ras.
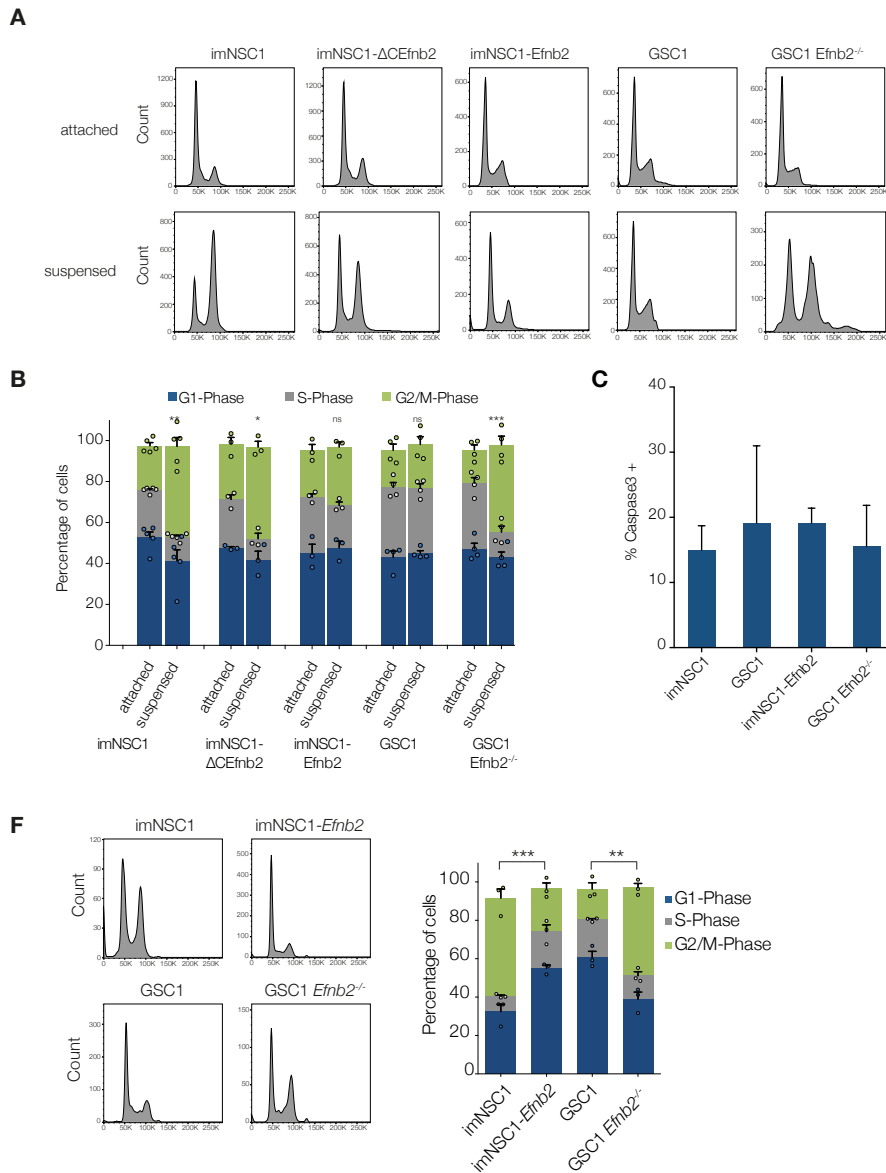
**Figure 23: Ephrin-B2 controls anchorage independent proliferation.** a) Representative FACS profiles of cells grown in attachment or methylcellulose for 72 h, showing DNA content by propidium iodide (PI) staining. b) Quantification of cell cycle phases from the FACS profiles in a. n=3-5 as indicated by the dots. Error bars depict s.e.m. c) Percentage of total number of caspase3 positive cells after 72 h suspension culture. d) Representative FACS profile plots of indicated cells isolated from the cortex of CD-1 nude mice 7 days after injection (left). Quantification of cell cycle phases from the FACS profiles (right). Error bars depict s.e.m. One way anova.

Strikingly, this Ras mediated cell cycle progression was again fully dependent on ephrinB2 reverse signalling as genetic deletion of *Efnb2* rescued the G2/M checkpoint and GSC1 *Efnb2$^{-/-}$* were unable to complete a full cell cycle in suspension (**Figure 23a,b**). In addition, we showed that overexpression of full-length but not ΔC *Efnb2* was sufficient to overcome the G2/M arrest of imNSC1 cells cultured in suspension. This was again not caused by increased apoptosis as shown in (**Figure 23c**). Thus, ephrinB2 controls progression through G2/M-Phase in suspension culture.

To assess whether a similar mechanism caused the inability of cells lacking expression of *Efnb2* to proliferate *in vivo* we injected imNSC1, imNSC1-*Efnb2* , GSC1 and GSC1 *Efnb2$^{-/-}$* into 6 week old CD-1 nude mice. The cells were then isolated 7 days later by dissecting the GFP positive cells out of the brain and digesting the tissue using papain to obtain single cells. Remarkably the cell cycle profiles of all cells were indistinguishable from the corresponding *in vitro* suspension cultures with GSC1 and imNSC1-*Efnb2* proliferating robustly and showing a relatively low percentage of cells in G2/M whereas imNSC1 and GSC1 *Efnb2$^{-/-}$* were strongly growth inhibited and up to 50% of all cells showed a 2n DNA content.

This data confirms that ephrinB2 drives gliomagenesis *in vivo* by enabling proliferation despite the absence of normal anchorage signals.

## 6.3   EphrinB2 drives anchorage-independent cytokinesis through RhoA

In a previous study a similar G2/M arrest of normal human fibroblasts in suspension was reported which could be bypassed by expression of oncogenic ras. This study identified a failure in progression through cytokinesis to be causative for this arrest (Thullberg et al., 2007). We therefore sought to understand whether a failure to progress cytokinesis is responsible for the arrest in our system as well. To this end we cultured cells in suspension in the presence of

EdU for six hours. As the typical duration of cytokinesis in mammalian cells is less than an hour, this experimental set up allowed us to distinguish between normally cycling binucleated cells (EdU positive cells) and cells which were arrested at cytokinesis (EdU negative).

We additionally stained the cultures with phalloidin and DAPI to detect cortical actin and nuclear DNA, respectively. As shown in **Figure 24,** we found that all methylcellulose cultures lacking ephrinB2 reverse signalling (imNSC1, imNSC1-$\Delta C Efnb2$ and GSC1 $Efnb2^{-/-}$) contained a much larger proportion of EdU negative, binucleated cells with decondensed chromatin compared to adherent conditions, indicative of an arrest at cytokinesis (Thullberg et al., 2007).
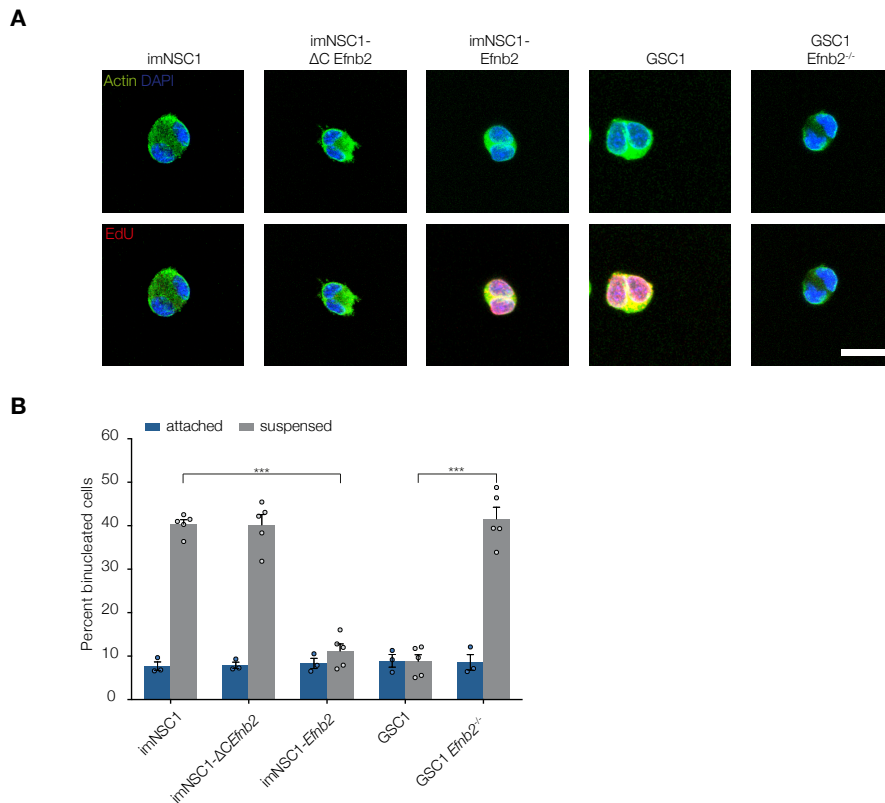


Figure 24: **Ephrin-B2 mediates progression through cytokinesis**. a) Representative immunofluorescence pictures of cells grown in methylcellulose suspension for 72 hours and stained for cortical actin (green),EdU (red) and DAPI (blue). Scale bar= 20µm. b) Quantification of the percentage of binucleated cells in the cultures shown in a. Error bars depict s.e.m., one way anova with Tukey post hoc test.

In contrast, cells with intact ephrinB2 reverse signalling (imNSC1-*Efnb2* and GSC1) had sim-

ilar percentages of binucleated cells in adhesion and suspension culture and binucleated cells were EdU positive almost without exception. This small percentage of binucleated cells most likely represents cells completing mitosis during normal division at the time of fixation. We thus concluded that ephrinB2 reverse signalling mediates anchorage independent cytokinesis. Cytokinesis is a highly complex process which integrates a multitude of signalling pathways to ensure that assembly of the contractile ring and abscission occurs at the right time in the right conditions. Amongst the downstream effectors of ephrinB2 Src, and RhoA have previously been linked to cytokinesis (Daar, 2012): RhoA plays a fundamental role in regulation constriction of the contractile ring (Jordan and Canman, 2012; Piekny et al., 2005) whereas Src signalling regulates the completion of abscission (Kasahara et al., 2007). We first tested whether Src and its critical substrate FAK were involved in mediating anchorage independent proliferation downstream of ephrinB2. For this we assessed p-Src and p-FAK expression levels of imNSC1, imNSC-*Efnb2* and GSC1 in attachment and methylcellulose suspension (**Figure 25a**). p-Src was undetectable in suspension cultures in all three cell types and p-Fak levels were also reduced to a comparable extent in all three cell types. Thus indicating that Src does not play a role in our system.

We next assessed the levels of RhoA-GTP, the activated form of RhoA by using a RhoA activation pulldown assay. This assay uses the Rho binding domain (RBD) to specifically enrich for the activated GTP-bound form of RhoA. We found that while levels of activated RhoA were low in suspended cells lacking ephrin-B2 reverse signalling (imNSC1,imNSC1-$\Delta$C*Efnb2* and GSC1 *Efnb2$^{-/-}$* ), they were greatly increased in cells that express high levels of full-length ephrinB2 (imNSC1-*Efnb2* , GSC1). This indicated a potential involvement of RhoA signalling in mediating progression through G2/M downstream of ephrinB2 (**Figure 25b**). To test this hypothesis we transfected all cells with either a constitutively active form of RhoA (RhoA-V14) or a dominant negative variant (RhoA-N19). Overexpression of RhoA-V14 in imNSC1, imNSC1$\Delta$C*Efnb2* and GSC1 *Efnb2$^{-/-}$* enabled progression through cytokinesis and caused a highly significant reduction of the percentage of cells in G2/M-Phase (**Figure 25c**). Consistent with this, overexpression of dominant negative RhoA-N19 in cells

with high levels of RhoA-GTP in suspension (imNSC1-*Efnb2* & GSC1) cause a cell-cycle arrest to similar extents as exhibited by imNSC1 cells. To further consolidate these results we also used a small-peptide inhibitor of Rho (C3) which blocks the exchange of GDP to GTP in RhoA. Again we observed an accumulation of GSC1 cells in G2/M-Phase consistent with the previous observation using overexpressing constructs (**Figure 25d**). Together these results confirm, that ephrinB2 reverse signalling indeed drives anchorage independent cytokinesis in a RhoA dependent manner.
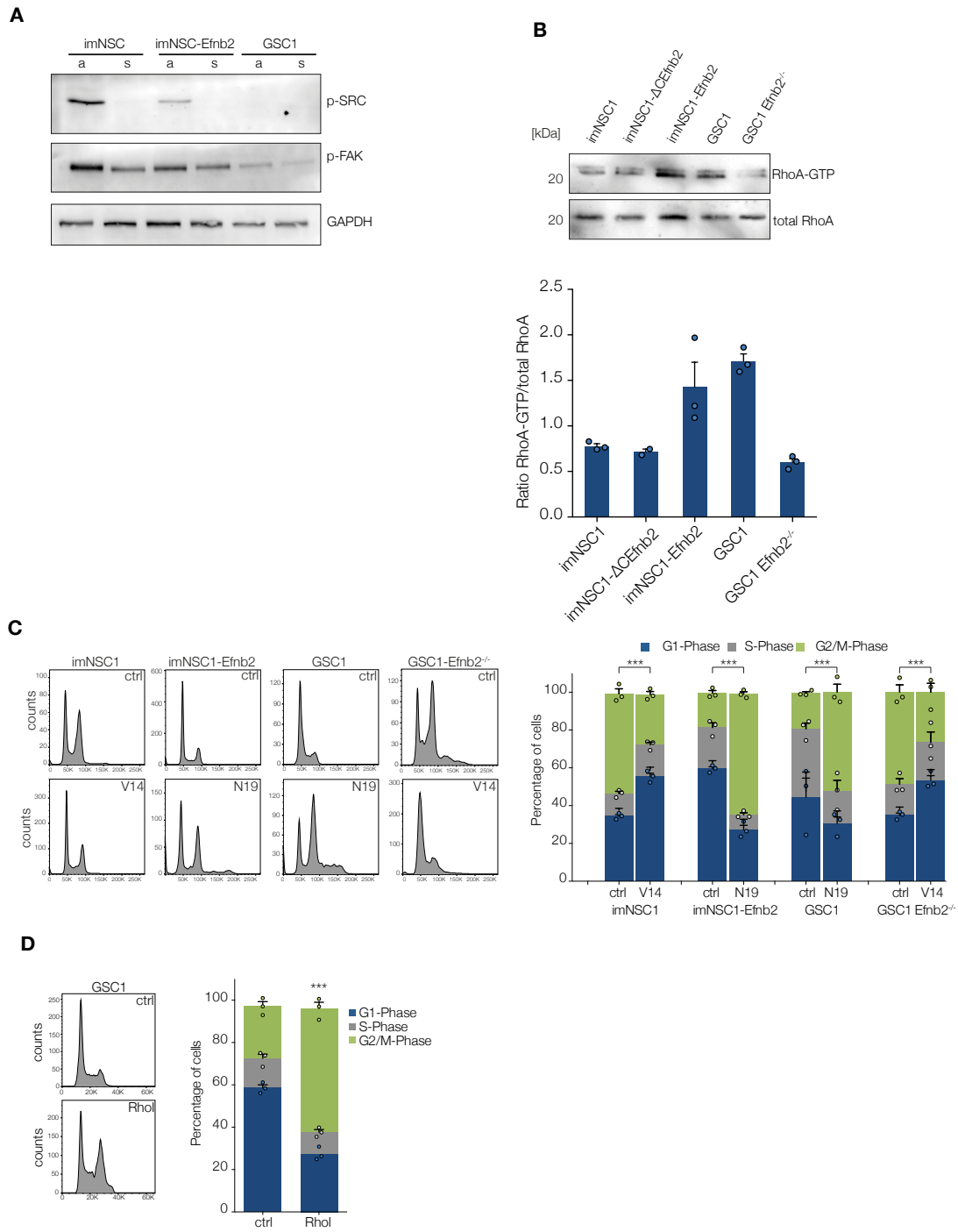
**Figure 25: RhoA controls anchorage independent proliferation downstream of ephrinB2.** a) Western blot analysis of depicted proteins in cells grown in attachment (a) or methylcellulose suspension (s) b) Western blot analysis of RhoA-GTP pulldown of cells grown in suspension (top). Quantification of the Western blot shown (bottom) c) Representative FACS profile plots of indicated cells grown in suspension transfected with either GFP-control vector (ctrl), constitutively active RhoA (V14) or dominant negative RhoA (N19) (left). The quantification of the cell cycle profile is shown on the right. Error bars depict s.e.m. One way ANOVA with Tukey post hoc test was used to calculate p values for differences in G2/M phase of each suspended culture relative to corresponding control infected cultures d)Representative FACS profile plots of GSC1 cells grown in suspension treated with either PBS (ctrl) or Rho inhibitor C3 (RhoI) (left). Quantification of the cell cycle profile is shown on the right. error bars depict s.e.m. One Way Anova with Tukey post hoc test to calculate p-values for differences in G2/M phase.

# 6.4 Conclusion

In this chapter we describe the surprising ability of ephrinB2 to act as a GBM oncogene and critical effector of the "Ras-transformed phenotype". We show that ephrinB2 is capable of inducing full transformation of immortalised neural stem cells and that in our model of mesenchymal GSCs it can substitute for oncogene ras: overexpression of *Efnb2* in largeT immortalised cells did indeed cause the formation of highly aggressive glioblastoma with nearly identical kinetics to ras-transformed neural stem cells and genetic deletion of *Efnb2* in GSCs dramatically reduced their tumourigenic potential, significantly prolonging the median survival time of injected mice Although ephrinB2 expression has been linked with increased tumourigenicity previously (Tu et al., 2012; Nakada et al., 2010) our study is the first to demonstrate a mechanism for this phenotype. We link ephrinB2 expression to the ability of GSCs to progress through cytokinesis in the absence of anchorage signals by maintaining high levels of activated RhoA.

Cytokinesis is initiated by the assembly of an actin-myosin ring around the cell equator which then begins to contract and physically separate the cytoplasms of the two daughter cells (Glotzer, 2005). It is well known, that members of the Rho family of GTPases are crucially involved in coordinating this process (Piekny et al., 2005). RhoA controls cytokinesis at various stages: It activates Formin, which promotes actin polymerisation and therefore the assembly of the contractile ring. Through activation of Rock it recruits myosin that generates the force necessary for the ingression of the contractile ring and finally it activates Citron K which regulates the final stages of cytokinesis (Piekny et al., 2005).

In contrast to perivascular invasion and the loss of compartmentalisation we find that progression through cytokinesis is not mediated by activation of Eph receptors on adjacent cells. Instead ephrinB2 reverse signalling enables cytokinesis in a cell autonomous manner irrespective of direct cell-cell interactions. EphrinB2 reverse signalling independent of Eph-receptor binding has been described before in regulating the morphology and motility of endothelial

cells (Bochenek et al., 2010) and a similar role for Eph independent ephrinB2 signalling was also described earlier in smooth muscle cells during blood-vessel wall assembly (Foo et al., 2006).

While we identified RhoA as downstream mediator of ephrinB2 we currently do not know how ephrinB2 leads to increased activation of RhoA. EphrinB reverse signalling has been studied much less extensively than Eph forward signalling, however some recurring themes evolve from the currently available literature: EphrinB ligands seem to be localised in lipid raft signalling complexes (Jiang et al., 2008) and are connected with a vast array of signalling networks through adapter proteins like Grb4 which bind to phosphorylated tyrosine residues through SH2 binding domains (Pasquale, 2008; Cowan and Henkemeyer, 2001; Xu and Henkemeyer, 2009). Interestingly Grb4 binds to a number of different proteins regulating Rho signalling: Dock180, a guanine nucleotide exchange factor activating RhoA (Siu et al., 2011), or Pak1 a known regulator of Rho exchange factors (Alberts et al., 2005).

Another possible downstream mediator of ephrinB2 is dishevelled which has been shown to act downstream of other ephrinB ligands (Tanaka et al., 2003). Dishevelled is a key component of the Wnt-signalling pathway and conveys Wnt signals from receptors to downstream effectors. Interestingly, it has been shown that Dishevelled also acts as an activator of RhoA in the non-canonical Wnt pathway (Gao and Chen, 2010). It is thought that binding of dishevelled to ephrins is again facilitated by Grb4 (Tanaka et al., 2003). While we have shown the importance ephrinB2 reverse signalling in our system, there is a clear need to identify the key molecules mediating this pathway. Future studies should explore the role of Grb4 and its many downstream effectors to gain a better understanding of this novel role for ephrinB2 in promoting progression through cytokinesis and tumourigenicity.

Thus we identified ephrinB2 as a *de novo* oncogene in mesenchymal glioblastoma. We show that ephrinB2 reverse signalling mediates anchorage independent cytokinesis through RhoA and can substitute for mutations in the ras pathway in driving tumourigenicity.

# Chapter 7

# EphrinB2 in human glioblastoma

## 7.1 EphrinB2 silencing suppresses GSC tumourigenesis

We have so far shown that ephrinB2 is a critical mediator of two key aspects of tumour formation in our murine GBM model: It enables perivascular invasion and drives cytokinesis in the absence of normal anchorage signals. To determine the relevance of these findings to human glioblastoma, we obtained a panel of human GSCs and GBM cell lines: U87 and U251 are well characterised primary human glioblastoma cell lines, which have been used extensively in the past. G7, G144, G166 and G26 are human glioblastoma stem cells isolated from individual patients by Steve Pollard et. al. (Pollard et al., 2009; Stricker et al., 2013).

Initially, we assessed *EFNB2* mRNA levels using quantitative RT-PCR (**Figure 26a**). We found that *EFNB2* expression was strongly increased in either highly invasive GSCs (G144) or GSCs originating from mesenchymal human GBM (G26) (Pollard et al., 2009; Stricker et al., 2013). We confirmed the expression levels using immunoblotting and found a similar trend with G26 expressing high levels of EphrinB2 (data not shown).

We next tested whether EphrinB2 expression affects tumourigenicity of human GSCs *in vivo*

. For these experiments we used G26 cells, as they showed the highest expression levels of EphrinB2 amongst the tested lines and were also derived from an NF1-deleted glioblastoma, and therefore most closely resembled our murine model. We introduced constructs stably expressing control shRNA (ctrl) or shRNA against *EFNB2* into G26-GSCs. shRNA1 yielded a knockdown of EphrinB2 on protein level of over 90% compared to scrambled controls, whereas shRNA2 less efficient (up to 50 % knockdown) (**Figure 26b**). We then transplanted $5\times10^4$ GFP-Luciferase tagged G26 ctrl or G26-shEFNB2 intracranially into the putamen of 6 week old CD1-nude mice and monitored their growth by bioluminescence imaging for 40 days(**Figure 26c**). Strikingly we observed a dramatic impairment of tumour formation and growth in the *EFNB2* knock-down group compared to scrambled control: control G26 cells formed glioblastoma with exponential kinetics, as previously reported (Pollard et al., 2009). In contrast, knockdown animals showed no evidence of tumourigenicity, and a rapid loss of bioluminescence signal was observed (**Figure 26d**). We continued monitoring the shEFNB2 group and saw no evidence of tumour growth beyond 100 days post injection.

To gain better insights into the mechanisms responsible for the inability of G26-shEFNB2 cells to proliferate and form tumours *in vivo* we performed a series of experiments: we first performed FACS analysis of G26 ctrl and shEFNB2 cells grown in attachment to determine whether the normal proliferative potential of G26 cells might have been affected by the expression of shEFNB2. Both cells showed very similar proliferation profiles and completely indistinguishable levels of BrdU incorporation after 8 h pulsing (**Figure 27a**).
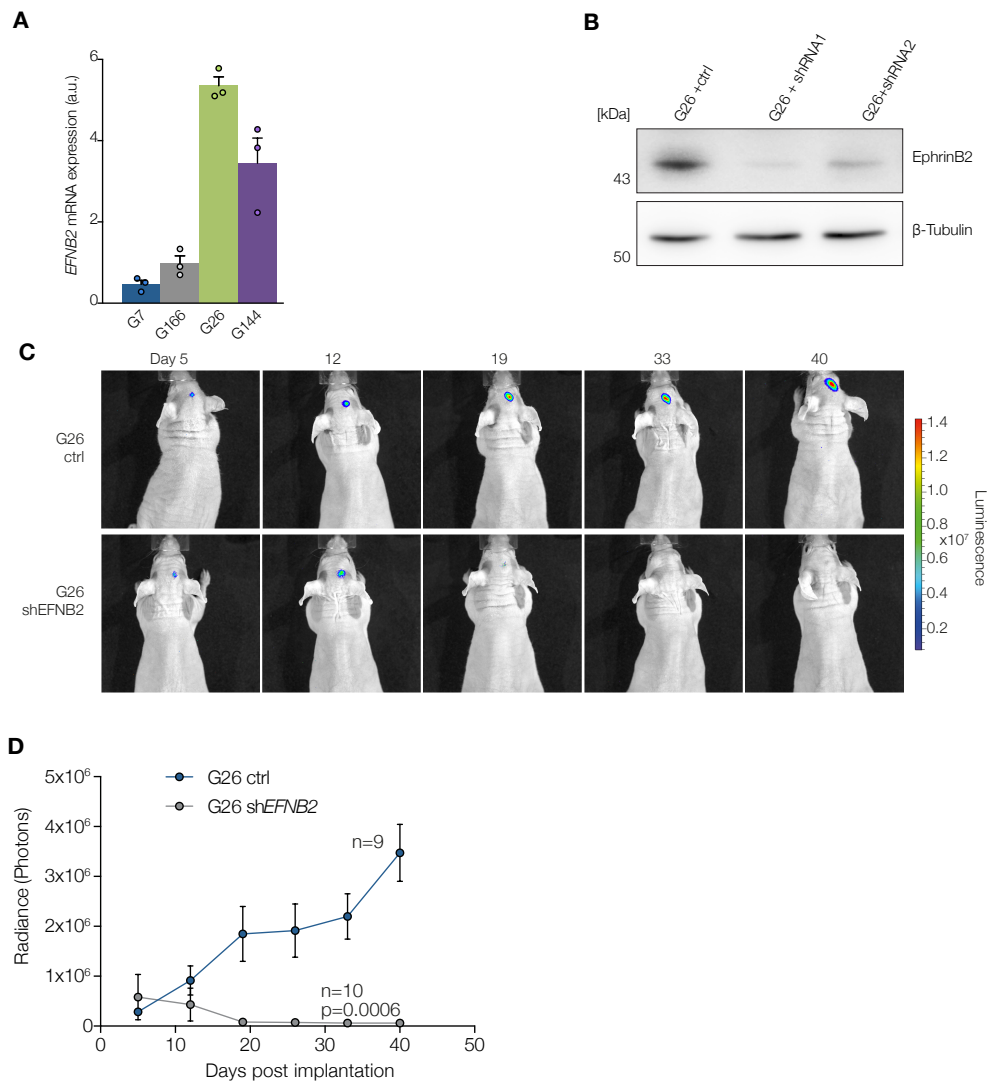
**Figure 26: EphrinB2 silencing prevents tumourigenesis *in vivo* .** a) Quantitative RT-PCR analysis of *EFNB2* expression levels in human GSC lines. Error bars depict s.e.m. b) Western blot analysis of EphrinB2 levels in G26 after infection with stably expressed control (ctrl) or *EFNB2* specific (shRNA1,2) shRNAs c) Representative bioluminescence images of mice injected with either ctrl or *EFNB2* knockdown (G26 shEFNB2) G26 CSCS and imaged at the specified days. d) Quantification of bioluminescence signal intensities over time in mice intracranially injected with either G26 ctrl or G26shEFNB2. Error bars depict s.e.m. Two way anova to calculate p-value for time-dependent differences between the groups. e) Representative FACS profile plots of G26 cells isolated 10 days after intracranial injection into CD1-nude mice (left). Quantification of the cell cycle profiles (right). Error bars depict s.e.m. One way anova with tukey post hoc test to calculate p-values for the difference in G2/M phase.
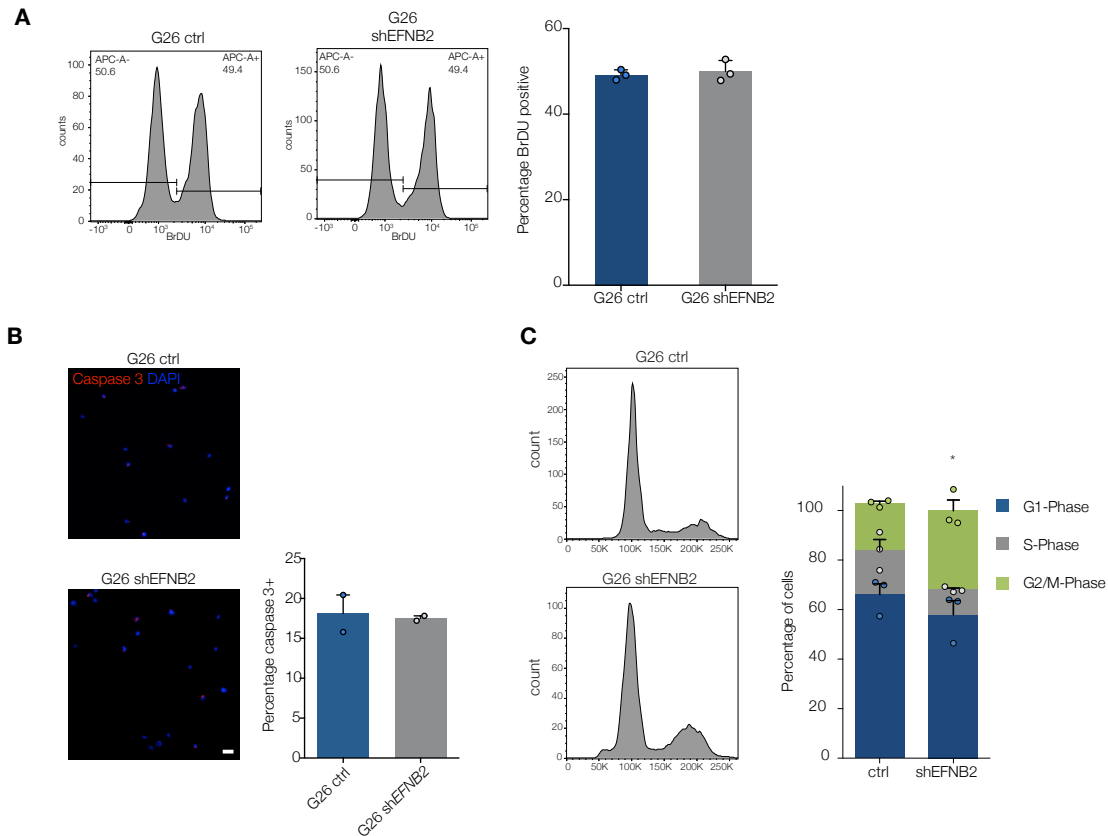
**Figure 27: EphrinB2 knockdown causes G2/M arrest in human GSC *in vivo* .** a) Representative FACS profile plots showing BrDU positive cells after 8 hour pulsing (left). Quantification of the percentage of BrDU positive cells (right). Error bars depict s.e.m. b) Representative immunofluorescence pictures of G26 ctrl and G26 shEFNB2 cells stained with caspase 3 (left). Quantification of the percentage of caspase+ cells (right). Error bars depict s.e.m. Scale bar = 50 µm c) FACS profile plot of G26 ctrl and G26 shEFNB2 cells isolated 10 days post intracranial injection into CD1-nude mice (left). Quantification of the cell cycle profile of three independent tumours (right). Error bars depict s.e.m. One way anova with tukey post hoc test to calculate p-values for the difference in G2/M phase

We next assessed whether shEFNB2 infected cells underwent apoptosis to a higher degree than control infected G26. No increase of caspase3+ cells could be observed both in normal growth conditions and after over night suspension culture in methylcellulose (**Figure 27b**). To understand, whether the inability of G26 shEFNB2 to proliferate *in vivo* was due to a cell cycle arrest similar to what we previously observed for our murine GSCs *in vitro* we recovered G26 ctrl and G26 shEFNB2 cells ten days after intracranial injection and examined their DNA profile using FACS following PI staining. Similar to ephrin-knockout murine cells, EFNB2 deficient G26 arrested in G2/M (**Figure 27c**). This indicates that EphrinB2 is required for

anchorage independent proliferation and progression through cytokinesis in human GSCs *in vivo* as well.

## 7.2 EphrinB2 is a therapeutic target for glioblastoma

We observed that shRNA knockdown of EphrinB2 is sufficient to prevent growth of glioblastoma in xenograft models. Next, we asked whether blocking EphrinB2 in pre-established tumours might be a feasible therapeutic approach to stop invasion and proliferation of GSCs. To this end we used an ephrinB2 blocking scFV human antibody fragment (B11) which was previously developed as a potential antiangiogenic therapeutic *in vivo* (Abéngozar et al., 2012). Single chain variable fragments, or scFv, are fusion proteins consisting of the variable region of the heavy($V_H$) and light chains($V_L$) of immunoglobulins, typically joined by a short linker peptide (Skerra and Plückthun, 1988). We implanted Luciferase-tagged G26 cells intracranially into immunocompromised CD-1 nude mice and monitored tumour growth using bioluminescent imaging. As soon as the signal intensities of individual exponentially growing tumours reached $1x10^6$ photons/s/cm² the mice were randomised into two groups with equal average bioluminescence (**Figure 28a**). A total dose of 400 μg B11 or PBS control was administered per animal in five separate intravenous injections over a period of 9 consecutive days as reported (Abéngozar et al., 2012; Binda et al., 2012). Glioblastoma are defined by abundant neovascularisation in later stages of the tumour development and ephrinB2 has previously been shown to control angiogenesis (Jain et al., 2007; Wang et al., 2010) To exclude the possibility that B11 affects tumour growth through blocking angiogenesis we specifically chose this treatment regime to assess B11 efficacy before the onset of neoangiogenesis and vascular sprouting. Remarkably treatment with B11 strongly suppressed tumour growth in all animals. The average tumour mass of B11 treated tumours was reduced by over 90% with one animal out of six showing complete recession of the observable tumour mass beyond 150 days post treatment (**Figure 28b,c**).
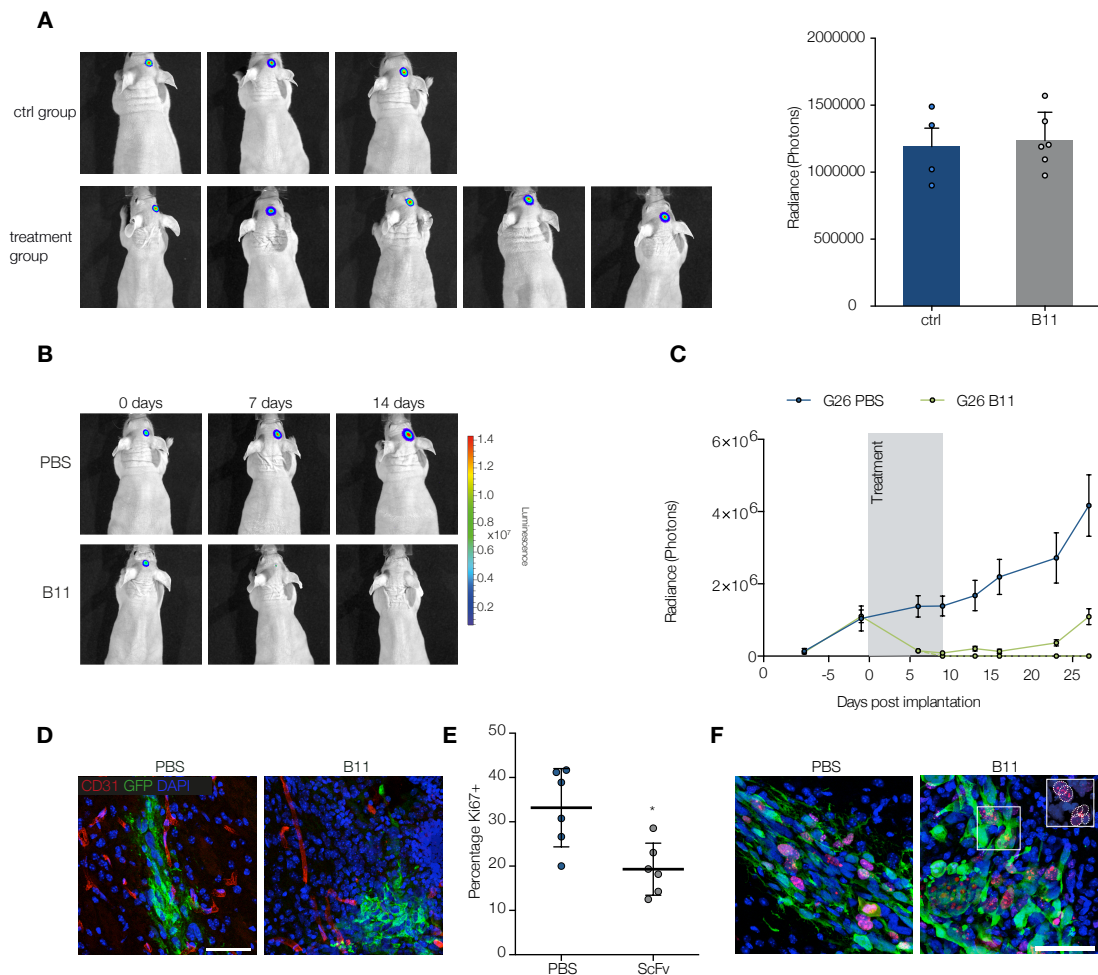
**Figure 28: Treatment with anti-Ephrin-B2 ScFv blocking antibody fragments inhibits tumour growth of pre-established GBMs**. a) Bioluminescence images of one complete cohort of Cd-1 nude mice at the start of the treatment (left). Quantification of the randomised groups (right). Error bars denote s.e.m. b,c) Representative images (a) and quantification (b) of bioluminescence radiance of PBS or anti Ephrin-B2 scFv antibody (B11) injected mice. Dotted line depicts radiance of the tumour that regressed completely. n=4 for PBS and 6 for B11 treated groups. d,e) Representative fluorescence images of control and treated G26 tumours 5 days after first B11 injection, stained for GFP to identify tumour cells, CD31 (red), to label the endogenous vasculature and the proliferation marker Ki67 (red). Note the absence of perivascular interactions and the presence of multinucleated cells (inset) in B11-treated tumours. Dotted circles demarcate individual nuclei within multinucleated cells. Scale bar=50μm

We analysed a panel of B11 and PBS treated tumours immediately after the third round of injections to examine the effects of ephrinB2 blocking *in vivo* . Immunofluorescence analysis of these tumours revealed abundant perivascular invasion at the tumour margin in PBS treated controls, as previously reported (Pollard et al., 2009). Intriguingly, the association with the vasculature was significantly reduced in B11-treated tumours also showing a much less organised overall structure of the tumour mass (**Figure 28d**). We also analysed B11 and PBS treated tumours for their percentage of proliferating cells staining for Ki67, a proliferation marker. We observed a significant difference in Ki67 positive cells in B11 treated tumours compared to PBS control (**Figure 28e**). Remarkably, while there were still Ki67 positive cells in B11 treated mice, these were often multinucleated, which was not observed in PBS treated tumours (**Figure 28f**). This is indicative of a failure to complete cytokinesis similar to the results we observed in our murine *Efnb2* knockout and human *EFNB2* knockdown models. Therefore, we concluded that B11 suppresses G26 tumourigenicity by inhibiting ephrinB2 dependent perivascular invasion and anchorage independent progression through cytokinesis.

To further confirm the tumour cell intrinsic effects of B11 we performed *in vitro* assays: We first tested the efficacy of B11 to rescue boundary formation of imNSC1-*Efnb2* and GSC1 with endothelial cells (**Figure 29a,b**). We found, that treatment with 20 μg/ml B11 but not control protein inhibited imNSC1-*Efnb2* and GSC1 migration into and over the endothelial monolayer, leading to significantly shorter boundary with endothelial cells in both cell types, thus at least partially restoring compartmentalisation. Additionally we treated GSC1 cells grown in methylcellulose suspension with 20 μg B11 or control protein and analysed their cell cycle profile using PI staining and FACS . Treatment with B11 caused a significant increased of cells in G2/M-Phase comparable to the effects of *EFNB2* knockdown. Additionally some cytotoxicity was observed as indicated by the increase of apoptotic or necrotic sub-G1 cell population (**Figure 29c**). From this we conclude that blocking ephrinB2 with specific scFv is a feasible approach to suppress tumourigenesis *in vivo* by directly targeting the invasion and proliferation of tumour cells independent of the effects B11 might have on angiogenesis.
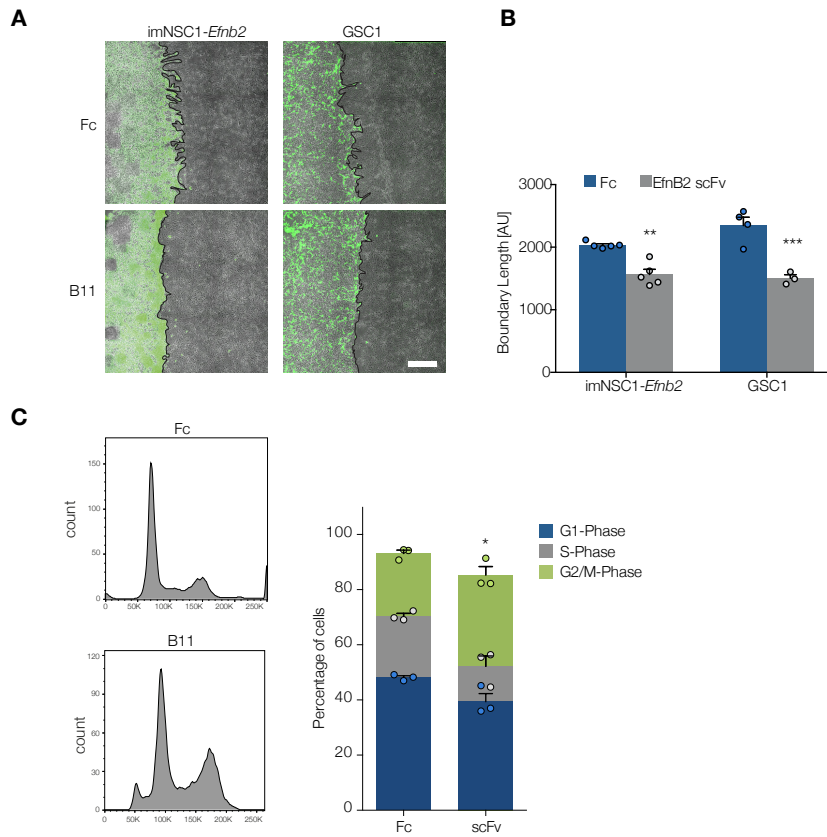
**Figure 29: Treatment with anti-Ephrin-B2 ScFv blocking antibody fragments rescues boundary formation and anchorage dependent G2/M arrest *in vitro* .** a) Merged Fluorescence and phase contrast still images taken from time-lapse microscopy experiments of GFP labelled imNSC1-*Efnb2* and GSC1 (green) migrating towards brain microvascular endothelial cells (unlabelled cells) treated with either 20 μg/ml anti ephrinB2 scFv (B11) or control protein (Fc). Scale bar = 500 μm b) Quantification of boundary length at 60 h. Error bars depict s.e.m. Students t-test. c) Representative FACS profile plots of GSC1 grown in suspension treated with 20 μg/ml B11 or control protein (Fc) (left). Quantification of the cell cycle profiles (right). Error bars depict s.e.m. One way anova to calculate the p-value of differences in G2/M phase

## 7.3 EphrinB2 expression in GBM correlates inversely with patient survival

To extend our findings to a larger cohort of human glioblastoma specimen we analysed the publicly available TCGA dataset (n=482). We first analysed *EFNB2* expression levels in GBM subtypes according to the classification by Verhaak et al., 2010. Here we found that mesenchymal and classical subtypes have significantly higher *EFNB2* levels than the average of all GBM

(**Figure 30a**).  In addition, in mesenchymal glioblastoma *EFNB2* was the only ephrinB ligand that was found significantly upregulated (**Figure 30b**).

Next, we split the cohort of tumours into *EFNB2* high (> median) and low (< median) expressors and assessed the overall patient survival.  Remarkably, *EFNB2* strongly correlated with decreased patient survival in glioblastoma (**Figure 30c**).  This correlation was maintained in the proneural and mesenchymal subtypes but not in neural or classical glioblastoma (**Figure 30d**).We then performed an unbiased correlation analysis to identify SNPs and CNVs which significantly correlated with differentially regulated *EFNB2* levels in the TCGA dataset. Remarkably, The gene alterations which showed the highest correlation with increased *EFNB2* expression were NF1 and p53, both defining mutations of the mesenchymal GBM subtype, and IDH1, almost exclusively mutated in the proneural subtype, respectively (**Figure 30e**). This further highlights the important role of *EFNB2* in mesenchymal and proneural glioblastoma.

Together, these findings strongly suggest an important role for EphrinB2 in the pathogenesis of human glioblastoma.

## 7.4  *EFNB2* is significantly increased in a wide variety of human tumours and inversely correlates with patient survival

*EFNB2* is highly expressed throughout development in almost all tissues and has been shown to be expressed in a variety of solid tumours.  Given the highly significant correlation of *EFNB2* expression with glioblastoma prognosis and survival we asked whether a similar *EFNB2* dependent mechanism might be involved in other tumour types as well.  For this we first compared the expression of *EFNB2* in a number of normal tissues with their malignant counterpart using the affy package for analysis of Affymetrix microarray data in R (Gautier et al.,
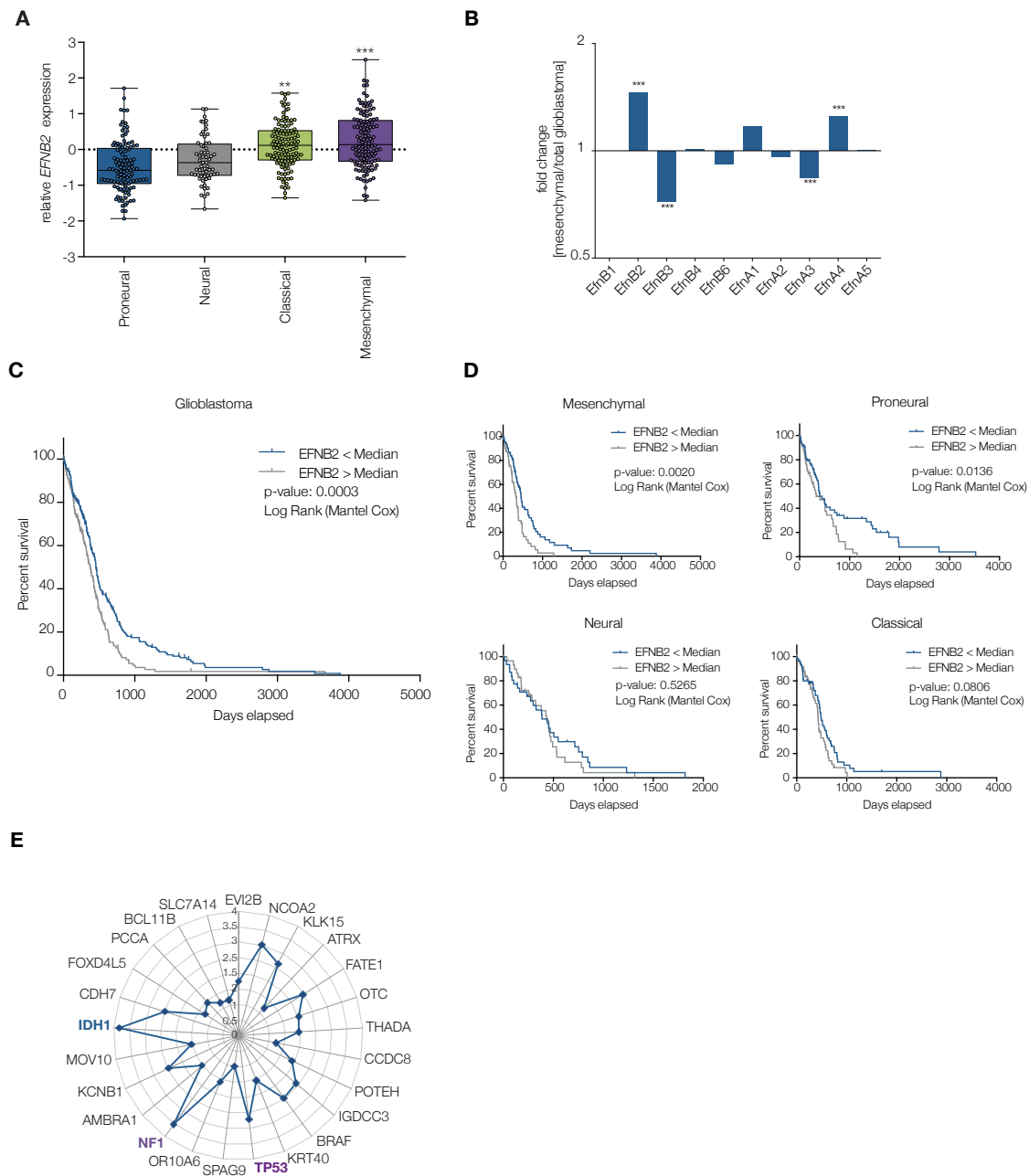
**Figure 30: EphrinB2 expression is increased in mesenchymal and proneural human GBM and correlates inversely with patient survival.** a) Relative mRNA expression levels of Ephrin-B2 in the four GBM subtypes of the TCGA dataset. One-way ANOVA with Tukey post-hoc test. b) fold change of all human EFN-genes in mesenchymal GBM compared to all other samples of the TCGA dataset. One-way anova with Tukey post hoc test. c) Kaplan Meier analysis of 482 human GBMs from the TCGA dataset stratified into high and low *EFNB2* expressors relative to the median expression value of the cohort. Log Rank Mantel Cox test. d) Kaplan Meier analysis of human GBM subtypes stratified into *EFNB2* high and low expressors. Log Rank Mantel Cox test. e) Radial plot depicting mutations most highly correlated with increased EFNB2 expression (and corresponding significance of the correlation) in the TCGA dataset
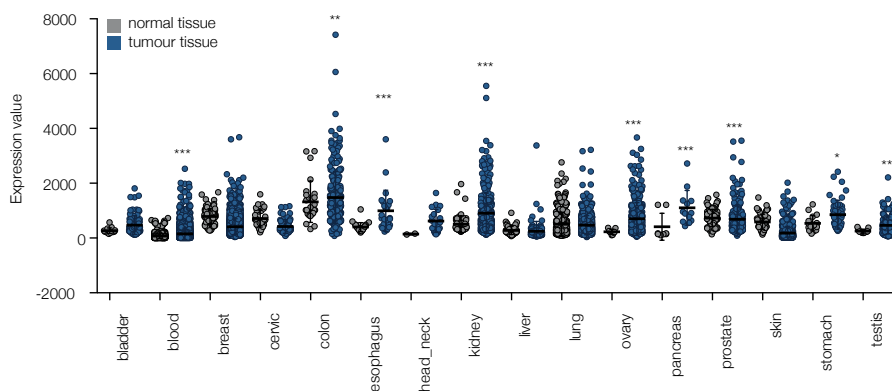
**Figure 31: EphrinB2 expression is increased in a wide variety of human tumours**. a) Relative expression of *EFNB2* in normal and tumour tissue. Analysis was performed using publicly available microarray data and the affy package in R.

2004). Surprisingly, *EFNB2* expression was significantly increased in a wide variety of human tumours including tumours of the colon, esophagus, kidney, ovary, pancreas, prostate, stomach and testis (**Figure 31a**).

For some of these tumours large cohorts of patients had been sequenced which allowed us to analyse the correlation of *EFNB2* expression and patient survival in these tumours. For this we used the online tool SurvExpress, a tool for the validation of biomarkers in cancer gene expression data which uses data sourced from a large number of publications and work from big consortiums like TCGA (Aguirre-Gamboa et al., 2013). We analysed colon, ovarian, kidney, pancreatic and prostate cancers to show the validity of this approach (**Figure 32a-e**). High *EFNB2* levels significantly correlated with decreased patient survival in both colon, ovarian and prostate cancer (**Figure 32a,b,e**). Interestingly the inverse correlation was found in kidney clear cell carcinoma (**Figure 32c**). For most of the remaining tumour types the available databases are too small to identify significant associations between gene expression and patient survival. One example is shown in **Figure 32d** depicting pancreatic cancer with an n of 100 sequenced tumours.

To validate this database based approach we performed another independent search using the PrognoScan tool, a database for meta-analysis of the prognostic value of genes (Mizuno et al.,
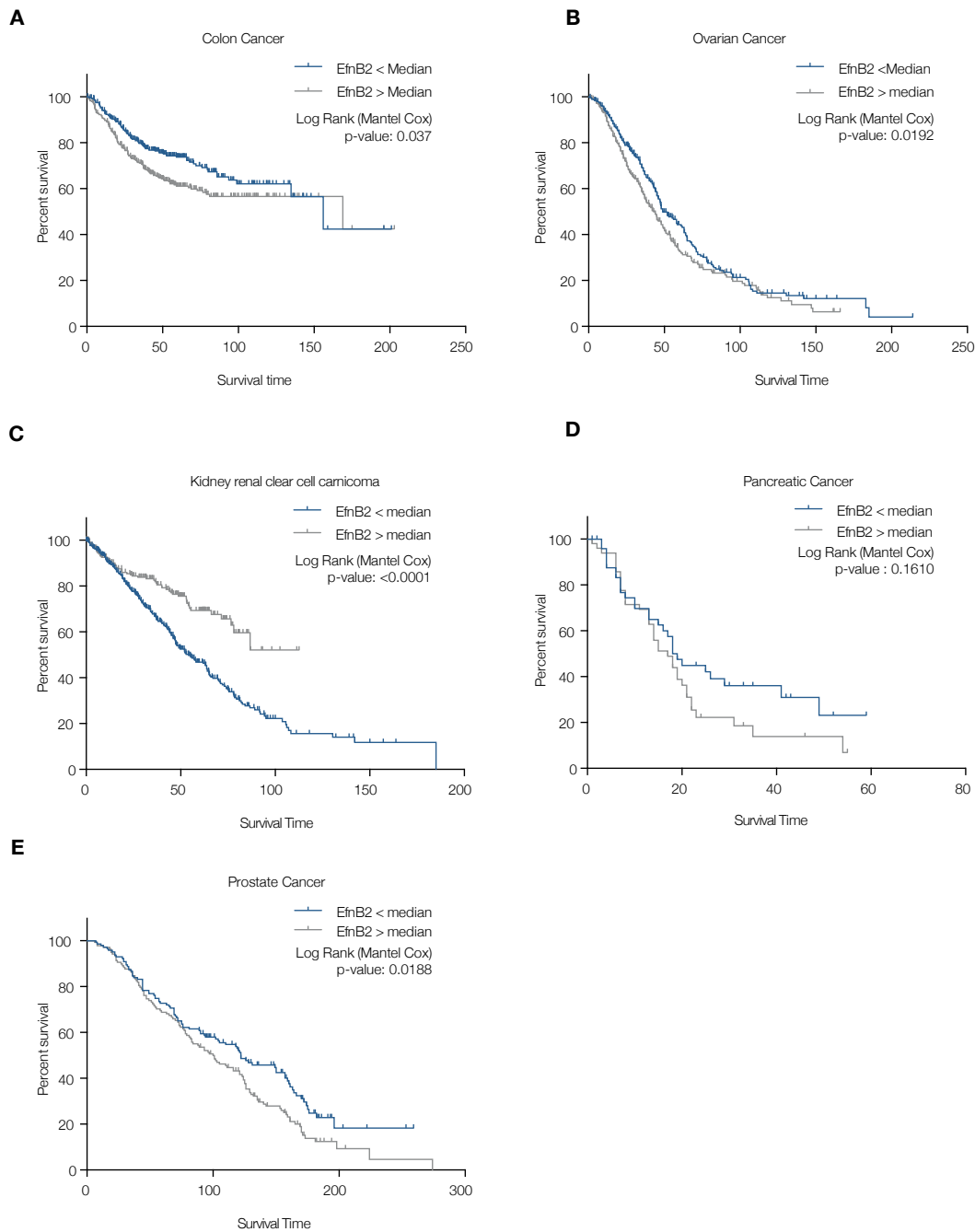
**Figure 32: EphrinB2 expression correlates inversely with patient survival in colon, ovarian and prostate cancer**. a-e) Kaplan Meier analysis of various human tumours stratified into *EFNB2* high and low expressors. Log Rank Mantel Cox test. a) Patient survival in colon cancer is significantly decreased in tumours expressing high *EFNB2* levels p-value = 0.037. Log Rank Mantel Cox b) High *EFNB2* correlate with decreased patient survival in ovarian cancer. p-value = 0.0192. Log Rank Mantel Cox c) In kidney renal clear cell carcinoma increased *EFNB2* strongly correlate positively with patient survival. p-value <0.0001. Log Rank Mantel Cox d) No significant association was observed in pancreatic cancer.
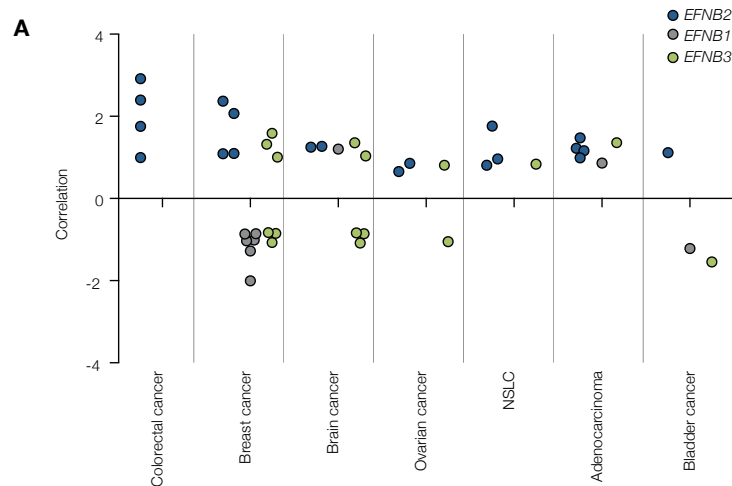
**Figure 33:** *EFNB2* **but not** *EFNB1* **or** *EFNB3* **is specifically overexpressed in a variety of human cancers**. a) Overview of a analysis of published microarray data using PrognoScan. Correlation with tumour tissue in comparison to the respective normal tissue is shown for *EFNB1* ,textitEFNB2 and textitEFNB3. Individual dots depict individual studies. Only significant correlations with a corrected p-value <0.05 are shown

2009). This allows a more direct approach scanning all publicly available microarray datasets irrespective of cancer type. To increase the rigour of this analysis we also included *EFNB1* and *EFNB3* as controls to exclude false positives. The results are shown in **Figure 33** and in the tables **Table 5**, **Table 6** and **Table 7** in the Appendix. This method again showed a highly significant correlation with high *EFNB2* levels and decreased survival in numerous patient cohorts. Interestingly *EFNB2* expression in colon cancer and ovarian cancer was again found to be significantly associated with a more malignant phenotype. In addition to that, a strong correlation is found in a variety of lung cancers, namely Non-Small Cell Lung Cancer (NSCLC) and Adenocarcinoma cohorts. We included *EFNB1* and *EFNB3* in this analysis to show that the observed effects are specific for *EFNB2*. Indeed, *EFNB2* was the only gene which consistently showed higher expression values in tumours compared to normal tissue and positively correlated with tumour progression (**Figure 33**).

Overall our findings suggest a more general role of *EFNB2* in a variety of tumours. We observe a strong correlation between decreased patient survival and high *EFNB2* levels in such different tissues as Lung, Colon and ovaries suggesting a common mechanism of ephrin-B2 mediated tumourigenicity.

## 7.5   Conclusion

In this chapter we show that knockdown of *EFNB2* in human xenograft glioblastoma models inhibited the establishment of intracranial tumours. We show that knockdown of *EFNB2* causes a a G2/M arrest and inability of hGSCs to progress through cytokinesis, identical to the phenotype observed in our murine GBM model. Significantly, treatment of pre-established glioblastoma with ephrinB2 blocking antibodies caused a strong reduction in tumour size and caused complete regression in one animal.

Preclinical studies often only assess the potential of a new treatment to delay the growth of injected tumours by pre-treating the cells rather than targeting established tumours (Day et al., 2013). Additionally, these studies often rely on direct perfusion into the brain using osmotic pumps (Binda et al., 2012) or viral delivery of knockdown constructs (Day et al., 2013). In contrast, we chose our treatment regime specifically to mimic human therapeutic paradigms by administrating B11 intravenously in clinically relevant doses and treating established glioblastoma. Importantly, during the treatment no side effects or toxicity were observed.

Glioma growth in animal models is usually characterised by two distinct vascular phases (Stiver, 2004): during early tumourigenesis small numbers of tumour cells co-opt preexisting blood vessels to meet their metabolic demand without the need for angiogenesis. With exponential tumour growth however, the existing vasculature alone quickly fails to provide sufficient nutrients to sustain further growth. This leads to tumour cells becoming hypoxic and upregulating expression of vascular endothelial growth factors (VEGF) which lead to the sprouting of new blood vessels and angiogenesis. This process typically occurs when a tumour reaches a size of 1-2 mm (Naumov et al., 2006). EphrinB2 is highly expressed on proliferating endothelial cells and is important for sprouting and formation of new vessels (Wang et al., 2010). We specifically chose to start treatment of our xenografts before an angiogenic switch occurred to avoid blocking angiogenesis without directly affecting the tumours cells,

as previously shown (Abéngozar et al., 2012; Sawamiphak et al., 2010). We further confirmed the direct effect of B11 on GSCs by analysing the treated tumours and found not only a reduction in size but also clear nuclear-abnormalities, with a large number of multinucleated cells, and a significant decrease in vascular association and alignment compared to control groups. Although we currently don't have direct evidence proving that the injected scFv is able to pass the intact blood brain barrier (BBB), the fact that it reaches its target cells in sufficient concentrations to cause observable effects strongly suggests that this is the case. This might be facilitated by a breakdown of the BBB by the initial injection, although disruption of the BBB is typically of short duration and reversible following introduction of a similar stab wound (Persson et al., 1976). A more likely explanation could be the nature of the GSCs itself: It has recently been shown that glioma cells associated with the vasculature dislodge astrocytic end feet and pericytes from endothelial cells and more importantly that even singly migrating cells are sufficient to disrupt the blood brain barrier locally (Watkins et al., 2014). It is nevertheless important to assess the potential of B11 (size 30kDa) to penetrate the BBB as previously reported for other scFv (Peter et al., 2013).This could be achieved by using fluorescently tagged B11 and tracing its distribution in the brain shortly after injection. A very similar approach is used to assess the leakiness of vessels using fluorescently labelled high molecular weight dextran injected intravenously (see Ottone et al., 2014). We currently do not know the mechanism of action by which the B11 blocks ephrinB2 reverse signalling. One possible explanation however, is that binding of the fragment interferes with ephrinB2 lateral clustering and therefore effectively inhibits activation and phosphorylation of intracellular downstream targets (compare Pasquale, 2005).

We found ephrinB2 drives human gliomagenesis in preclinical xenograft models through the same mechanisms identified in our murine mesenchymal GSC model. To further this conclusion we analysed patient samples using the TCGA database. We have shown that *Efnb2* in murine GSCs is upregulated in a NF1/ras dependent manner and indeed a strong correlation with *EFNB2* expression and the mesenchymal subtype was observed. Moreover, not only was *EFNB2* identified as core gene of the mesenchymal GBM signature previously (Carro et al.,

2010), it also inversely correlated with patient survival in mesenchymal and proneural GBM and directly with the mutations defining both pathways in our analysis.

Eph/signalling is a critical mediator of a large number of processes in almost all tissues during throughout development (Klein, 2012). Interestingly, developmental gene programs are known to be re-activated in a variety of solid tumours (Naxerova et al., 2008) and EphrinB2 specifically has been shown to be expressed in a variety of solid tumours. We therefore analysed a wider set of human tumours to identify potential links between tumour progression and *EFNB2* expression. Surprisingly we found a strong correlation between high *EFNB2* levels and worse prognosis in Lung, ovarian and colon cancer using different *in silico* approaches.

Interestingly, both colon and ovarian cancers are highly vascularised tumours that show a high rate of tumour recurrence, similar to glioblastoma. Both also contain a defined cancer stem cell population and there is some evidence suggesting a quiescent stem cell population as likely source for these tumours (Flesken-Nikitin et al., 2013; Gostjeva and Thilly, 2005). Various reports additionally suggest a cross-regulation between these CSCs and endothelial cells similar to the vascular niche described in glioblastoma (Lin et al., 2013; Pasquier and Rafii, 2013). In agreement with our *in silico* analysis, there have been reports about a correlation between increased ephrinB2 expression and tumour grade in ovarian cancer (Alam et al., 2008). It would be interesting to assess whether ephrinB2 plays a similar role in regulating cytokinesis in ovarian or colon cancer stem cells.

In the previous chapter we have identified ephrinB2 as *de novo* oncogene in a murine model of glioblastoma. Here we show that this observation is not only limited to a murine system but that ephrinB2 expression drives tumourigenesis in human glioblastoma stem cells *in vivo* . Furthermore we show that ephrinB2 expression correlated with a progressively worse prognosis in human glioblastoma and surprisingly a variety of other highly vascularised and aggressive tumours.

# Significance and future directions


This study describes the important role of ephrin/Eph signalling during gliomagenesis and significantly expands our current knowledge about how the vasculature can act as a tumour suppressing niche in a healthy organism.

In particular we have shown, that ephrinB2 expressed on endothelial cells acts as a tumour suppressor which limits the tumourigenic potential of neural stem cells in two ways: First, it compartmentalises normal neural stem cells and inhibits perivascular invasion. Secondly it also limits their proliferation through activation of p53 and subsequent cell-cycle arrest. p53 is classically known as a DNA damage response gene, however it has become more and more apparent that it serves a more general role in stem cells: p53 is constitutively expressed in a number of stem cells and its deletion causes overproliferation and abnormal differentiation patterns (Solozobova and Blattner, 2011). In the subventricular zone p53 is constitutively expressed at high levels in neural stem cells despite the fact, that apoptosis is a very rare event in this cell population until their more differentiated progeny reaches the olfactory bulb as neuroblasts (Meletis et al., 2006; Biebl et al., 2000) It is therefore tempting to speculate that loss of p53 in gliomagenesis might not primarily be required to avoid apoptotic stimuli but rather to enable mutated stem cells to escape the proliferation-restricting stem cell niche.

So far we have not identified any director mediators that link Eph signalling and p53 activation but it would be of great interest to further pursue the candidates we have identified using hypothesis-driven and unbiased approaches to understand the underlying mechanism.

Interestingly, it has been shown, that endothelial cells secret BMP's which negatively regulate proliferation of stem cells in the subventricular zone. This arrest was rescued by p53 ablation but only partially when blocking BMP signalling (Mathieu et al., 2008). It is possible, that Eph and BMP signalling pathways converge on an activator of p53 and cooperate to regulate neural progenitor proliferation. It would be therefore intriguing to study the potential cooperation of Eph and Smad signalling in this context. Eph/ephrin is highly important in a large variety of other stem cell niches and this combined with the fact, that p53 loss is an early event in tumourigenicity in a large number of other tumours (Rivlin et al., 2011) suggests a more general role of this signalling pathway.

Endothelial ephrinB2 however not only limits the proliferation of stem cells, but also inhibits their migration. It is crucial for a healthy organism to strictly control the positioning of stem cells in their respective niches as failure to do so would enable potentially unchecked dispersion of a population of cells with nearly unlimited proliferative potential. Recently Niola and colleagues described an elegant synchronicity of stemness and cell positioning of neural stem cells: They showed that Id proteins, a family of key transcription factors which prevent premature differentiation of stem cells, also directly control key mediators of cell adhesion and act to preserve anchorage of NSCs in their specialised niche (Niola et al., 2012). Whereas this is a distinctly cell-intrinsic mechanism, it seems as if vascular ephrinB2 performs a similar dual role in the SVZ: It directly controls stem cell maintenance through p53 and ensures correct positioning through compartmentalisation. This steady state of quiescence and tight anchorage in the niche however has to be overcome once a stem cell becomes activated, divides and then migrates out of the SVZ along the rostral-migratory stream both as part of regular cell turnover or in response to injuries like a stroke (Zhang et al., 2004; Lim and Alvarez-Buylla, 2014). It would be of great interest to understand how and through which signalling pathways this robust spatial and divisional control is subdued to ensure that stem cells can respond to an increased demand of differentiated progeny.

We further discovered, that ephrinB2 upregulation in a MAPK dependent manner helps ma-

lignant neural stem cells to overcome the compartmentalisation by endothelial cells but even more importantly also enhances the intrinsic tumourigenic capabilities of GSCs by enabling anchorage independent cytokinesis. Interestingly, we found that two key aspects of glioma-genesis, anchorage independent proliferation and perivascular invasion are mediated by the same molecule through very distinct signalling mechanisms: perivascular invasion depends on Eph forward signalling whereas anchorage independent proliferation is cell autonomous and requires ephrinB2 reverse signalling. Bidirectional signalling is a distinctive feature of Eph/ephrin molecules and distributes greatly to the ability of Eph receptors and ligands to mediate a great variety of distinct biological processes but also complicates the understanding of Eph/ephrin signalling in a disease context (Pasquale, 2008). There has been a long-standing debate about the dichotomy of Eph/ephrin signalling in tumour progression: various studies have provided extensive evidence of ephrins and Eph receptors acting both tumour suppressive and promoting in the same tumours (Pasquale, 2010; Nakada et al., 2011). Our data offers a simple new explanation for this: it is well conceivable, that tumour protective signalling pathways are hijacked by mutated cancer cells to achieve the opposite aim. As such, both tumour promoting and suppressing effects can be mediated by the same molecule depending on the specific intercellular interactions, differences in forward and reverse signalling and the complex stoichiometry of Eph/ephrin clusters on the individual cell surfaces (see Janes et al., 2012; Pasquale, 2005).

Intriguingly, the novel mechanism for perivascular invasion we have discovered in glioblas-toma differs significantly from other reports which identify downregulation of Eph receptors as cause for increased invasiveness in colorectal and prostate cancer (Astin et al., 2010; Cortina et al., 2007). We propose a model in which GSCs escape niche regulation by homotypic cell interactions which causes permanently high levels of Eph activation and leads to saturation of this signalling pathway. This in turn causes an insensitivity of GSCs to compartmentalis-ing vascular stimuli. Interestingly, it has already been reported, that phosphorylation of both EphB2 receptor and ephrinB2 ligand is crucial for glioma migration and invasion *in vivo* (Nakada et al., 2004, 2010) which is in agreement with our proposed model (**Figure 34)**.

Immortalised neural stem cell
(ephrinB2 low)

Glioblastoma stem cell
(ephrinB2 high)

Endothelial cells

Compartmentalisation

imNSC

GSC

Invasion

ephrinB2
Eph
p-Eph

Eph signalling responsive to acute
stimulation by endothelial ephrinB2

Constitutive Eph signalling in tumour cells
- no response to endothelial stimulation
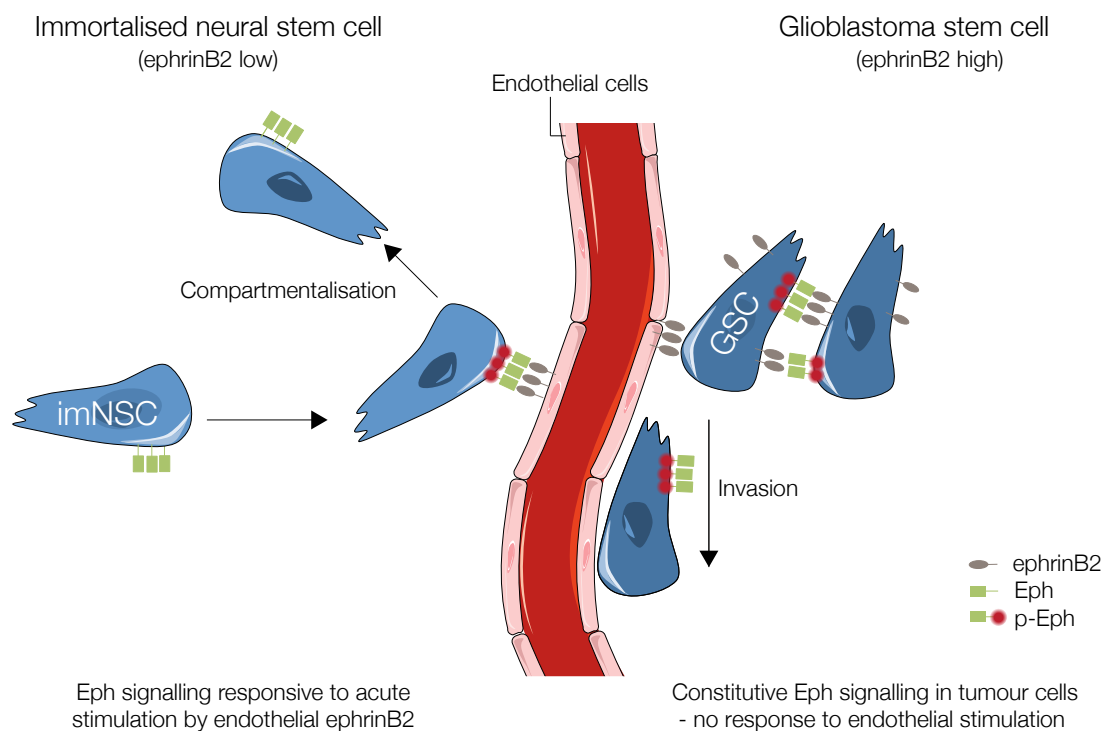
**Figure 34: Model of ephrinB2 mediated perivascular invasion.** Endothelial ephrinB2 compartmentalises normal neural stem cells by activating Eph signalling. GSCs overexpress ephrinB2 and have continuously saturated levels of activated Eph-signalling. They become insensitive to compartmentalising stimuli from the vasculature and are able to invade perivascularly.

This suggests, that absolute levels of specific Eph receptors and ligands expressed on a cell might not be the crucial determinant for cell behaviour. Instead the key factor might be the activation state of this protein in comparison to other Eph receptors and ligands. More research is needed however to understand this effect in more detail.

One key aspect which remains unclear is how single cells are able to continue migrating perivascularly once they lost homotypic cell-interactions as a means of overcoming compartmentalisation. One possibility is the following: initially GSCs rely on homotypic interactions to saturate Eph signalling and become insensitive to vascular ephrinB2. Once they are in contact and migrating along the vasculature however, the permanent stimulation of Eph signalling through endothelial ephrinB2 maintains the high phosphorylation levels. As the levels of Eph activation remain steady throughout this, the cells perceives no change in the microenvironment and continues migrating even though, stimulating ephrinB2 ligands were first supplied

by neighbouring tumour cells and then by endothelial cells. One important limitation of this simple model is, that if invading cells transiently loose contact with the vasculature they would become compartmentalised again if they again try to invade perivascularly. It has to be noted however, that *in vivo* migrating GSCs not only contact endothelial cells but also other cell types present in the perivascular space. Amongst them are astrocytes, which are also known to express high levels of ephrinB2 and might contribute to the saturation of Eph signalling in migrating GSCs (Ashton et al., 2012). Additionally, it is possible, that expression of ephrinB2 in GSCs to some extent inhibits the transduction of Eph signalling in cis for example by competing with bindings partners of the receptor. A similar mechanism of cis-inhibition has already been observed by Falivelli and colleagues (Falivelli et al., 2013). To truly understand the mechanism of ephrinB2 enabled perivascular invasion we should perform a more detailed analysis of singly migrating GSCs.

We specifically chose the transforming mutations in our murine tumour model to generate GSCs resembling mesenchymal glioblastoma. This subtype is generally considered as the most aggressive (Phillips et al., 2006); however it has to be noted, that glioblastoma is one of the most aggressive and invasive tumours known, irrespective of subtype. This therefore raises the important question of whether a similar ephrin-B2 dependent mechanism is also involved in other GBM subtypes and, if not whether specific genetic mutations help these cells to circumvent compartmentalisation, for example by altering the expression or function of other Eph receptors or ephrin ligands. We have shown, that our approach is successful in linking specific genetic mutations to phenotypic changes in Nf1 mutated mesenchymal glioblastoma and one could easily adopt the protocol to analyse GSCs with other stereotypical genetic aberrations like EGFR amplification or IDH1 mutations. *In silico* analysis using the publicly available TCGA database confirmed a strong correlation between *EFNB2* levels and decreased patient survival and predicted an important role for this ligand in mesenchymal and proneural subclasses. Interestingly, perivascularly invading proneural tumour cells appear to be slowly proliferative which might hint at a potential stem cell like phenotype of these invading cells, similar to mesenchymal glioblastoma (Sabit et al., 2014). It seems to be

clear, that tumour stem cells need to bypass vascular compartmentalisation through changes in Eph/ephrin expression levels and it is likely that different proteins of this family might be involved in different glioblastoma subtypes. Using the *in vitro* and *in vivo* tools we have established, we are able to pinpoint the underlying genetic mutations to phenotypical changes in perivascular invasion and tumourigenicity and it should therefore be a priority to widen our findings from one mesenchymal GSC line to a broader spectrum of GSCs of all subtypes.

The factors enabling a specific cell within a tumour to become invasive have been the subject of a long-standing and very intriguing debate. Mounting evidence in glioblastoma suggests, that it is indeed glioma stem cells, that are not only driving tumour recurrence after treatment, but are also largely responsible for tumour infiltration and invasion (Inoue et al., 2010; Venere et al., 2011). This is in agreement with our study and similar publications which employ a stem cell based model for glioblastoma formation: extensive invasion is observed in these xenografts, whereas injection of differentiated tumour cells only leads to the generation of well defined lesions but no formation of diffusely infiltrative tumours (Cheng et al., 2011). Interestingly, it has been reported that following chemotherapy, invasion of glioblastoma cells is strongly enhanced which not only hints at surviving GSCS as drivers of invasion but even at a potential suppression of tumour invasion by differentiated tumour cells (Velpula et al., 2012). The efficacy of anti-ephrinB2 treatment in inhibiting glioblastoma progression in our stem cell based model indicated that this therapy would be able to target GSCs specifically and might therefore be a valid approach to attack the most critical subset of cells within GBM. In addition, we observed a robust increase of ephrinB2 levels in GSCs compared to normal neural stem cells and other normal tissue. This would predict a relatively specific therapeutic approach with limited side effect consistent with the absence of any observed toxicity or other adverse effects in our xenograft models.

Gliomablastoma growth heavily relies on the association of glioblastoma stem cells with the vasculature (Calabrese et al., 2007). This highly vascularised nature led to previous attempts to employ anti-angiogenic therapies in the treatment of glioblastoma. Indeed, many anti-

angiogenic therapies are currently in trials and bevacizumab a monoclonal antibody targeting VEGF is currently approved under the name Avastin® to treat recurring glioblastoma. However despite initially showing great promise Avastin® resulted in no improvement of overall patient survival time as glioblastoma rapidly developed tumour escape mechanisms (Wick et al., 2011). An important adaptive mechanism of tumour resistance to anti-VEGF therapy is the co-option of blood vessels, a mechanism by which tumour cells obtain a blood supply by simply homing to and migrating along the preexisting vasculature (Donnem et al., 2013). Interestingly ephrinB2 is a key mediator of angiogenesis both in a physiological and tumour context (Sawamiphak et al., 2010). It might be a highly promising therapeutic approach to target the invasive capabilities of glioblastoma stem cells at the same time as inhibiting angiogenesis. This way, increased invasion and vascular cooption could be prevented and the cancer stem cell resistance circumvented. It has already been shown, that B11 robustly inhibits tumour angiogenesis in pancreas, colon and lung cancer models (Abéngozar et al., 2012), whereas we show a direct effect on glioblastoma cells. Treating with specific anti-ephrinB2 antibodies therefore tackles not only proliferation and invasion of GSCs directly, but could also inhibit angiogenesis and therefore effectively inhibit three pathways at once. Whilst this is intriguing, it might be more promising to combine anti-ephrinB2 treatment with antiangiogenic therapies, like anti-VEGF treatment to test whether tumour recurrence rates can be reduced. Additionally while our approach shows great promise to treat the stem cell compartment of glioblastomas this only compromises a relatively small proportion of the tumour mass (Singh et al., 2003) and specific ablation of the stem cell population causes a considerable residual tumour to remain behind (Chen et al., 2012). Thus to target the bulk of the tumour it might be beneficial to combine the stem cell specific anti-ephrinB2 therapy with classical chemotherapeutics like the commonly prescribed Carmustine or temozolomide. This combinatorial strategy might be successful in removing both the stem cell compartment and the more differentiated tumour mass completely, and might therefore significantly increase the time of progression free survival (Chaichana et al., 2011).

This study mainly focussed on perivascular migration as a route of invasion for glioblastoma,

the prevalent route of glioblastoma spread in many mouse models based on glioblastoma stem cells (Farin et al., 2006). However extensive invasion along other existing structures like myelinated fibres in white matter tracts(perifascicular) and perineuronal migration has been frequently observed in glioblastoma (Giese and Westphal, 1996). To fully understand glioblastoma invasion it is crucial to study these pathways of invasion as well using the *in vitro* and *in vivo* assays we have established in our lab. It has previously been reported, that the ability of glioblastoma cell lines to migrate on coated myelin differs dramatically between different glioblastoma cell lines and it would be of great interest to better understand proteins controlling perifascicular invasion (Giese et al., 1996).

Overall, our work identified ephrinB2 as highly attractive target for the treatment of GBM. We show how eph/ephrin signalling acts as a tumour suppressor at early tumour stages and is then hijacked by glioblastoma stem cells to overcome this inhibition. EphrinB2 is, to our knowledge, the first target protein which in itself would be an effective "combinatorial therapy": by targeting ephrinB2 we were able to inhibit both perivascular invasion and proliferation of glioblastoma stem cells **(Figure 35)**, therefore paving new avenues for future, more effective, glioblastoma therapies which will hopefully result in improving the survival chances of patients.
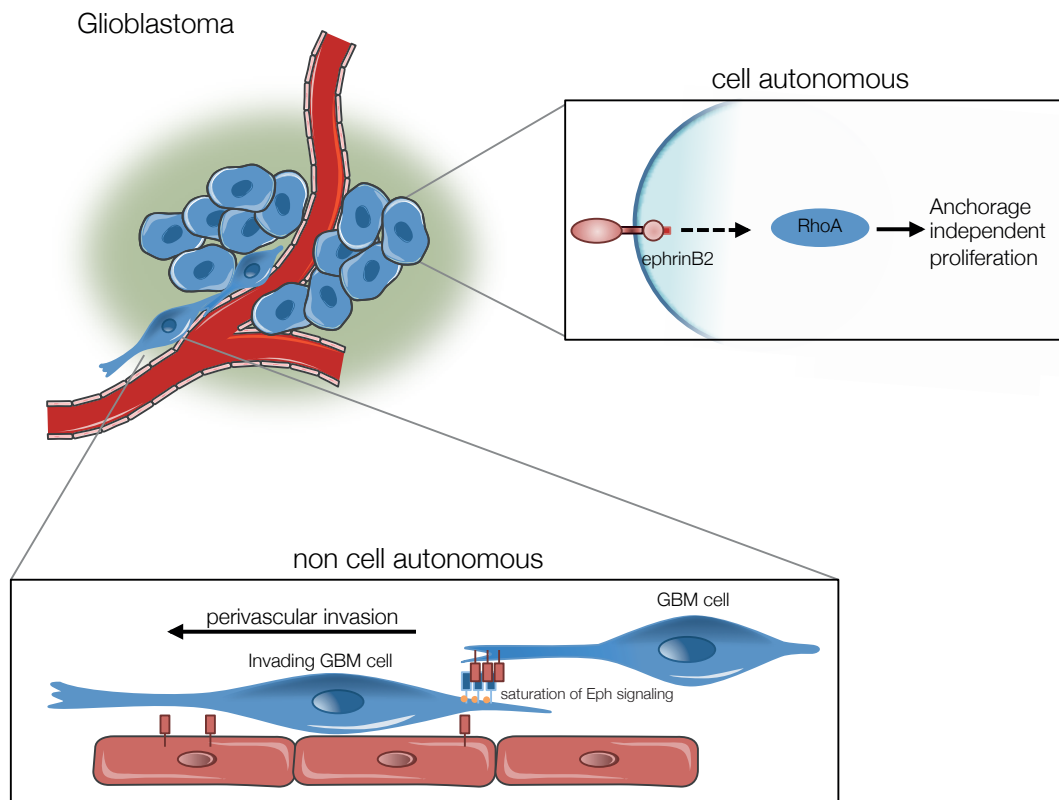
**Figure 35: Model of ephrinB2 mediated tumourigenicity.** ephrinB2 expression influences GSC behaviour in two complementary ways: It enables perivascular invasion by saturating Eph signalling and therefore desensitising GSCs to endothelial compartmentalisation in a cell-contact dependent manner. Additionally it enables anchorage independent proliferation cell-autonomously by mediating progression through cytokinesis in a RhoA dependent manner

# Bibliography

Abel, T. W., Clark, C., Bierie, B., Chytil, A., Aakre, M., Gorska, A., and Moses, H. L. (2009). GFAP-Cre-mediated activation of oncogenic K-ras results in expansion of the subventricular zone and infiltrating glioma. *Molecular cancer research : MCR*, 7(5):645--53.

Abéngozar, M. A., de Frutos, S., Ferreiro, S., Soriano, J., Perez-Martinez, M., Olmeda, D., Marenchino, M., Cañamero, M., Ortega, S., Megias, D., Rodriguez, A., and Martínez-Torrecuadrada, J. L. (2012). Blocking ephrinB2 with highly specific antibodies inhibits angiogenesis, lymphangiogenesis, and tumor growth. *Blood*, 119(19):4565--76.

Agarwal, S., Manchanda, P., Vogelbaum, M. A., Ohlfest, J. R., and Elmquist, W. F. (2013). Function of the blood-brain barrier and restriction of drug delivery to invasive glioma cells: findings in an orthotopic rat xenograft model of glioma. *Drug metabolism and disposition: the biological fate of chemicals*, 41(1):33--9.

Aguirre-Gamboa, R., Gomez-Rueda, H., Martínez-Ledesma, E., Martínez-Torteya, A., Chacolla-Huaringa, R., Rodriguez-Barrientos, A., Tamez-Peña, J. G., and Treviño, V. (2013). SurvExpress: an online biomarker validation tool and database for cancer gene expression data using survival analysis. *PloS one*, 8(9):e74250.

Al-Hajj, M., Wicha, M. S., Benito-Hernandez, A., Morrison, S. J., and Clarke, M. F. (2003). Prospective identification of tumorigenic breast cancer cells. *Proceedings of the National Academy of Sciences of the United States of America*, 100(7):3983--8.

Alam, S. M., Fujimoto, J., Jahan, I., Sato, E., and Tamaya, T. (2008). Coexpression of

EphB4 and ephrinB2 in tumour advancement of ovarian cancers. *British journal of cancer*, 98(4):845--51.

Alberts, A. S., Qin, H., Carr, H. S., and Frost, J. A. (2005). PAK1 negatively regulates the activity of the Rho exchange factor NET1. *The Journal of biological chemistry*, 280(13):12152--61.

Alberts, B., Johnson, A., J., L., Raff, M., Roberts, K., and Walter, P. (2008). *Molecular Biology of the Cell*. Garland Science, 5 edition.

Alcantara Llaguno, S., Chen, J., Kwon, C.-H., Jackson, E. L., Li, Y., Burns, D. K., Alvarez-Buylla, A., and Parada, L. F. (2009). Malignant astrocytomas originate from neural stem/progenitor cells in a somatic tumor suppressor mouse model. *Cancer cell*, 15(1):45--56.

Ali, S. H. and DeCaprio, J. A. (2001). Cellular transformation by SV40 large T antigen: interaction with host proteins. *Seminars in cancer biology*, 11(1):15--23.

Allen, E. (1912). *The cessation of mitosis in the central nervous system of the Albino rat*. Waverley Press].

Alvarez-Buylla, A., Herrera, D. G., and Wichterle, H. (2000). The subventricular zone: source of neuronal precursors for brain repair. *Progress in brain research*, 127:1--11.

Armesilla-Diaz, A., Bragado, P., Del Valle, I., Cuevas, E., Lazaro, I., Martin, C., Cigudosa, J. C., and Silva, A. (2009). p53 regulates the self-renewal and differentiation of neural precursors. *Neuroscience*, 158(4):1378--89.

Arvanitis, D. and Davy, A. (2008). Eph/ephrin signaling: networks. *Genes & development*, 22(4):416--29.

Ashton, R. S., Conway, A., Pangarkar, C., Bergen, J., Lim, K.-I., Shah, P., Bissell, M., and Schaffer, D. V. (2012). Astrocytes regulate adult hippocampal neurogenesis through ephrin-B signaling. *Nature neuroscience*, 15(10):1399--406.

Astin, J. W., Batson, J., Kadir, S., Charlet, J., Persad, R. A., Gillatt, D., Oxley, J. D., and Nobes, C. D. (2010). Competition amongst Eph receptors regulates contact inhibition of locomotion and invasiveness in prostate cancer cells. *Nature cell biology*, 12(12):1194--204.

Baccelli, I. and Trumpp, A. (2012). The evolving concept of cancer and metastasis stem cells. *The Journal of cell biology*, 198(3):281--93.

Bachoo, R. M., Maher, E. A., Ligon, K. L., Sharpless, N. E., Chan, S. S., You, M. J., Tang, Y., DeFrances, J., Stover, E., and Weissleder, R. (2002). Epidermal growth factor receptor and Ink4a/ArfConvergent mechanisms governing terminal differentiation and transformation along the neural stem cell to astrocyte axis. *Cancer Cell*, 1(3):269--277.

Bae, K.-M., Parker, N. N., Dai, Y., Vieweg, J., and Siemann, D. W. (2011). E-cadherin plasticity in prostate cancer stem cell invasion. *American journal of cancer research*, 1(1):71--84.

Baker, G. J., Yadav, V. N., Motsch, S., Koschmann, C., Calinescu, A.-A., Mineharu, Y., Camelo-Piragua, S. I., Orringer, D., Bannykh, S., Nichols, W. S., DeCarvalho, A. C., Mikkelsen, T., Castro, M. G., and Lowenstein, P. R. (2014). Mechanisms of glioma formation: iterative perivascular glioma growth and invasion leads to tumor progression, VEGF-independent vascularization, and resistance to antiangiogenic therapy. *Neoplasia (New York, N.Y.)*, 16(7):543--61.

Bao, S., Wu, Q., Sathornsumetee, S., Hao, Y., Li, Z., Hjelmeland, A. B., Shi, Q., McLendon, R. E., Bigner, D. D., and Rich, J. N. (2006). Stem cell-like glioma cells promote tumor angiogenesis through vascular endothelial growth factor. *Cancer research*, 66(16):7843--8.

Batlle, E., Henderson, J. T., Beghtel, H., van den Born, M. M., Sancho, E., Huls, G., Meeldijk, J., Robertson, J., van de Wetering, M., Pawson, T., and Clevers, H. (2002). $\beta$-Catenin and TCF Mediate Cell Positioning in the Intestinal Epithelium by Controlling the Expression of EphB/EphrinB. *Cell*, 111(2):251--263.

Beauchesne, P. (2011). Extra-neural metastases of malignant gliomas: myth or reality? *Cancers*, 3(1):461--77.

Benner, E. J., Luciano, D., Jo, R., Abdi, K., Paez-Gonzalez, P., Sheng, H., Warner, D. S., Liu, C., Eroglu, C., and Kuo, C. T. (2013). Protective astrogenesis from the SVZ niche after injury is controlled by Notch modulator Thbs4. *Nature*, 497(7449):369--73.

Bernstein, J. J. and Woodard, C. A. (1995). Glioblastoma cells do not intravasate into blood vessels. *Neurosurgery*, 36(1):124--32; discussion 132.

Bhat, K. P. L., Salazar, K. L., Balasubramaniyan, V., Wani, K., Heathcock, L., Hollingsworth, F., James, J. D., Gumin, J., Diefes, K. L., Kim, S. H., Turski, A., Azodi, Y., Yang, Y., Doucette, T., Colman, H., Sulman, E. P., Lang, F. F., Rao, G., Copray, S., Vaillant, B. D., and Aldape, K. D. (2011). The transcriptional coactivator TAZ regulates mesenchymal differentiation in malignant glioma. *Genes & development*, 25(24):2594--609.

Biebl, M., Cooper, C. M., Winkler, J., and Kuhn, H. (2000). Analysis of neurogenesis and programmed cell death reveals a self-renewing capacity in the adult rat brain. *Neuroscience Letters*, 291(1):17--20.

Binda, E., Visioli, A., Giani, F., Lamorte, G., Copetti, M., Pitter, K. L., Huse, J. T., Cajola, L., Zanetti, N., DiMeco, F., De Filippis, L., Mangiola, A., Maira, G., Anile, C., De Bonis, P., Reynolds, B. A., Pasquale, E. B., and Vescovi, A. L. (2012). The EphA2 receptor drives self-renewal and tumorigenicity in stem-like tumor-propagating cells from human glioblastomas. *Cancer cell*, 22(6):765--80.

Binns, K. L., Taylor, P. P., Sicheri, F., Pawson, T., and Holland, S. J. (2000). Phosphorylation of Tyrosine Residues in the Kinase Domain and Juxtamembrane Region Regulates the Biological and Catalytic Activities of Eph Receptors. *Molecular and Cellular Biology*, 20(13):4791--4805.

Blakemore, W. F. (1969). The ultrastructure of the subependymal plate in the rat. *Journal of anatomy*, 104(Pt 3):423--33.

Blouw, B., Song, H., Tihan, T., Bosze, J., Ferrara, N., Gerber, H.-P., Johnson, R. S., and Bergers, G. (2003). The hypoxic response of tumors is dependent on their microenvironment. *Cancer Cell*, 4(2):133--146.

Bochenek, M. L., Dickinson, S., Astin, J. W., Adams, R. H., and Nobes, C. D. (2010). Ephrin-B2 regulates endothelial cell morphology and motility independently of Eph-receptor binding. *Journal of cell science*, 123(Pt 8):1235--46.

Bonizzi, G., Cicalese, A., Insinga, A., and Pelicci, P. G. (2012). The emerging role of p53 in stem cells. *Trends in molecular medicine*, 18(1):6--12.

Bonnet, D. and Dick, J. E. (1997). Human acute myeloid leukemia is organized as a hierarchy that originates from a primitive hematopoietic cell. *Nature medicine*, 3(7):730--7.

Brantley-Sieders, D. M. and Chen, J. (2004). Eph receptor tyrosine kinases in angiogenesis: from development to disease. *Angiogenesis*, 7(1):17--28.

Bruce, V., Olivieri, G., Eickelberg, O., and Miescher, G. C. (1999). Functional activation of EphA5 receptor does not promote cell proliferation in the aberrant EphA5 expressing human glioblastoma U-118 MG cell line. *Brain research*, 821(1):169--76.

Brückner, K., Pasquale, E. B., and Klein, R. (1997). Tyrosine phosphorylation of transmembrane ligands for Eph receptors. *Science (New York, N.Y.)*, 275(5306):1640--3.

Burger, P. C., Vogel, F. S., Green, S. B., and Strike, T. A. (1985). Glioblastoma multiforme and anaplastic astrocytoma. Pathologic criteria and prognostic implications. *Cancer*, 56(5):1106--11.

Cabarcas, S. M., Mathews, L. A., and Farrar, W. L. (2011). The cancer stem cell niche--there goes the neighborhood? *International journal of cancer. Journal international du cancer*, 129(10):2315--27.

Calabrese, C., Poppleton, H., Kocak, M., Hogg, T. L., Fuller, C., Hamner, B., Oh, E. Y., Gaber, M. W., Finklestein, D., Allen, M., Frank, A., Bayazitov, I. T., Zakharenko, S. S.,

Gajjar, A., Davidoff, A., and Gilbertson, R. J. (2007). A perivascular niche for brain tumor stem cells. *Cancer cell*, 11(1):69--82.

Carro, M. S., Lim, W. K., Alvarez, M. J., Bollo, R. J., Zhao, X., Snyder, E. Y., Sulman, E. P., Anne, S. L., Doetsch, F., Colman, H., Lasorella, A., Aldape, K., Califano, A., and Iavarone, A. (2010). The transcriptional network for mesenchymal transformation of brain tumours. *Nature*, 463(7279):318--25.

Chaichana, K. L., Zaidi, H., Pendleton, C., McGirt, M. J., Grossman, R., Weingart, J. D., Olivi, A., Quiñones Hinojosa, A., and Brem, H. (2011). The efficacy of carmustine wafers for older patients with glioblastoma multiforme: prolonging survival. *Neurological research*, 33(7):759--64.

Charles, N., Ozawa, T., Squatrito, M., Bleau, A.-M., Brennan, C. W., Hambardzumyan, D., and Holland, E. C. (2010). Perivascular nitric oxide activates notch signaling and promotes stem-like character in PDGF-induced glioma cells. *Cell stem cell*, 6(2):141--52.

Chen, J., Li, Y., Yu, T.-S., McKay, R. M., Burns, D. K., Kernie, S. G., and Parada, L. F. (2012). A restricted cell population propagates glioblastoma growth after chemotherapy. *Nature*, 488(7412):522--6.

Cheng, L., Wu, Q., Guryanova, O. A., Huang, Z., Huang, Q., Rich, J. N., and Bao, S. (2011). Elevated invasive potential of glioblastoma stem cells. *Biochemical and biophysical research communications*, 406(4):643--8.

Chow, L. M. L., Endersby, R., Zhu, X., Rankin, S., Qu, C., Zhang, J., Broniscer, A., Ellison, D. W., and Baker, S. J. (2011). Cooperativity within and among Pten, p53, and Rb pathways induces high-grade astrocytoma in adult brain. *Cancer cell*, 19(3):305--16.

Chumley, M. J., Catchpole, T., Silvany, R. E., Kernie, S. G., and Henkemeyer, M. (2007). EphB receptors regulate stem/progenitor cell proliferation, migration, and polarity during hippocampal neurogenesis. *The Journal of neuroscience : the official journal of the Society for Neuroscience*, 27(49):13481--90.

Cichowski, K. and Jacks, T. (2001). NF1 Tumor Suppressor Gene Function. *Cell*, 104(4):593--604.

Collins, A. T., Berry, P. A., Hyde, C., Stower, M. J., and Maitland, N. J. (2005). Prospective identification of tumorigenic prostate cancer stem cells. *Cancer research*, 65(23):10946--51.

Conover, J. C., Doetsch, F., Garcia-Verdugo, J. M., Gale, N. W., Yancopoulos, G. D., and Alvarez-Buylla, a. (2000). Disruption of Eph/ephrin signaling affects migration and proliferation in the adult subventricular zone. *Nature neuroscience*, 3(11):1091--7.

Cortina, C., Palomo-Ponce, S., Iglesias, M., Fernández-Masip, J. L., Vivancos, A., Whissell, G., Humà, M., Peiró, N., Gallego, L., Jonkheer, S., Davy, A., Lloreta, J., Sancho, E., and Batlle, E. (2007). EphB-ephrin-B interactions suppress colorectal cancer progression by compartmentalizing tumor cells. *Nature genetics*, 39(11):1376--83.

Cowan, C. A. and Henkemeyer, M. (2001). The SH2/SH3 adaptor Grb4 transduces B-ephrin reverse signals. *Nature*, 413(6852):174--9.

Cremona, C. A. and Lloyd, A. C. (2009). Loss of anchorage in checkpoint-deficient cells increases genomic instability and promotes oncogenic transformation. *Journal of cell science*, 122(Pt 18):3272--81.

Cuddapah, V. A., Robel, S., Watkins, S., and Sontheimer, H. (2014). A neurocentric perspective on glioma invasion. *Nature reviews. Neuroscience*, 15(7):455--65.

Curtis, M. A., Kam, M., Nannmark, U., Anderson, M. F., Axell, M. Z., Wikkelso, C., Holtå s, S., van Roon-Mom, W. M. C., Björk-Eriksson, T., Nordborg, C., Frisén, J., Dragunow, M., Faull, R. L. M., and Eriksson, P. S. (2007). Human neuroblasts migrate to the olfactory bulb via a lateral ventricular extension. *Science (New York, N.Y.)*, 315(5816):1243--9.

Daar, I. O. (2012). Non-SH2/PDZ reverse signaling by ephrins. *Seminars in cell & developmental biology*, 23(1):65--74.

Dai, Y., Ning, X., Han, G., and Li, W. (2015). Assessment of the Association between Isocitrate Dehydrogenase 1 Mutation and Mortality Risk of Glioblastoma Patients. *Molecular neurobiology*.

Davidson, G. and Niehrs, C. (2010). Emerging links between CDK cell cycle regulators and Wnt signaling. *Trends in cell biology*, 20(8):453--60.

Day, B. W., Stringer, B. W., Al-Ejeh, F., Ting, M. J., Wilson, J., Ensbey, K. S., Jamieson, P. R., Bruce, Z. C., Lim, Y. C., Offenhäuser, C., Charmsaz, S., Cooper, L. T., Ellacott, J. K., Harding, A., Leveque, L., Inglis, P., Allan, S., Walker, D. G., Lackmann, M., Osborne, G., Khanna, K. K., Reynolds, B. A., Lickliter, J. D., and Boyd, A. W. (2013). EphA3 maintains tumorigenicity and is a therapeutic target in glioblastoma multiforme. *Cancer cell*, 23(2):238--48.

Day, B. W., Stringer, B. W., and Boyd, A. W. (2014). Eph receptors as therapeutic targets in glioblastoma. *British journal of cancer*, 111(7):1255--61.

de Groot, J. F., Fuller, G., Kumar, A. J., Piao, Y., Eterovic, K., Ji, Y., and Conrad, C. A. (2010). Tumor invasion after treatment of glioblastoma with bevacizumab: radiographic and pathologic correlation in humans and mice. *Neuro-oncology*, 12(3):233--42.

De Marchis, S., Bovetti, S., Carletti, B., Hsieh, Y.-C., Garzotto, D., Peretto, P., Fasolo, A., Puche, A. C., and Rossi, F. (2007). Generation of distinct types of periglomerular olfactory bulb interneurons during development and in adult mice: implication for intrinsic properties of the subventricular zone progenitor population. *The Journal of neuroscience : the official journal of the Society for Neuroscience*, 27(3):657--64.

Delgado, A. C., Ferrón, S. R., Vicente, D., Porlan, E., Perez-Villalba, A., Trujillo, C. M., D'Ocón, P., and Fariñas, I. (2014). Endothelial NT-3 delivered by vasculature and CSF promotes quiescence of subependymal neural stem cells through nitric oxide induction. *Neuron*, 83(3):572--85.

Demuth, T. and Berens, M. E. (2004). Molecular mechanisms of glioma cell migration and invasion. *Journal of neuro-oncology*, 70(2):217--28.

Dirks, P. B. (2001). Glioma migration: clues from the biology of neural progenitor cells and embryonic CNS cell migration. *Journal of neuro-oncology*, 53(2):203--12.

Doetsch, F. (2003). A niche for adult neural stem cells. *Current opinion in genetics & development*, 13(5):543--50.

Doetsch, F., Caillé, I., Lim, D. A., García-Verdugo, J. M., and Alvarez-Buylla, A. (1999a). Subventricular zone astrocytes are neural stem cells in the adult mammalian brain. *Cell*, 97(6):703--16.

Doetsch, F., Garcia-Verdugo, J. M., and Alvarez-Buylla, A. (1999b). Regeneration of a germinal layer in the adult mammalian brain. *Proceedings of the National Academy of Sciences*, 96(20):11619--11624.

Donnem, T., Hu, J., Ferguson, M., Adighibe, O., Snell, C., Harris, A. L., Gatter, K. C., and Pezzella, F. (2013). Vessel co-option in primary human tumors and metastases: an obstacle to effective anti-angiogenic treatment? *Cancer medicine*, 2(4):427--36.

Dow, L. E., Kauffman, J. S., Caddy, J., Zarbalis, K., Peterson, A. S., Jane, S. M., Russell, S. M., and Humbert, P. O. (2007). The tumour-suppressor Scribble dictates cell polarity during directed epithelial migration: regulation of Rho GTPase recruitment to the leading edge. *Oncogene*, 26(16):2272--82.

Dravis, C. and Henkemeyer, M. (2011). Ephrin-B reverse signaling controls septation events at the embryonic midline through separate tyrosine phosphorylation-independent signaling avenues. *Developmental biology*, 355(1):138--51.

Du, J., Fu, C., and Sretavan, D. W. (2007). Eph/ephrin signaling as a potential therapeutic target after central nervous system injury. *Current pharmaceutical design*, 13(24):2507--18.

Eph Nomenclature Committee (1997). Unified nomenclature for Eph family receptors and their ligands, the ephrins. Eph Nomenclature Committee. *Cell*, 90(3):403--4.

Eriksson, P. S., Perfilieva, E., Björk-Eriksson, T., Alborn, A. M., Nordborg, C., Peterson, D. A., and Gage, F. H. (1998). Neurogenesis in the adult human hippocampus. *Nature medicine*, 4(11):1313--7.

Falivelli, G., Lisabeth, E. M., Rubio de la Torre, E., Perez-Tenorio, G., Tosato, G., Salvucci, O., and Pasquale, E. B. (2013). Attenuation of eph receptor kinase activation in cancer cells by coexpressed ephrin ligands. *PloS one*, 8(11):e81445.

Farin, A., Suzuki, S. O., Weiker, M., Goldman, J. E., Bruce, J. N., and Canoll, P. (2006). Transplanted glioma cells migrate and proliferate on host brain vasculature: a dynamic analysis. *Glia*, 53(8):799--808.

Ferrón, S. R., Andreu-Agulló, C., Mira, H., Sánchez, P., Ángeles Marqués-Torrejón, M., and Fariñas, I. (2007). A combined ex/in vivo assay to detect effects of exogenously added factors in neural stem cells. *Nature Protocols*, 2(4):849--859.

Flesken-Nikitin, A., Hwang, C.-I., Cheng, C.-Y., Michurina, T. V., Enikolopov, G., and Nikitin, A. Y. (2013). Ovarian surface epithelium at the junction area contains a cancer-prone stem cell niche. *Nature*, 495(7440):241--5.

Foo, S. S., Turner, C. J., Adams, S., Compagni, A., Aubyn, D., Kogata, N., Lindblom, P., Shani, M., Zicha, D., and Adams, R. H. (2006). Ephrin-B2 controls cell motility and adhesion during blood-vessel-wall assembly. *Cell*, 124(1):161--73.

Freedman, V. (1974). Cellular tumorigenicity in nude mice: Correlation with cell growth in semi-solid medium. *Cell*, 3(4):355--359.

Friedmann-Morvinski, D., Bushong, E. A., Ke, E., Soda, Y., Marumoto, T., Singer, O., Ellisman, M. H., and Verma, I. M. (2012). Dedifferentiation of neurons and astrocytes by oncogenes can induce gliomas in mice. *Science (New York, N.Y.)*, 338(6110):1080--4.

Fukai, J., Yokote, H., Yamanaka, R., Arao, T., Nishio, K., and Itakura, T. (2008). EphA4 promotes cell proliferation and migration through a novel EphA4-FGFR1 signaling pathway in the human glioma U251 cell line. *Molecular cancer therapeutics*, 7(9):2768--78.

Galan-Moya, E. M., Le Guelte, A., Lima Fernandes, E., Thirant, C., Dwyer, J., Bidere, N., Couraud, P.-O., Scott, M. G. H., Junier, M.-P., Chneiweiss, H., and Gavard, J. (2011). Secreted factors from brain endothelial cells maintain glioblastoma stem-like cell expansion through the mTOR pathway. *EMBO reports*, 12(5):470--6.

Galli, R., Binda, E., Orfanelli, U., Cipelletti, B., Gritti, A., De Vitis, S., Fiocco, R., Foroni, C., Dimeco, F., and Vescovi, A. (2004). Isolation and characterization of tumorigenic, stem-like neural precursors from human glioblastoma. *Cancer research*, 64(19):7011--21.

Gao, C. and Chen, Y.-G. (2010). Dishevelled: The hub of Wnt signaling. *Cellular signalling*, 22(5):717--27.

Gautier, L., Cope, L., Bolstad, B. M., and Irizarry, R. A. (2004). affy--analysis of Affymetrix GeneChip data at the probe level. *Bioinformatics (Oxford, England)*, 20(3):307--15.

Genander, M. (2012). Eph and ephrins in epithelial stem cell niches and cancer. *Cell adhesion & migration*, 6(2):126--30.

Genander, M. and Frisén, J. (2010). Ephrins and Eph receptors in stem cells and cancer. *Current opinion in cell biology*, 22(5):611--6.

Genander, M., Holmberg, J., and Frisén, J. (2010). Ephrins negatively regulate cell proliferation in the epidermis and hair follicle. *Stem cells (Dayton, Ohio)*, 28(7):1196--205.

Giese, A., Kluwe, L., Laube, B., Meissner, H., Berens, M. E., and Westphal, M. (1996). Migration of human glioma cells on myelin. *Neurosurgery*, 38(4):755--64.

Giese, A., Rief, M. D., Loo, M. A., and Berens, M. E. (1994). Determinants of human astrocytoma migration. *Cancer research*, 54(14):3897--904.

Giese, A. and Westphal, M. (1996). Glioma invasion in the central nervous system. *Neurosurgery*, 39(2):235--50; discussion 250--2.

Gil-Perotin, S., Marin-Husstege, M., Li, J., Soriano-Navarro, M., Zindy, F., Roussel, M. F., Garcia-Verdugo, J.-M., and Casaccia-Bonnefil, P. (2006). Loss of p53 induces changes in the behavior of subventricular zone cells: implication for the genesis of glial tumors. *The Journal of neuroscience : the official journal of the Society for Neuroscience*, 26(4):1107--16.

Gilbertson, R. J. and Rich, J. N. (2007). Making a tumour's bed: glioblastoma stem cells and the vascular niche. *Nature reviews. Cancer*, 7(10):733--6.

Girouard, S. D. and Murphy, G. F. (2011). Melanoma stem cells: not rare, but well done. *Laboratory investigation; a journal of technical methods and pathology*, 91(5):647--64.

Glaser, T., Pollard, S. M., Smith, A., and Brüstle, O. (2007). Tripotential differentiation of adherently expandable neural stem (NS) cells. *PloS one*, 2(3):e298.

Glotzer, M. (2005). The molecular requirements for cytokinesis. *Science (New York, N.Y.)*, 307(5716):1735--9.

Goldman, S. A. and Chen, Z. (2011). Perivascular instruction of cell genesis and fate in the adult brain. *Nature neuroscience*, 14(11):1382--9.

Gómez-Gaviro, M. V., Scott, C. E., Sesay, A. K., Matheu, A., Booth, S., Galichet, C., and Lovell-Badge, R. (2012). Betacellulin promotes cell proliferation in the neural stem cell niche and stimulates neurogenesis. *Proceedings of the National Academy of Sciences of the United States of America*, 109(4):1317--22.

Gostjeva, E. V. and Thilly, W. G. (2005). Stem cell stages and the origins of colon cancer: a multidisciplinary perspective. *Stem cell reviews*, 1(3):243--51.

Gürsel, D. B., Shin, B. J., Burkhardt, J.-K., Kesavabhotla, K., Schlaff, C. D., and Boockvar, J. A. (2011). Glioblastoma stem-like cells-biology and therapeutic implications. *Cancers*, 3(2):2655--66.

Hatano, M., Eguchi, J., Tatsumi, T., Kuwashima, N., Dusak, J. E., Kinch, M. S., Pollack, I. F., Hamilton, R. L., Storkus, W. J., and Okada, H. (2005). EphA2 as a glioma-associated antigen: a novel target for glioma vaccines. *Neoplasia (New York, N.Y.)*, 7(8):717--22.

Heinemeyer, T., Wingender, E., Reuter, I., Hermjakob, H., Kel, A. E., Kel, O. V., Ignatieva, E. V., Ananko, E. A., Podkolodnaya, O. A., Kolpakov, F. A., Podkolodny, N. L., and Kolchanov, N. A. (1998). Databases on transcriptional regulation: TRANSFAC, TRRD and COMPEL. *Nucleic acids research*, 26(1):362--7.

Henkemeyer, M., Marengere, L. E., McGlade, J., Olivier, J. P., Conlon, R. A., Holmyard, D. P., Letwin, K., and Pawson, T. (1994). Immunolocalization of the Nuk receptor tyrosine kinase suggests roles in segmental patterning of the brain and axonogenesis. *Oncogene*, 9(4):1001--14.

Himanen, J.-P., Chumley, M. J., Lackmann, M., Li, C., Barton, W. A., Jeffrey, P. D., Vearing, C., Geleick, D., Feldheim, D. A., Boyd, A. W., Henkemeyer, M., and Nikolov, D. B. (2004). Repelling class discrimination: ephrin-A5 binds to and activates EphB2 receptor signaling. *Nature neuroscience*, 7(5):501--9.

Himanen, J. P., Rajashankar, K. R., Lackmann, M., Cowan, C. A., Henkemeyer, M., and Nikolov, D. B. (2001). Crystal structure of an Eph receptor-ephrin complex. *Nature*, 414(6866):933--8.

Hindley, A. and Kolch, W. (2002). Extracellular signal regulated kinase (ERK)/mitogen activated protein kinase (MAPK)-independent functions of Raf kinases. *Journal of cell science*, 115(Pt 8):1575--81.

Hirai, H., Maru, Y., Hagiwara, K., Nishida, J., and Takaku, F. (1987). A novel putative tyrosine kinase receptor encoded by the eph gene. *Science (New York, N.Y.)*, 238(4834):1717--20.

Holland, E. C., Celestino, J., Dai, C., Schaefer, L., Sawaya, R. E., and Fuller, G. N. (2000).

Combined activation of Ras and Akt in neural progenitors induces glioblastoma formation in mice. *Nature genetics*, 25(1):55--7.

Holland, S. J., Gale, N. W., Gish, G. D., Roth, R. A., Songyang, Z., Cantley, L. C., Henke-meyer, M., Yancopoulos, G. D., and Pawson, T. (1997). Juxtamembrane tyrosine residues couple the Eph family receptor EphB2/Nuk to specific SH2 domain proteins in neuronal cells. *The EMBO journal*, 16(13):3877--88.

Holtmaat, A., Bonhoeffer, T., Chow, D. K., Chuckowree, J., De Paola, V., Hofer, S. B., Hübener, M., Keck, T., Knott, G., Lee, W.-C. A., Mostany, R., Mrsic-Flogel, T. D., Nedivi, E., Portera-Cailliau, C., Svoboda, K., Trachtenberg, J. T., and Wilbrecht, L. (2009). Long-term, high-resolution imaging in the mouse neocortex through a chronic cranial window. *Nature protocols*, 4(8):1128--44.

Huang, C.-Y. and Tan, T.-H. (2012). DUSPs, to MAP kinases and beyond. *Cell & bioscience*, 2(1):24.

Humbert, P., Russell, S., and Richardson, H. (2003). Dlg, Scribble and Lgl in cell polarity, cell proliferation and cancer. *BioEssays : news and reviews in molecular, cellular and developmental biology*, 25(6):542--53.

Humbert, P. O., Grzeschik, N. A., Brumby, A. M., Galea, R., Elsum, I., and Richardson, H. E. (2008). Control of tumourigenesis by the Scribble/Dlg/Lgl polarity module. *Oncogene*, 27(55):6888--907.

Huntley, M. A., Bien-Ly, N., Daneman, R., and Watts, R. J. (2014). Dissecting gene expression at the blood-brain barrier. *Frontiers in neuroscience*, 8:355.

Ignatova, T. N., Kukekov, V. G., Laywell, E. D., Suslov, O. N., Vrionis, F. D., and Steindler, D. A. (2002). Human cortical glial tumors contain neural stem-like cells expressing as-troglial and neuronal markers in vitro. *Glia*, 39(3):193--206.

Ihrie, R. a. and Alvarez-Buylla, A. (2011). Lake-front property: a unique germinal niche by the lateral ventricles of the adult brain. *Neuron*, 70(4):674--86.

Inda, M.-D.-M., Bonavia, R., and Seoane, J. (2014). Glioblastoma multiforme: a look inside its heterogeneous nature. *Cancers*, 6(1):226--39.

Inoue, A., Takahashi, H., Harada, H., Kohno, S., Ohue, S., Kobayashi, K., Yano, H., Tanaka, J., and Ohnishi, T. (2010). Cancer stem-like cells of glioblastoma characteristically express MMP-13 and display highly invasive activity. *International journal of oncology*, 37(5):1121--31.

Jain, R. K., di Tomaso, E., Duda, D. G., Loeffler, J. S., Sorensen, A. G., and Batchelor, T. T. (2007). Angiogenesis in brain tumours. *Nature reviews. Neuroscience*, 8(8):610--22.

Janes, P. W., Griesshaber, B., Atapattu, L., Nievergall, E., Hii, L. L., Mensinga, A., Chheang, C., Day, B. W., Boyd, A. W., Bastiaens, P. I., Jorgensen, C., Pawson, T., and Lackmann, M. (2011). Eph receptor function is modulated by heterooligomerization of A and B type Eph receptors. *The Journal of Cell Biology*, 195(6):1033--45.

Janes, P. W., Nievergall, E., and Lackmann, M. (2012). Concepts and consequences of Eph receptor clustering. *Seminars in cell & developmental biology*, 23(1):43--50.

Jeon, S. H., Yoon, J.-Y., Park, Y.-N., Jeong, W.-J., Kim, S., Jho, E.-H., Surh, Y.-J., and Choi, K.-Y. (2007). Axin inhibits extracellular signal-regulated kinase pathway by Ras degradation via beta-catenin. *The Journal of biological chemistry*, 282(19):14482--92.

Jiang, G., Freywald, T., Webster, J., Kozan, D., Geyer, R., DeCoteau, J., Narendran, A., and Freywald, A. (2008). In human leukemia cells ephrin-B-induced invasive activity is supported by Lck and is associated with reassembling of lipid raft signaling complexes. *Molecular cancer research : MCR*, 6(2):291--305.

Jones, D. L. and Wagers, A. J. (2008). No place like home: anatomy and function of the stem cell niche. *Nature reviews. Molecular cell biology*, 9(1):11--21.

Jordan, S. N. and Canman, J. C. (2012). Rho GTPases in animal cell cytokinesis: an occupation by the one percent. *Cytoskeleton (Hoboken, N.J.)*, 69(11):919--30.

Kalo, M. S. and Pasquale, E. B. (1999). Multiple in vivo tyrosine phosphorylation sites in EphB receptors. *Biochemistry*, 38(43):14396--408.

Kasahara, K., Nakayama, Y., Nakazato, Y., Ikeda, K., Kuga, T., and Yamaguchi, N. (2007). Src signaling regulates completion of abscission in cytokinesis through ERK/MAPK activation at the midbody. *The Journal of biological chemistry*, 282(8):5327--39.

Kemper, E. M., Leenders, W., Küsters, B., Lyons, S., Buckle, T., Heerschap, A., Boogerd, W., Beijnen, J. H., and van Tellingen, O. (2006). Development of luciferase tagged brain tumour models in mice for chemotherapy intervention studies. *European journal of cancer (Oxford, England : 1990)*, 42(18):3294--303.

Klein, R. (2009). Bidirectional modulation of synaptic functions by Eph/ephrin signaling. *Nature neuroscience*, 12(1):15--20.

Klein, R. (2012). Eph/ephrin signalling during development. *Development (Cambridge, England)*, 139(22):4105--9.

Kokovay, E., Goderie, S., Wang, Y., Lotz, S., Lin, G., Sun, Y., Roysam, B., Shen, Q., and Temple, S. (2010). Adult SVZ lineage cells home to and leave the vascular niche via differential responses to SDF1/CXCR4 signaling. *Cell stem cell*, 7(2):163--73.

Korkaya, H., Liu, S., and Wicha, M. S. (2011). Breast cancer stem cells, cytokine networks, and the tumor microenvironment. *The Journal of clinical investigation*, 121(10):3804--9.

Kornack, D. R. and Rakic, P. (2001). The generation, migration, and differentiation of olfactory neurons in the adult primate brain. *Proceedings of the National Academy of Sciences of the United States of America*, 98(8):4752--7.

Kullander, K. and Klein, R. (2002). Mechanisms and functions of Eph and ephrin signalling. *Nature reviews. Molecular cell biology*, 3(7):475--86.

Lathia, J. D., Gallagher, J., Heddleston, J. M., Wang, J., Eyler, C. E., Macswords, J., Wu, Q., Vasanji, A., McLendon, R. E., Hjelmeland, A. B., and Rich, J. N. (2010). Integrin alpha 6 regulates glioblastoma stem cells. *Cell stem cell*, 6(5):421--32.

Lathia, J. D., Li, M., Hall, P. E., Gallagher, J., Hale, J. S., Wu, Q., Venere, M., Levy, E., Rani, M. R. S., Huang, P., Bae, E., Selfridge, J., Cheng, L., Guvenc, H., McLendon, R. E., Nakano, I., Sloan, A. E., Phillips, H. S., Lai, A., Gladson, C. L., Bredel, M., Bao, S., Hjelmeland, A. B., and Rich, J. N. (2012). Laminin alpha 2 enables glioblastoma stem cell growth. *Annals of neurology*, 72(5):766--78.

Laussu, J., Khuong, A., Gautrais, J., and Davy, A. (2014). Beyond boundaries-Eph:ephrin signaling in neurogenesis. *Cell adhesion & migration*, 8(4):349--59.

Lee, H.-S., Nishanian, T. G., Mood, K., Bong, Y.-S., and Daar, I. O. (2008). EphrinB1 controls cell-cell junctions through the Par polarity complex. *Nature cell biology*, 10(8):979--86.

Leon, S. P., Folkerth, R. D., and Black, P. M. (1996). Microvessel density is a prognostic indicator for patients with astroglial brain tumors. *Cancer*, 77(2):362--72.

Leventhal, C., Rafii, S., Rafii, D., Shahar, A., and Goldman, S. A. (1999). Endothelial trophic support of neuronal production and recruitment from the adult mammalian subependyma. *Molecular and cellular neurosciences*, 13(6):450--64.

Levison, S. W. and Goldman, J. E. (1993). Both oligodendrocytes and astrocytes develop from progenitors in the subventricular zone of postnatal rat forebrain. *Neuron*, 10(2):201--12.

Lewis, P. (1968). A quantitative study of cell proliferation in the subependymal layer of the adult rat brain. *Experimental Neurology*, 20(2):203--207.

Lhoták, V., Greer, P., Letwin, K., and Pawson, T. (1991). Characterization of elk, a brain-specific receptor tyrosine kinase. *Molecular and cellular biology*, 11(5):2496--502.

Li, C., Heidt, D. G., Dalerba, P., Burant, C. F., Zhang, L., Adsay, V., Wicha, M., Clarke, M. F., and Simeone, D. M. (2007). Identification of pancreatic cancer stem cells. *Cancer research*, 67(3):1030--7.

Li, J.-J., Liu, D.-P., Liu, G.-T., and Xie, D. (2009). EphrinA5 acts as a tumor suppressor in glioma by negative regulation of epidermal growth factor receptor. *Oncogene*, 28(15):1759--68.

Li, L. and Xie, T. (2005). Stem cell niche: structure and function. *Annual review of cell and developmental biology*, 21:605--31.

Ligon, K. L., Huillard, E., Mehta, S., Kesari, S., Liu, H., Alberta, J. A., Bachoo, R. M., Kane, M., Louis, D. N., Depinho, R. A., Anderson, D. J., Stiles, C. D., and Rowitch, D. H. (2007). Olig2-regulated lineage-restricted pathway controls replication competence in neural stem cells and malignant glioma. *Neuron*, 53(4):503--17.

Lim, D. A. and Alvarez-Buylla, A. (2014). Adult neural stem cells stake their ground. *Trends in neurosciences*, 37(10):563--71.

Lin, S.-P., Lee, Y.-T., Yang, S.-H., Miller, S. A., Chiou, S.-H., Hung, M.-C., and Hung, S.-C. (2013). Colon cancer stem cells resist antiangiogenesis therapy-induced apoptosis. *Cancer letters*, 328(2):226--34.

Liu, D.-P., Wang, Y., Koeffler, H. P., and Xie, D. (2007). Ephrin-A1 is a negative regulator in glioma through down-regulation of EphA2 and FAK. *International journal of oncology*, 30(4):865--71.

Liu, Y.-X., Wang, J., Guo, J., Wu, J., Lieberman, H. B., and Yin, Y. (2008). DUSP1 is controlled by p53 during the cellular response to oxidative stress. *Molecular cancer research : MCR*, 6(4):624--33.

Lois, C. and Alvarez-Buylla, A. (1994). Long-distance neuronal migration in the adult mammalian brain. *Science (New York, N.Y.)*, 264(5162):1145--8.

Louis, D. N., Ohgaki, H., Wiestler, O. D., Cavenee, W. K., Burger, P. C., Jouvet, A., Scheithauer, B. W., and Kleihues, P. (2007). The 2007 WHO classification of tumours of the central nervous system. *Acta neuropathologica*, 114(2):97--109.

Lugassy, C., Haroun, R. I., Brem, H., Tyler, B. M., Jones, R. V., Fernandez, P. M., Patierno, S. R., Kleinman, H. K., and Barnhill, R. L. (2002). Pericytic-like angiotropism of glioma and melanoma cells. *The American Journal of dermatopathology*, 24(6):473--8.

Lun, M., Lok, E., Gautam, S., Wu, E., and Wong, E. T. (2011). The natural history of extracranial metastasis from glioblastoma multiforme. *Journal of neuro-oncology*, 105(2):261--73.

Luo, L. and Flanagan, J. G. (2007). Development of continuous and discrete neural maps. *Neuron*, 56(2):284--300.

MacDonald, B. T., Tamai, K., and He, X. (2009). Wnt/beta-catenin signaling: components, mechanisms, and diseases. *Developmental cell*, 17(1):9--26.

Malanchi, I., Santamaria-Martínez, A., Susanto, E., Peng, H., Lehr, H.-A., Delaloye, J.-F., and Huelsken, J. (2012). Interactions between cancer stem cells and their niche govern metastatic colonization. *Nature*, 481(7379):85--9.

Marquardt, T., Shirasaki, R., Ghosh, S., Andrews, S. E., Carter, N., Hunter, T., and Pfaff, S. L. (2005). Coexpressed EphA receptors and ephrin-A ligands mediate opposing actions on growth cone navigation from distinct membrane domains. *Cell*, 121(1):127--39.

Mathieu, C., Sii-Felice, K., Fouchet, P., Etienne, O., Haton, C., Mabondzo, A., Boussin, F. D., and Mouthon, M.-A. (2008). Endothelial cell-derived bone morphogenetic proteins control proliferation of neural stem/progenitor cells. *Molecular and cellular neurosciences*, 38(4):569--77.

Meletis, K., Wirta, V., Hede, S.-M., Nistér, M., Lundeberg, J., and Frisén, J. (2006). p53

suppresses the self-renewal of adult neural stem cells. *Development (Cambridge, England)*, 133(2):363--9.

Mentlein, R., Hattermann, K., and Held-Feindt, J. (2012). Lost in disruption: role of proteases in glioma invasion and progression. *Biochimica et biophysica acta*, 1825(2):178--85.

Miao, H., Burnett, E., Kinch, M., Simon, E., and Wang, B. (2000). Activation of EphA2 kinase suppresses integrin function and causes focal-adhesion-kinase dephosphorylation. *Nature cell biology*, 2(2):62--9.

Mizuno, H., Kitada, K., Nakai, K., and Sarai, A. (2009). PrognoScan: a new database for meta-analysis of the prognostic value of genes. *BMC medical genomics*, 2(1):18.

Montana, V. and Sontheimer, H. (2011). Bradykinin promotes the chemotactic invasion of primary brain tumors. *The Journal of neuroscience : the official journal of the Society for Neuroscience*, 31(13):4858--67.

Mrugala, M. M. (2013). Advances and Challenges in the Treatment of Glioblastoma: A Clinician's Perspective. *Discovery Medicine*, 15(83):221--230.

Murai, K. K. and Pasquale, E. B. (2003). 'Eph'ective signaling: forward, reverse and crosstalk. *Journal of cell science*, 116(Pt 14):2823--32.

Nagasaka, K., Nakagawa, S., Yano, T., Takizawa, S., Matsumoto, Y., Tsuruga, T., Nakagawa, K., Minaguchi, T., Oda, K., Hiraike-Wada, O., Ooishi, H., Yasugi, T., and Taketani, Y. (2006). Human homolog of Drosophila tumor suppressor Scribble negatively regulates cell-cycle progression from G1 to S phase by localizing at the basolateral membrane in epithelial cells. *Cancer science*, 97(11):1217--25.

Nakada, M., Anderson, E. M., Demuth, T., Nakada, S., Reavie, L. B., Drake, K. L., Hoelzinger, D. B., and Berens, M. E. (2010). The phosphorylation of ephrin-B2 ligand promotes glioma cell migration and invasion. *International journal of cancer. Journal international du cancer*, 126(5):1155--65.

Nakada, M., Drake, K. L., Nakada, S., Niska, J. A., and Berens, M. E. (2006). Ephrin-B3 ligand promotes glioma invasion through activation of Rac1. *Cancer research*, 66(17):8492--500.

Nakada, M., Hayashi, Y., and Hamada, J.-i. (2011). Role of Eph/ephrin tyrosine kinase in malignant glioma. *Neuro-oncology*, 13(11):1163--70.

Nakada, M., Niska, J. A., Miyamori, H., McDonough, W. S., Wu, J., Sato, H., and Berens, M. E. (2004). The phosphorylation of EphB2 receptor regulates migration and invasion of human glioma cells. *Cancer research*, 64(9):3179--85.

Nakano, I. (2015). Stem cell signature in glioblastoma: therapeutic development for a moving target. *Journal of neurosurgery*, 122(2):324--30.

Nam, S. C., Kim, Y., Dryanovski, D., Walker, A., Goings, G., Woolfrey, K., Kang, S. S., Chu, C., Chenn, A., Erdelyi, F., Szabo, G., Hockberger, P., and Szele, F. G. (2007). Dynamic features of postnatal subventricular zone cell motility: a two-photon time-lapse study. *The Journal of comparative neurology*, 505(2):190--208.

Naumov, G. N., Akslen, L. A., and Folkman, J. (2006). Role of angiogenesis in human tumor dormancy: animal models of the angiogenic switch. *Cell cycle (Georgetown, Tex.)*, 5(16):1779--87.

Naxerova, K., Bult, C. J., Peaston, A., Fancher, K., Knowles, B. B., Kasif, S., and Kohane, I. S. (2008). Analysis of gene expression in a developmental context emphasizes distinct biological leitmotifs in human cancers. *Genome biology*, 9(7):R108.

Nelson, W. G. and Kastan, M. B. (1994). DNA strand breaks: the DNA template alterations that trigger p53-dependent DNA damage response pathways. *Molecular and cellular biology*, 14(3):1815--23.

Nie, K., Molnár, Z., and Szele, F. G. (2010). Proliferation but not migration is associated

with blood vessels during development of the rostral migratory stream. *Developmental neuroscience*, 32(3):163--72.

Nikolova, Z., Djonov, V., Zuercher, G., Andres, A. C., and Ziemiecki, A. (1998). Cell-type specific and estrogen dependent expression of the receptor tyrosine kinase EphB4 and its ligand ephrin-B2 during mammary gland morphogenesis. *Journal of cell science*, 111 ( Pt 1:2741--51.

Niola, F., Zhao, X., Singh, D., Castano, A., Sullivan, R., Lauria, M., Nam, H.-s., Zhuang, Y., Benezra, R., Di Bernardo, D., Iavarone, A., and Lasorella, A. (2012). Id proteins synchronize stemness and anchorage to the niche of neural stem cells. *Nature cell biology*, 14(5):477--87.

Noren, N. K. and Pasquale, E. B. (2004). Eph receptor-ephrin bidirectional signals that target Ras and Rho proteins. *Cellular signalling*, 16(6):655--66.

Nowakowski, J., Cronin, C. N., McRee, D. E., Knuth, M. W., Nelson, C. G., Pavletich, N. P., Rogers, J., Sang, B.-C., Scheibe, D. N., Swanson, R. V., and Thompson, D. A. (2002). Structures of the Cancer-Related Aurora-A, FAK, and EphA2 Protein Kinases from Nanovolume Crystallography. *Structure*, 10(12):1659--1667.

Oh, T., Fakurnejad, S., Sayegh, E. T., Clark, A. J., Ivan, M. E., Sun, M. Z., Safaee, M., Bloch, O., James, C. D., and Parsa, A. T. (2014). Immunocompetent murine models for the study of glioblastoma immunotherapy. *Journal of translational medicine*, 12(1):107.

Ohgaki, H. and Kleihues, P. (2005). Epidemiology and etiology of gliomas. *Acta neuropathologica*, 109(1):93--108.

Oliver, T. G. and Wechsler-Reya, R. J. (2004). Getting at the root and stem of brain tumors. *Neuron*, 42(6):885--8.

Ottone, C., Krusche, B., Whitby, A., Clements, M., Quadrato, G., Pitulescu, M. E., Adams,

R. H., and Parrinello, S. (2014). Direct cell-cell contact with the vascular niche maintains quiescent neural stem cells. *Nature cell biology*, 16(11):1045--1056.

Ozawa, T., Wang, J., Hu, L. J., Bollen, A. W., Lamborn, K. R., and Deen, D. F. (2002). Growth of human glioblastomas as xenografts in the brains of athymic rats. *In vivo (Athens, Greece)*, 16(1):55--60.

Pacholska, A., Wirth, T., Samaranayake, H., Pikkarainen, J., Ahmad, F., and Ylä-Herttuala, S. (2012). Increased invasion of malignant gliomas after 15-LO-1 and HSV-tk/ganciclovir combination gene therapy. *Cancer gene therapy*, 19(12):870--4.

Palmer, A., Zimmer, M., Erdmann, K. S., Eulenburg, V., Porthin, A., Heumann, R., Deutsch, U., and Klein, R. (2002). EphrinB phosphorylation and reverse signaling: regulation by Src kinases and PTP-BL phosphatase. *Molecular cell*, 9(4):725--37.

Parrinello, S., Noon, L. A., Harrisingh, M. C., Wingfield Digby, P., Rosenberg, L. H., Cremona, C. A., Echave, P., Flanagan, A. M., Parada, L. F., and Lloyd, A. C. (2008). NF1 loss disrupts Schwann cell-axonal interactions: a novel role for semaphorin 4F. *Genes & development*, 22(23):3335--48.

Pasquale, E. B. (2005). Eph receptor signalling casts a wide net on cell behaviour. *Nature reviews. Molecular cell biology*, 6(6):462--75.

Pasquale, E. B. (2008). Eph-ephrin bidirectional signaling in physiology and disease. *Cell*, 133(1):38--52.

Pasquale, E. B. (2010). Eph receptors and ephrins in cancer: bidirectional signalling and beyond. *Nature reviews. Cancer*, 10(3):165--80.

Pasquier, J. and Rafii, A. (2013). Role of the microenvironment in ovarian cancer stem cell maintenance. *BioMed research international*, 2013:630782.

Persson, L., Hansson, H. A., and Sourander, P. (1976). Extravasation, spread and cellular

uptake of Evans blue-labelled albumin around a reproducible small stab-wound in the rat brain. *Acta Neuropathologica*, 34(2):125--136.

Peter, J.-C., Rossez, H., Weckering, M., Zipfel, G., Lecourt, A.-C., Owen, J. B., Banks, W. A., and Hofbauer, K. G. (2013). Protective effects of an anti-melanocortin-4 receptor scFv derivative in lipopolysaccharide-induced cachexia in rats. *Journal of cachexia, sarcopenia and muscle*, 4(1):79--88.

Phillips, H. S., Kharbanda, S., Chen, R., Forrest, W. F., Soriano, R. H., Wu, T. D., Misra, A., Nigro, J. M., Colman, H., Soroceanu, L., Williams, P. M., Modrusan, Z., Feuerstein, B. G., and Aldape, K. (2006). Molecular subclasses of high-grade glioma predict prognosis, delineate a pattern of disease progression, and resemble stages in neurogenesis. *Cancer cell*, 9(3):157--73.

Piekny, A., Werner, M., and Glotzer, M. (2005). Cytokinesis: welcome to the Rho zone. *Trends in cell biology*, 15(12):651--8.

Pietsch, T. and Wiestler, O. D. (1997). Molecular neuropathology of astrocytic brain tumors. *Journal of neuro-oncology*, 35(3):211--22.

Pitz, M. W., Desai, A., Grossman, S. A., and Blakeley, J. O. (2011). Tissue concentration of systemically administered antineoplastic agents in human brain tumors. *Journal of neuro-oncology*, 104(3):629--38.

Poliakov, A., Cotrina, M., and Wilkinson, D. G. (2004). Diverse roles of eph receptors and ephrins in the regulation of cell migration and tissue assembly. *Developmental cell*, 7(4):465--80.

Pollard, S. M., Yoshikawa, K., Clarke, I. D., Danovi, D., Stricker, S., Russell, R., Bayani, J., Head, R., Lee, M., Bernstein, M., Squire, J. A., Smith, A., and Dirks, P. (2009). Glioma stem cell lines expanded in adherent culture have tumor-specific phenotypes and are suitable for chemical and genetic screens. *Cell stem cell*, 4(6):568--80.

Puche, A. C. and Bovetti, S. (2011). Studies of adult neural stem cell migration. *Methods in molecular biology (Clifton, N.J.)*, 750:227--40.

Qin, Y., Capaldo, C., Gumbiner, B. M., and Macara, I. G. (2005). The mammalian Scribble polarity protein regulates epithelial cell adhesion and migration through E-cadherin. *The Journal of cell biology*, 171(6):1061--71.

Quail, D. F., Taylor, M. J., and Postovit, L.-M. (2012). Microenvironmental regulation of cancer stem cell phenotypes. *Current stem cell research & therapy*, 7(3):197--216.

Radke, J., Bortolussi, G., and Pagenstecher, A. (2013). Akt and c-Myc induce stem-cell markers in mature primary p53 / astrocytes and render these cells gliomagenic in the brain of immunocompetent mice. *PloS one*, 8(2):e56691.

Ramírez-Castillejo, C., Sánchez-Sánchez, F., Andreu-Agulló, C., Ferrón, S. R., Aroca-Aguilar, J. D., Sánchez, P., Mira, H., Escribano, J., and Fariñas, I. (2006). Pigment epithelium-derived factor is a niche signal for neural stem cell renewal. *Nature neuroscience*, 9(3):331--9.

Recht, L., Jang, T., Savarese, T., and Litofsky, N. S. (2003). Neural stem cells and neuro-oncology: quo vadis? *Journal of cellular biochemistry*, 88(1):11--9.

Ridley, A. (1977). Immunological aspects of gliomas. *Proceedings of the Royal Society of Medicine*, 70(12):867--9.

Rivlin, N., Brosh, R., Oren, M., and Rotter, V. (2011). Mutations in the p53 Tumor Suppressor Gene: Important Milestones at the Various Steps of Tumorigenesis. *Genes & cancer*, 2(4):466--74.

Robinson, V., Smith, A., Flenniken, A. M., and Wilkinson, D. G. (1997). Roles of Eph receptors and ephrins in neural crest pathfinding. *Cell and tissue research*, 290(2):265--74.

Sabit, H., Nakada, M., Furuta, T., Watanabe, T., Hayashi, Y., Sato, H., Kato, Y., and

Hamada, J.-i. (2014). Characterizing invading glioma cells based on IDH1-R132H and Ki-67 immunofluorescence. *Brain tumor pathology*, 31(4):242--6.

Sadahiro, H., Yoshikawa, K., Ideguchi, M., Kajiwara, K., Ishii, A., Ikeda, E., Owada, Y., Yasumoto, Y., and Suzuki, M. (2014). Pathological features of highly invasive glioma stem cells in a mouse xenograft model. *Brain tumor pathology*, 31(2):77--84.

Sadot, E., Geiger, B., Oren, M., and Ben-Ze'ev, A. (2001). Down-regulation of beta-catenin by activated p53. *Molecular and cellular biology*, 21(20):6768--81.

Sahin, M., Greer, P. L., Lin, M. Z., Poucher, H., Eberhart, J., Schmidt, S., Wright, T. M., Shamah, S. M., O'connell, S., Cowan, C. W., Hu, L., Goldberg, J. L., Debant, A., Corfas, G., Krull, C. E., and Greenberg, M. E. (2005). Eph-dependent tyrosine phosphorylation of ephexin1 modulates growth cone collapse. *Neuron*, 46(2):191--204.

Sampieri, K. and Fodde, R. (2012). Cancer stem cells and metastasis. *Seminars in Cancer Biology*, 22(3):187--193.

Sanai, N., Tramontin, A., Quiñones Hinojosa, A., Barbaro, N., Gupta, N., Kunwar, S., Lawton, M., McDermott, M., Parsa, A., Verdugo, J., and Others (2004). Unique astrocyte ribbon in adult human brain contains neural stem cells but lacks chain migration. *Nature*, 427(6976):740--744.

Sawamiphak, S., Seidel, S., Essmann, C. L., Wilkinson, G. a., Pitulescu, M. E., Acker, T., and Acker-Palmer, A. (2010). Ephrin-B2 regulates VEGFR2 function in developmental and tumour angiogenesis. *Nature*, 465(7297):487--91.

Scherer, H. J. (1940). Cerebral Astrocytomas and Their Derivatives. *Am J Cancer*, 40(2):159--198.

Schofield, R. (1978). The relationship between the spleen colony-forming cell and the haemopoietic stem cell. *Blood cells*, 4(1-2):7--25.

Shen, Q., K Goderie, S., Jin, L., Karanth, N., Sun, Y., Abramova, N., Vincent, P., Pumiglia, K., and Temple, S. (2004). Endothelial cells stimulate self-renewal and expand neurogenesis of neural stem cells. *Science*, 304(5675):1338--1340.

Shen, Q., Wang, Y., Kokovay, E., Lin, G., Chuang, S.-M., Goderie, S. K., Roysam, B., and Temple, S. (2008). Adult SVZ stem cells lie in a vascular niche: a quantitative analysis of niche cell-cell interactions. *Cell stem cell*, 3(3):289--300.

Singh, S. K., Clarke, I. D., Terasaki, M., Bonn, V. E., Hawkins, C., Squire, J., and Dirks, P. B. (2003). Identification of a Cancer Stem Cell in Human Brain Tumors. *Cancer Res.*, 63(18):5821--5828.

Singh, S. K., Hawkins, C., Clarke, I. D., Squire, J. A., Bayani, J., Hide, T., Henkelman, R. M., Cusimano, M. D., and Dirks, P. B. (2004). Identification of human brain tumour initiating cells. *Nature*, 432(7015):396--401.

Siu, M. K., Wong, C. H., Xia, W., Mruk, D. D., Lee, W. M., and Cheng, C. Y. (2011). The $\beta$1-integrin-p-FAK-p130Cas-DOCK180-RhoA-vinculin is a novel regulatory protein complex at the apical ectoplasmic specialization in adult rat testes. *Spermatogenesis*, 1(1):73--86.

Skerra, A. and Plückthun, A. (1988). Assembly of a functional immunoglobulin Fv fragment in Escherichia coli. *Science (New York, N.Y.)*, 240(4855):1038--41.

Smith, J. S. and Jenkins, R. B. (2000). Genetic alterations in adult diffuse glioma: occurrence, significance, and prognostic implications. *Frontiers in bioscience : a journal and virtual library*, 5:D213--31.

Solozobova, V. and Blattner, C. (2011). p53 in stem cells. *World journal of biological chemistry*, 2(9):202--14.

Stein, E., Huynh-Do, U., Lane, A. A., Cerretti, D. P., and Daniel, T. O. (1998). Nck recruit-

ment to Eph receptor, EphB1/ELK, couples ligand activation to c-Jun kinase. *The Journal of biological chemistry*, 273(3):1303--8.

Stiver, S. I. (2004). Angiogenesis and its role in the behavior of astrocytic brain tumors. *Frontiers in bioscience : a journal and virtual library*, 9:3105--23.

Stock, J. K., Giadrossi, S., Casanova, M., Brookes, E., Vidal, M., Koseki, H., Brockdorff, N., Fisher, A. G., and Pombo, A. (2007). Ring1-mediated ubiquitination of H2A restrains poised RNA polymerase II at bivalent genes in mouse ES cells. *Nature cell biology*, 9(12):1428--35.

Stricker, S. H., Feber, A., Engström, P. G., Carén, H., Kurian, K. M., Takashima, Y., Watts, C., Way, M., Dirks, P., Bertone, P., Smith, A., Beck, S., and Pollard, S. M. (2013). Widespread resetting of DNA methylation in glioblastoma-initiating cells suppresses malignant cellular behavior in a lineage-dependent manner. *Genes & development*, 27(6):654--69.

Sun, Y., Aiga, M., Yoshida, E., Humbert, P. O., and Bamji, S. X. (2009). Scribble interacts with beta-catenin to localize synaptic vesicles to synapses. *Molecular biology of the cell*, 20(14):3390--400.

Suzuki, S. O. and Goldman, J. E. (2003). Multiple Cell Populations in the Early Postnatal Subventricular Zone Take Distinct Migratory Pathways: A Dynamic Study of Glial and Neuronal Progenitor Migration. *J. Neurosci.*, 23(10):4240--4250.

Takakura, N. (2012). Formation and regulation of the cancer stem cell niche. *Cancer science*, 103(7):1177--81.

Tan, N. Y. and Khachigian, L. M. (2009). Sp1 phosphorylation and its regulation of gene transcription. *Molecular and cellular biology*, 29(10):2483--8.

Tanaka, M., Kamo, T., Ota, S., and Sugimura, H. (2003). Association of Dishevelled with

Eph tyrosine kinase receptor and ephrin mediates cell repulsion. *The EMBO journal*, 22(4):847--58.

Tavazoie, M., Van der Veken, L., Silva-Vargas, V., Louissaint, M., Colonna, L., Zaidi, B., Garcia-Verdugo, J. M., and Doetsch, F. (2008). A specialized vascular niche for adult neural stem cells. *Cell stem cell*, 3(3):279--88.

TCGA (2008). Comprehensive genomic characterization defines human glioblastoma genes and core pathways. *Nature*, 455(7216):1061--8.

Tetsu, O. and McCormick, F. (1999). Beta-catenin regulates expression of cyclin D1 in colon carcinoma cells. *Nature*, 398(6726):422--6.

Theus, M. H., Ricard, J., Bethea, J. R., and Liebl, D. J. (2010). EphB3 limits the expansion of neural progenitor cells in the subventricular zone by regulating p53 during homeostasis and following traumatic brain injury. *Stem cells (Dayton, Ohio)*, 28(7):1231--42.

Thiery, J. P. (2002). Epithelial-mesenchymal transitions in tumour progression. *Nature reviews. Cancer*, 2(6):442--54.

Thullberg, M., Gad, A., Le Guyader, S., and Strömblad, S. (2007). Oncogenic H-Ras V12 promotes anchorage-independent cytokinesis in human fibroblasts. *Proceedings of the National Academy of Sciences of the United States of America*, 104(51):20338--43.

Todaro, M., Alea, M. P., Di Stefano, A. B., Cammareri, P., Vermeulen, L., Iovino, F., Tripodo, C., Russo, A., Gulotta, G., Medema, J. P., and Stassi, G. (2007). Colon cancer stem cells dictate tumor growth and resist cell death by production of interleukin-4. *Cell stem cell*, 1(4):389--402.

Trovó-Marqui, A. B. and Tajara, E. H. (2006). Neurofibromin: a general outlook. *Clinical genetics*, 70(1):1--13.

Tso, C.-L., Freije, W. A., Day, A., Chen, Z., Merriman, B., Perlina, A., Lee, Y., Dia, E. Q., Yoshimoto, K., Mischel, P. S., Liau, L. M., Cloughesy, T. F., and Nelson, S. F. (2006).

Distinct transcription profiles of primary and secondary glioblastoma subgroups. *Cancer research*, 66(1):159--67.

Tu, Y., He, S., Fu, J., Li, G., Xu, R., Lu, H., and Deng, J. (2012). Expression of EphrinB2 and EphB4 in glioma tissues correlated to the progression of glioma and the prognosis of glioblastoma patients. *Clinical & translational oncology : official publication of the Federation of Spanish Oncology Societies and of the National Cancer Institute of Mexico*, 14(3):214--20.

Uhrbom, L., Dai, C., Celestino, J. C., Rosenblum, M. K., Fuller, G. N., and Holland, E. C. (2002). Ink4a-Arf loss cooperates with KRas activation in astrocytes and neural progenitors to generate glioblastomas of various morphologies depending on activated Akt. *Cancer research*, 62(19):5551--8.

Velpula, K. K., Rehman, A. A., Chelluboina, B., Dasari, V. R., Gondi, C. S., Rao, J. S., and Veeravalli, K. K. (2012). Glioma stem cell invasion through regulation of the interconnected ERK, integrin $\alpha6$ and N-cadherin signaling pathway. *Cellular signalling*, 24(11):2076--84.

Venere, M., Fine, H. A., Dirks, P. B., and Rich, J. N. (2011). Cancer stem cells in gliomas: identifying and understanding the apex cell in cancer's hierarchy. *Glia*, 59(8):1148--54.

Verhaak, R. G. W., Hoadley, K. A., Purdom, E., Wang, V., Qi, Y., Wilkerson, M. D., Miller, C. R., Ding, L., Golub, T., Mesirov, J. P., Alexe, G., Lawrence, M., O'Kelly, M., Tamayo, P., Weir, B. A., Gabriel, S., Winckler, W., Gupta, S., Jakkula, L., Feiler, H. S., Hodgson, J. G., James, C. D., Sarkaria, J. N., Brennan, C., Kahn, A., Spellman, P. T., Wilson, R. K., Speed, T. P., Gray, J. W., Meyerson, M., Getz, G., Perou, C. M., and Hayes, D. N. (2010). Integrated genomic analysis identifies clinically relevant subtypes of glioblastoma characterized by abnormalities in PDGFRA, IDH1, EGFR, and NF1. *Cancer cell*, 17(1):98--110.

von Bülow, C., Hayen, W., Hartmann, A., Mueller-Klieser, W., Allolio, B., and Nehls, V. (2001). Endothelial capillaries chemotactically attract tumour cells. *The Journal of pathology*, 193(3):367--76.

Vredenburgh, J. J., Desjardins, A., Herndon, J. E., Dowell, J. M., Reardon, D. A., Quinn, J. A., Rich, J. N., Sathornsumetee, S., Gururangan, S., Wagner, M., Bigner, D. D., Friedman, A. H., and Friedman, H. S. (2007). Phase II trial of bevacizumab and irinotecan in recurrent malignant glioma. *Clinical cancer research : an official journal of the American Association for Cancer Research*, 13(4):1253--9.

Wang, H. U., Chen, Z. F., and Anderson, D. J. (1998). Molecular distinction and angiogenic interaction between embryonic arteries and veins revealed by ephrin-B2 and its receptor Eph-B4. *Cell*, 93(5):741--53.

Wang, L.-F., Fokas, E., Juricko, J., You, A., Rose, F., Pagenstecher, A., Engenhart-Cabillic, R., and An, H.-X. (2008). Increased expression of EphA7 correlates with adverse outcome in primary and recurrent glioblastoma multiforme patients. *BMC cancer*, 8:79.

Wang, Y., Nakayama, M., Pitulescu, M. E., Schmidt, T. S., Bochenek, M. L., Sakakibara, A., Adams, S., Davy, A., Deutsch, U., Lüthi, U., Barberis, A., Benjamin, L. E., Mäkinen, T., Nobes, C. D., and Adams, R. H. (2010). Ephrin-B2 controls VEGF-induced angiogenesis and lymphangiogenesis. *Nature*, 465(7297):483--6.

Wang, Y., Yang, J., Zheng, H., Tomasek, G. J., Zhang, P., McKeever, P. E., Lee, E. Y.-H. P., and Zhu, Y. (2009). Expression of mutant p53 proteins implicates a lineage relationship between neural stem cells and malignant astrocytic glioma in a murine model. *Cancer cell*, 15(6):514--26.

Watkins, S., Robel, S., Kimbrough, I. F., Robert, S. M., Ellis-Davies, G., and Sontheimer, H. (2014). Disruption of astrocyte-vascular coupling and the blood-brain barrier by invading glioma cells. *Nature communications*, 5:4196.

Wick, W., Wick, A., Weiler, M., and Weller, M. (2011). Patterns of progression in malignant glioma following anti-VEGF therapy: perceptions and evidence. *Current neurology and neuroscience reports*, 11(3):305--12.

Winkler, F., Kienast, Y., Fuhrmann, M., Von Baumgarten, L., Burgold, S., Mitteregger, G., Kretzschmar, H., and Herms, J. (2009). Imaging glioma cell invasion in vivo reveals mechanisms of dissemination and peritumoral angiogenesis. *Glia*, 57(12):1306--15.

Wybenga-Groot, L. E., Baskin, B., Ong, S. H., Tong, J., Pawson, T., and Sicheri, F. (2001). Structural basis for autoinhibition of the Ephb2 receptor tyrosine kinase by the unphosphorylated juxtamembrane region. *Cell*, 106(6):745--57.

Wykosky, J. and Debinski, W. (2008). The EphA2 receptor and ephrinA1 ligand in solid tumors: function and therapeutic targeting. *Molecular cancer research : MCR*, 6(12):1795--806.

Xu, N.-J. and Henkemeyer, M. (2009). Ephrin-B3 reverse signaling through Grb4 and cytoskeletal regulators mediates axon pruning. *Nature neuroscience*, 12(3):268--76.

Yamaguchi, Y. and Pasquale, E. B. (2004). Eph receptors in the adult brain. *Current opinion in neurobiology*, 14(3):288--96.

Yamashita, Y. M., Yuan, H., Cheng, J., and Hunt, A. J. (2010). Polarity in stem cell division: asymmetric stem cell division in tissue homeostasis. *Cold Spring Harbor perspectives in biology*, 2(1):a001313.

Yan, G.-N., Yang, L., Lv, Y.-F., Shi, Y., Shen, L.-L., Yao, X.-H., Guo, Q.-N., Zhang, P., Cui, Y.-H., Zhang, X., Bian, X.-W., and Guo, D.-Y. (2014). Endothelial cells promote stem-like phenotype of glioma cells through activating the Hedgehog pathway. *The Journal of pathology*, 234(1):11--22.

Ye, J., Wu, D., Wu, P., Chen, Z., and Huang, J. (2014). The cancer stem cell niche: cross talk between cancer stem cells and their microenvironment. *Tumour biology : the journal of the International Society for Oncodevelopmental Biology and Medicine*, 35(5):3945--51.

Yin, Y., Liu, Y.-X., Jin, Y. J., Hall, E. J., and Barrett, J. C. (2003). PAC1 phosphatase

is a transcription target of p53 in signalling apoptosis and growth suppression. *Nature*, 422(6931):527--31.

Yuan, X., Curtin, J., Xiong, Y., Liu, G., Waschsmann-Hogiu, S., Farkas, D. L., Black, K. L., and Yu, J. S. (2004). Isolation of cancer stem cells from adult glioblastoma multiforme. *Oncogene*, 23(58):9392--400.

Zhang, R., Zhang, Z., Zhang, C., Zhang, L., Robin, A., Wang, Y., Lu, M., and Chopp, M. (2004). Stroke transiently increases subventricular zone cell division from asymmetric to symmetric and increases neuronal differentiation in the adult rat. *The Journal of neuroscience : the official journal of the Society for Neuroscience*, 24(25):5810--5.

Zhu, T. S., Costello, M. a., Talsma, C. E., Flack, C. G., Crowley, J. G., Hamm, L. L., He, X., Hervey-Jumper, S. L., Heth, J. a., Muraszko, K. M., DiMeco, F., Vescovi, A. L., and Fan, X. (2011). Endothelial cells create a stem cell niche in glioblastoma by providing NOTCH ligands that nurture self-renewal of cancer stem-like cells. *Cancer research*, 71(18):6061--72.

Zhu, Y., Guignard, F., Zhao, D., Liu, L., Burns, D. K., Mason, R. P., Messing, A., and Parada, L. F. (2005). Early inactivation of p53 tumor suppressor gene cooperating with NF1 loss induces malignant astrocytoma. *Cancer cell*, 8(2):119--30.

Zhu, Y., Romero, M. I., Ghosh, P., Ye, Z., Charnay, P., Rushing, E. J., Marth, J. D., and Parada, L. F. (2001). Ablation of NF1 function in neurons induces abnormal development of cerebral cortex and reactive gliosis in the brain. *Genes & development*, 15(7):859--76.

Zhu, Z., Khan, M. A., Weiler, M., Blaes, J., Jestaedt, L., Geibert, M., Zou, P., Gronych, J., Bernhardt, O., Korshunov, A., Bugner, V., Lichter, P., Radlwimmer, B., Heiland, S., Bendszus, M., Wick, W., and Liu, H.-K. (2014). Targeting self-renewal in high-grade brain tumors leads to loss of brain tumor stem cells and prolonged survival. *Cell stem cell*, 15(2):185--98.

Zisch, A. H., Pazzagli, C., Freeman, A. L., Schneller, M., Hadman, M., Smith, J. W., Ruoslahti, E., and Pasquale, E. B. (2000). Replacing two conserved tyrosines of the EphB2 receptor with glutamic acid prevents binding of SH2 domains without abrogating kinase activity and biological responses. *Oncogene*, 19(2):177--87.

Zong, H., Verhaak, R. G. W., and Canoll, P. (2012). The cellular origin for malignant glioma and prospects for clinical advancements. *Expert review of molecular diagnostics*, 12(4):383--94.

# Appendix

**Table 4:** Overview of tumours in which *EFNB2* expression correlated with decreased survival

| Cancer type | Cohort | corrected p-value | correlation |
| --- | --- | --- | --- |
| Adenocarcinoma | Nagoya (1995-1999, 2002-2004) | 0.0012784 | 1.16378 |
| Breast cancer | UCSF | 0.001830238 | 2.36732 |
| NSCLC | Nagoya (1995-1996) | 0.00192527 | 1.76569 |
| Adenocarcinoma | NCCRI | 0.00198601 | 1.47671 |
| Glioma | UCLA (1996-2003) | 0.00517395 | 1.2468 |
| Glioma | CBTTB, MGH, BWH, CH | 0.00761859 | 1.27132 |
| Colorectal cancer | Berlin | 0.00921191 | 2.91548 |
| Colorectal cancer | Melbourne | 0.0106433 | 0.995391 |
| Ovarian cancer | AOCS, RBH, WH, NKI-AVL (1992-2006) | 0.0123721 | 0.856288 |
| Breast cancer | UCSF | 0.0156387 | 2.06875 |
| NSCLC | Seoul (1995-2005) | 0.0266104 | 0.812794 |
| Colorectal cancer | Berlin | 0.0182768 | 1.75469 |
| Bladder cancer | CNUH | 0.0246226 | 1.11386 |
| Colorectal cancer | Berlin | 0.0259612 | 2.39903 |
| NSCLC | Seoul (1995-2005) | 0.0266104 | 0.812794 |
| Adenocarcinoma | NCCRI | 0.0391651 | 1.22188 |

**Table 6 Continued:** Overview of tumours in which *EFNB2* expression correlated with decreased survival

| Cancer type | Cohort | corrected p-value | correlation |
| --- | --- | --- | --- |
| Adenocarcinoma | Nagoya (1995-1999, 2002-2004) | 0.0473717 | 0.961708 |
| Ovarian cancer | AOCS, RBH, WH, NKI-AVL (1992-2006) | 0.0484524 | 0.659146 |

**Table 5:** Overview of tumours in which *EFNB1* expression correlated with decreased survival

| Cancer type | Cohort | corrected p-value | correlation |
|---|---|---|---|
| Breast cancer | Duke (1990-2001) | 0.000891795 | -2.00311 |
| Breast cancer | Duke | 0.0102873 | -1.00889 |
| Breast cancer | Uppsala, Oxford, Stockholm, IGR, GUYT, CRH (1980-1998) | 0.0107961 | -1.03226 |
| Breast cancer | Rotterdam (1980-1995) | 0.0171224 | -0.858444 |
| Breast cancer | Uppsala, Oxford, Stockholm, IGR, GUYT, CRH (1980-1998) | 0.0178735 | -0.864373 |
| Breast cancer | MGH (1987-2000) | 0.0224134 | 1.23689 |
| Brain cancer | MDA | 0.0250715 | 1.20635 |
| Bladder cancer | CNUH | 0.0254188 | -1.21998 |
| Adenocarcinoma | NCCRI | 0.0271007 | 0.86434 |

**Table 6:** Overview of tumours in which *EFNB2* expression correlated with decreased survival

| Cancer type | Cohort | corrected p-value | correlation |
| --- | --- | --- | --- |
| Adenocarcinoma | Nagoya (1995-1999, 2002-2004) | 0.0012784 | 1.16378 |
| Breast cancer | UCSF | 0.001830238 | 2.36732 |
| NSCLC | Nagoya (1995-1996) | 0.00192527 | 1.76569 |
| Adenocarcinoma | NCCRI | 0.00198601 | 1.47671 |
| Glioma | UCLA (1996-2003) | 0.00517395 | 1.2468 |
| Glioma | CBTTB, MGH, BWH, CH | 0.00761859 | 1.27132 |
| Colorectal cancer | Berlin | 0.00921191 | 2.91548 |
| Colorectal cancer | Melbourne | 0.0106433 | 0.995391 |
| Ovarian cancer | AOCS, RBH, WH, NKI-AVL (1992-2006) | 0.0123721 | 0.856288 |
| Breast cancer | UCSF | 0.0156387 | 2.06875 |
| NSCLC | Seoul (1995-2005) | 0.0266104 | 0.812794 |
| Colorectal cancer | Berlin | 0.0182768 | 1.75469 |
| Bladder cancer | CNUH | 0.0246226 | 1.11386 |
| Colorectal cancer | Berlin | 0.0259612 | 2.39903 |
| NSCLC | Seoul (1995-2005) | 0.0266104 | 0.812794 |
| Adenocarcinoma | NCCRI | 0.0391651 | 1.22188 |
| Adenocarcinoma | Nagoya (1995-1999, 2002-2004) | 0.0473717 | 0.961708 |
| Ovarian cancer | AOCS, RBH, WH, NKI-AVL (1992-2006) | 0.0484524 | 0.659146 |

**Table 7:** Overview of tumours in which *EFNB3* expression correlated with decreased survival

| Cancer type | Cohort | corrected p-value | correlation |
|---|---|---|---|
| Adenocarcinoma | Nagoya (1995-1999, 2002-2004) | 1.44E-06 | -1.54462 |
| Brain cancer | MDA | 0.00273962 | 1.00748 |
| Adenocarcinoma | CAN/DF | 0.00274028 | 1.39703 |
| Breast cancer | Duke | 0.00307694 | -1.08188 |
| Breast cancer | EMC | 0.00487172 | -0.859015 |
| Brain cancer | NCI (1974-2001) | 0.0115523 | -16.6031 |
| Ovarian cancer | Duke | 0.0125169 | 0.836825 |
| Breast cancer | Stockholm (1994-1996) | 0.02453 | 1.35686 |
| Breast cancer | Uppsala (1987-1989) | 0.0251273 | 1.03413 |
| Breast cancer | Duke (1990-2001) | 0.0258922 | 1.62677 |
| Brain cancer | MDA | 0.0259832 | -1.05024 |
| Breast cancer | Montpellier, Bordeaux, Turin (1989-2001) | 0.0459283 | -0.837453 |